INVESTIGATING THE ROLE OF SYNCYTIOTROPHOBLAST-DERIVED EXTRACELLULAR VESICLES IN THE PATHOGENESIS OF PREECLAMPSIA



Dr Prassana Varun Logenthiran

Linacre College

A thesis submitted for the degree of Doctor of Philosophy

Trinity Term 2024

45,000 words

This thesis is submitted to the University of Oxford

in partial fulfilment of the

Doctor of Philosophy degree requirement.

This thesis is the product of my original research and investigation. It represents my own scholarly contribution, except for any citations or collaborations explicitly mentioned within the text.

Copyright © Prassana Varun Logenthiran

All rights reserved.

உ

சிவன் அவன் என் சிந்தையுள் நின்ற அதனால்

அவன் அருளாலே அவன் தாள் வணங்கி...

- சிவபுராணம்

Shiva is fully established in my mind..

Therefore, with his grace, I bow to his holy feet…

- *Shivapuranam*

In loving memory of

Yogeswarie Logenthiran ***(1952 - 2021)***

whose unwavering love and support fuelled my every step !

This thesis is dedicated to you, *Amma*,

for always believing in my ability to

achieve my dreams !

Acknowledgements

Since embarking on my DPhil journey, the thought of writing this acknowledgement has lingered in the back of my mind. Even now, with the thesis complete, expressing my gratitude proves a significant challenge. These past years have been a whirlwind of transformative growth. I've pushed myself beyond imagined limits, embraced strategic work ethic, and dared to dream even bigger. Growing up in Sri Lanka, a world seemingly distant from the hallowed halls of Oxford, I held onto a fervent dream of pursuing a research career in obstetric medicine and placental diseases. This journey, fuelled by a relentless pursuit of knowledge, has ultimately led me here. Looking back, it's not just the hours poured into research that define this experience. The true difference lies in the exceptional people I've encountered throughout my DPhil. These individuals, with their unwavering support and guidance, have been instrumental in helping me navigate this path and turn my aspirations into reality.

Throughout this journey, I've felt a guiding hand from above, a divine presence lighting the path when doubts threatened to cloud my vision. This unwavering belief in a higher power has offered solace and strength, reminding me that even the most ambitious dreams can be achieved with faith and perseverance. Closer to home, my deepest appreciation goes to the ones who nurtured my dreams from the very beginning – my parents (Rajanathan Logenthiran & Yogeswarie Logenthiran). Their unwavering love and belief in my potential have been the bedrock of my journey. I am ever grateful for their emotional and financial assistance during this odyssey. Words cannot express the profound sense of loss I experienced with the passing of my mother during my DPhil. Yet, her spirit and the values she instilled in me continue to be my guiding light, a radiant beacon from heaven that shines even brighter in moments of hardship. The lessons she imparted, the sacrifices she made, and the love she showered upon me are the very foundation upon which I stand today. My gratitude extends to all my teachers, who from a young age recognized my spark and nurtured my curiosity. Their dedication to imparting

knowledge has shaped my academic foundation and instilled in me a lifelong love of learning. To all of you, from the divine to the earthly, my sincerest thanks. You have played a pivotal role in shaping me into the researcher I am today.

Professor Manu Vatish, your guidance and support have transcended the traditional supervisor-student relationship. You have embodied the very essence of mentorship, becoming a father figure when I needed a steady hand, a brother when I craved camaraderie, and a friend when solace was most necessary. Beyond the confines of your supervisory role, you've consistently offered invaluable help during the darkest phases of my DPhil journey. Your unwavering support extended far beyond the lab, and your genuine interest in my well-being was truly heart-warming. You've always championed what was best for me, even when it meant redefining my career path. Your willingness to guide me through such a pivotal decision speaks volumes about your dedication to your students. This thesis wouldn't exist without your unwavering belief in my abilities, *Manu*. Your encouragement acted as a constant "hype-man," fuelling my motivation during challenging times. Your enthusiasm for my research, coupled with your insightful feedback, was an invaluable resource throughout the entire process. Thank you for being my sounding board, a safe space where I could voice my doubts and aspirations. I am incredibly grateful for your guidance, which served as my conscience, ensuring I stayed true to my academic and personal values.

My deepest gratitude extends to the exceptional faculty at the Nuffield Department of Women's and Reproductive Health who have fostered my academic journey. Emeritus Professor Chris Redman, a stalwart figure in obstetric medicine, has been an inspiration since my medical school days. Your dedication to the field ignited my passion for pursuing research in obstetric medicine. Dr. Sofia Cerdeira, my co-supervisor, has been an invaluable asset and a good friend. Your constructive criticism pushed me to constantly question and refine my research direction. This insightful questioning proved instrumental in shaping a more robust research project. Dr. Wei

Zhang, a senior postdoctoral researcher, deserves special thanks for his ever-present support. Your expertise in research methodology and laboratory techniques significantly aided my progress. My heartfelt appreciation goes to Dr. Carolina Motta Mejia for inducting me into the world of wet lab research. Coming from a background without prior research experience, your guidance was instrumental in equipping me with the necessary skills to navigate the lab environment. I would also like to thank Dr. Neva Kandzija for the stimulating academic interactions. Your insights have significantly shaped my research methods and techniques, allowing me to approach my project with greater sophistication. I would like to extend a special mention to Prof. Benedikt Kessler and Dr. Zhanru Yu of the Target Discovery Institute, University of Oxford, for their invaluable support with gas chromatography-mass spectrometry. Additionally, I am deeply grateful to Prof. Naveed Akbar of the Department of Cardiovascular Medicine, University of Oxford, for his insightful guidance in planning and executing endothelial cell-based studies.

Dr. Toluwalase Awoyemi, or "*General Tolu*" as we affectionately call him, has been more than just a colleague; he's become a friend, a brother, and a true mentor. His unwavering belief in me pushed me to reach heights I never thought possible. Whenever self-doubt crept in, his infectious enthusiasm and "can-do" attitude acted as a powerful antidote. Let's just say, his motivational skills would put any life coach to shame! Dr. Maryam Rahbar has been a delightful constant: a good friend, a fantastic host, and a patient listener (especially during my not-so-successful experimental trials!). Her warm hospitality extended far beyond the confines of the lab, with her frequent dinner invitations becoming a welcome respite from the demands of research – and let's not forget the delicious food! Dr. Shuhan Jiang deserves a special mention for instilling a healthy dose of scientific rigor in my approach. Not only was she a steadfast partner in the often-laborious world of lab experiments, but she also possessed an uncanny ability to explain complex scientific concepts with remarkable clarity. This fantastic trio understood the importance of a well-rounded life, ensuring that research wasn't the only thing on my plate. They

were instrumental in creating a vibrant social space and keeping my psychological and social well-being in check. For that, I am truly grateful!

Our lab, "Team Manu," truly embodies the spirit of a scientific family. I extend my sincere gratitude to Rannya Ri, Will Cooke, Emily Mazey, Gabriel Jones, Catarina Palma Dos Reis, Morganne Wilbourne, Faheem Seedat, Cathy Wang, Qing Cao, Qian Chen, Ezekiel Musa, Angga Lokeswara, Bryony Davies, and Emily Hyde. Each of you has played a role in creating a supportive and stimulating research environment. A special thanks goes to Dr. Gabriel Jones for his invaluable expertise in statistical analysis, data interpretation, and data visualization. His guidance helped me navigate the complexities of data analysis and effectively communicate my research findings. Similarly, Dr. Will Cooke deserves recognition for his time and patience in refining my PCR techniques, a crucial aspect of my research methodology. My appreciation also extends to Emily Mazey for her willingness to share her knowledge and guide me through the intricacies of tissue culture, a skillset that proved essential for this project. My heartfelt appreciation to Morganne Wilbourne for her continuous support with bioinformatic analysis that helped me navigate coding related challenges. Together, Team Manu has fostered a collaborative atmosphere where knowledge is shared freely, and challenges are tackled as a united front. Thank you for your camaraderie and unwavering support throughout my DPhil journey.

My deepest gratitude extends to the dedicated research midwives, Fenella Roseman and Lotoyah Carty, who played a pivotal role in facilitating patient recruitment and sample collection. Furthermore, I am incredibly grateful to all the patients who generously participated in this study. Your willingness to donate biological samples is a testament to your altruism and underscores the importance of patient participation in advancing medical research. The success of this project would not have been possible without your invaluable contribution.

I'm incredibly fortunate to have a wonderful extended family here in the UK who made me feel right at home. My heartfelt thanks go to Priya and Sritharan, Kavitha and Devnath, and Kovika and Gunaparan families for their unwavering love, support, and warm hospitality. Your homes became havens where I could relax and recharge, and the delicious home-cooked meals were a constant reminder of the warmth and comfort of family. My gratitude also extends to my dear friends in UK: Niranchana and Suresh, Shivanthy and Suseenthiran, Jeyakumar, Krisha and Kamalanathan, Parthipan, Sanjeev, Saisanjeev, Sujeevan, Bawany and Jeyarupan, Shayani and Thiru, Nira and George, and Ann. You've all been a source of immense joy and support throughout my DPhil journey. Whether it was lending a listening ear, sharing a laugh, or simply being there for me, your friendship has been a true blessing. Thank you for making United Kingdom feel like a second home.

My deepest appreciation extends to my extended family back in Sri Lanka, whose unwavering belief and trust in my endeavours fuelled my spirit throughout this journey. Knowing they were cheering me on from afar instilled a sense of purpose and determination. Furthermore, I am grateful for the friends who stood by me during challenging times, offering a shoulder to lean on and unwavering support. My heartfelt thanks go to the Gunasekaran family, Dr. Uthayasanker, Gireshanth, Sugirthan, and Thileepan. Your presence, even miles away, was a constant source of strength and comfort. Thank you for reminding me that I was never alone on this journey.

My journey to this point wouldn't have been possible without the guidance and support I received from exceptional mentors in Sri Lanka. Professor Chandrika Wijeratne, Professor Susirith Mendis, Professor Sharaine Fernando, Professor Savithri Wimalasekara, and Professor Priyadarshika Hettiarachchi – your belief in my potential and early exposure to academic research ignited a passion for knowledge and set me on this path. I am deeply grateful for your invaluable insights and encouragement. Furthermore, I would like to express my sincere

appreciation to the Department of Physiology at the Faculty of Medicine, General Sir John Kotelawala Defence University (2019-2020) and the Department of Physiology at the Faculty of Medical Sciences, University of Sri Jayewardenepura (2020 - present) for their unwavering support in pursuing my DPhil degree. Their understanding and flexibility allowed me to balance my academic commitments in Sri Lanka with the demands of this doctoral program. I am incredibly grateful to the AHEAD project for their generous scholarship (2021-2023) that provided financial means to complete this DPhil degree.

As I reflect on this journey, the immense sacrifices made by my family hold a place of profound gratitude. To my father, your unwavering love and unwavering belief in my dreams have been the silent pillars of strength throughout my life. Anushala, my dear sister, and Suthan (my brother-in-law), the distance couldn't diminish the bond we share. Thank you for always being a source of support, encouragement, and joy. Ruksha, my dearest wife, words cannot express the depth of my appreciation. You not only shouldered the weight of our life in Sri Lanka but also held space for my dreams to flourish here in the UK. I know these years were challenging, with Raghavardhini, our daughter, missing her father's bedtime stories and playful hugs. The miles couldn't erase the love we shared, and the joy of reuniting as a family is a feeling I will forever cherish. To my aunt, Gnaneshwary, and mother-in-law, Mahendradevi, your support and well wishes have been a constant source of warmth. Thank you for embracing Ruksha and Raghavardhini during my absence. This thesis is a testament to the unwavering love and support of my entire family. You have all, in your own unique way, helped me navigate the challenges and celebrate the triumphs of this DPhil journey. As I embark on the next chapter, I do so with a heart brimming with gratitude for the love and sacrifices that made this achievement possible.

Table of contents

ACKNOWLEDGEMENTS ..... **V**

TABLE OF CONTENTS ..... **XI**

LIST OF FIGURES ..... **XV**

LIST OF TABLES ..... **XVI**

LIST OF ABBREVIATIONS ..... **XVII**

ABSTRACT ..... **- 1 -**

INTRODUCTION ..... **- 3 -**

1.1 OVERVIEW ..... **- 4 -**

1.2 PREECLAMPSIA ..... **- 5 -**

1.2.1 Definition and classification ..... - 5 -

1.2.2 Disease burden ..... - 7 -

1.3 CLINICAL APPROACHES TO PREECLAMPSIA ..... **- 8 -**

1.3.1 Prediction ..... - 8 -

1.3.2 Prevention ..... - 12 -

1.3.3 Diagnosis ..... - 13 -

1.3.4 Management ..... - 13 -

1.3.4.1 Place of care ..... *- 14 -*

1.3.4.2 Regular monitoring ..... *- 14 -*

1.3.4.3 Pharmacotherapy ..... *- 15 -*

1.3.4.4 Timed delivery ..... *- 22 -*

1.3.5 Long-term complications ..... - 22 -

1.4 PATHOPHYSIOLOGY OF PREECLAMPSIA ..... **- 24 -**

1.4.1 Overview ..... - 24 -

1.4.2 Placental origins of preeclampsia ..... - 24 -

1.4.3 Placental stress to maternal syndrome of preeclampsia ..... - 25 -

1.5 SYNCYTIOTROPHOBLAST-DERIVED EXTRACELLULAR VESICLES ..... **- 27 -**

1.5.1 Classification of syncytiotrophoblast-derived extracellular vesicles ..... - 27 -

1.5.2 Biogenesis of syncytiotrophoblast-derived extracellular vesicles ..... - 28 -

1.5.2.1 Biogenesis of small syncytiotrophoblast-derived extracellular vesicles ..... *- 28 -*

1.5.2.2 Biogenesis of medium/large syncytiotrophoblast-derived extracellular vesicles ..... *- 30 -*

1.5.3 Preferential sorting of cargo into syncytiotrophoblast-derived extracellular vesicles ..... - 30 -

1.5.4 Cellular entry mechanisms of syncytiotrophoblast-derived extracellular vesicles ..... - 32 -

1.5.5 Role of syncytiotrophoblast-derived extracellular vesicles in preeclampsia ..... - 35 -

1.5.6 Diagnostic potential of syncytiotrophoblast-derived extracellular vesicles ..... - 36 -

1.6 CONCLUSION ..... - 37 -
1.7 AIMS ..... - 38 -
MATERIALS AND METHODS ..... - 39 -
2.1 GENERAL METHODS ..... - 40 -
2.1.1 Human participants ..... - 40 -
2.1.2 Introduction and clarification of nomenclatures used in the thesis ..... - 41 -
2.1.3 Isolation and enrichment of STB-EVs by placental *ex vivo* dual lobe perfusion ..... - 42 -
2.1.4 Characterisation of STB-EVs isolated by placental ex-vivo dual lobe perfusion ..... - 48 -
2.1.4.1 Transmission electron microscopy ..... - 48 -
2.1.4.2 Flow cytometry ..... - 49 -
2.1.4.3 Nanoparticle tracking analysis ..... - 53 -
2.1.4.4 Western blot analysis ..... - 54 -
2.1.4.5 Bicinchoninic acid (BCA) protein assay ..... - 57 -
2.2 SPECIFIC METHODS ..... - 61 -
2.2.1 Immunohistochemistry ..... - 61 -
2.2.2 Capillary electrophoresis and western blot analysis using Jess ..... - 63 -
2.2.3 Gas chromatography mass spectrometry ..... - 64 -
2.2.4 Methods for validation of selected miRNA with quantitative polymerase chain reaction (qPCR) ... - 67 -
2.2.4.1 RNA extraction from STB-EVs ..... - 67 -
2.2.4.2 RNA extraction from serum EVs ..... - 68 -
2.2.4.3 Complimentary DNA synthesis for miRNA synthesis ..... - 69 -
2.2.4.4 Quantitative polymerase chain reaction (qPCR) ..... - 71 -
2.2.5 Cell culture: human cerebral microvascular endothelial cells (hCMEC/D3) ..... - 75 -
2.2.6 Cell proliferation and viability assay ..... - 76 -
2.2.7 Cell migration assay ..... - 78 -
2.2.8 Identification of angiogenesis-related protein expression using human angiogenesis array kit. - 79 -
2.2.9 Protein-protein interaction network construction and cluster analysis ..... - 81 -
2.2.10 VCAM-1 expression analysis following TNF-α stimulation ..... - 81 -
ISOLATION, ENRICHMENT AND CHARACTERIZATION OF SYNCYTIOTROPHOBLAST-DERIVED EXTRACELLULAR VESICLES ..... - 84 -
ABSTRACT ..... - 85 -
3.1 INTRODUCTION ..... - 86 -
3.2 AIMS ..... - 88 -
3.3 METHODS OF ISOLATION AND ENRICHMENT FOR PLACENTAL EVS ..... - 89 -
3.3.1 Methods for isolation and enrichment of EVs ..... - 89 -
3.3.2 Isolation and enrichment of trophoblast derived EVs ..... - 92 -
3.3.2.1 Mechanical STB-EV isolation ..... - 92 -
3.3.2.2 In vitro explant culture-derived STB-EVs ..... - 93 -

3.3.2.3 Ex vivo placental perfusion derived STB-EVs - 96 -
3.3.2.4 Cultured human choriocarcinoma-derived cell line (BeWo) derived EVs - 97 -
3.3.2.5 Cultured trophoblast derived cell line derived EVs - 97 -
3.3.2.6 Cytotrophoblast derived EVs - 98 -
3.4 METHODS - 99 -
3.5 RESULTS - 100 -
3.5.1 Patient demographics and clinical characteristics - 100 -
3.5.2 Characterisation of syncytiotrophoblast-derived extracellular vesicles - 100 -
3.5.2.1 Transmission electron microscopy - 100 -
3.5.2.2 Nanoparticle tracking analysis - 101 -
3.5.2.3 Western blotting - 101 -
3.5.2.4 Flow cytometry - 101 -
3.6 DISCUSSION - 106 -
3.7 CONCLUSION - 112 -
3.8 NEXT STEPS - 112 -
SYNCYTIOTROPHOBLAST-DERIVED EXTRACELLULAR VESICLES CARRY FUNCTIONAL KYNURENINE METABOLIZING ENZYMES - 113 -
ABSTRACT - 114 -
4.1 INTRODUCTION - 116 -
4.1.1 The kynurenine pathway - 117 -
4.1.4 Kynurenine in pregnancy - 120 -
4.2 AIMS - 122 -
4.3 METHODS - 122 -
4.4 RESULTS - 123 -
4.4.1 Transcriptomic analysis of placental lysate and STB-EVs shows expression of KYNME - 123 -
4.4.2 Demographics and clinical characteristics - 123 -
4.4.3 Syncytiotrophoblast layer is selectively enriched for KYNME - 126 -
4.4.4 Placental lysates express KYNME - 126 -
4.4.5 Identification of KYNME expression in STB-EVs - 126 -
4.4.6 Functional Assessment of KYNME in STB-EVs - 129 -
4.5 DISCUSSION - 133 -
4.6 CONCLUSION - 138 -
4.7 FUTURE DIRECTION - 138 -
MEDIUM/LARGE SYNCYTIOTROPHOBLAST-DERIVED EXTRACELLULAR VESICLES CARRY ANTI-ANGIOGENIC MICRO RNA IN EARLY-ONSET PREECLAMPSIA - 140 -
ABSTRACT - 141 -

5.1 INTRODUCTION ..... - 143 -
5.1.1 Differentially expressed miRNAs in preeclamptic m/l STB-EVs ..... - 145 -
5.1.2 Angiogenesis ..... - 147 -
5.1.3 Endothelial dysfunction in preeclampsia ..... - 149 -
5.1.4 Cerebral circulation in preeclampsia ..... - 149 -
5.2 AIMS ..... - 151 -
5.3 METHODS ..... - 151 -
5.4 RESULTS ..... - 152 -
5.4.1 Patient characteristics of the m/lSTB-EV samples used for validation ..... - 152 -
5.4.2 qPCR validation of selected miRNA targets on m/lSTB-EVs ..... - 152 -
5.4.3 Patient characteristics of the serum extracellular vesicles used for validation ..... - 157 -
5.4.4 qPCR validation of *hsa-miR-9-5p* on serum EV samples ..... - 157 -
5.4.5 *hsa-miR-9-5p* attenuates hCMEC/D3 proliferation ..... - 160 -
5.4.6 *hsa-miR-9-5p* attenuates hCMEC/D3 migration ..... - 162 -
5.4.7 *hsa-miR-9-5p* alters the angiogenic-protein profile of hCMEC/D3 ..... - 165 -
5.4.8 Protein-protein interaction network and functional enrichment of differentially expressed angiogenesis-related proteins ..... - 165 -
5.4.9 miR-9-5p does not affect the ability of hCMEC/D3's response to TNF-α stimuli ..... - 174 -
5.5 DISCUSSION ..... - 176 -
5.6 CONCLUSION ..... - 183 -
5.7 FUTURE DIRECTION ..... - 183 -
PREDICTIVE VALUE OF SFLT-1:PLGF RATIO IN WOMEN WITH SUSPECTED PREECLAMPSIA IN SRI LANKA – CLINICAL TRIAL ..... - 185 -
6.1 INTRODUCTION ..... - 186 -
6.2 STUDY PROTOCOL ..... - 188 -
6.3 TRIAL PROGRESS ..... - 223 -
SUMMARY AND FUTURE DIRECTION ..... - 227 -
7.1 SUMMARY ..... - 228 -
7.2 FUTURE WORK ..... - 232 -
LIST OF PUBLICATIONS ..... - 235 -
8.1 PUBLISHED PAPERS ..... - 235 -
8.2 SUBMITTED MANUSCRIPTS (UNDER REVIEW) ..... - 236 -
8.3 ABSTRACTS ..... - 237 -
REFERENCES ..... - 239 -

List of figures

Figure 1 - Algorithm for antihypertensive therapy ..... - 16 -
Figure 2 - Two-stage theory of PE ..... - 26 -
Figure 3 - Biogenesis of extracellular vesicles ..... - 31 -
Figure 4 – Cellular entry mechanisms of extracellular vesicles ..... - 34 -
Figure 5 - Illustration of *ex vivo* dual lobe placental perfusion setup ..... - 45 -
Figure 6 - Illustration of differential ultracentrifugation process ..... - 47 -
Figure 7 – Schematic representation for isolating STB-EVs from placental explants ..... - 95 -
Figure 8 – STB-EV characterisation. ..... - 104 -
Figure 9 – Representative flow cytometry data of 10K STB-EV pellet. ..... - 105 -
Figure 10 - The kynurenine pathway of tryptophan degradation ..... - 118 -
Figure 11 - Normalized counts of mRNAs coding for KYNME expressed in placental tissue and STB-EVs ..... - 125 -
Figure 12 - KYNME expression on placental tissue ..... - 127 -
Figure 13 - KYNMEs are expressed by STB-EVs ..... - 128 -
Figure 14 - 2D/3D GC-MS representation of kynurenine ..... - 130 -
Figure 15 - STB-EVs isolated from normal pregnancy break down kynurenine ..... - 131 -
Figure 16 - Serum kynurenine levels in normal and preeclamptic pregnancies ..... - 132 -
Figure 17 - Multiple functions of endothelial cells ..... - 148 -
Figure 18 - RNA Sequencing and qPCR data of selected miRNA targets ..... - 156 -
Figure 19 - Log fold changes for *hsa-miR-9-5p* in m/lSTB-EVs and serum EVs ..... - 159 -
Figure 20 - miR-9-5p attenuates microvascular endothelial cell proliferation ..... - 161 -
Figure 21 - Optimization experiments for wound healing assay ..... - 163 -
Figure 22 - miR-9-5p attenuates hCMEC/D3 cell migration ..... - 164 -
Figure 23 - Altered angiogenesis-related protein profile of hCMEC/D3 ..... - 167 -
Figure 24 – PPI network of differentially expressed angiogenesis-related proteins ..... - 169 -
Figure 25 - Regulators of endothelial cell proliferation ..... - 170 -
Figure 26 - Regulators of endothelial cell migration ..... - 171 -
Figure 27 - VCAM-1 expression in cell culture supernatants ..... - 175 -
Figure 28 - Ethics approval for the clinical trial in Sri Lanka ..... - 226 -

List of tables

Table 1 - Clinical risk factors of preeclampsia ..... - 10 -
Table 2 - Clinical risk assessment for preeclampsia ..... - 11 -
Table 3 - First line antihypertensive medications for non-severe hypertension in pregnancy - 17 -
Table 4 - Antihypertensive medications for severe hypertension ..... - 19 -
Table 5 - Dosing regimen for magnesium sulfate ..... - 20 -
Table 6 - Monitoring guidelines while administering magnesium sulfate ..... - 21 -
Table 7 - Indications for delivery with preeclampsia at any gestational age ..... - 23 -
Table 8 - Instrument parameters for the BD Bioscience's LSR II flow cytometer ..... - 52 -
Table 9 - Reagents used for western blot ..... - 59 -
Table 10 - Antibodies used in western blot ..... - 60 -
Table 11 - qPCR primers, miRNA sequence and assay ID ..... - 74 -
Table 12 - Summary of EV isolation techniques ..... - 90 -
Table 13 - Demographic and clinical characteristics ..... - 102 -
Table 14 - Mean sizes of the 10K and 150K STB-EV pellets ..... - 103 -
Table 15 - Demographic and clinical characteristics ..... - 124 -
Table 16 - List of upregulated miRNAs in m/lSTB-EVs ..... - 146 -
Table 17 - Patient characteristics of m/lSTB-EV samples ..... - 154 -
Table 18 - Log fold change and log fold standard error of selected miRNAs ..... - 155 -
Table 19 - Patient characteristics of serum samples ..... - 158 -
Table 20 - Log fold changes of differentially expressed angiogenesis-related proteins in hCMEC/D3 treated with miR-9-5p (10 nM) ..... - 168 -
Table 21 - Gene ontology terms (biological processes) associated with established PPI network ..... - 172 -
Table 22 - KEGG pathways associated with established PPI network ..... - 173 -

LIST OF ABBREVIATIONS

ACEI – angiotensin converting enzyme inhibitors

AGE-RAGE – advanced glycation end products-receptors for advanced glycation end products

AGO2 – argonaute 2

Ahr – aryl hydrocarbon receptor

AHT – antihypertensive medication

AKI – acute kidney injury

ALIX – ALG-2-interacting protein X

ALT – alanine transaminase

ANGPT2 – angiopoietin 2

APLS – antiphospholipid syndrome

APOA1 – apolipoprotein A1

APOA2 – apolipoprotein A2

ARB – angiotensin receptor blockers

ASA – acetyl salicylic acid

AST – aspartate transaminase

ATCC – American Type Culture Collection

BBB – blood brain barrier

BCA – bicinchoninic acid

BMI – body mass index

BP – blood pressure

BSA – bovine serum albumin

C/I – contraindicated

$CaCl_2$ – calcium chloride

cDNA – complementary deoxyribonucleic acid

cGMP –guanosine 3’-5’-cyclic monophosphate

CHMP4 – charged multivesicular body protein 4a

CI – confidence interval

CNS – central nervous system

CS – antenatal corticosteroids

Ct – cycle threshold

CTB – cytotrophoblast

CTG – cardiotocography

Cu^{+} – cuprous ions

Cu^{2+} – cupric ions

CXCL16 – C-X-C motif chemokine ligand 16

CXCL8 – C-X-C motif chemokine ligand 8 (interleukin 8)

CXCR4 – C-X-C motif chemokine receptor 4

Cyt. C – cytochrome C

DBP – diastolic blood pressure

ddH_2O – double distilled water

DEMs – differentially expressed miRNAs

DEPs – differentially expressed proteins

DIC – disseminated intravascular coagulation

dL – decilitre

DMEM – Dulbecco's modified Eagle's medium

DNA – deoxyribonucleic acid

DPPIV – dipeptidyl peptidase-4

dUC – differential ultracentrifugation

ECM – extracellular matrix

EGF – endothelial growth factor

EGFR – endothelial growth factor receptor

EGM-2 – endothelial growth medium 2

EI – electron ionization

ELISA – enzyme-linked immunosorbent assay

EM – electron microscopy

eNOS – endothelial nitric oxide synthase

EOPE – early-onset preeclampsia

ERCC – External RNA Control Consortium

ESCRT – endosomal complex required for transport

eSTB-EVs – explant culture derived STB-EVs

EVs – extracellular vesicles

FBS – foetal bovine serum

FC – fold change

FCS – foetal calf serum

FDR – false discovery rate

Fe^{2+} – ferrous ions

Fe^{3+} – ferric ions

FGF2 – fibroblast growth factor 2

FLT1 – fms-like tyrosine kinase 1

FLT4 – fms-like tyrosine kinase 4

FMF – Fetal Medicine Forum

FMO-1 – Fluorescence minus one

fPBS – filtered phosphate-buffered saline

g – gram

GC – gas chromatography

GCxGC-MS – gas chromatography coupled with tandem mass spectrometry

GDM – gestational diabetes mellitus

Gest. age – gestational age

GPI – glycosylphosphatidylinositol

GTP – guanosine triphosphate

H_2O_2 – hydrogen peroxide

HBSS – Hanks balanced salt solution

hCMEC/D3 – human cerebral microvascular endothelial cells

HEPES – 4-(2-Hydroxyethyl)piperazine-1-ethane-sulfonic acid

HIF-1 – hypoxia inducible factor 1

HIF-1α – hypoxia inducible factor 1α

HLA – human leukocyte antigen

HRP – horseradish peroxidase

HSP70 – heat shock (70kDa) protein

ht. – height

HUVECs – human umbilical vein endothelial cells

IDO – indoleamine 2,3-diooxygenase

IDO1 – indoleamine 2,3-diooxygenase 1

IDO2 – indoleamine 2,3-diooxygenase 2

IFN-γ – interferon γ

IGFBP3 – insulin-like growth factor binding protein 3

IHC – immunohistochemistry

IL – interleukins

ILVs – intraluminal vesicles

IM – intramuscular

INHBA – activin A

INR – international normalized ratio

IPA – isopropanol

ISEV – International Society for Extracellular Vesicles

ISSHP – International Society for the Study of Hypertension

IU – international units

IUGR – intrauterine growth restriction

IV – intravenous

JAK-STAT – Janus kinase-signal transducers and activators of transcription

K:T ratio – kynurenine:tryptophan ratio

KAT-III – Kynurenine aminotransferase III

KDR – kinase insert domain receptor

KEGG – Kyoto Encyclopaedia of Genes and Genomes

KMO – Kynurenine monooxygenase

Kyn – kynurenine

KYNME – kynurenine metabolising enzymes

KYNU – Kynureninase

L – litre

LA – long acting

LBW – low birthweight

LEP – leptin

LFC – log_2 fold change

LOPE – late-onset preeclampsia

LSE – log standard error

m/lEVs – medium/large extracellular vesicles

m/lSTB-EVs – medium/large syncytiotrophoblast-derived extracellular vesicles

MAPK – mitogen-activated protein kinase

MEM – modified Eagle's medium

mg – milligram

$MgSO_4$ – magnesium sulfate

miRNA – microRNA

MISEV – Minimal Information for Studies of Extracellular Vesicles

mmHg – millimeter mercury

mmol – millimole

MMP9 – matrix metalloproteinase-9

MR – modified release

mRNAs – messenger RNAs

MS – mass spectrometry

MSTFA – methyl-N-(trimethylsilyl)trifluoroacetamide

MVBs – multivesicular bodies

MW – molecular weight

NaCl – sodium chloride

NDWRH – Nuffield Department for Women's and Reproductive Health

NF-κB – nuclear factor kappa B

NK cells – natural killer cells

nm – nano meter

NO – nitric oxide

NP – normal pregnancies

NPV – negative predictive value

NS – normal saline

NTA – nanoparticle tracking analysis

OR – odds ratio

PA – prolonged acting

PBS – phosphate-buffered saline

PDGFA – platelet derived growth factor-AA

PDGFB – platelet derived growth factor-BB

PE – preeclampsia

PEG – polyethylene glycol

PF4 – platelet factor 4

PFA – paraformaldehyde

PGF – placental growth factor

pH – power of hydrogen

PI3Ks – phosphoinositide 3-kinases

PIERS – Preeclampsia Integrated Estimate of Risk

PIGF – placental growth factor

PKG – protein kinase G

PLAP – placental alkaline phosphatase

PLG – plasminogen

PMT – photomultiplier tube

PPARγ – peroxisome proliferator-activated receptor γ

PPI – protein-protein interaction

PrCr – protein-to-creatinine ratio

PRES – posterior reversible encephalopathy syndrome

PRL – prolactin

PVDF – polyvinylidene difluoride

QC – quality control

qPCR – quantitative polymerase chain reaction

R^2 – radii squared

RBC – red blood cell

RCF – relative centrifugal force

REA – recombinant engineered antibodies

RNA – ribonucleic acid

RNA Seq – ribonucleic acid sequencing

RPM – revolutions per minute

RPS – resistive pulse sensing

RR – relative risk

SBP – systolic blood pressure

SDS – sodium dodecyl sulphate

SDS-PAGE – sodium dodecyl sulphate-polyacrylamide gel electrophoresis

SEM – standard error of mean

sEng – soluble endoglin

SERPINB5 – serpin B5

sEVs – small extracellular vesicles

sFlt-1 – soluble fms-like tyrosine kinase-1

sFLT-1:PlGF ratio - soluble fms-like tyrosine kinase-1:placental growth factor ratio

SGA – small for gestational age

SIGLEC6 – sialic acid binding immunoglobulin-like lectin 6

SLE – systemic lupus erythematous

SSC – side scatter

sSTB-EVs – small syncytiotrophoblast-derived extracellular vesicles

STB – syncytiotrophoblast

STB-EVs – syncytiotrophoblast-derived extracellular vesicles

STRING – Search Tool for the Retrieval of Interacting Genes

TBST – tris-buffered saline

TDO – tryptophan 2,3-dioxygenase

TEK – TEK tyrosine kinase (angiopoietin-1 receptor)

TEM – transmission electron microscopy

TFA – trifluoracetic acid

TGF-β – transforming growth factor β

TGFB1 – transforming growth factor β1

THBS1 – thrombospondin 1

THBS2 – thrombospondin 2

TLR – Toll-like receptor

TMCS – chlorotrimethylsilane

TNF-α – tumour necrosis factor-α

tRNA – transfer ribonucleic acid

Trp – tryptophan

TSG – tumour suppressor gene

TSG101 – tumour susceptibility gene-101

UK – United Kingdom

USA – United States of America

VASH1 – vasohibin 1

VCAM-1 – vascular cell adhesion molecule 1

VEGF – vascular endothelial growth factor

VEGFA – vascular endothelial growth factor A

VEGFC – vascular endothelial growth factor C

VEGFR2 – vascular endothelial growth factor receptor 2

WBC – white blood cell

WCHG – Welcome Centre for Human Genetics

wt. – weight

XL – extended release

y – years

ε-ACA – ε-aminohexanoic acid

μg – microgram

μL – microlitre

μmol – micromole

ABSTRACT

TITLE: **INVESTIGATING THE ROLE OF SYNCYTIOTROPHOBLAST-DERIVED EXTRACELLULAR VESICLES IN THE PATHOGENESIS OF PREECLAMPSIA**

NAME: Dr Prassana Varun Logenthiran

COLLEGE: Linacre College

DEGREE: D.Phil. in Women's and Reproductive Health

TERM: Trinity Term

YEAR: 2024

Introduction: Preeclampsia (PE), a multi-systemic disorder of pregnancy affecting 2-8% of women globally, is one of the leading causes of maternal and neonatal morbidity and mortality. PE is diagnosed by *de novo* hypertension and end-organ damage. Although precise mechanisms are not fully elucidated, placenta is involved in the pathogenesis. Syncytiotrophoblast-derived extracellular vesicles (STB-EVs), which are membrane-bound biomolecules ranging between 30 – 1000 nm in size are gaining attention due to their diagnostic potential and their role in pathogenesis of PE. This thesis explores the roles of STB-EVs in pregnancy, focusing on the effects of their cargo (proteins and miRNA) on altering maternal physiology in PE and their potential to serve as non-invasive biomarkers. This research aimed to establish reliable protocols for isolating STB-EVs and to investigate their protein and genetic cargo, particularly focusing on kynurenine metabolising enzymes (KYNMEs) and microRNAs (miRNAs) relevant to preeclampsia.

Aims: The study's objectives included isolating and characterizing STB-EVs, analysing their protein (kynurenine metabolising enzymes, KYNME) and genetic cargo (*hsa-miR-9-5p*), and exploring their functional implications PE.

Methods: STB-EVs were isolated and enriched using *ex vivo* dual lobe placental perfusion and differential ultracentrifugation. Characterisation involved nanoparticle tracking analysis, western blotting, transmission electron microscopy, and flow cytometry. The protein cargo, particularly KYNMEs and their functionality, were analysed using immunohistochemistry, capillary electrophoresis and western blotting, and gas chromatography-mass spectrometry. Differentially expressed microRNAs were validated using quantitative polymerase chain reaction and their functional impacts were assessed *in vitro* on cerebral microvascular endothelial cells via assays for cell proliferation, viability and migration.

Results: The isolation protocol successfully enriched STB-EVs. STB-EVs from normal and PE pregnancies contained KYNMEs with no significant differences between the two groups. Serum kynurenine levels were significantly lower in preeclamptic pregnancies. KYNMEs on STB-EVs demonstrated a dose-dependent attenuation of kynurenine levels *in vitro*. Additionally, differentially expressed miRNAs were validated, with *hsa-miR-9-5p* identified as a key target over-expressed in medium/large STB-EVs and serum EVs in preeclampsia. miR-9-5p attenuated cell proliferation and migration and altered the expression of angiogenesis-related proteins in cerebral microvascular endothelial cells.

Conclusion: This thesis for the first time highlights the potential role of STB-EVs in kynurenine pathway and describes the anti-angiogenic effect of *hsa-miR-9-5p* on cerebral microvascular endothelial cells. The findings suggest that STB-EVs could be critical in regulating vascular and angiogenic responses in preeclampsia, providing a foundation for further understanding of the pathogenesis and future diagnostic strategies.

CHAPTER 1

INTRODUCTION

1.1 Overview

Preeclampsia (PE) is a complex hypertensive disorder of pregnancy, arises due to placental dysfunction. A stressed placenta initiates a cascade of events by releasing soluble factors and placental-derived extracellular vesicles into the maternal circulation. These factors serve as messengers that trigger endothelial dysfunction, vasospasm, and immune activation in susceptible individuals, creating a vicious cycle of inflammation, ultimately leading to hypoperfusion and end-organ dysfunction. The culmination of these processes manifests as the maternal syndrome of PE, a condition with significant morbidity and mortality risks for both mother and foetus.

Preeclampsia remains a significant obstetrical challenge due to several key limitations. Firstly, despite ongoing efforts, early and reliable screening for PE remains elusive. This is partly due to the complex and multifaceted nature of the disease, with no single definitive biomarker currently available. As a result, many cases of PE are diagnosed only after the onset of clinical symptoms, potentially limiting timely intervention. Secondly, a comprehensive understanding of the underlying pathophysiology of PE is still lacking. While placental dysfunction is recognized as a central factor, the specific mechanisms by which a stressed placenta triggers the cascade of events leading to PE are not fully elucidated. This incomplete knowledge hinders the development of targeted therapies aimed at addressing the root causes of the disease. Finally, the only definitive treatment for established PE is delivery of the placenta, a strategy that inevitably leads to prematurity and its associated complications for the foetus. The lack of effective therapeutic options beyond delivery underscores the critical need for alternative treatment approaches.

These limitations collectively compel researchers to delve deeper into the role of placental-derived factors in PE pathogenesis. Investigating the mechanisms by which these factors contribute to the disease may offer valuable insights for the development of novel diagnostic tools and therapeutic strategies. By unravelling the communication between stressed placenta and the maternal systems, we aimed to identify potential targets for intervention, ultimately leading to improved outcomes for both mothers and foetuses affected by PE.

1.2 Preeclampsia

1.2.1 Definition and classification

The International Society for the Study of Hypertensive Disorders of Pregnancy (ISSHP) outlines the clinical definition of preeclampsia (PE)[1,2]. Diagnosis hinges on *de novo* hypertension accompanied by one or more of the following conditions at ≥ 20 weeks' gestation:

- Proteinuria
- Other maternal end-organ dysfunction
- Uteroplacental dysfunction

Hypertension is defined as a systolic blood pressure (SBP) exceeding 140 mmHg or a diastolic blood pressure (DBP) exceeding 90 mmHg based on an average of at least two measurements. In addition to hypertension, the presence of at least one of the following criteria is required for a PE diagnosis:

Proteinuria: The urine protein-to-creatinine ratio (PrCr) measured in a spot (random) urine sample exceeding ≥ 30 mg/mmol (in the absence of a urinary tract infection)[3,4]; or albumin-to-creatinine ratio (ACR) ≥ 8 mg/mmol[5]; or urine protein ≥ 0.3 g/day in a complete 24-hour urine collection; or ≥ 2+ by urinary dipstick (if confirmatory testing is not available)[6,7].

Other maternal end-organ dysfunction, including:

- **Neurological complications** (e.g., eclampsia, altered mental status, blindness, stroke, clonus)
- **Pulmonary oedema**
- **Haematological complications** (e.g., platelet count < 150,000 / μL, disseminated intravascular coagulation, haemolysis)
- **Acute kidney injury (AKI)** (serum creatinine ≥ 90 μmol/L or 1 mg/dL)
- **Liver involvement** (e.g., elevated transaminases; ALT or AST > 40 IU/L, with or without right upper quadrant or epigastric abdominal pain)

Uteroplacental dysfunction

- Placental abruption
- Angiogenic imbalance
- Fetal growth restriction
- Abnormal umbilical artery Doppler waveform analysis
- Intrauterine foetal death

Classification of PE into placental and maternal categories[8], as well as into early-onset PE (EOPE), diagnosed before 34 weeks of gestation, and late-onset PE (LOPE), diagnosed after 34 weeks[9], are commonly utilized. The placental and maternal subtypes correspond to EOPE and LOPE, respectively, and are believed to exhibit distinct etiopathogenesis and clinical manifestations. Another classification system divides PE into three categories: early-onset PE (< 34 weeks), intermediate-onset PE (34-36 weeks), and late-onset PE (> 36 weeks)[10]. Additionally, PE can be categorized into preterm PE (< 37 weeks) and term PE (> 37 weeks)[11].

The traditional categorization of PE into non-severe and severe stages has become less applicable in recent years. This shift is due, in part, to the potential for rapid deterioration of disease without warning and the inherent high-risk nature of PE for all affected women[1,2]. However, blood pressure severity remains a relevant clinical indicator, with classifications including mild (140/90 – 149/99 mmHg), moderate (150/100 – 159/109 mmHg), and severe (≥160/110 mmHg)[12].

1.2.2 Disease burden

Preeclampsia is a significant global health concern, with a prevalence ranging from 2% to 8%[1,13], particularly affecting low- and middle-income countries posing short- and long-term adverse morbidity and mortality risks to both the mother and the foetus[14–16]. Hypertensive disorders in pregnancy are estimated to cause approximately 30,000 maternal deaths and 500,000 perinatal deaths annually[17]. In the United Kingdom, nulliparous women have the highest incidence of PE, with approximately 4.9% affected[18]. Maternal complications due to PE include acute respiratory distress syndrome, seizures, and cerebrovascular accidents, while long-term effects include persistent endothelial dysfunction, cardiovascular changes, and increased risk of renal disease, diabetes, and cardiovascular events[19–21]. Among offspring, PE increases the risk of growth restriction and perinatal mortality. Delivery of the placenta remains the only cure for PE, and thus results in iatrogenic prematurity, contributing to neonatal morbidity and long-term health risks, including metabolic and cardiovascular diseases[22,23].

1.3 Clinical approaches to preeclampsia

1.3.1 Prediction

Historically two approaches have been commonly adopted to identify women at increased risk for PE and who could potentially benefit from preventive interventions. A traditional count of clinical risk factors and more recent multivariate modelling of clinical, ultrasonographic, and laboratory assessment of uteroplacental perfusion and function are used for risk stratification.

Traditional screening for risk of preeclampsia is advocated by most of the established clinical practice guidelines[24]. Large-scale epidemiological studies have identified clinical risk factors (Table 1) that are independently assessed and summarized as a count of any factor that confers high risk or one or more factors that confer a moderate risk (summarized in Table 2)[25]. Even though this approach is simple, the sensitivity is low for both early-onset PE (~40%) and late-onset PE (~35%) with a screen-positive rate of approximately 10%[26].

On the other hand, competing-risk model of the Fetal Medicine Forum (FMF), one of the widely used multivariable model supported by the largest body of evidence, uses components most used in other models (i.e., maternal ethnic/racial background, BMI, blood pressure, ultrasonographic assessment of uterine artery pulsatility index, and angiogenic markers)[27]. These multivariable models have higher detection rates when used at 11 – 13 weeks' gestation for EOPE and at 35 – 36 weeks' gestation for term PE, with a positive screening rate of 10%[27].

More recently the placental derived soluble factors; placental growth factor (PlGF) and soluble fms-like tyrosine kinase-1 (sFlt-1) have gained more attraction as potential biomarkers for early screening for PE. Several studies have shown that both sFlt-1 and PlGF are altered in the

maternal plasma/serum in women with PE prior to the onset of disease[28–32]. In PE, circulating levels of serum sFlt-1 are elevated and PlGF are decreased[33,34]. A higher ratio of sFlt-1:PlGF is shown to be associated with increased risk of PE and considered a better predictor of PE risk than either biomarker alone[34–39]. An sFlt-1:PlGF ratio ≤ 38 has negative predictive value of 99.3% (95% CI: 97.9 – 99.9) with 80% sensitivity (95% CI: 51.9 – 95.7) and 78.3% specificity (95% CI: 74.6 – 81.7) for excluding PE in the subsequent week in women whom PE was suspected[40]. Ratio > 85 in pregnant women (< 34 weeks) had a sensitivity of 88.0% (95% CI: 81.3 – 100.0); specificity of 99.5% (95% CI: 97.7 – 100.0) and positive likelihood ratio (LR) of 176 (95% CI: 24.88 – 1245) to detect PE[41].

Table 1 - Clinical risk factors of preeclampsia

Risk factor	Mean RR/OR	95% CI
Antiphospholipid syndrome[42]	9.72	4.34 – 21.75
Previous history of PE[42,43]	7.19	5.85 – 8.83
Insulin dependent diabetes mellitus[42]	3.56	2.54 – 4.99
Multifoetal gestation[42]	2.93	2.04 – 4.21
Nulliparity[42]	2.91	1.28 – 6.61
Family history of PE[42]	2.90	1.70 – 4.93
Obesity[42]	2.47	1.66 – 3.67
Father is a product of PE pregnancy[44]	2.10	1.00 – 4.30
Age > 40 years[42]	1.96	1.34 – 2.87
Pregnancy with a male who has fathered a PE pregnancy who begins a new relationship[45]	1.80	1.20 – 2.60
Donor insemination[46]	1.60	1.40 – 1.80
Chronic hypertension[42]	1.38	1.01 – 1.87

OR – odds ratio; RR – relative risk; CI – confidence interval

Table 2 - Clinical risk assessment for preeclampsia

Risk level	Risk factors
High[a]	• History of preeclampsia • Multifoetal gestation • Chronic hypertension • Pregestational type 1 or 2 diabetes mellitus • Renal disease • Autoimmune disease (SLE, APLS)
Moderate[b]	• Nulliparity • Obesity • Family history of PE • Lower income[*] • Age > 35 • Personal history of LBW or SGA or previous adverse pregnancy outcome or > 10-year pregnancy interval • In vitro conception

[a] Includes single risk factors that are consistently associated with greatest risk for PE. Incidence of PE is likely to be at least 8% in a population of pregnant women having 1 of these risk factors.

[b] Factors independently associated with moderate risk of PE. Combination of multiple moderate-risk factors place a pregnant woman at higher risk for PE.

[*] Associated with increased risk due to environmental, social, and historical inequalities shaping health exposures, access to health care, and unequal distribution of resources, not biological predispositions.

SLE – systemic lupus erythematous; APLS – antiphospholipid syndrome; LBW – low birth weight; SGA; small for gestational age

1.3.2 Prevention

As delivery of the placenta remains the only proven method to resolve preeclampsia, its prevention becomes a critical focus in healthcare. Preventive strategies for PE have focused on targeting key pathways implicated in the disease process, including angiogenic imbalance, endothelial activation, oxidative stress, vasoconstriction, and systemic inflammation.

Acetyl salicylic acid (ASA, *aspirin*) is shown to reduce the risk of PE in a dose dependent manner (RR, 0.82; 95% CI, 0.77 – 0.88) in addition to lowering the incidence of serious maternal complications, preterm birth, delivery of small for gestational age neonates, and foetal and neonatal mortality[47]. The ASPRE trial demonstrated a significant reduction in the incidence of preeclampsia (PE) in women identified as high-risk. Daily low-dose aspirin (150 mg) administered between 11 and 13 weeks of gestation resulted in a 60% reduction in PE compared to the placebo group (OR, 0.38; 95% CI, 0.20-0.74)[48]. Moderate-intensity exercise (brisk walking, water aerobics, stationary cycling with moderate effort, resistance training, and household chores such as washing windows or gardening) for more than 140 minutes per week reduced the risk of PE (OR, 0.59; 95% CI, 0.37 – 0.90)[49]. Regardless of the time of initiation during pregnancy, calcium supplementation (500 – 1000 mg per day) reduced the risk of PE (RR, 0.49; 95% CI, 0.39 – 0.61)[50,51]. The effect of calcium supplementation had greatest benefit in women who consumed low calcium diet (RR, 0.36; 95 % CI, 0.20 – 0.65); and who were at high risk of developing PE (RR, 0.22; 95 % CI, 0.12 – 0.42)[52]. Use of pravastatin (20 mg per day)[53] or folic acid (4 mg per day)[54] did not prevent preeclampsia. Efficacy of low-molecular weight heparin in preventing PE remains uncertain[55] and newer candidates (e.g., metformin) are being considered for which safety in pregnancy has been well established[56,57].

1.3.3 Diagnosis

For women identified as high-risk for PE based on multivariable or clinical risk factor screening in early pregnancy, pragmatic approaches may improve the early diagnosis of the clinical syndrome. These approaches include increased frequency of antenatal care visits, maternal self-monitoring of blood pressure, frequent maternal laboratory testing for end-organ involvement (thrombocytopenia, elevated creatinine, or aminotransferase levels, or angiogenic imbalance), and third-trimester foetal assessment using ultrasound to monitor growth or Doppler velocimetry to assess blood flow in the umbilical and middle cerebral arteries. Timely diagnosis allows the clinicians to identify the women at risk for adverse pregnancy outcomes and determine the best course of management. The diagnosis of preeclampsia is based on the definition proposed by ISSHP that includes *de novo* hypertension with evidence of one of the following presenting after 20 weeks of gestation: proteinuria, or other maternal end-organ dysfunction, or uteroplacental dysfunction[2]. Women who develop PE before 34 weeks (EOPE) are more prone to have end-organ involvement, foetal growth restriction, and haemodynamic profile of low cardiac output and increased total peripheral resistance compared to women who develop LOPE[58]. This emphasizes the importance of timing of the diagnosis.

1.3.4 Management

Despite the absence of a definitive cure beyond placental delivery, advancements in managing preeclampsia (PE) have demonstrably reduced its associated mortality and morbidity for women with access to advanced healthcare. These strategies significantly reduce PE-associated mortality and morbidity. The place of care, regular monitoring, pharmacotherapy, and timed delivery are just a few successful interventions that highlight the effectiveness of managing PE, even in the absence of a permanent solution.

1.3.4.1 Place of care

Owing to the inherent nature of rapid deterioration of preeclampsia, it is recommended to assess and manage women with preeclampsia in a hospital setting which has the facilities to undertake emergent delivery and care for sick mothers and neonates[59].

1.3.4.2 Regular monitoring

Routine monitoring constitutes a fundamental pillar in managing preeclampsia by facilitating the confirmation of the diagnosis in suspected cases and enabling the detection of potential complications that may arise in established PE. Prospective studies involving pregnant women suspected with PE have shown that measurement of sFlt-1:PlGF ratio is useful to identify women who will develop PE in the next 1 to 4 weeks[40,60].

Externally validated fullPIERS (Preeclampsia Integrated Estimate of Risk) model has been shown to predict the adverse maternal outcomes, provided the components incorporated in the model are assessed twice a week. The components of fullPIERS model include: gestational age, chest pain or dyspnoea, pulse oximetry measurement, platelet count, serum creatinine and AST or ALT levels[61,62]. The inclusion of the angiogenic biomarker profile in the fullPIERS model did not enhance the prediction of adverse maternal outcomes compared to using the fullPIERS model by itself[63,64].

1.3.4.3 Pharmacotherapy

Despite ongoing research, no medication exists to definitively treat established PE. Existing clinical trials have largely focused on interventions for early-onset preeclampsia, with the main goal being to prolong pregnancy.

A. Antihypertensives

Hypertension in pregnancy should be treated with antihypertensives to achieve the target blood pressure to reduce the likelihood of developing severe hypertension[65] and stroke[66]. ISSHP defines the target blood pressure as the diastolic blood pressure (DBP) of 85 mmHg[2,65]. The simplified focus on DBP resulted in concurrent control of systolic blood pressure (SBP), achieving a mean blood pressure of 133/85 mmHg with antihypertensive therapy[65]. Figure 1 illustrates the algorithm used for initiation and cessation of antihypertensives based on the target blood pressure (adopted from the CHIPS trial[65]).

The choice of antihypertensive medications is governed by the severity of hypertension. Initial antihypertensive therapy for non-severe hypertension is monotherapy from the listed first-line drugs (labetalol, nifedipine and methyldopa) which are proven to be safe in pregnancy and their benefits outweigh any potential risks[67]. Table 3 summarizes the first line antihypertensives in non-severe hypertension in pregnancy, their dose titration, potential adverse effects, and contraindications (adopted from ISSHP recommendations[2]). Angiotensin converting enzyme inhibitors (ACEI) and angiotensin receptor blockers (ARB) are not considered safe in pregnancy owing to their foetal renal toxicity (ARB > ACEI) and its consequences, including still birth[68].

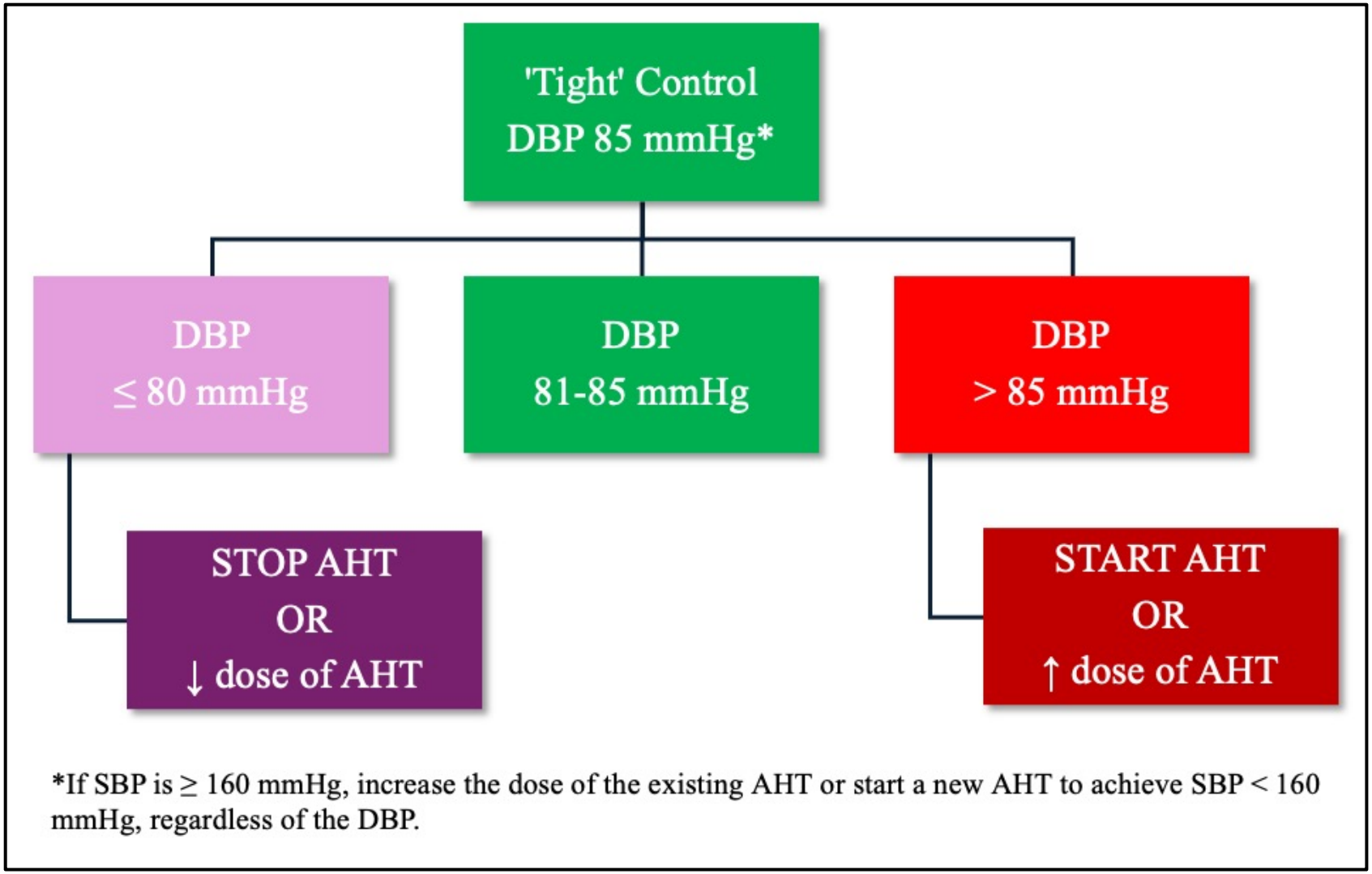


Figure 1 - Algorithm for antihypertensive therapy

SBP – systolic blood pressure; DBP – diastolic blood pressure; AHT – antihypertensive medication

Table 3 - First line antihypertensive medications for non-severe hypertension in pregnancy

First-line Antihypertensives	Adverse Effects / Contraindications	Dosage (mg)					
		Low	*If BP not controlled*	**Medium**	*If BP not controlled*	**High**	**Maximum**
Labetalol	C/I in poorly controlled asthma[69]. May cause neonatal bradycardia & hypoglycaemia[70].	100 mg 3 – 4 times/day	Proceed to **MEDIUM** dose of the same low-dose medication	200 mg 3 – 4 times/day	Consider **ADDING** another low-dose drug rather than going to high dose of the same drug(s) for a maximum of 3 medications[71]	300 mg 3 – 4 times/day	**1200 mg/day**
Nifedipine PA or MR	C/I in aortic stenosis.	10 mg 2 – 3 times/day		20 mg 2 – 3 times/day		30 mg 2 – 3 times/day	**120 mg/day**
Nifedipine XL or LA		30 mg once a day		30 mg twice a day		30 mg mane and 60 mg nocte	**120 mg/day**
Methyldopa	May cause maternal depression.	250 mg 3 – 4 times/day		500 mg 3 – 4 times/day		750 mg 3 times/day	**2250 mg/day**

PA – prolonged acting; MR – modified release; XL – extended release; LA – long acting; C/I – contraindicated

Severe hypertension (BP ≥ 160/110 mmHg) is considered as a surrogate marker of adverse maternal and foetal outcomes and there is global consensus that it should be treated urgently[72]. Treatment within 60 minutes has shown to decrease the incidence of severe maternal morbidity[73]. Most frequently used antihypertensives to control severe hypertension are parenteral labetalol and hydralazine, and oral nifedipine[74]. There was no difference in effectiveness between IV labetalol and either oral nifedipine or IV hydralazine[75], but target BP was achieved much quicker with nifedipine compared to IV hydralazine[76]. Table 4 outlines the choice of antihypertensives, recommended dosing and preferred routes of administration in managing severe hypertension.

B. Magnesium sulfate

Magnesium sulfate is recommended to women with PE who have proteinuria (≥3+) and severe hypertension (BP ≥ 160/110 mmHg), or hypertension with neurological signs and symptoms of "imminent eclampsia" (headache, visual disturbances, or clonus) for eclampsia prevention and for women with eclampsia to prevent recurrent seizures[77–79]. Tables 5 and 6 outline the dosing regimen and monitoring guidelines respectively for magnesium sulfate[1,77].

C. Antenatal corticosteroids

For women with preeclampsia who are less than 34 weeks pregnant and anticipate delivery within the next 7 days, a single course of antenatal corticosteroids (CS) is recommended to reduce the incidence of neonatal death and neonatal morbidity, including respiratory distress and ventricular haemorrhage[80]. Furthermore, for women with singleton pregnancies and preeclampsia who have not received a prior course of CS, a single course of CS can be administered during the 34–37-week gestational window if delivery is imminent[81].

Table 4 - Antihypertensive medications for severe hypertension

First-line drug[a]	Rout of administration and Dosage units	0 min	30 min	60 min	90 min	120 min	150 min
Labetalol	Oral – mg	200	-	200	-	200	-
	Intermittent IV – mg	10 – 20	20 – 40	40 – 80	40 – 80	40 – 80	40 – 80
	IV infusion – mg/min	0.5 – 2.0	→	→	→	→	→
Nifedipine	Oral capsule – mg	5 – 10	10	-	10	-	10
	Oral tablet (PA/MR) – mg	10	-	10	-	10	-
Hydralazine	Intermittent IV – mg	5	5 – 10	5 – 10	5 – 10	-	-
Methyldopa[b]	Oral – mg	1000	-	-	-	-	-

[a] Objective of initiating treatment is to maintain SBP < 160 mmHg and DBP < 110 mmHg within 180 minutes

[b] If other medications unavailable or for *in utero* transfer without monitoring

PA – prolonged acting; MR – modified release; IV - intravenous

Table 5 - Dosing regimen for magnesium sulfate

Dosing	IV administration	Combined IV and IM administration
Loading dose	4 g $MgSO_4$ IV in 100 mL NS infused over 20 minutes	4 g $MgSO_4$ IV in 100 mL NS infused over 20 minutes *AND* 5 g IM into each gluteus muscle
Maintenance	1 g/hr IV in NS infusion	5 g IM into one gluteus muscle every 4 hours
Duration	Until 24 hours after last eclamptic seizure or birth, whichever is later	

IV – intravenous; IM – intramuscular; NS – normal saline; $MgSO_4$ – Magnesium sulfate

Table 6 - Monitoring guidelines while administering magnesium sulfate

Monitoring	Observations	Signs of toxicity[c]
Maternal		
Upon completion of loading dose	Reflexes	Decreased or absent reflexes
Every 30 minutes	Blood pressure Heart rate Respiratory rate Pulse oximetry	Lower BP Lower HR or arrythmias < 12/min for 15 mins O2 saturation < 94% for 15 min
Every hour	Urine output[a] Reflexes	< 30 mL/hr for 4 hrs Decreased or absent reflexes
Symptoms[b]	-	CNS – excessive drowsiness, slurred speech Neuromuscular – muscle weakness
Fetal		
≥ 26 weeks	Continuous CTG	
< 26 weeks	Intermittent foetal heart rate auscultation every 30 mins	

[a] Foley catheterization is recommended.
[b] Symptoms of toxicity should be distinguished from well-known side effects (flushing of the skin, metallic taste in the mouth, sweating, nausea, vomiting, chest heaviness, and palpitations).
[c] If toxicity is suspected, stop the $MgSO_4$ infusion and take blood for serum magnesium. If toxicity is confirmed, administer 10% calcium gluconate (10 mL in 100 mL normal saline over 10 minutes).
CTG – cardiotocography; CNS – central nervous system

1.3.4.4 Timed delivery

In managing preeclampsia, careful consideration is given to the timing of delivery to optimize outcomes for both mother and baby. When the pregnancy is in pre-viable stage (< 24 weeks) and both the mother and foetus face significant risks of complications or death, termination of pregnancy should be considered as the recommended course of action[82,83]. Additionally, regardless of gestational age, if severe complications arise that threaten the mother or foetus (Table 7)[84], delivery is necessary. Finally, even in uncomplicated pregnancies, HYPITAT trial typically recommends delivery at term (≥ 37 weeks) to minimize risks for the mother while ensuring favourable outcomes for the new-born[85].

1.3.5 Long-term complications

Mounting evidence confirms the increased risk of long-term health complications in women with a history of preeclampsia. These women exhibit a heightened susceptibility to developing a range of complications, including hypertension, diabetes mellitus, stroke, venous thromboembolism, vascular dementia, and chronic kidney disease[86–88].

Table 7 - Indications for delivery with preeclampsia at any gestational age

Maternal or foetal complications
• Abnormal neurological features (e.g., eclampsia, severe intractable headache, or repeated visual scotomata) • Repeated episodes of severe hypertension despite maintenance treatment with three classes of antihypertensive drugs • Pulmonary oedema • Progressive thrombocytopaenia or platelet count < 50 x 10^9 /L • Transfusion of any blood product • Abnormal and rising serum creatinine • Abnormal and rising liver enzymes • Hepatic dysfunction (INR > 2 in absence of DIC or warfarin treatment), haematoma or rupture • Placental abruption with evidence of maternal or foetal compromise • Non-reassuring foetal status (including death)

INR – international normalized ratio; DIC – disseminated intravascular coagulation

1.4 Pathophysiology of preeclampsia

1.4.1 Overview

Preeclampsia is a multifaceted condition originating at the maternal-foetal interface, with effects that span various organ systems[89,90]. The pathogenesis of preeclampsia is predominantly centred around disturbances in placental function, distinguishing it as primarily a placental disorder. This distinction is underscored by the resolution of symptoms upon removal of the placenta. Although preeclampsia is often viewed as a distinct entity, particularly its early-onset form, it is part of a broader spectrum of pregnancy complications collectively referred to as "disorders of placentation" or the "great obstetrical syndromes" (encompassing late spontaneous miscarriage, placental abruption, foetal growth restriction, pre-term rupture of membranes, and premature delivery)[91]. Preeclampsia manifests clinically with abnormalities in trophoblast invasion, a process that initiates early in pregnancy, even before the onset of recognizable symptoms[89,92]. This underscores the challenge in diagnosing and managing the condition, as the underlying pathophysiological mechanisms may be at play long before the onset of clinical manifestations.

1.4.2 Placental origins of preeclampsia

Normal implantation involves trophoblast invasion of the decidualized endometrium, leading to spiral artery remodelling and obliteration of tunica media of myometrial spiral arteries, allowing enhanced blood flow to the placenta independent of maternal vasomotor changes[93]. However, in preeclampsia, trophoblasts fail to adopt an endothelial phenotype, resulting in impaired invasion and incomplete spiral artery remodelling resulting in reduced placental blood flow[89]. The resultant placental ischemia leads to oxidative stress of the syncytiotrophoblast (STB), the cell type that forms the epithelial covering of the placental chorionic villi in contact with the

maternal circulation, is one of the hallmarks in early-onset PE[94,95]. The stressed STB layer releases angiogenic markers such as soluble fms-like tyrosine kinase-1 (sFlt-1) and soluble endoglin (sEng) and syncytiotrophoblast-derived extracellular vesicles (STB-EVs) which mediate downstream effects, including endothelial dysfunction and vasoconstriction, contributing to the clinical features of preeclampsia[90,96–98]. Conversely, late-onset preeclampsia (LOPE) may arise from a mismatch between normal maternal perfusion and the increased metabolic demands of the placenta and foetus, exacerbated by maternal factors such as obesity, hypertension, or increased predisposition to inflammation[99].

1.4.3 Placental stress to maternal syndrome of preeclampsia

The classic two-stage model (Fig. 2) describes the pathogenesis of preeclampsia, focusing on placental dysfunction and the subsequent maternal response. In stage 1, inadequate development of uterine blood vessels leads to placental malperfusion, placental ischaemia, and oxidative stress. The stressed placenta responds by releasing factors into the maternal circulation. These factors, in stage 2, are thought to trigger systemic inflammation and endothelial dysfunction, ultimately manifesting as the maternal syndrome of preeclampsia, characterized by hypertension and features of end-organ damage[100]. Emerging evidence suggests that blood flow to various maternal organs is reduced even before the onset of clinical symptoms and physiological assessments reveal signs of vasospasm, activation of coagulation cascade, and reduced plasma volume[101–103]. The severity of the initial placental malperfusion is associated with higher levels of placental senescence[104], maternal serum pro-inflammatory cytokines[105], cell-free foetal DNA[106], leptin[107], STB-EVs[108], sFLT-1[109], and lower levels of PlGF[110]. Differences in the maternal responses to these messengers will mediate the clinical manifestations of the maternal syndrome.

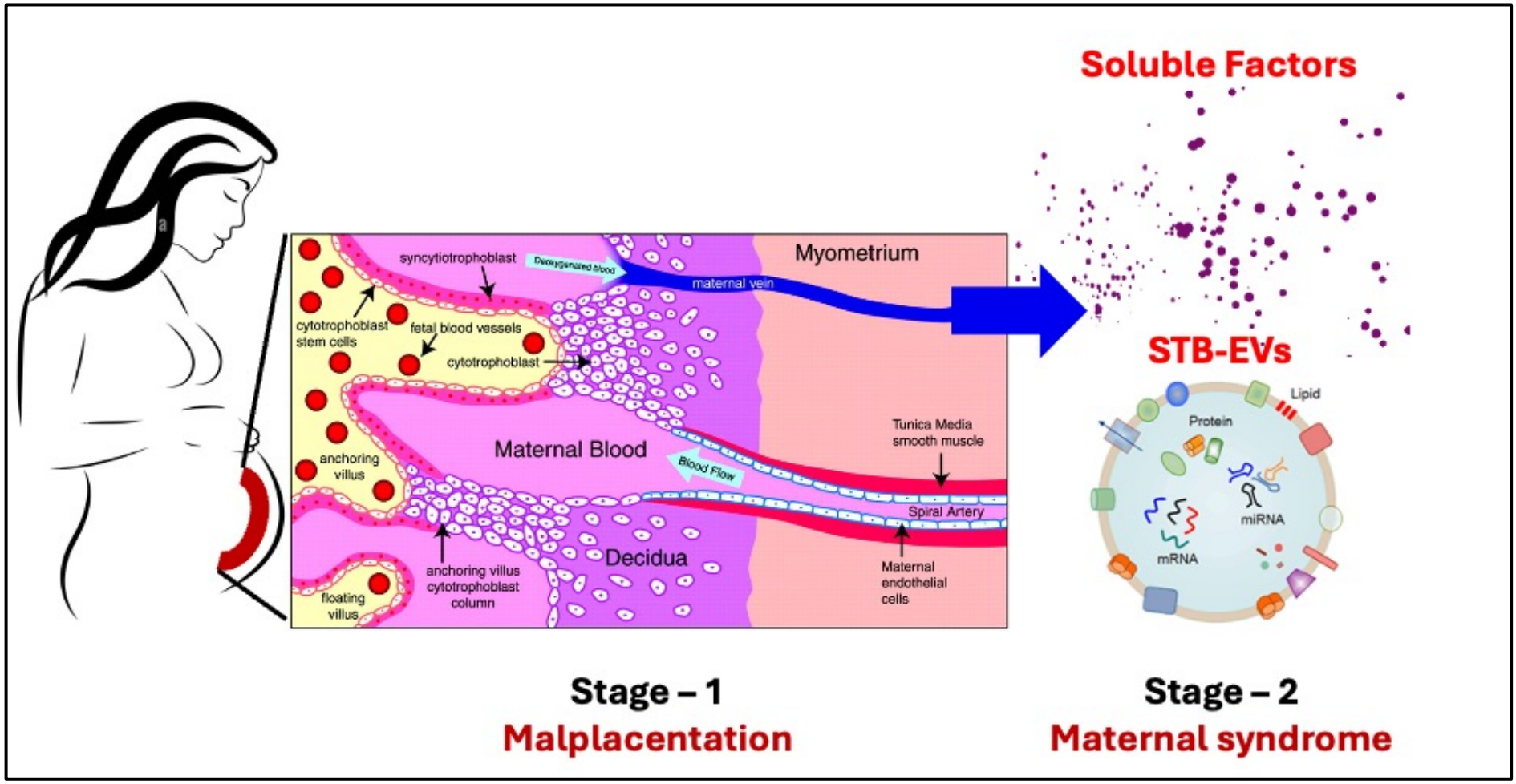


Figure 2 - Two-stage theory of PE

Malplacentation (stage 1) leading to placental ischaemia and oxidative stress resulting in release of soluble factors and STB-EVs into maternal circulation, mediating the maternal syndrome. STB-EVs carry biomolecules including proteins, genetic material, and lipids.

1.5 Syncytiotrophoblast-derived extracellular vesicles

Extracellular vesicles (EVs) are small lipid membrane-bound particles released by cells and act as signalling molecules in various biological systems. One specific type of EV is the syncytiotrophoblast-derived extracellular vesicle (STB-EV). These double-walled membrane spherical structures released from the syncytiotrophoblast (a placental cell layer) facilitate cell-to-cell communication during pregnancy. STB-EVs travel through the maternal circulation and influence both normal pregnancy physiology and disease states, such as gestational diabetes and preeclampsia.

Like other EVs, STB-EVs interact with recipient cells through two primary mechanisms: (a) internalization of the entire vesicle or (b) direct interaction between surface molecules on the STB-EV and the recipient cell membrane. The terminology for STB-EVs has evolved considerably since their discovery, with terms like placental debris[111], placental microparticles[112], placental EVs[113], and syncytiotrophoblast microparticles[114] used historically. The most recent and preferred nomenclature is syncytiotrophoblast-derived extracellular vesicles (STB-EVs)[115,116].

1.5.1 Classification of syncytiotrophoblast-derived extracellular vesicles

STB-EVs, like all EVs, can be categorized based on their biogenesis into established subtypes: microvesicles, exosomes, and apoptotic bodies[117]. However, they can also be categorized into small (< 200 nm) or medium/large (200 nm to 1000 nm) EVs based on their physical characteristics[117,118]. For the purpose of this thesis, the size-based categorization was revised to < 220 nm (small) and > 220 nm (medium/large) due to limitations in available filtration equipment in the laboratory (220 nm filter instead of 200 nm filter).

Apoptotic bodies are much larger structures (1-5 μm) formed during cellular disassembly processes, including plasma membrane blebbing, apoptotic membrane protrusion, and fragmentation[119,120]. Unlike microvesicles and exosomes, apoptotic bodies are associated with programmed cell death and were therefore excluded from further analysis in this thesis.

1.5.2 Biogenesis of syncytiotrophoblast-derived extracellular vesicles

Two potential mechanisms contribute to the generation of STB-EVs. The primary pathway, illustrated in Figure 3A, is the classical pathway. This well-established mechanism involves the production of STB-EVs from activated syncytiotrophoblast cells[108,121]. These STB-EVs encompass a range of sizes, including small STB-EVs (including exosomes), medium/large STB-EVs (including microvesicles), and potentially other types of extracellular vesicles. A less-studied alternative pathway also contributes to STB-EV generation[122]. This pathway involves the shedding of small microparticles from detached syncytial aggregates, resembling the release of platelets from circulating megakaryocytes[122].

1.5.2.1 Biogenesis of small syncytiotrophoblast-derived extracellular vesicles

Small STB-EV (sSTB-EV; including exosomes) biogenesis unfolds through a multistep process depicted in Figure 3.A. Early endosomes, formed by invagination of the plasma membrane, mature into multivesicular bodies (MVBs) containing intraluminal vesicles (ILVs). MVBs can be further categorized as secretory MVBs or degradative MVBs, with secretory MVBs fusing with the plasma membrane to release sSTB-EVs, while degradative MVBs fuse with lysosomes for degradation[123,124]. The formation of ILVs involves inward budding of the MVB membrane, enriched with the lipid ceramide (produced from sphingomyelin and sphingosine by ceramidase and sphingomyelinase respectively)[124,125]. This

ceramide enrichment organizes the membrane into raft-like microdomains, which play a crucial role in sorting proteins and RNA cargo destined for incorporation into ILVs[125,126]. Cellular RNA interacts with the MVB surface and is selectively packaged into ILVs based on its affinity for these raft-like regions[127]. Finally, MVBs fuse with the plasma membrane, releasing the encapsulated ILVs as small EVs into the extracellular space via endosomal complex required for transport (ESCRT) dependent or independent endosomal pathways[124,128,129].

In the ESCRT-dependent pathway, the endosomal membrane gets organized into specialized units highly enriched for tetraspanins (e.g., CD63 – marker for sSTB-EVs including exosomes). The enriched tetraspanins facilitate interaction between themselves and gangliosides[130], transmembrane or cytosolic proteins and cholesterol[131] to form functional microdomains on the membrane. Subsequently, the ESCRT multi-protein complexes (ESCRT-0, ESCRT-I, ESCRT-II, and ESCRT-III) work in a stepwise manner to promote membrane budding and release of sSTB-EVs[132]. ESCRT 0 and I subunits cluster ubiquitylated cargo on the microdomains of the MVB membrane and facilitate recruitment of ESCRT II and III subcomplexes. ESCRT I and II then work together to initiate membrane budding, while ESCRT III completes the process. A key player in ESCRT III function is ALG-2-interacting protein X (ALIX)[133], which binds to tumour susceptibility gene-101 (TSG101) of ESCRT I and charged multivesicular body protein 4a (CHMP4) of ESCRT III, promoting final membrane scission[134]. ALIX also contributes to sSTB-EV biogenesis through a separate interaction with syntenin[135].

Small EV biogenesis can also occur through ESCRT-independent pathways. One such alternate pathway involves the ceramide pathway, where neutral sphingomyelinase II generates ceramide, a lipid that facilitates the formation of membrane subdomains similar to those observed in the ESCRT pathway[136]. Tetraspanins, including CD9, CD63, CD81, and CD82, also seem to play a role in ESCRT-independent sorting mechanisms. This is supported

by studies demonstrating defective small EV biogenesis in animal models lacking these tetraspanins[137,138].

1.5.2.2 Biogenesis of medium/large syncytiotrophoblast-derived extracellular vesicles

Medium/large STB-EV (m/lSTB-EV, including microvesicles) biogenesis, compared to small STB-EVs, remains less explored. However, it appears to be triggered by stressful stimuli[139,140] that cause a calcium influx into the cell, activating enzymes like floppases, flippases, and scramblases, leading to the exposure and translocation of phosphatidylserine to the outer leaflet of the plasma membrane[129,141]. This translocation is then followed by two key events: outward budding of the plasma membrane and contraction of the cytoskeletal structures mediated by actin-myosin interactions (Figure 3.A). These combined mechanisms ultimately result in the deportation of m/lSTB-EVs from the cell surface.

1.5.3 Preferential sorting of cargo into syncytiotrophoblast-derived extracellular vesicles

Despite ongoing research, the specific mechanisms governing cargo sorting into STB-EVs remain unexplored. However, general mechanisms for sorting cargo into EVs are likely apply to STB-EVs as well. For instance, cytosolic proteins like heat shock (70kDa) protein (HSP70) are co-sorted with ubiquitous small EV proteins, while glycosylphosphatidylinositol (GPI)-anchored membrane proteins are recruited due to their affinity for lipid rafts[142]. The ESCRT complex sorts mono-ubiquitinated transmembrane proteins into ILVs (ultimately released as EVs) in an ESCRT-dependent pathway[142,143]. Notably, both mono- and poly-ubiquitinated proteins can also be sorted independent of ESCRT by factors like sphingolipids, tetraspanins, and ceramide[144,145].

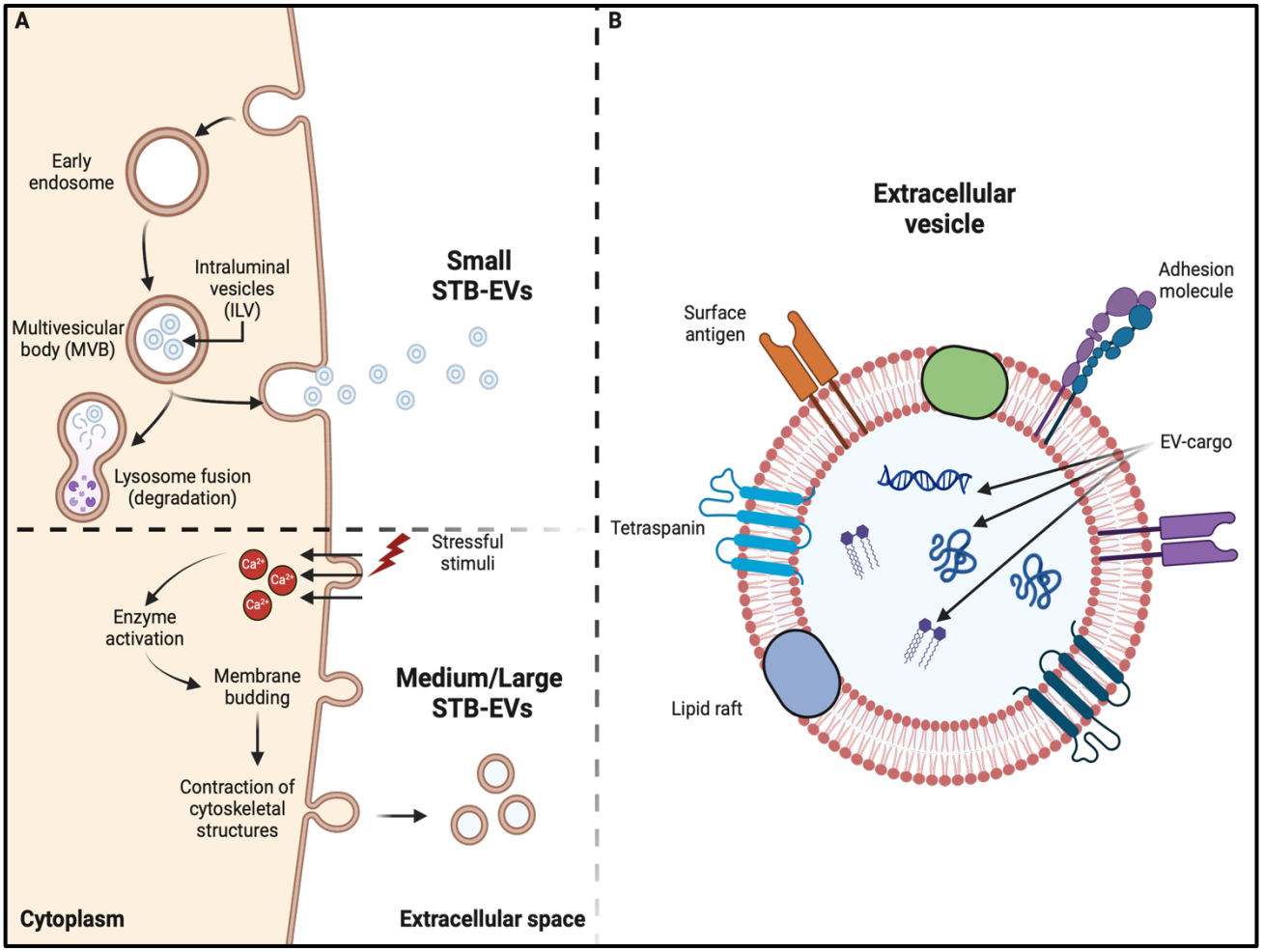


Figure 3 - Biogenesis of extracellular vesicles

A) Illustration of biogenesis of exosomes (a subtype of sSTB-EVs) from the early endosome and multivesicular body and biogenesis of microvesicles (a subtype of m/lSTB-EVs) from plasma membrane budding. **B)** Illustration of an extracellular vesicle. EVs contain a wide variety of molecules, such as nucleic acids, proteins, and lipids. All the content at both the membrane and soluble levels represents the cell of origin the EVs are released from. Created with BioRender.com

Small RNAs, particularly microRNAs, contain specific motifs that influence preferential sorting into exosomes[146]. Garcia-Martin et al. identified unique sequences/ sorting motifs (EXOmotifs) enriched in small EVs that bind to RNA-binding proteins Alyref and Fus, facilitating their sorting[146]. Additionally, the KRAS-MEK signalling pathway and various proteins (major vault protein, Y-box binding protein-1, hnRNPA2B1, caveolin-1, neural sphingomyelinase-2, and argonaut-2) are all implicated in miRNA sorting[147–150]. Notably, hnRNPA2B1, a SUMOylated (small ubiquitin RNA modifier) RNA-binding protein, helps identify specific miRNA motifs (like the GAGAG motif in the 3' region) for sorting[151]. Furthermore, tetraspanin-enriched microdomains may concentrate RNA-binding proteins like the ESCRT II subcomplex within membrane subdomains, potentially influencing sorting[147]. While extensive reviews exist on microRNA sorting by Groot et al.[147] and general EV sorting mechanisms by Anand et al.[152] and Villarroya-Beltri et al.[142], much less is known about sorting mechanisms for metabolites, lipids, mRNA, or other RNA subtypes beyond microRNAs into EVs.

1.5.4 Cellular entry mechanisms of syncytiotrophoblast-derived extracellular vesicles

Ever since the discovery of EVs' ability to influence recipient cells, understanding their uptake mechanisms has become a major research focus. Several pathways have been identified (Figure 4), including endocytosis[153], clathrin- and caveolin-dependent endocytosis[154], lipid raft-mediated endocytosis[155], phagocytosis[156], macropinocytosis[157] and membrane fusion[158]. The specific endocytosis pathway utilized by a cell appears to depend on the EV's origin and involves: heparan sulfate proteoglycans[159], galectin 5[160], CD91[161], calcium[162] or fibronectin[163].

Clathrin- and caveolin-dependent pathways are mediated by dynamin[157] and neuroactive ligand receptors[154] for function, while lipid raft-mediated endocytosis utilizes glycosphingolipids[164], cholesterol[165], or ERK1/2 signalling[166]. Macropinocytosis involves proton pumps or sodium/proton exchangers[157], while phagocytosis is mediated by phosphoinositide 3-kinases (PI3Ks)[167] or phosphatidylserine[157] and membrane fusion via sodium absorption[158]. Regarding STB-EVs specifically, Cronqvist et al. proposed endocytosis or membrane fusion as potential uptake mechanisms in human coronary artery endothelial cells[168]. Vargas et al. observed a syncytin-1 and -2 dependent uptake of small villous cytotrophoblast STB-EVs by BeWo cells, suggesting an alternative pathway[169]. However, a comprehensive investigation into whether STB-EV uptake differs from other EVs or varies between different sized STB-EVs is still lacking.

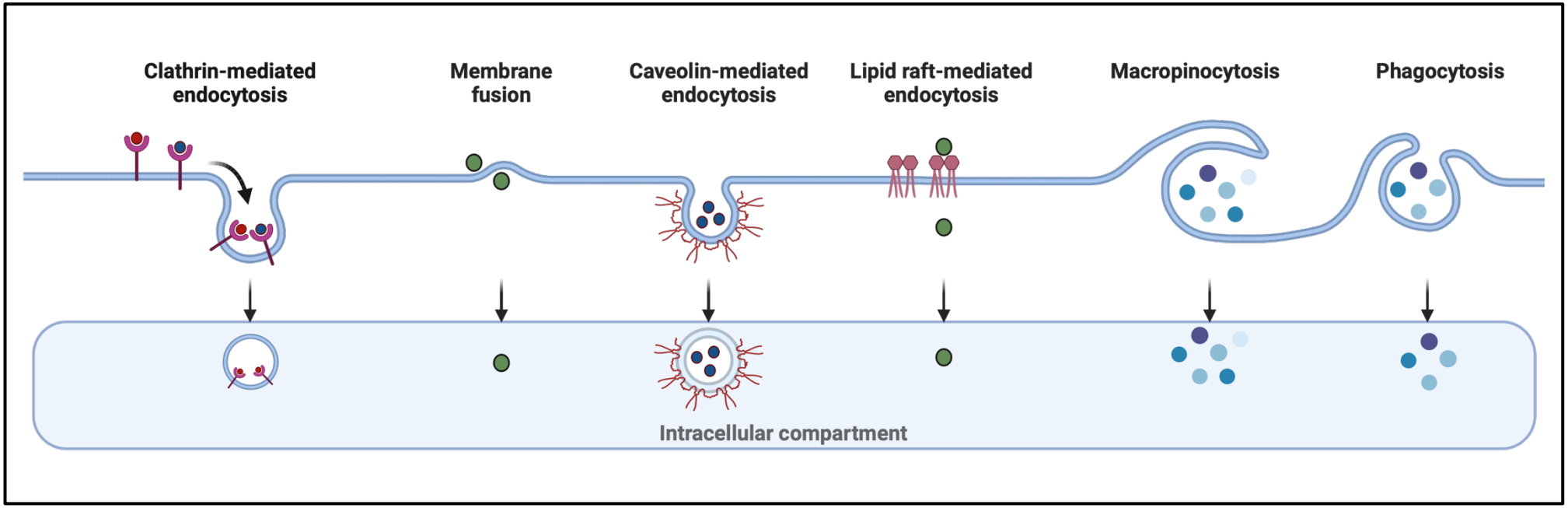


Figure 4 – Cellular entry mechanisms of extracellular vesicles

EVs from donor cells are internalized by the recipient cells via endocytosis (clathrin-, caveolin-, and lipid raft-mediated), membrane fusion, macropinocytosis, and phagocytosis. Once internalized, the EVs are absorbed into the intracellular compartments and their cargo are deposited intracellularly. Created with BioRender.com

1.5.5 Role of syncytiotrophoblast-derived extracellular vesicles in preeclampsia

In preeclampsia, STB-EVs exhibit a proinflammatory phenotype, particularly in EOPE[170,171]. Studies differentiating the phenotypes of STB-EVs (i.e., EOPE vs. LOPE) have shown that LOPE STB-EVs are less likely to produce a proinflammatory response in THP1 cells compared to normal pregnancy (NP) STB-EVs, in contrast to EOPE STB-EVs[172]. STB-EVs can induce the elaboration of proinflammatory cytokines such as tumour necrosis factor (TNF)-α, IL-1, IL-8, and IL-6 in neutrophils, B- and T-cells, and monocytes[173,174], which can be inhibited by blocking Toll-like receptor (TLR) signalling or targeting the nuclear factor kappa B (NF-κB)[175].

PE STB-EVs are also anti-angiogenic and contribute to endothelial dysfunction. Endothelial nitric oxide synthase (eNOS) activity is reduced in PE STB-EVs, potentially contributing to the vascular dysfunction and hypertension observed in PE[176]. In pregnant animal studies, injection of preeclamptic EVs resulted in arterial vasoconstriction, decreased maternal body weight, increased maternal blood pressure, and an increase in circulating sFlt-1[177].

PE STB-EVs enhance cellular oxidative stress by inducing endoplasmic reticulum and mitochondrial membrane ruffling and can cause endothelial dysfunction by transferring functional microRNAs or mitochondrial DNA from dysfunctional syncytiotrophoblast[168]. They can bind proangiogenic factors (vascular endothelial growth factor, placental growth factor, and transforming growth factor-β), disrupt cultured human umbilical vein endothelial cell monolayers[178], and inhibit endothelial tube formation *in vitro*, leading to anti-angiogenesis[122].

Furthermore, PE STB-EVs promote abnormal coagulation. Tannetta et al. noted that PE STB-EVs could activate platelets by increasing protein tyrosine phosphorylation, which can be inhibited with aspirin[179]. PE STB-EVs also express procoagulant proteins such as tissue factor[180], anionic phospholipids[181], and plasminogen activator inhibitors-1[182], contributing to the abnormal coagulation observed in preeclampsia.

1.5.6 Diagnostic potential of syncytiotrophoblast-derived extracellular vesicles

Since the discovery of EVs, their cargo has been extensively studied for its diagnostic potential. Similar to other EVs, syncytiotrophoblast-derived extracellular vesicles carry genetic material, proteins, lipids, and other metabolites. This unique cargo has generated significant interest in STB-EVs as a source for non-invasive placental biopsies.

In preeclampsia, STB-EV miRNAs have been investigated as potential biomarkers by analysing cell-free miRNAs in circulation (plasma or serum) and linking them to the placenta. Several studies have reported various miRNA targets as potential biomarker candidates for PE, including *hsa-miR-574-5p, hsa-miR-181a, miR-122, miR-758, hsa-miR-517-5p, hsa-miR-520-5p, hsa-miR-521, hsa-miR-542-3p, hsa-miR-4313, hsa-miR-23c, hsa-miR-191, miR-210,* and *miR-25*[183–187].

Several other studies have identified differentially expressed proteins on STB-EVs in PE. Gardiner et al. reported a 2-10-fold increase in tissue factor activity in PE STB-EVs compared to NP[180]. Tanetta et al. found upregulation of Flt-1, an antiangiogenic tyrosine kinase that binds VEGF, in PE STB-EVs[178]. Rajakumar et al. noted that soluble Flt-1 (sFlt-1) is highly expressed in sSTB-EVs in PE, contributing to endothelial dysfunction and vasoconstriction[122].

Other proteins reported as upregulated in PE STB-EVs include neprilysin (NEP), a metalloendopeptidase that inactivates bioactive peptides[188], and transthyretin, a protein essential for foetal development[189,190]. A novel glycosylated form of SIGLEC6, which regulates immune cell activation and clonal expansion, was also identified as differentially expressed in PE STB-EVs[191].

1.6 Conclusion

Preeclampsia, a complex pregnancy disorder impacting multiple organ systems, presents significant challenges in elucidating its pathogenesis, diagnosis, and treatment. The placenta, central to this pathology, releases soluble factors and syncytiotrophoblast-derived extracellular vesicles (STB-EVs). Notably, STB-EVs in preeclampsia exhibit pro-inflammatory, anti-angiogenic, and pro-coagulatory properties, additionally contributing to endothelial dysfunction. These findings collectively highlight their potential role in the pathogenesis of preeclampsia. Furthermore, ongoing research into the unique cargo of PE STB-EVs holds promise for developing biomarkers for early prediction, diagnosis, and disease monitoring. Given these compelling findings, in this thesis I aim to investigate the role of syncytiotrophoblast-derived extracellular vesicles in the pathogenesis of preeclampsia.

1.7 Aims

This thesis aims to achieve the following objectives:

1. **Isolate, enrich, and characterize syncytiotrophoblast-derived extracellular vesicles (STB-EVs) (Chapter 3).**

   This initial step will establish a foundation for further investigation of STB-EVs in subsequent experiments.

2. **Characterize the protein cargo of STB-EVs with a focus on kynurenine metabolising enzymes and assess their functional activity in an *in vitro* setting (Chapter 4).**

   This will explore the role of kynurenine metabolising enzymes within STB-EVs and their potential contribution to pathogenesis of preeclampsia.

3. **Validate differentially expressed microRNAs in the genetic cargo of STB-EVs and assess the functional impact of a specific miRNA (*hsa-miR-9-5p*) on cerebral microvascular endothelial cells (Chapter 5).**

   This will validate a specific miRNA *(hsa-miR-9-5p)* in STB-EVs and serum EVs of women with EOPE and investigate its influence on cerebral microvascular endothelial cell function.

4. **Establish a clinical trial in Sri Lanka to evaluate the sFlt-1:PlGF ratio as a potential biomarker for predicting preeclampsia in women with suspected symptoms (Chapter 6).**

   In parallel to the investigation of STB-EVs, this clinical trial will explore the use of a readily measurable biomarker for early preeclampsia diagnosis. Additionally, a biobank of stratified serum and plasma samples will be established to support future research endeavours.

CHAPTER 2:

MATERIALS AND METHODS

2.1 General Methods

2.1.1 Human participants

Ethical approval for this study was granted by the Central Oxfordshire Research Ethics Committee C (reference numbers: 07/H0607/74 & 07/H0606/148). Pregnant women undergoing elective caesarean sections prior to onset of labour were prospectively recruited from the maternity ward at the Women's Centre, John Radcliffe Hospital, Oxford. Research midwives facilitated the process of obtaining written informed consent from all participants before collecting placenta and/or blood samples.

Inclusion criteria for placenta and blood collection encompassed both normal pregnancies (NP) and pregnancies diagnosed with early-onset preeclampsia (EOPE). EOPE was defined as onset of preeclampsia (*de novo* hypertension (systolic blood pressure, SBP>140mmHg and diastolic blood pressure, DBP>90mmHg) with either new-onset proteinuria, or evidence of other maternal end-organ dysfunction (including liver, kidney, neurological); haematological involvement; or uteroplacental dysfunction)[1] before 34 weeks of gestation, and confirmed by an sFLT-1:PlGF ratio > 85[192], while normal pregnancies (NP) were defined as singleton pregnancy with no history of preeclampsia, hypertensive disorders, or other complication is pregnancy, and had a sFLT-1:PlGF ratio < 38[192].

Placentae were retrieved in the operating theatre and were perfused within 10 minutes. Blood samples were collected in plastic serum tubes (BD Vacutainer) using a 21-gauge needle from the left antecubital fossa under sterile conditions. These blood samples were processed immediately after collection. The samples were centrifuged (Thermo Multifuge X3R) at a rate

of 3,000 RPM for 10 minutes at 21°C to separate the serum. The serum was then aliquoted and stored at -80°C until analysis.

Placental biopsies were collected from the maternal facing surface (without the decidual layer) for protein expression analysis. Placental lysates were prepared using RIPA buffer (150 mM NaCl,50mM Tris pH 8.0, 0.1% SDS, 1% Triton X100, 0.5% sodium deoxycholate; ThermoFisher Scientific) and a protease inhibitor cocktail (Sigma Aldrich) and were subsequently subjected to a bicinchoninic acid (BCA) protein assay (Sigma Aldrich). The lysates were then stored at -20°C until analysis.

2.1.2 Introduction and clarification of nomenclatures used in the thesis

During the initial enrichment and characterisation stages, crude preparations containing medium/large STB-EVs (m/lSTB-EVs) and small STB-EVs (sSTB-EVs) were referred to as 10K STB-EV and 150K STB-EV pellets, respectively, based on their differential ultracentrifugation steps (10,000 x g and 150,000 x g). Following characterisation by a validated method, such as Nanoparticle Tracking Analysis (NTA) and/or flow cytometry, the 10K STB-EV pellets were verified to be enriched for medium/large EVs falling within the expected size range of ≥ 200 nm up to 1000 nm and 150K STB-EV pellets contained small EVs measuring less than 200 nm[117]. Due to limitations in available filtration equipment (220 nm instead of 200 nm) in our laboratory, the size-based classification of EVs was adjusted. Small STB-EVs were defined as less than 220 nm, and m/lSTB-EVs were defined as ≥ 220 nm. Subsequently, the placental (syncytiotrophoblast) origin of the EVs was confirmed by the presence of placental alkaline phosphatase, a protein specific to syncytiotrophoblast cells.

To reflect this validated size distribution and cellular origin, and to enhance clarity for the remainder of the thesis, the nomenclature of STB-EVs was subsequently revised. Henceforth, the 10K STB-EV and 150K STB-EV pellet designations will be referred to as m/lSTB-EVs and sSTB-EVs, respectively.

2.1.3 Isolation and enrichment of STB-EVs by placental *ex vivo* dual lobe perfusion

This section describes the protocol for isolation and enrichment of STB-EVs from human placentae by placental *ex vivo* dual lobe perfusion and differential ultracentrifugation as previously described by our group[179,193–196]. Strict adherence to standardized protocols is critical for the successful isolation of EVs with minimal contamination from other cellular components.

Placental *ex vivo* perfusion: Following caesarean delivery, placentae were promptly transported to the laboratory in a clean plastic bucket with pre-warmed Hanks' balanced salt solution (HBSS, Gibco) to minimize temperature fluctuations that could compromise the integrity of EVs. HBSS is a balanced physiological salt solution that helps to maintain cellular integrity during transport[197].

Upon arrival at the laboratory, an intact peripheral lobe devoid of any visible signs of postpartum villus disruption was chosen for further processing. Damage to these structures could potentially introduce cellular debris and compromise the purity of the isolated STB-EV population.

The chosen placental lobe was then cannulated at the chorionic plate, the foetal facing surface of the placenta. Cannulation involved insertion of small tubes into the branches of umbilical artery and vein (perfusing the chosen placental lobe) to establish a closed perfusion circuit. The chosen lobe was perfused with 0.1 μm filtered (Stericup-VP, Merck Millipore) M-199 tissue culture medium (Medium 199 supplemented with L-glutamine and Earle's salts; 0.8% dextran

20; 0.5% w/v bovine serum albumin (BSA) (Sigma, UK); and 2.75 g/L sodium bicarbonate; pH 7.4), 5000 IU/L sodium heparin (Fannin, UK), and 100,000 IU streptokinase (Oxford Hospitals). Medium 199 with L-glutamine and Earle's salt provides a suitable nutritional environment to maintain cell viability during the perfusion process; 0.8% Dextran 20, a high molecular weight polysaccharide, exerts an oncotic pressure effect to maintain vascular integrity and prevent leakage of cellular components during perfusion; 0.5% BSA minimizes non-specific binding of EVs to surfaces within the perfusion apparatus; and 5000 U/L sodium heparin (anticoagulant) and 100,000 IU streptokinase (thrombolytic agent), prevent blood clotting within the vascular network of the placental lobe. The perfusion process was controlled at a flow rate of 5 mL/min.

Following initial cannulation and perfusion of the foetal circulation, the entire placenta was carefully inverted to position the maternal surface facing upwards and was laid in a Perspex water jacket maintained at 37°C. The maternal surface is the placental interface in direct contact with the uterine wall. This reorientation facilitated perfusion of the maternal circulation. A pre-formulated tissue culture medium, identical to the one used for the foetal circuit (Medium 199 supplemented with L-glutamine and Earle's salts; 0.8% dextran 20; 0.5% BSA (Sigma)) but lacking heparin, was then perfused through six strategically placed 1.7 mm foetal feeding tubes (Pennine Healthcare) positioned on the maternal surface. The controlled flow rate for maternal perfusion was set at 20 mL/min.

To ensure proper equilibration of the entire placental lobule with the perfusion solution, the perfusion process continued for a designated period of 20 minutes. Following equilibration, the maternal circuit was closed, and a volume of 600 mL of perfusion medium was retained within the closed circuit to maintain tissue hydration and preserve cellular integrity. Perfusion media (foetal and maternal) were kept warm in a 37°C water bath, and the maternal perfusion medium was continuously oxygenated with 95% v/v O_2 and 5% v/v CO_2. The stability of the preparation was continuously monitored by measuring the volume of the effluent exiting the foetal circuit.

This served as an indicator of potential leaks or disruptions within the perfusion system. After a three-hour perfusion period, the maternal perfusate was collected to harvest STB-EVs. Illustrative representation of placental *ex-vivo* dual lobe perfusion set-up is shown in Figure 5.

STB-EV isolation and enrichment: Collected maternal perfusate was subjected to differential serial ultracentrifugation to eliminate cellular debris and isolate EVs. The perfusate was centrifuged twice at 1,500 x g for 10 minutes at 4°C using a refrigerated centrifuge (Beckman Coulter Avanti J-20XP) equipped with a swing-out rotor (Beckman Coulter JS-5.3). This initial low-speed centrifugation steps effectively remove any remaining intact cells (e.g. red blood cells) and cellular debris from the perfusate. The resulting supernatant, enriched for EVs was carefully collected and pooled for further processing.

The pooled supernatant was then subjected to ultracentrifugation at 10,000 x g (designated as 10K) for 35 minutes at 4°C in a swing bucket centrifuge (7,700 RPM; Beckman L8-80M ultracentrifuge and SW 32 Ti swinging-bucket rotor). This centrifugation step pellets a fraction enriched for larger EVs, including medium/large STB-EVs (m/lSTB-EVs). The resultant pellets were carefully recovered and designated as 10K STB-EV pellets. These pellets were then washed with filtered phosphate-buffered saline (fPBS) and pooled by ultracentrifugation at 10,000 x g for 35 minutes at 4°C to remove residual contaminants from the perfusion solution. The final pellet was resuspended in fresh fPBS for further analysis or storage.

An aliquot of the resuspended 10K STB-EV pellet fraction was utilized for subsequent STB-EV identification and characterisation. The remaining were aliquoted to achieve a protein concentration of approximately 2-5 µg/µL (determined using a Pierce BCA protein assay kit) and stored at -80°C for later use as recommended[118].

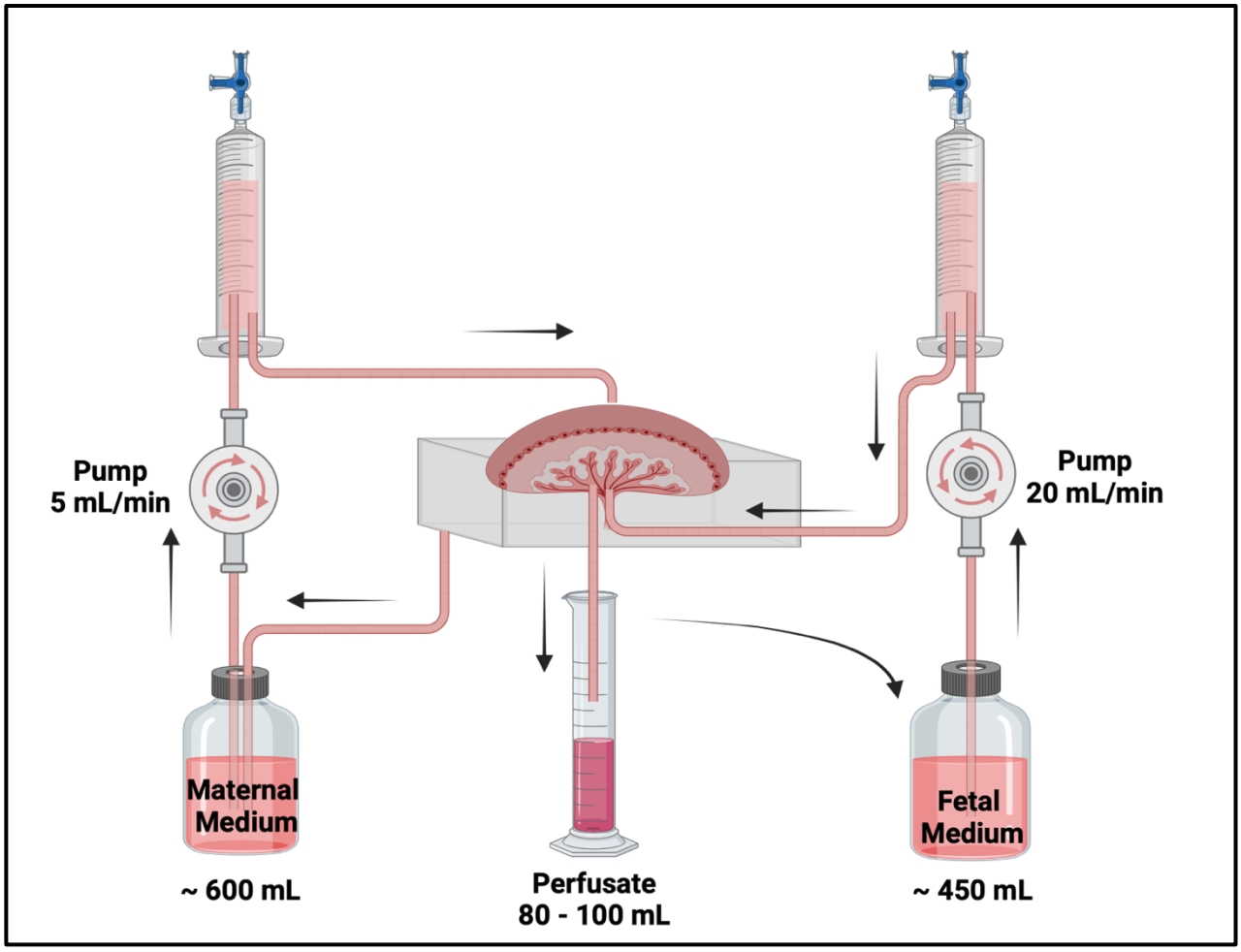


Figure 5 - Illustration of *ex vivo* dual lobe placental perfusion setup

The placenta perfusion system comprises the foetal circuit on the right and the maternal circuit on the left. Maternal circuit is a closed circuit. The maternal medium moves through the tubes from the maternal medium bottle to perfuse the maternal side of the identified cotyledon. The maternal perfusate is then returned through the tubing to the maternal medium bottle. The foetal circuit is manually closed. The foetal medium moves through the tubes from the foetal medium bottle to perfuse the foetal side of the identified cotyledon. The foetal perfusate is then measured every twenty minutes to determine flow rate consistency and emptied manually into the foetal medium bottle. The illustration was created with BioRender.com

Following the isolation of the 10K STB-EV fraction, the remaining post-10K supernatant was subjected to further purification. This supernatant is anticipated to be enriched for smaller EVs, including small STB-EVs (sSTB-EVs). To enrich sSTB-EVs, the supernatant was first passed through a 0.22 μm filter (Stericup-VP, Merk Millipore) to remove any remaining larger particles. The filtrate obtained after passing through the 0.22 μm filter, was then subjected to ultracentrifugation at 150,000 x g for 125 minutes at 4°C in a swing bucket centrifuge (29,600 RPM; Beckman L8-80M ultracentrifuge and SW 32 Ti swinging-bucket rotor). This ultra-high-speed centrifugation step effectively pellets a population enriched for smaller EVs, including sSTB-EVs. The resulting pellets were designated as 150K STB-EV pellets. Similar to the 10K STB-EV pellets, the 150K STB-EV pellets were washed with fPBS, resuspended in fresh fPBS, aliquoted into appropriate volumes, and stored at -80°C for subsequent analyses as recommended[118]. Schematic illustration of differential serial ultracentrifugation is shown in Figure 6.

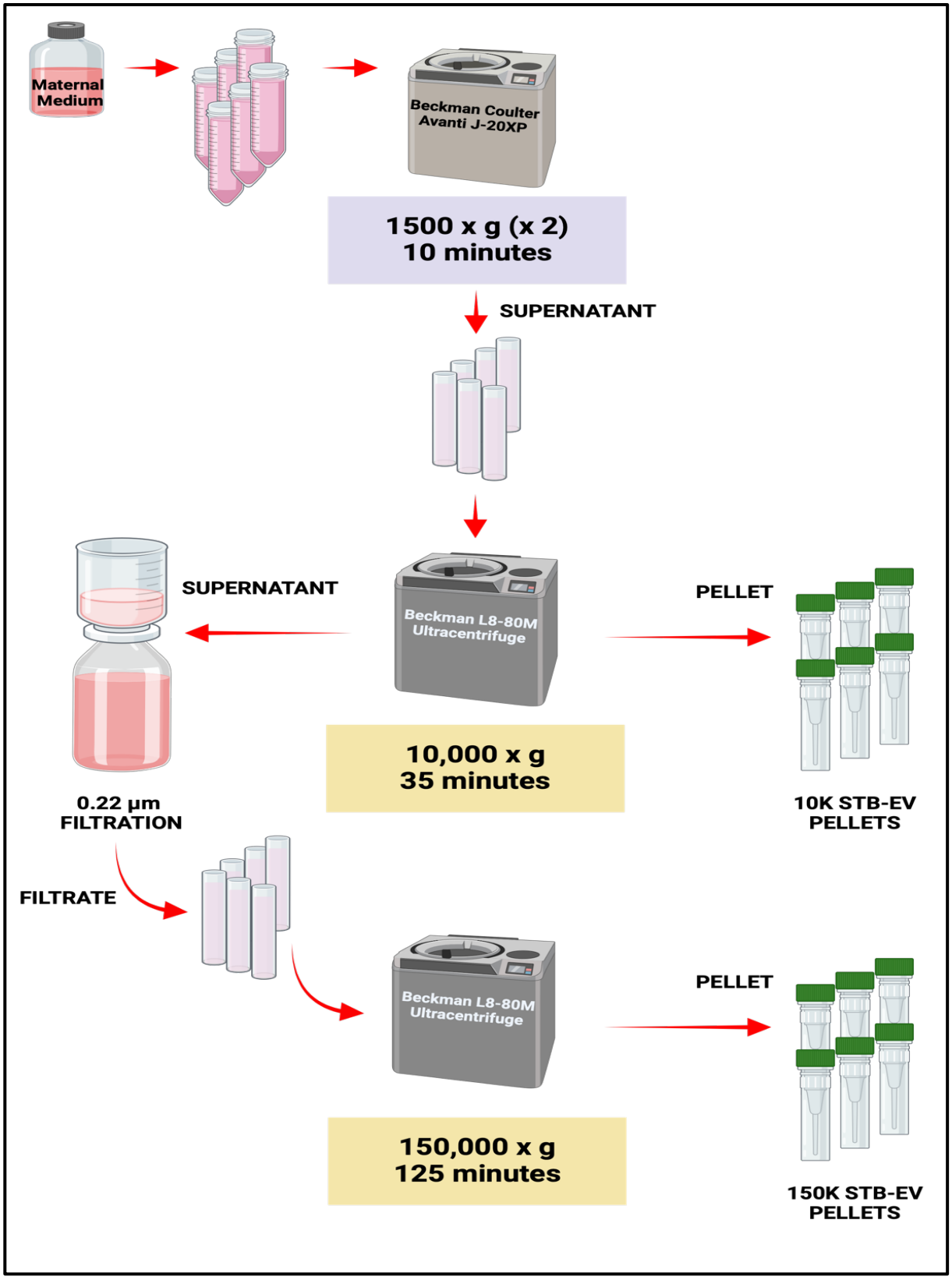


Figure 6 - Illustration of differential ultracentrifugation process

The maternal perfusate undergoes differential ultracentrifugation (10,000 x g and 150,000 x g) to pellet medium/large and small extracellular vesicles. The pellets are then subjected to characterisation studies to confirm their size distribution, tissue of origin and presence of extracellular vesicle markers. The objects in the illustration are not to scale and do not represent their actual size proportions. Illustration created with BioRender.com

2.1.4 Characterisation of STB-EVs isolated by placental ex-vivo dual lobe perfusion

2.1.4.1 Transmission electron microscopy

STB-EV characterisation by transmission electron microscopy (TEM) was outsourced to Dr. Errin Johnson at the Sir William Dunn School of Pathology, University of Oxford. This approach ensured access to specialized expertise and high-resolution TEM instrumentation for optimal data acquisition.

Sample preparation: STB-EV pellets were resuspended in phosphate-buffered saline (PBS) to achieve a final concentration ranging from 0.1 to 0.3 µg/µL. This suspension was then used for negative staining, a technique that enhances the contrast between the STB-EVs and the background for optimal visualization under TEM. Ten microliters of the resuspended STB-EV were carefully applied to freshly glow-discharged carbon Formvar-coated 300 mesh copper grids. Following a 2-minute incubation period, excess liquid was removed using filter paper. The grids were then negatively stained with 2% uranyl acetate solution for 10 seconds. Afterward, the grids were further blotted with filter paper and allowed to air-dry completely.

Imaging: TEM imaging was performed at the Sir William Dunn School of Pathology using an FEI Tecnai 12 TEM operating at an acceleration voltage of 120 kV. Images were captured with a Gatan OneView CMOS camera.

2.1.4.2 Flow cytometry

This section details the flow cytometric analysis of medium/large STB-EVs, performed with the assistance of Dr. Wei Zhang (Senior Postdoctoral Researcher, NDWRH, University of Oxford).

Instrumentation and quality control: Analyses were conducted using a BD LSR II flow cytometer (BD Biosciences) equipped with blue, violet, and red lasers. Daily quality control (QC) was a critical step to ensure instrument stability and optimal performance. CS&T beads (BD Biosciences) were employed for daily QC, establishing the photomultiplier tube (PMT) voltage for each fluorescent detector, except for side scatter (SSC). SSC PMT voltage was determined using Apogee beads mix (1493, Apogee Flow System, UK), setting a threshold to trigger on 0.59 μm silica beads and above for all analysed 10K STB-EV pellets. Additionally, a background noise threshold of 200 was applied on the SSC channel to remove noise below 0.59 μm silica beads. A flow rate of 10 μL/min was achieved using TruCount beads (BD Biosciences). The flow rate was calculated by dividing the events obtained within the TruCount bead gate by the lot-specific number of beads in each TruCount tube and then dividing this value by the acquisition time.

Sample preparation and staining: 10K STB-EV pellets were diluted with fPBS to achieve a desired flow rate of approximately 400 events/second. To minimize spectral overlap between fluorochromes used for antibody conjugation and M/L STB-EV intrinsic fluorescence, fluorochrome compensation was performed using BD CompBeads (BD Biosciences) and recombinant engineered antibodies (REA) compbeads (Miltenyl Biotech). Additionally, BODIPY FL N-(2-aminoethyl)-maleimide [505/513 nm] (bioM, Molecular Probes) was employed to stain M/L STB-EVs. BioM binds to protein cysteine residues and thiol groups, enabling clear distinction between stained particles and background noise.

Antibody titrations were conducted independently to achieve optimal staining intensity for both STB-EVs and compensation beads. Events exceeding the staining intensity of compensation beads were excluded from further analysis to ensure accurate data interpretation.

For antibody staining, 100 µL aliquots of diluted 10K STB-EV pellet samples (containing M/L STB-EVs) were incubated with specific antibodies for 15 minutes at room temperature. Subsequently, the samples were transferred to ultrafree 0.22 nm filter units (Merk Millipore) and centrifuged at 800 x g for two minutes at room temperature to remove unbound antibodies. The following antibodies were utilized for flow cytometric analysis:

- Fc receptor blocker (Miltenyl, UK) – to prevent non-specific Fc receptor binding.
- Phycoerythrin (PE) conjugated placenta alkaline phosphatase (PLAP) – to identify syncytiotrophoblast-derived EVs.
- PE Vio770 conjugated anti-classical HLA class I and II – to exclude co-isolated white blood cell (WBC) EVs.
- Pacific blue conjugated CD41 – to identify co-isolated platelet EVs.
- CD235a – to identify co-isolated red blood cell (RBC) EVs.

For sample staining, 90 µL of 10K STB-EV pellet was incubated with 10 µL of Fc receptor blocker for 10 minutes at 4°C and then stained with phycoerythrin conjugated PLAP; PE Vio770 conjugated anti-classical HLA class I and II; pacific blue conjugated CD41 and CD235a in the dark for 10 minutes at room temperature. Following incubation, samples were transferred to ultrafree 0.2 µm filter units (Merk Millipore) and centrifuged at 800 x g for 2-3 minutes to remove unbound antibodies and eliminate EVs smaller than the filter pore size. Retained 10K STB-EVs on the filter membrane were recovered using 90 µL of fPBS.

Recovered 10K STB-EVs were further stained with BODIPY FL N-(2-aminoethyl)-maleimide [505/513 nm] (Molecular Probes) at a final concentration of 0.5 nM for 10 minutes in the dark at room temperature. Samples were then diluted to 500 µL and analysed on the flow cytometer to monitor the event rate. If necessary, subsequent dilutions were made to achieve a flow rate of ≤ 400 events/second and prevent swarming. Each patient sample analysis involved a 100 µL diluted sample analysed at 10 µL/minute for a total duration of 10 minutes.

Fluorescence minus one (FMO-1) controls were included for each fluorochrome to account for background noise and autofluorescence. Samples were re-acquired after treatment with 2% nonidet P-40 (NP-40) (Sigma) to differentiate between vesicular and non-vesicular particles. Data and figures were generated with the Flowjo software version 10 (Tree Star Inc., Ashland, OR). Table 8 shows the instrument parameters used for the flow cytometric analysis.

Table 8 - Instrument parameters for the BD Bioscience's LSR II flow cytometer

Laser	Detector	LP mirror	BP filter	Flurochrome	Marker
Blue	A	735	780/60	PE-Vio770	HLA – I & II, CD41a, CD235a/b
Blue	D	550	575/26	PE	PLAP
Blue	E	505	530/30	BioM	Protein dye
Blue	F, SSC		488/10		

BP – band pass; BioM – BODIPY FL N-(2-aminoethyl)-maleimide; PE – phycoerythrin; HLA – human leukocyte antigen; PLAP – placental alkaline phosphatase

2.1.4.3 Nanoparticle tracking analysis

This section describes the characterisation of STB-EV size and concentration using nanoparticle tracking analysis (NTA) with the NanoSight NS500 system (Malvern Panalytical).

Instrumentation and calibration: The NanoSight NS500 system employs a 405 nm laser, an sCMOS camera, and nanoparticle tracking analysis (NTA) software version 2.3 (Build 0033). This system utilizes a modified Stokes-Einstein equation to determine the size and concentration of EVs within a sample. Briefly, the laser beam is directed towards the sample chamber through a glass prism, illuminating the EVs. Scattered light from individual EVs is then captured by the camera and analysed by the NTA software. Prior to sample analysis, instrument performance verification was performed using commercially available silica nanoparticles of a defined size (100 nm, Polysciences, Inc.).

Sample preparation and analysis: STB-EV samples were diluted with fPBS to achieve a concentration suitable for optimal NTA analysis, typically ranging from 1:10,000 to 1:100,000 dilutions, based on the initial sample concentration. Automated injection of the diluted samples into the NanoSight chamber was facilitated by a 1 mL syringe. A standardized script was employed for all EV measurements: prime, delay: 5, capture: 60, repeat: 4. Images of the analysed samples were captured with optimized camera settings at Level 12 (shutter speed: 15 ms; gain: 350). Consistency in NTA post-acquisition settings was maintained across all samples. Each video recording was analysed using the NTA software to extract the size and concentration profiles of the STB-EVs within the sample.

2.1.4.4 Western blot analysis

Western blotting was utilized to further characterize placental homogenates and STB-EV pellets. All STB-EVs were probed with:

- Placental Alkaline Phosphatase (PLAP) (1.67 µg/µL) – In-house antibody specific to syncytiotrophoblast-derived proteins, indicating placental origin (1:1000 dilution).
- CD63 (200 µg/mL) (Sc-59286, Santa Cruz Biotechnology) – Extracellular marker enriched in EVs, particularly in 150K STB-EV pellets (1:1000 dilution).
- TSG101 (200 µg/mL) (Sc-7964, Santa Cruz Biotechnology) – Extracellular marker enriched in EVs, particularly in 150K STB-EV pellets (1:1000 dilution).
- ALIX (200 µg/mL) (Sc-53538, Santa Cruz Biotechnology) – Extracellular marker enriched in EVs, particularly in 150K STB-EV pellets (1:1000 dilution).
- Cytochrome C (200 µg/mL) (Sc-13156, Santa Cruz Biotechnology) – Negative control marker present in all cells and homogenates but not EVs (1:1000 dilution).

Antibody selections were performed in accordance with recommendations established by the International Society for Extracellular Vesicles (ISEV)[117].

Sample preparation: Protein concentration in placental homogenates and STB-EV pellets was quantified using a bicinchoninic acid (BCA) assay. Following protein quantification, equal amounts of protein (20-40 µg) were carefully measured and combined with predetermined volume of 4X Laemmli buffer (180 mM Tris-Cl (pH 6.8); 6% SDS; 30% glycerol; 0.3% 2-mercaptoethanol; and 0.0015% bromophenol blue, BioRad). Laemmli buffer serves a multitude of purposes in SDS-PAGE. It provides a reducing environment through the presence of β-mercaptoethanol, which disrupts disulfide bonds and linearizes protein structures. The SDS component acts as a detergent, denaturing proteins and ensuring they adopt a uniform negative

charge proportional to their molecular weight. The inclusion of glycerol in the Laemmli buffer contributes to sample viscosity, facilitating loading during electrophoresis. Finally, the Tris-HCl buffer maintains a consistent pH throughout the sample preparation and electrophoresis stages. β-mercaptoethanol was included in the Laemmli buffer used for PLAP, Cytochrome C, TSG101, and ALIX samples, as these proteins contain disulfide bonds that require reduction for optimal separation during electrophoresis. Conversely, β-mercaptoethanol was omitted from the Laemmli buffer used for CD63 samples, to preserve the protein's native structure. The samples were diluted to 20 µL with double distilled water (ddH_2O). Samples were then heated at 70°C for ten minutes for protein denaturation and an equal volume of sample was loaded.

Electrophoresis and membrane transfer: Electrophoresis was performed under reducing conditions (with β-mercaptoethanol) for PLAP, Cytochrome C, Syntenin, and ALIX, and under non-reducing conditions (without β-mercaptoethanol) for CD63. Precision Plus Protein™ Dual Colour Standards (Bio-Rad Laboratories Ltd.) served as protein size markers. Proteins were separated on NuPAGE TM 4-12% Bis-Tris Gel 1.0 mm x 10 well gels (Invitrogen by Thermo Fisher Scientific) at 150 V for 1-1.5 hours in a Novex minicell tank (Invitrogen, UK) filled with NuPAGE™ MOPS SDS running buffer (Novex by Life Technologies).

Following electrophoretic separation, proteins were transferred from the gel to polyvinylidene (PVDF) membranes (Bio-Rad) using a semi-dry transfer technique. Three distinct buffer solutions were employed during the transfer process, each serving a specific purpose:

- Anode Buffer Solution (Solution 1): This buffer, containing 300 mM Tris and 10% methanol at a pH of 10.4, serves two primary functions. High Tris concentration provides buffering capacity, maintaining a consistent pH throughout the transfer process and the inclusion of methanol facilitates protein denaturation and promotes protein interaction with the PVDF membrane.

- Anode Buffer Solution (Solution 2): This buffer, composed of 25 mM Tris, 20% methanol, and a pH of 10.4, acts as an intermediate layer between Solution 1 and the gel. Its composition is similar to Solution 1, ensuring a gradual transition in buffer conditions between the anode and the gel.
- Cathode Buffer Solution: This buffer, containing 25 mM Tris, 40 mM ε-aminohexanoic acid (ε-ACA), and 20% methanol at a pH of 10.4, plays a crucial role in protein transfer efficiency. ε-ACA functions as a spacer molecule. It minimizes protein interactions with the cathode buffer chamber, preventing non-specific protein adsorption and facilitating efficient protein transfer towards the PVDF membrane. Tris and methanol contribute to buffer capacity and protein denaturation, respectively.

Four filter paper sheets were pre-saturated in Anode Buffer Solution 1; two filter paper sheets were pre-saturated in Anode Buffer Solution 2; and three filter paper sheets were pre-saturated in Cathode Buffer Solution. Pre-saturating the filter papers ensures efficient protein transfer.

The assembled transfer cassette was then subjected to a constant voltage of 25 V for a duration of 45 minutes within the Novex semi-dry transfer apparatus (Life Technologies, UK).

Western blotting: PVDF membranes were blocked for one hour with 5% Blotto (2B Scientific) in 0.1% TBST (Tris-buffered saline (*20 mM Tris; 137 mM NaCl; pH 7.6*) and 1% Tween-20, Sigma) followed by overnight incubation with primary antibodies (PLAP, ALIX, Cytochrome C, Syntenin, and CD63).

After overnight incubation and washing steps with TBST (three times, each for five minutes), membranes were incubated with corresponding secondary antibodies, anti-mouse (P044701-2), or anti-rabbit (P044801-2) polyclonal goat immunoglobulins conjugated with horseradish peroxidase (HRP) (1:2000 dilution, Dako UK Ltd, Cambridge, UK) for one hour at room temperature. Membranes were then washed again with TBST (three times, each for five minutes)

and treated with the EZ-ECL chemiluminescence detection kit for HRP (Biological Industries Israel Beit Haemek, Israel) for one minute before being developed using both a gel documentation system (G-Box, Syngene, Cambridge UK) running GeneSys (version 1.5.0.0, Syngene) and a chemiluminescence film (Amersham HyperfilmTM ECL (enhanced chemiluminescence); GE Healthcare Limited, Buckinghamshire UK) to obtain the band intensity for each lane. Table 9 and 10 summarizes the list of reagents and antibodies used for western blot analysis, respectively.

2.1.4.5 Bicinchoninic acid (BCA) protein assay

Protein content in fresh STB-EVs and placental homogenate samples was determined using the BCA protein assay kit (Pierce). This colorimetric assay relies on the ability of BCA to chelate cupric ions (Cu^{2+}) in an alkaline environment. Proteins present in the samples reduce Cu^{2+} to cuprous ions (Cu^{+}), which subsequently form a purple-coloured complex with BCA. The absorbance of this complex at a specific wavelength (562 nm) is directly proportional to the protein concentration in the sample. A bovine serum albumin (BSA) stock solution (1 mg/mL) was serially diluted in fPBS to generate protein concentration standards (0.0625 mg/mL, 0.125 mg/mL, 0.25 mg/mL, 0.5 mg/mL, and 1.0 mg/mL). These standards were used to establish a standard curve for protein quantification.

Sample preparation: STB-EVs and placental homogenate samples were diluted in fPBS at 1:5 and 1:10 dilution ratio. Twelve and a half microliters (12.5 µL) of each BSA standard and diluted sample were added to a 96-well plate. One hundred microliters (100 µL) of BCA reagent mix, prepared by combining BCA solution (Thermo Scientific) and copper II sulphate solution (Thermo Scientific) in a 50:1 ratio, were added to each well.

Colorimetric detection and protein quantification: The plate was covered with aluminium foil and incubated on a shaker for 5 minutes at room temperature. Subsequently, the plate was incubated at 37°C for 30 minutes to facilitate colour change. All reactions were performed in duplicate to enhance data reliability. Following incubation, the absorbance of the samples and standards was measured at a wavelength of 562 nm using a FLUOStar OPTIMA (BMG) plate reader. The measured absorbance values for the standards were plotted against their corresponding protein concentrations to generate a standard curve. The protein concentration in each sample was then extrapolated from the standard curve based on its measured absorbance value.

Table 9 - Reagents used for western blot

Buffers	Power of hydrogen (pH)	Constituents
4X Laemmeli (reducing) buffer	6.8	9 parts 4X Laemmeli buffer 1 part β-mercaptoethanol
4X Laemmeli (non-reducing) buffer		4X Laemmeli buffer
Anode buffer solution 1	10.4	300 mM Tris base (36.34 g/L) 100% methanol (20 mL/L) 980 mL ddH_2O
Anode buffer solution 2	10.4	25 mM Tris base (3.0 g/L) 100% methanol (20 mL/L) 980 mL ddH_2O
Cathode buffer solution	9.4	25 mM Tris base (3.0 g/L) 40 nM 6-aminocaproic acid (5.2 g/L) 100% methanol (20 mL/L) 980 mL ddH_2O
10X TBS	8.0	NaCl (87.6 g) Tris base (12.1 g) 700 mL ddH_2O
TBST	8.0	10X TBS 0.1% Tween (1 mL) 900 mL ddH_2O
5% Milk in TBST		5 g Blotto in 100 mL TBST

Table 10 - Antibodies used in western blot

Antibody	Concentration	Dilution	Antigen	Manufacturer
Anti-PLAP	1.6 µg/µL	1:1000	PLAP	In-house antibody
Anti-ALIX	200 µg/µL	1:1000	ALIX	Santa Cruz Biotechnology
Anti-TSG101	xx µg/mL	1:1000	TSG101	Santa Cruz Biotechnology
Anti-CD63	200 µg/µL	1:1000	CD63	Santa Cruz Biotechnology
Anti-Cyt. C	200 µg/µL	1:1000	Cyt. C	Santa Cruz Biotechnology
Anti-KYNU	200 µg/µL	1:1000	KYNU	R&D
Anti-KMO	200 µg/µL	1:1000	KMO	R&D
Anti-KAT-III	200 µg/µL	1:1000	KAT-III	MyBioSource
Anti-mouse/rabbit immunoglobulin HRP conjugate		1:2000	Mouse/Rabbit immunoglobulins	Dako UK Ltd

Cyt.C – Cytochrome C; KYNU – Kynureninase; KMO – Kynurenine monooxygenase; KAT-III – Kynurenine aminotransferase III; PLAP – placental alkaline phosphatase; TSG – tumour suppressor gene

2.2 Specific methods

2.2.1 Immunohistochemistry

The following section details the methods employed for processing placental tissues obtained via biopsy and subsequent immunohistochemical (IHC) staining for target proteins. IHC staining was performed with the assistance of Maryam Rahbar (NDWRH, University of Oxford).

Tissue fixation and sectioning: Placental tissues were immersed in a 4% v/v paraformaldehyde (PFA) solution to preserve cellular morphology and were dehydrated through a series of graded alcohols and xylene. The tissue was then infiltrated and embedded in paraffin wax blocks to facilitate sectioning. Paraffin blocks were sectioned at a precise thickness of 10 μm using a microtome. These thin sections were mounted onto glass slides for further processing.

Immunohistochemical staining: Paraffin wax was removed from the tissue sections using a series of xylene and graded alcohol washes, followed by rehydration in water. To enhance the accessibility of target antigens within the tissue, sections were subjected to heat-induced epitope retrieval in a citrate buffer solution (10 mM sodium citrate, pH 6.0) for 10 minutes. This process facilitates antibody binding to the target protein. Endogenous peroxidase activity within the tissue was blocked using a 3% v/v hydrogen peroxide (H_2O_2) solution in PBS to prevent non-specific staining. To minimize background staining due to non-specific antibody binding, sections were incubated with a solution of 10% v/v foetal calf serum (FCS) (Sigma Aldrich, UK) in PBS containing Tween 20 (PBS-T) for one hour at room temperature. Tissue sections were incubated overnight at 4°C with a solution containing 1% FCS and primary antibodies specific to the target proteins of interest.

The primary antibodies used included:

- Anti-Kynureninase (KYNU) primary antibody (1 μg/mL, OriGene, USA)
- Anti-Kynurenine 3-Hydroxylase (KAT-III) primary antibody (1 μg/mL, Santa Cruz Biotechnology, USA)
- Anti-Kynurenine Monooxygenase (KMO) primary antibody (1 μg/mL, MyBioSource, USA)
- Non-immune mouse IgG1 control antibody (1 μg/mL, BioLegend, UK)

All primary antibodies were diluted in PBS-T. The non-immune mouse IgG1 served as a negative control for non-specific antibody binding. Following primary antibody incubation, sections were washed and incubated with an α-anti-mouse IgG secondary antibody conjugated to HRP (Life Technologies, UK) in 10% v/v FCS for one hour at room temperature. This secondary antibody binds specifically to the Fc region of the mouse primary antibodies used previously.

Detection and visualization: Tissue sections were washed extensively and then incubated with a HRP Substrate Kit with Nickel 3,3'-diaminobenzidine (DABVector Laboratories, USA) to visualize the location of the target proteins. DAB reacts with the bound secondary antibody-enzyme complex, resulting in a brown precipitate at the site of antigen localisation. Hematoxylin solution (Thermo Fisher, UK) was applied to stain cell nuclei for better visualization of cellular morphology under the microscope. The slides were dehydrated in graded ethanol and mounted with Depex (WPR).

Microscopy and image acquisition: Stained slides were examined using a Leica DMIRE 2 microscope. Images of the stained sections were captured using a Hamamatsu Orca digital camera and HCI software for further analysis.

2.2.2 Capillary electrophoresis and western blot analysis using Jess

This section describes the multiplexed immunoassay utilizing the Jess instrument (ProteinSimple) to quantify three target proteins: kynureninase (KYNU), kynurenine monooxygenase (KMO), and kynurenine Aminotransferase (KAT-III) in diluted pooled STB-EVs (mixture of m/lSTB-EVs and sSTB-EVs). This multiplex immunoassay allows for simultaneous detection of target proteins in a single experiment, improving efficiency and data throughput.

Sample preparation: Diluted pooled STB-EV samples were prepared from both normal pregnancy (NP, n=3) and early onset pre-eclampsia (EOPE, n=3) placental perfusions. Diluted liver cell lysate served as a positive control for KYNU, KMO, and KAT-III [kynurenine metabolising enzymes (KYNME)] detection. Liver tissue expresses KYNME, ensuring proper antibody response and signal generation. Diluted placental tissue lysate served as a positive control for PLAP detection. Placental tissue is rich in PLAP, confirming antibody specificity for the target protein in the STB-EVs.

Specific primary antibodies were chosen for each target protein:

- Goat anti-KYNU (R&D Systems, UK) diluted 1:10
- Rabbit anti-KMO (R&D Systems, UK) diluted 1:10
- Rabbit anti-KAT-111 (MyBioSource, USA) diluted 1:10
- Mouse anti-PLAP (NDOG2 in-house antibody) diluted 1:50

The dilution factors for each antibody were optimized to balance sensitivity and signal intensity.

Immunoassay procedure: Diluted pooled STB-EVs, positive controls, and protein samples were combined with the manufacturer-supplied fluorescent master mix. Heating at 95°C for 5 minutes facilitated protein denaturation and antibody binding accessibility. The protein samples, blocking reagent, primary antibodies (mentioned above), secondary horseradish peroxidase (HRP)-conjugated antibodies (ready-to-use detection modules specific for each primary antibody source), total protein detection reagent, chemiluminescent substrate, and wash buffer were all dispensed into designated wells in the Jess instrument's microplate. The plate was then loaded into the instrument, and proteins were automatically drawn into individual capillaries within a 13/25 capillary cassette, separating proteins based on size (12-230 kDa).

Data analysis: The Jess instrument utilizes proprietary Compass software for data acquisition and analysis. This software allows for automated signal detection, quantification, and generation of protein expression profiles.

2.2.3 Gas chromatography mass spectrometry

This section details the methodology employed for sample preparation and analysis by gas chromatography coupled with tandem mass spectrometry (GCxGC-MS).

Sample preparation: Frozen serum samples obtained from gestationally age-matched women diagnosed with EOPE (n = 9) and control subjects with normal pregnancies (n = 9) were thawed in a water bath set at 37°C. Kynurenine solution was prepared by dissolving 25 mg of L-Kynurenine [molecular weight: 208.22 mg/mmol, (Sigma Aldrich)] in 1200 mL of fPBS to achieve a final concentration of 100 µmol/L. The stock solution was diluted with fPBS (1:10) to achieve the desired concentration of 10 µmol/L. Two hundred microlitres (200 µL) of kynurenine solutions in 0.5 mL Eppendorf tubes were treated with (a) control solution [5 µL; (2.5 µL of STB-EVs (1 µg / µL) denatured with 2.5 µL of 100% trifluoracetic acid (Sigma

Aldrich)]; (b) 1 µg of STB-EV [5 µL; (1 µL of STB-EVs (1 µg/µL) diluted in 4 µL of fPBS)]; and (c) 5 µg of STB-EV [5 µL; (5 µL of STB-EVs (1 µg/µL)] for 5 minutes and 60 minutes duration in a shaker at 37°C. Five microlitres (5 µL) of 100% TFA was used as stop reagent to cease enzymatic activity.

Metabolite extraction: Unless otherwise specified, metabolite extraction was performed at room temperature. To a bead beater tube containing 100 µL of sample (kynurenine solution after treating with control and experimental conditions or serum), 800 µL of extraction solvent (isopropanol (IPA) with 1% trifluoracetic acid (TFA)) and 2.5 µL of internal standard solution (myristic acid-14,14,14-d3 in IPA, 1 mg/mL) were added. The mixture was homogenized in a bead beater (Precellys 24, Bertin Technologies) using a three-cycle protocol (5000 RPM x 20 seconds) with chilling between cycles using a dry ice bath. Following homogenization, the samples were incubated at -80°C for 60 minutes and then centrifuged at 13,000 x g for 20 minutes at 4°C. The aqueous supernatant was collected and transferred to a glass vial for overnight drying under vacuum (Speedvac).

Chemical derivatization: Chemical derivatization was performed according to a previously published method[198]. Briefly, the dried samples were resuspended in a 1:1:1 v/v mixture of N-Methyl-N-(trimethylsilyl)trifluoroacetamide (MSTFA) with 1% chlorotrimethylsilane (TMCS) and pyridine. The mixture was incubated for one hour at 60°C with shaking at 1200 rpm. Samples were then cooled to room temperature and directly injected for GCxGC-MS analysis.

GCxGC-MS analysis: The prepared samples were immediately analysed using a GCxGC-MS system consisting of a gas chromatograph coupled to a quadrupole mass spectrometer (Shimadzu GCMS-QP2010 Ultra) and a Shimadzu AOC-20i/s autosampler.

Chromatographic separation: The first-dimension separation utilized a SHM-5MS capillary column (30 m × 0.25 mm i.d. × 0.25 μm film thickness, Shimadzu). The second-dimension separation employed a BPX-50 capillary column (5 m × 0.15 mm i.d. × 0.15 μm film thickness, SGE).

Gas chromatography (GC) conditions: Helium gas served as the carrier gas at a constant inlet head pressure of 73 psi. The modulation period was set to 4 seconds. Samples were injected at 280°C with split ratios of either 1:1 or 1:10. The oven temperature program began with an initial hold at 100°C for 2 minutes, followed by a ramp to 220°C at 30°C/min with a hold at 220°C for 1 minute. Subsequently, the temperature increased to 280°C at 5°C/min with a hold for 1 minute, and finally reached a final temperature of 300°C with a hold for 2 minutes.

Mass spectrometry (MS) conditions: The interface temperature to the mass spectrometer was set at 300°C, and the ion source temperature was maintained at 230°C. The mass spectrometer operated at scan speeds ranging from 5000 to 20000 amu, covering a mass-to-charge ratio (m/z) range of 45–600. Electron ionization (EI) spectra were acquired at an ionization energy of 70 eV.

Data processing and analysis: Raw GCxGC-MS data were processed using a combination of software programs: GCMSsolution software (v2.72/4.20, Shimadzu), Chromsquare software (v2.1.6, Shimadzu), and GC Image (v2.3). In-house libraries including NIST 11/s, OA_TMS, FA_ME, and YUTDI were employed for data analysis.

Kynurenine annotation and quantification: Kynurenine was identified by comparing its retention time (adjusted to the internal standard myristic acid-14,14,14-d3) and mass spectrum with those of an external standard. Quantification of kynurenine was performed using the GCMS Solution software (v4.2) via accumulated single ion monitoring (m/z 307).

2.2.4 Methods for validation of selected miRNA with quantitative polymerase chain reaction (qPCR)

STB-EV RNA extraction and complementary DNA synthesis and quantitative polymerase chain reaction for selected miRNA targets were performed with the help of Toluwalase Awoyemi (NDWRH, University of Oxford). Serum EV RNA extraction and complementary DNA synthesis and quantitative polymerase chain reaction for selected miRNA targets were performed later.

2.2.4.1 RNA extraction from STB-EVs

This section details the methodology employed for m/lSTB-EVs RNA extraction. Total RNA was extracted from m/lSTB-EV samples using the ExoRNeasy Maxi Kit (Qiagen) according to the manufacturer's instructions. Prior to RNA isolation, samples were normalized based on protein content (200 μg) to ensure consistent RNA yield across samples. Each sample was then adjusted to a final volume of 200 μL with RNAse free water.

Carrier RNA and internal controls: To enhance RNA extraction efficiency and provide internal references for downstream analysis, two types of RNA controls were spiked into each STB-EV sample:

- M2 Phage RNA: 2 μL of a 1:25 dilution of a 5 nM stock solution of M2 Phage RNA was added to each sample. M2 Phage RNA serves as a carrier RNA, facilitating the binding and isolation of smaller RNA species present in EVs.
- External RNA Control Consortium (ERCC) RNA Spike-in Mix (Thermo Fisher Scientific): 1 μL of a 1:10,000 dilution of the ERCC RNA Spike-in Mix was added to each sample. The ERCC mix contains a defined set of synthetic RNA transcripts with varying lengths,

allowing for the evaluation of RNA integrity and potential biases during library preparation and sequencing.

RNA purification: The prepared sample mix (200 µL) containing m/lSTB-EVs, carrier RNA, and internal controls was loaded onto the ExoRNeasy Maxi Kit column. The column purification steps were followed as per the manufacturer's protocol to isolate high-quality RNA.

RNA quality assessment: The purity of the isolated RNA was initially evaluated using a Nanodrop spectrophotometer (NanoDrop 1000 software). All samples exhibited a 260/280 nm absorbance ratio greater than 1.8, which indicates a high degree of RNA purity with minimal protein contamination. Subsequently, the isolated RNA samples were sent to the Welcome Centre for Human Genetics (WCHG) for further analysis using a Bioanalyser (Agilent Technologies). The Bioanalyser provides information on RNA concentration and the RNA Integrity Number (RIN). However, it is important to acknowledge that RIN values are not necessarily indicative of RNA quality for EV-derived RNA. This is because EV-associated RNA is typically fragmented and lacks the prominent 18S and 28S ribosomal RNA peaks used in the RIN calculation[199]. All m/lSTB-EV samples yielded RIN values between 1 and 3.

2.2.4.2 RNA extraction from serum EVs

This section details the processing of frozen serum samples for subsequent serum EV RNA extraction. Frozen serum samples obtained from gestationally age-matched women diagnosed with EOPE (n = 8) and control subjects with normal pregnancies (n = 8) were thawed in a water bath set at 37°C.

RNA isolation: Following thawing, 800 µL of each serum sample were loaded onto individual ExoRNeasy Midi Kit (Qiagen) columns. The subsequent column purification steps were performed as per the manufacturer's instructions to isolate high-quality RNA from the serum samples.

Internal control: To normalize RNA yield across samples and facilitate downstream analysis, a *cel-miR-39* spike-in control was added to each serum sample. An aliquot of 1 µL from a 5 nM working solution of *cel-miR-39* (Integrated DNA Technologies, 100 nmol RNA Oligo) was introduced into each sample. *cel-miR-39* is a synthetic RNA molecule not naturally present in human serum. Its presence allows for normalization of RNA extraction efficiency and serves as an internal reference for subsequent analyses.

RNA quality assessment: The purity of the isolated RNA was evaluated using a Nanodrop spectrophotometer (NanoDrop 1000 software). All samples exhibited a 260/280 nm absorbance ratio greater than 1.8.

2.2.4.3 Complimentary DNA synthesis for miRNA synthesis

Complementary DNA (cDNA) was synthesised from the isolated RNA samples (m/lSTB-EVs and serum EVs) using the TaqMan™ Advanced miRNA cDNA Synthesis Kit (Applied Biosystems, A28007). All reaction steps were performed on ice following the manufacturer's instructions to ensure optimal enzyme activity and minimize RNA degradation.

Reverse transcription: The reverse transcription reaction consisted of four sequential stages:

- **Poly(A) tailing:** MicroRNAs (miRNAs) are short, non-coding RNA molecules that lack a poly(A) tail at the 3' end, unlike messenger RNAs (mRNAs). This lack of a poly(A) tail presents a challenge for reverse transcription enzymes. To overcome this hurdle, an artificial poly(A) tail was added to the 3' end of each miRNA molecule, facilitating its recognition and subsequent reverse transcription.
- **Adaptor ligation:** An adaptor oligonucleotide was then ligated to the poly(A) tail, providing a primer binding site for the reverse transcriptase enzyme.
- **Reverse transcription:** The reverse transcription reaction was carried out using a reverse transcriptase enzyme to convert the single-stranded RNA molecules (miRNAs) into their complementary double-stranded cDNA counterparts.
- **miR-amplification:** An additional amplification step was included in the protocol to enrich the reverse-transcribed miRNA targets. This step helps to improve the sensitivity of downstream qPCR analysis.

Each reverse transcription reaction was performed in a G-Storm™ thermocycler (G-storm) using the thermal cycling conditions specified by the manufacturer's protocol. Following reverse transcription, 10 µL aliquots of the cDNA samples were subjected to preamplification. Un-amplified cDNA samples were aliquoted and stored at -80°C for future use.

Preamplified cDNA samples were diluted 1:5 with nuclease-free 0.1X TE buffer before use in subsequent qPCR reactions. In cases where qPCR analysis could not be performed on the same day as preamplification, aliquots of the diluted preamplified cDNA were stored at either 4°C (for less than 2 days) or -20°C (for less than a month) to minimize potential degradation.

2.2.4.4 Quantitative polymerase chain reaction (qPCR)

Based on the fold-change observed in the RNA sequencing data obtained from Toluwalase Awoyemi's (NDWRH, University of Oxford) previous work, six microRNAs (miRNAs) were chosen for validation using qPCR: *hsa-miR-3196; hsa-miR-4488; hsa-miR-4516; hsa-miR-9-5p; hsa-miR-210-3p; and hsa-miR-193b-5p*. Table 11 summarizes the miRNA primers used in the experiment.

qPCR analysis using TaqMan™ gene expression assay: TaqMan™ gene expression assays (Applied Biosystems, USA) were employed for the validation of these differentially expressed miRNAs.

qPCR master mix preparation: A qPCR master mix was prepared for each reaction plate. The master mix contained the following components per reaction:

- 1 µL of 20X TaqMan™ Gene Expression Assay for the specific miRNA of interest
- 10 µL of 2X TaqMan™ Gene Expression Master Mix (contains Taq DNA polymerase, dNTPs, and optimized buffer conditions)
- 7 µL of RNase-free water

Eighteen microliters (18 µL) of this master mix were added to each well of a 96-well reaction plate (MicroAmp™ Optical 96-Well Reaction Plate, Thermo Fisher Scientific) containing 2 µL of preamplified cDNA sample. The plate was then sealed with a MicroAmp™ Optical Adhesive Film to prevent evaporation during thermal cycling.

Real-time PCR conditions: The qPCR reactions were carried out on a QuantStudio™ 3 Real-Time PCR System (Thermo Fisher Scientific) using the following cycling parameters:

- Hold: 50°C for 2 minutes (enzyme activation)
- Hold: 95°C for 20 seconds (initial denaturation)
- Followed by forty (40) cycles of:
    - Denaturation: 95°C for 1 second
    - Annealing/Extension: 60°C for 20 seconds (FAM™ channel acquisition)

Fluorescence data was collected during the annealing/extension step of each cycle. The QuantStudio™ Design and Analysis Desktop Software (Thermo Fisher Scientific) automatically generated cycle threshold (Ct) values based on the fluorescence intensity curves. All miRNAs tested were detected before 30^{th} cycle.

Data analysis and normalization: Raw Ct values obtained from the software were exported to an Excel spreadsheet for further analysis. *hsa-miR-30d-5p* was selected as the internal reference miRNA for normalization of STB-EV qPCR data.

This selection was based on the following criteria identified from the RNA sequencing data:

- Fold change (FC) less than 0.001 between PE and normal samples (minimal differential expression)
- Low standard error indicating consistent expression levels

The stability of *hsa-miR-30d-5p* as a reference gene was further validated using an independent qPCR experiment. *cel-miR-39-3p* was used as the reference for normalization of serum EV qPCR data.

Fold change (FC) calculation and statistical analysis: FC values for each target miRNA relative to *hsa-miR-30d-5p / cel-miR-39-3p* were calculated using the $2^{-\Delta\Delta Ct}$ method[200]. Statistical analysis was performed on ΔCt values using one-tailed Student's *t-test* to assess significant differences in miRNA expression between groups. A *p*-value of less than 0.05 was considered statistically significant. GraphPad Prism (*v10.2.2*, Boston, MA, USA) was used to create graphical representations of the data. Fold-change values are presented with error bars representing the standard error.

Table 11 - qPCR primers, miRNA sequence and assay ID

MicroRNA primers	MicroRNA sequence	Assay ID
hsa-miR-3196	CGGGGCGGCAGGGGCCUC	483159_mir
hsa-miR-4488	AGGGGGCGGGCUCCGGCG	478906_mir
hsa-miR-4516	GGGAGAAGGGUCGGGGC	478303_mir
hsa-miR-9-5p	UCUUUGGUUAUCUAGCUGUAUGA	478214_mir
hsa-miR-210-3p	CUGUGCGUGUGACAGCGGCUGA	477970_mir
hsa-miR-193b-5p	CGGGGUUUUGAGGGCGAGAUGA	478742_mir
hsa-miR-30d-5p	CUUUCAGUCAGAUGUUUGCUGC	479362_mir
cel-miR-39-3p	UCACCGGGUGUAAAUCAGCUUG	478293_mir

2.2.5 Cell culture: human cerebral microvascular endothelial cells (hCMEC/D3)

Human cerebral microvascular endothelial cells (hCMEC/D3) used in the experiments were kindly donated by Professor Yvonne Couch (Radcliffe Department of Medicine, University of Oxford).

The first step involved preparing the flasks for cell attachment. T75 (75 cm^2) flasks were coated with gelatin (Sigma Aldrich) solution (diluted to 1% v/v with autoclaved deionised water), providing a suitable surface for hCMEC/D3 adhesion. The cells were cultured in complete EGM-2 endothelial cell growth medium supplemented with Bullet Kit (Lonza) and 1% v/v penicillin-streptomycin antibiotics cocktail. This rich medium contains essential nutrients, antibiotics to prevent bacterial contamination, and various growth factors that stimulate hCMEC/D3 proliferation and maintain their specific characteristics.

hCMEC/D3 were passaged from a confluent T75 flask for re-seeding. The spent culture medium was removed, and the adherent cells were then gently washed with PBS to remove any residual serum proteins or debris from the culture medium. Trypsin, a protease enzyme, is introduced to break down the protein linkages between the hCMEC/D3 and the gelatin-coated flask surface. The incubation time with trypsin was carefully monitored to ensure sufficient detachment of the cells without harming them. After trypsinization, the inactivating solution, containing 10% FBS in complete EGM-2 medium, was added to stop the trypsin's activity and prevent further cell damage. The cell suspension was then collected and centrifuged at 1300 RPM for 3 minutes to pellet the detached hCMEC/D3. The resultant supernatant was carefully discarded without disturbing the cell pellet and the pellet was resuspended in 1 – 2 mL of fresh complete EGM-2 medium.

Following centrifugation, the viable cell count was determined using a trypan blue exclusion assay. Trypan blue is a dye that only penetrate cells with compromised membranes, staining them blue. Viable cells, with intact membranes, remain unstained. By combining the cell suspension with trypan blue and using an automated cell counter, the total number of viable hCMEC/D3 was accurately determined.

The seeding density of hCMEC/D3 were determined as 6 – 7 x 10^6 cells per flask. The calculated volume of the cell suspension is then transferred to a new gelatin-coated flask containing fresh complete EGM-2 medium. The flask was incubated at 37°C in a humidified atmosphere with 20% O_2 and 5% CO_2. The medium was changed every 2-3 days to replenish essential nutrients and remove waste products. When hCMEC/D3 reached near confluency, typically covering about 80% - 90% of the flask surface, they were passaged again to maintain a healthy and actively growing cell population or for use in downstream experiments. Gentle pipetting techniques were used while handling hCMEC/D3, to minimize cell damage, as they were sensitive to shear stress. All experiments using hCMEC/D3 in this thesis were completed between passages of 40 – 45.

2.2.6 Cell proliferation and viability assay

Cell proliferation assay: To assess the effect of *hsa-miR-9-5p* on human cerebral microvascular endothelial cell (hCMEC/D3) proliferation, a colorimetric cell viability assay was performed. hCMEC/D3 were seeded at a density of 2 X 10^5 cells/well in 12-well plates (coated with 1% gelatin) and allowed to adhere overnight. The cells were then treated with either vehicle control (mirVana™ miRNA Mimic, Negative Control #1, ThermoFisher) or two different concentrations of *hsa-miR-9-5p* mimic [(5nM and 10nM), mirVana™ miRNA Mimic, ThermoFisher] for 2, 24, and 48 hours. Lipofectamine RNAiMAX transfection reagent

(ThermoFisher) was used for the transfection of hCMEC/D3 with the miRNA mimics as described in the manufacturer protocol.

Cell counting and viability determination: Following treatment, cell number and viability were determined using a trypan blue exclusion assay. After each time point, cells were detached from each well using trypsin. After trypsinization 10% FBS in complete EGM-2 medium was added and the cell suspension was collected and centrifuged at 1300 RPM for 3 minutes to pellet the detached hCMEC/D3. The resultant supernatant was discarded the pellet was resuspended in 500 µL of fresh complete EGM-2 growth medium. An aliquot of 10 µL of the cell suspension was then mixed with an equal volume of trypan blue stain. Trypan blue is a vital dye that can permeate the cell membrane of dead or damaged cells, staining their cytoplasm blue. Conversely, viable cells with intact membranes remain unstained and appear bright under a microscope.

The total number of cells (both viable and dead) was determined using TC20^{TM} automated cell counter (Bio-Rad). The percentage of viable cells was then calculated by dividing the number of unstained (viable) cells by the total number of cells counted and multiplying by 100. This method provides a quantitative assessment of cell viability within each treatment group.

The cell proliferation assay was performed independently three times to ensure reproducibility of the results. Following the final time point (48 hours), remaining cells from each treatment group were collected as cell lysates using Lysis Buffer [1% Igepal CA-630, 20 mM Tris-HCl (pH 8.0), 137 mM NaCl, 10% glycerol, 2 mM EDTA, 10 µg/mL Aprotinin, 10 µg/mL Leupeptin, and 10 µg/mL Pepstatin] for further analysis with Proteome Profiler^{TM} Array (R&D Systems).

2.2.7 Cell migration assay

To assess the migratory capacity of human cerebral microvascular endothelial cells in response to *hsa-miR-9-5p* miRNA mimic and negative control, a wound healing assay was performed.

Cell seeding and gap creation: Human cerebral microvascular endothelial cells were seeded at a density of 2 x 10^4 cells/well in a 2-well insert with a defined width of 500 µm (Ibidi) placed in the wells of a 12 well culture plate (coated with 1% gelatin). This insert creates a standardized gap between the seeded cells upon removal. After overnight incubation to allow for cell attachment and spreading, the inserts were carefully removed, creating a uniform cell-free area in each well.

Treatment and image capture: Following insert removal, the cells were treated with either EGM-2 growth medium or negative scramble (mirVana™ miRNA Mimic, Negative Control #1, ThermoFisher) or different concentrations (1.25 nM, 2.5 nM, 5 nM and 10 nM) of *hsa-miR-9-5p* (ThermoFisher).

To establish optimal conditions for the migration assay, two preliminary experiments were conducted. Experiment A compared the migration of cells in EGM-2 growth medium. This experiment aimed to determine the optimal assay duration, with 16 hours being chosen as the time it takes for cells to migrate across the gap. Experiment B then focused on identifying the optimal dose of the *hsa-miR-9-5p* mimic. Cells were treated with 5 nM to 10 nM concentrations of *hsa-miR-9-5p*, and negative scramble, and their migration was compared between 0 and 16 hours. This experiment revealed 10 nM to be the most effective concentration for the miRNA mimic. Finally, the effect of *hsa-miR-9-5p* (10 nM) on hCMEC/D3 migration was measured every 2 hours from 0 to 16 hours, with an additional time point captured at 24 hours.

Both treatment and control conditions were performed in triplicate wells for statistical analysis. Brightfield images of the cell cultures were captured at regular intervals (every 2 hours) using an Olympus CKX53 microscope equipped with a 4x objective lens.

Quantification of cell migration: ImageJ2 software (*v2.14.0/1.54f*; NIH, USA) was used to analyse the captured images. The area of the cell-free gap was measured at each time point for treatment and control groups. Graphical representation was generated in R (*v4.3.1*) software, plotting the cell-free gap area and time for both treatment and control group. The mean area of cell-free wound gap was compared at each time point using unpaired T-test with Bonferroni correction and the statistical significance was set at $p < 0.05$.

2.2.8 Identification of angiogenesis-related protein expression using human angiogenesis array kit

The expression profile of proteins associated with angiogenesis was determined using the Proteome Profiler™ Human Angiogenesis Antibody Array Kit (R&D Systems), following the manufacturer's instructions. This kit employs a nitrocellulose membrane containing an array of 55 pre-spotted antibodies targeting key proteins involved in angiogenesis.

Cell lysis and protein extraction: Human cerebral microvascular endothelial cells were treated as previously described (Section 2.2.6) with either vehicle control or *hsa-miR-9-5p* (10 nM) for 48 hours. Following treatment, the cells were washed thoroughly with fPBS and centrifuged at 1300 rpm for 3 minutes to form a cell pellet. The supernatant was carefully aspirated to avoid disturbing the pellet. The cell pellet was then lysed using a lysis buffer containing 1% Igepal CA-630, 20 mM Tris-HCl (pH 8.0), 137 mM NaCl, 10% glycerol, 2 mM EDTA, 10 µg/mL Aprotinin, 10 µg/mL Leupeptin, and 10 µg/mL Pepstatin according to manufacturer protocol (R&D Systems). Briefly, the lysis buffer was added to the pellet, followed by resuspension with

pipetting. The suspension was then rocked at 2–8°C for 30 minutes to facilitate cell lysis. After rocking, the lysate was centrifuged at 14,000 x g for 5 minutes to separate the cellular debris from the soluble protein fraction. The clarified supernatant, containing the extracted proteins, was carefully collected into a clean microcentrifuge tube for protein quantification using the BCA assay (described previously). The lysates were used immediately for the subsequent proteome array experiment.

Antibody array processing: Aliquots of 1.5 mL of each sample (supernatant + array buffer 4) were then combined with 15 µL of the biotinylated detection antibody cocktail provided in the kit. This mixture was incubated for 1 hour at room temperature to allow for specific binding between the biotinylated antibodies and the target proteins present in the cell lysate supernatants. The nitrocellulose membranes containing the antibody array were subsequently blocked (using array buffer 7) according to the manufacturer's instructions to minimize non-specific binding. The blocked membranes were then incubated with the cell lysate supernatant + antibody mixtures overnight at 2–8°C on a rocking platform to facilitate efficient capture of the target proteins by the immobilized antibodies on the array. After overnight incubation, the membranes were washed thoroughly using the provided wash buffer to remove unbound materials.

Chemiluminescent detection and quantification of protein expression: Following the washing steps, streptavidin-conjugated horseradish peroxidase (HRP) and chemiluminescent detection reagents were added sequentially to the membranes according to the manufacturer's protocol. The streptavidin-HRP binds to the biotinylated detection antibodies, while the chemiluminescent substrate generates a light signal upon reaction with HRP. The intensity of the chemiluminescent signal on the membranes was captured using X-ray film. Higher signal intensity corresponded to a greater abundance of the specific protein captured by the corresponding antibody on the array. The captured X-ray film was then scanned using a transmission-mode scanner, and the resulting image file was analysed using ImageJ2 software

(*v2.14.0/1.54f*; NIH, USA) with the Protein Array Analyzer plugin. The intensity of the chemiluminescent signal for each spot on the array was quantified and normalized to the reference spots. Log transformed data of differential expression of proteins were considered for data interpretation.

2.2.9 Protein-protein interaction network construction and cluster analysis

Protein-protein interaction (PPI) network of differentially expressed angiogenesis-related proteins identified from the Proteome Profiler™ Human Angiogenesis Antibody Array Kit analysis was constructed using the Search Tool for the Retrieval of Interacting Genes (STRING) database (*v11.5*) (https://string-db.org)[201]. The list comprising differentially expressed angiogenesis-related proteins was uploaded onto the platform, and the network was filtered to exhibit interactions solely with a high confidence score (≥ 0.7). To enhance the visualization of the PPI network and elucidate additional biological processes and molecular functions, a second shell comprising ten interacting proteins was incorporated based on known protein-protein interactions. After network establishment, pertinent gene ontology terms encompassing biological processes, cellular components, and molecular functions, alongside Kyoto Encyclopedia of Genes and Genomes (KEGG) pathways, were delineated.

2.2.10 VCAM-1 expression analysis following TNF-α stimulation

This section describes the evaluation of VCAM-1 protein expression in human cerebral microvascular endothelial cells following stimulation with tumour necrosis factor-α (TNF-α) as described previously[202]. VCAM-1 is a cell adhesion molecule upregulated on the endothelial cell surface during inflammatory activation. This experiment aimed to investigate whether *hsa-miR-9-5p* treatment modulates VCAM-1 expression in response to TNF-α stimulation.

Cell seeding and pre-treatment: hCMEC/D3 were seeded at a density of 1 x 10^5 cells per well in a 12-well plate pre-coated with 1% gelatin solution. The cells were then incubated under standard culture conditions to allow for proliferation and adherence.

miR-9-5p treatment: Once the cells reached approximately 80% confluence, they were divided into two groups: Vehicle control; and *hsa-miR-9-5p* (10 nM). Each group was cultured in triplicate wells for statistical analysis. hCMEC/D3 were treated with their respective conditions (vehicle control or *hsa-miR-9-5p*) for 48 hours.

TNF-α stimulation and supernatant collection: Following the 48-hour pre-treatment period, the cell culture supernatants were removed from each well. The cells were then gently washed with 1 mL of fPBS to remove any residual treatment media. One millilitre of fresh supplemented EGM-2 growth medium was added to each well. In the treatment groups designated for TNF-α stimulation, the medium was further supplemented with recombinant human TNF-α (R&D Systems) at a final concentration of 10 ng/mL. The control groups were treated with equal volume of fresh supplemented EGM-2 growth medium. The cells were then incubated with control or TNF-α for an additional 16 hours to induce VCAM-1 expression. After the 16-hour stimulation period, the supernatants from each well were carefully collected and centrifuged at 1,000 x g for 10 minutes to pellet any cellular debris. The clarified supernatants were transferred to clean Eppendorf tubes and were analysed immediately.

VCAM-1 detection by ELISA: VCAM-1 protein levels in the cell culture supernatants were quantified using the commercially available human VCAM-1/CD106 DuoSet ELISA kit (R&D Systems) according to the manufacturer's instructions. This ELISA assay employs a sandwich immunoassay format to specifically detect and quantify VCAM-1 protein present in the samples.

Briefly, the ELISA involves a series of incubation steps with capture and detection antibodies coated onto a microtiter plate. The amount of bound VCAM-1 is then determined using a colorimetric horseradish peroxidase (HRP) enzymatic reaction. The intensity of the colorimetric signal is directly proportional to the concentration of VCAM-1 protein in the sample, allowing for its quantification by measuring absorbance at a specific wavelength using a microplate reader.

CHAPTER 3:

ISOLATION, ENRICHMENT AND CHARACTERIZATION OF SYNCYTIOTROPHOBLAST-DERIVED EXTRACELLULAR VESICLES

Abstract

Introduction: Syncytiotrophoblast-derived extracellular vesicles (STB-EVs) are gaining interest due to their potential roles in pregnancy. I aimed to establish a protocol for isolating and enriching medium/large STB-EVs (m/lSTB-EVs) and small STB-EVs (sSTB-EVs) from placental perfusate.

Methods: Placental perfusate was obtained after *ex vivo* dual lobe perfusion. Differential ultracentrifugation (dUC) was employed for enrichment, with centrifugation parameters reported following ISEV guidelines. Characterisation involved particle number quantification (NTA), protein composition analysis (Western blot), transmission electron microscopy (TEM), flow cytometry, and particle size analysis (NTA).

Results: The dUC protocol successfully enriched m/lSTB-EVs and sSTB-EVs. Particle quantification revealed higher concentrations of sSTB-EVs compared to m/lSTB-EVs. Western blot confirmed the presence of EV marker proteins (CD63, TSG101, and ALIX) and the absence of a negative marker (cytochrome C), indicating EV purity. TEM visualized cup-shaped EVs with a lipid bilayer membrane. NTA analysis confirmed size distribution consistent with expected ranges for both STB-EV sub-types.

Conclusion: This study presents a detailed protocol for STB-EV isolation and enrichment, acknowledging limitations of dUC regarding co-precipitation of contaminants. The multi-faceted characterisation approach strengthens the evidence for successful isolation of bona fide STB-EVs. The established protocol enables further investigations into the functional roles and potential applications of placental EVs in pregnancy-related research and therapeutics.

3.1 Introduction

Extracellular vesicles (EVs) represent a heterogeneous population of particles released by cells. These particles are delimited by a phospholipid bilayer membrane and lack the capacity for self-replication, as they do not contain a functional nucleus[117,118]. Despite initial attempts to categorize extracellular vesicles (EVs) based on their biogenesis – "exosomes" originating from internal compartments and "ectosomes" (also known as microvesicles or microparticles) budding from the cell surface[203,204] – this classification system faces significant limitations. Current isolation techniques often collect a heterogeneous mixture of EVs, making it difficult to differentiate them based solely on their origin. This lack of clear differentiation creates a problem for interpreting research findings. Studies based on isolated "exosomes" or "ectosomes" likely contain a broader range of EVs, potentially obscuring the specific functions of each subtype.

To address this challenge, the International Society for Extracellular Vesicles (ISEV) recommends reserving terms like "exosome" and "ectosome" for situations where researchers have demonstrably purified specific EV populations. In most cases, current methods cannot definitively isolate EVs based solely on their biogenesis pathway. Therefore, the ISEV encourages the use of operational terms like "medium/large EVs" (> 200nm) and "small EVs" (< 200nm) to acknowledge this limitation[117,118].

EVs are emerging as crucial players in cell-to-cell communication[205] as they act as messengers, shuttling various cargo molecules, including proteins, lipids, and nucleic acids (DNA, mRNA, miRNA) between cells[205–208]. This intercellular communication is essential for maintaining tissue homeostasis and coordinating complex physiological processes throughout the body. The specific cargo carried by EVs allows them to influence the recipient cell's behaviour in various ways. Proteins on the EV surface interact with receptors on target cells, triggering signalling

pathways that alter gene expression and cellular function[209,210]. The encapsulated nucleic acids in the EVs can be delivered to recipient cells, potentially influencing their protein synthesis and overall activity[211,212].

Placental EVs play a pivotal role in intercellular communication modulating complex physiological and pathological processes in pregnancy.

Placental EVs in physiological pregnancy: EVs act as critical regulators of temporal sequences and cell-to-cell signalling impacting processes like embryogenesis and embryo-maternal cross talks[213]. Placental EVs are known to mediate communication between the foetus and the mother[214,215]. They carry signalling molecules, such as miRNAs, that (a) modify the transcriptome of maternal endometrial cells facilitating extracellular matrix remodelling and subsequent placental establishment[216,217]; and (b) regulate trophoblast cell invasion[218] and uterine spiral artery remodelling[219,220] to ensure successful implantation. Placental EVs promote maternal immune tolerance and prevent foetal rejection by transferring their cargo to maternal immune cells such as Natural Killer (NK) cells[221–223], macrophages[224–226], and T cells[221,227,228]. Placental EVs in maternal circulation modulate endothelial cell migration and contribute to the vascular adaptation seen in pregnancy to accommodate hypervolaemia[229]. Placental EVs are known to promote angiogenesis by delivering pro-angiogenic factors to endothelial cells[196,230], facilitating the development of new blood vessels that supply oxygen and nutrients to the developing baby.

Placental EVs in pathological pregnancy: The communication capabilities of placental EVs can also be exploited during pathological processes like preeclampsia (PE)[231] and gestational diabetes mellitus (GDM)[232]. Placental EVs are proinflammatory in early onset preeclampsia (EOPE)[233,234] expressing more proinflammatory cytokines (TNF-α, IL-1, IL-6, IL-8) in neutrophils; B- and T-lymphocytes; and monocytes[173,174]. Preeclamptic EVs (a) demonstrate

reduced endothelial nitric oxide synthase (eNOS) activity, contributing to vascular dysfunction and hypertension[235]; (b) enhance cellular oxidative stress and endothelial dysfunction by transferring miRNAs and mitochondrial DNA from dysfunctional syncytiotrophoblasts[236]; and (c) scavenge proangiogenic factors (PlGF, VEGF, TGF- β) and inhibit endothelial tube formation *in vitro*, translating to anti-angiogenesis[122]. Placental EVs in preeclampsia promote abnormal coagulation by activating platelets[237] and expressing procoagulant factors, such as tissue factor[238], anionic phospholipids[181], and plasminogen activator inhibitor-I[182]. Placental EVs in GDM (a) differentially express miRNAs that are involved in insulin regulation and glucose metabolism[239,240] and (b) express 8-fold more Dipeptidyl peptidase IV (DPPIV), which favours insulin resistance by decreasing circulating glucagon like peptide-1[232].

3.2 Aims

The aims of this chapter are:

1. to review the existing techniques for placental EV isolation and enrichment
2. to describe the isolation, enrichment, and characterisation of STB-EVs as prescribed in the minimal information for studies of extracellular vesicles 2018 (MISEV2018)[117] and MISEV 2023[118].

3.3 Methods of isolation and enrichment for placental EVs

3.3.1 Methods for isolation and enrichment of EVs

Methods for EV isolation in general are based on the principles of centrifugation, filtration, precipitation, and affinity interaction[241]. Isolation of EVs from complex biological samples often require a combination of different techniques such as differential centrifugation[242–244]; density gradient centrifugation[243,244]; ultrafiltration[244]; affinity-based method precipitation[243–245]; and size exclusion chromatography[243,244,246]. Each of these methods' present advantages and disadvantages. The choice of the method of isolation and enrichment is guided by the biological source material and planned downstream experiments.

Different isolation techniques, their principles, advantages, and disadvantages reported in the guidelines presented by ISEV[117,118,247] are summarised in table 12.

Table 12 - Summary of EV isolation techniques

Method	Principle	Advantages	Disadvantages
Differential centrifugation	EV isolation with consequent centrifugation steps (from 300 x g to 150,000 x g): cells, platelets and large apoptotic bodies depleted by low-speed centrifugation. Larger EVs (~10,000 x g) and smaller EVs (~150000 x g) are then pelleted.	Most used Intermediate recovery and specificity	Time consuming EV protein aggregates, lipoprotein particles, and other contaminants may sediment
Density gradient centrifugation	EV isolation by establishing density gradients of sucrose / iohexol / iodixanol.	High purity	Applicable to small volume of samples
Ultrafiltration	EVs filtered at different MW cut-offs.	Recovery and purity dependent on consequent centrifugation	Low specificity EV may adhere to filter Filtering may damage EVs
Precipitation	EVs precipitated with organic solvents / chemical compounds such as PEG, sodium acetate or protamine.	High recovery Fast Easy to perform	Low specificity Co-precipitation of contaminants (lipoproteins)
Size exclusion chromatography	EVs separated by their ability to pass through a resin packed column.	High purity	Not suitable for larger volumes of sample

Affinity isolation	EVs bind to specific antibodies against EV-specific surface antigens.	High purity	Low recovery Requires specific antibody
Microfluidic devices	On-chip EV isolation including immunoaffinity capture, size-based filtration, and physical trapping.	High throughput Low processing time	Not suitable for larger volumes of sample
Nanoscale flow cytometric sorting	Fluorescent labelled EVs sorted using flow cytometer	Very specific High purity	Time consuming

MW – molecular weight; PEG – polyethylene glycol

3.3.2 Isolation and enrichment of trophoblast derived EVs

In trophoblast-derived extracellular vesicle (EV) isolation, methods typically fall within two overarching categories: (a) tissue-based and (b) cell-based approaches. Tissue-based methods, such as mechanical isolation, placental explant culture, and placental perfusion, are utilized to generate syncytiotrophoblast-derived EVs (STB-EVs). On the other hand, cell-based methods involve the use of trophoblast-derived cell lines, such as those derived from the BeWo cell line or trophoblast-derived cell lines from either the first or second trimester of pregnancy. The method used to isolate placental EVs can significantly influence their cargo and downstream effects[248,249]. Therefore, it is essential to critically evaluate the available methods and select the appropriate method or methods for placental EV isolation.

3.3.2.1 Mechanical STB-EV isolation

The process for generating mechanical STB-EVs (mSTB-EVs) involves several steps. Initially, 10 to 20 g of placental tissue are spread out manually and then rapidly washed in ice-cold isotonic $CaCl_2$ solution followed by ice-cold Kreb's physiological saline. This step removes much of the blood from intervillous space. Subsequently, the placental tissue is transferred to ice-cold 0.9% normal saline and subjected to gentle mechanical agitation at 0°C for a duration of 30 minutes using a magnetic stirrer. This enabled spreading out of chorionic microvilli so that their surfaces are well irrigated. Mechanical agitation is followed by a series of differential centrifugation steps aimed at isolating the desired mSTB-EVs. The first centrifugation step is performed at 800 x g for 10 minutes to remove red cells and cellular debris. This is followed by a centrifugation at 10,000 x g for 5 minutes to eliminate larger particles and intracellular debris. Finally, a centrifugation at 100,000 x g for 60 minutes is conducted to pellet the mSTB-EVs[250]. Even though the described procedure is simple, rapid and provides a good yield of mSTB-EVs,

there is co-precipitation of other contaminants reducing the purity of the pellet. Gupta *et al*. have compared the effect of STB-EVs generated by mechanical disruption, explant culture and placental perfusion on human umbilical vein endothelial cells (HUVEC)[251] and have demonstrated that mSTB-EVs inhibited HUVEC proliferation; disrupted HUVEC monolayer; and induced apoptosis compared to EVs isolated by other methods. Thus, it is now established that mechanical disruption of placental villi is a poor method for collecting physiologically relevant trophoblast derived EVs[251].

3.3.2.2 *In vitro* explant culture-derived STB-EVs

Traditionally placental EVs have been collected by culturing placental villous explants in a minimally disruptive static system for 24-96 hours followed by differential centrifugation for EV isolation[252]. The process of isolating *in vitro* explant culture-derived STB-EVs (eSTB-EVs) involves two main steps:

***In vitro* placental explant culture**[253]**:** This step is performed in a laminar flow hood under sterile conditions. Once the placenta is received, the top 2 mm of the maternal facing placenta is dissected and discarded and ~2 cm^3 (x 3) of underlying villous placental tissues are dissected out. The dissected tissue is rinsed thoroughly in sterile PBS. Washed pieces of tissue are further dissected into explants of approximately 400 mg. As shown in figure 7, the inserts are placed in a 12-well culture plate, creating two compartments. Placental explants are placed in the upper compartment and 3 mL of advanced DMEM/F12 (supplemented with 10% v/v foetal bovine serum (FBS); 5 ng / mL epidermal growth factor (EGF); 5 µg / mL insulin; 10 µg / mL transferrin; 20 nM sodium selenite; 400 U/L human chorionic gonadotropin; 100 U / mL penicillin; 100 µg / mL streptomycin; and 0.25 µg / mL amphotericin B) is added. The plates are sealed with micropore tape and cultured in an incubator set at 37°C, 20% O_2, and 5% CO_2 for 24 – 72 hours.

Isolation of EVs[253]**:** Following the incubation period, the cultured medium containing the STB-EVs undergoes a series of differential ultracentrifugation steps. Centrifugation at 2000 x g for 5 minutes at 4°C to sediment red cells and other contaminating cellular debris and the supernatant enriched in STB-EVs is collected and ultracentrifuged to isolate of m/lSTB-EVs (20,000 x g for 60 minutes at 4°C) and sSTB-EVs (100,000 x g for 60 minutes at 4°C). The pellets are resuspended in sterile fPBS for characterisation and downstream analysis.

While both placental explant culture and perfusion techniques effectively isolate STB-EVs from intact term placentae, limitations arise when dealing with first-trimester or early second-trimester samples. These early placentas are often smaller and lack the extensive villous development necessary for successful perfusion. In this scenario, explant culture becomes the primary viable isolation method[253]. However, a key drawback of explant culture is the generally lower yield of EVs compared to placental perfusion.

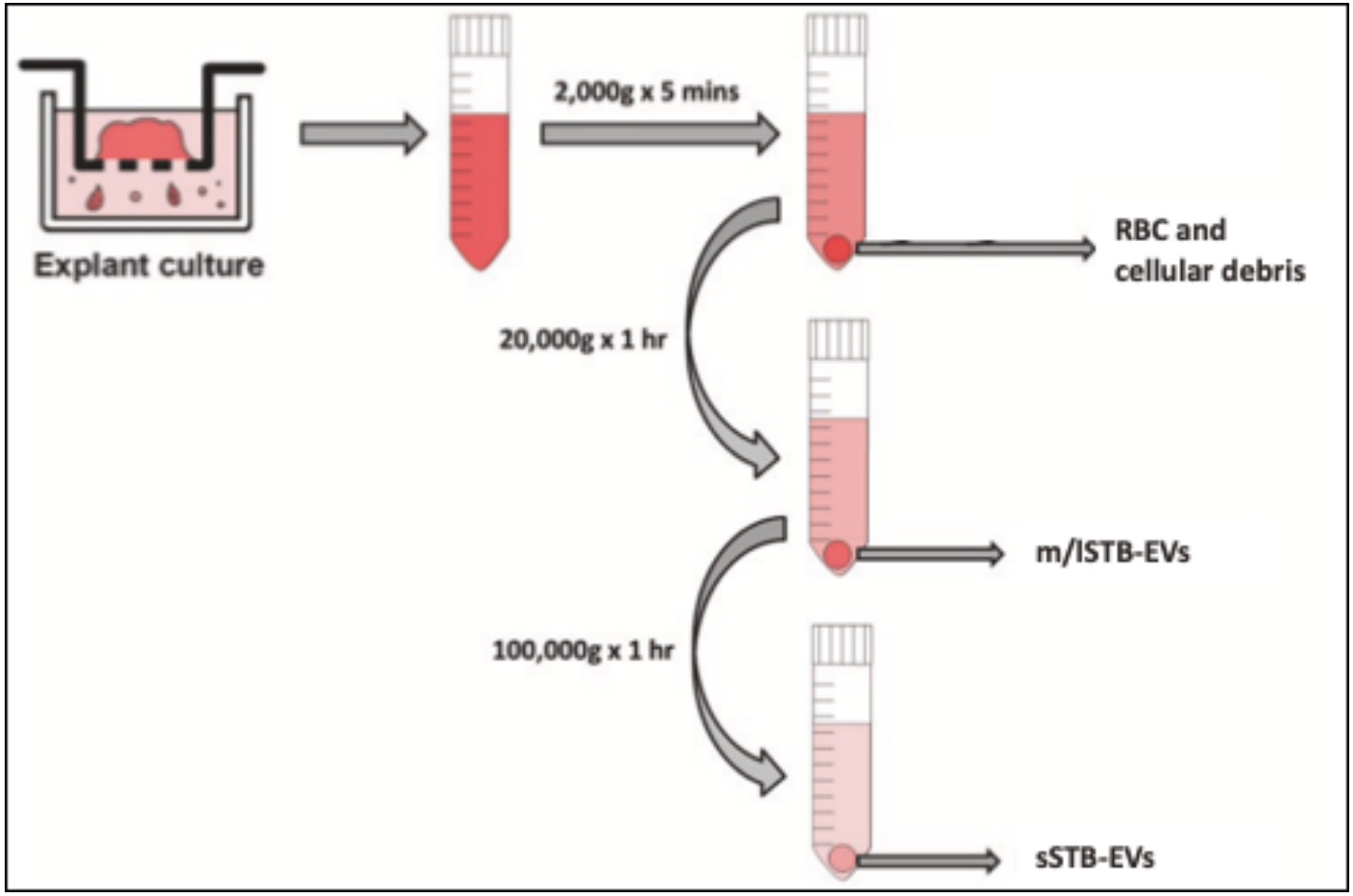


Figure 7 – Schematic representation for isolating STB-EVs from placental explants

(adapted from Tong, M. & Chamley, L.W. (2018)[253])

3.3.2.3 *Ex vivo* placental perfusion derived STB-EVs

The *ex vivo* dual perfusion technique establishes physiological perfusion conditions within a human placenta. This involves perfusing buffer solutions through two separate and independent circulatory systems (maternal and foetal). By mimicking the *in vivo* utero-placental and foeto-placental circulations, this technique facilitates a quantitative understanding of several processes, including solute transfer and release of endogenous substances[253].

The detailed method of *ex vivo* dual lobe placental perfusion is described in detail in section 2.1.3 and extensively reported by our group [179,193–196]. In brief, a chosen placental cotyledon is cannulated on both the foetal (with a flow rate of 6 to 12 mL/min and pressure of 50 to 90 mmHg) and maternal (with a flow rate of 10 to 20 mL/min and pressure of 80 to 140 mmHg) facing sides of the placenta and perfused with supplemented M-199 medium for three hours. Subsequently, the resulting maternal perfusate undergoes differential centrifugation at 1500 x g for 15 minutes (twice) to remove cellular debris, followed by centrifugation at 10,000 x g for 35 minutes at 4°C to isolate m/lSTB-EVs, and finally, centrifugation at 150,000 x g for 125 minutes at 4°C to isolate sSTB-EVs.

Dual lobe placental perfusion has the unique advantage of providing high yield of STB-EVs (compared to explant culture) allowing wide range of downstream analysis. But it is a laborious process requiring specialised equipment and technical expertise and has higher STB-EVs production failure rate.

3.3.2.4 Cultured human choriocarcinoma-derived cell line (BeWo) derived EVs

BeWo cell derived EVs are derived by culturing BeWo cells in Dulbecco's modified Eagle's medium (DMEM) supplemented with L-glutamine, 4500 mg/L glucose, and penicillin/streptomycin, but lacking sodium bicarbonate. Heat-inactivated foetal bovine serum (FBS) is used for initial cell growth. Once the cell growth reaches approximately 90% confluence, the medium is replaced with fresh medium containing exosome depleted FBS. The cells are then incubated for an additional 48 hours to allow for EV secretion. The conditioned culture medium, containing the secreted EVs, is collected for further processing. Differential centrifugation is performed in two steps: first at 800 x g for 5 minutes and then at 2,000 x g for 10 minutes, to remove both large cell debris and remaining cellular components. The resulting supernatant is then concentrated using a 100 kDa ultrafiltration membrane, which allows EVs to pass through while filtering out larger proteins and other macromolecules. Finally, ultracentrifugation at 120,000 x g for 2 hours at 4°C pellets the EVs by sedimenting them based on their density. The isolated EV pellet is then gently resuspended in a small volume of fresh phosphate buffered saline (PBS) for further analysis[254].

3.3.2.5 Cultured trophoblast derived cell line derived EVs

Trophoblast cell line derived EVs are isolated by culturing ATCC No. CRL-1584, a villous 3A cytotrophoblast first trimester placental cell line from American Type Culture Collection (ATCC)[255], which is widely used as an *in vitro* placental model[256,257]. The cells are first cultured in 10% modified Eagle's medium (MEM) supplemented with foetal bovine serum (FBS) and antibiotics, at 37°C in a 5% CO_2 atmosphere. After 24 hours, the culture supernatants containing secreted EVs are collected. To remove any remaining cells, the supernatants undergo a two-step differential centrifugation process: first at 300 x g for 5 minutes and then at 800 x g for 5 minutes.

Next, ultracentrifugation at a high force of 100,000 x g for 90 minutes at 4°C pellets the EVs based on their density. The isolated EV pellet is then washed twice with fresh PBS to remove any residual contaminants. Finally, the pellet is resuspended in a small volume of fresh 10% MEM media for further analysis[258].

3.3.2.6 Cytotrophoblast derived EVs

Cytotrophoblasts (CTB) are isolated from second trimester placentae according to established protocol[259]. CTBs are cultured in Dulbecco's Modified Eagle Medium/Ham's F-12 (DMEM/H-21), supplemented with Nutridoma-SP (a commercial supplement), sodium pyruvate, HEPES buffer, glutamine, penicillin/streptomycin, and gentamicin. After an initial incubation period, the medium containing unattached immune cells and other unwanted cells is removed and replaced with fresh serum-free medium to create a more purified CTB population. Following a further 36-38 hours of culture, the conditioned medium, now enriched with EVs secreted by the CTBs, is processed for EV isolation. A low-speed centrifugation at 400 x g for 5 minutes removes any remaining intact cells. The supernatant is then subjected to two additional centrifugations at increasing speeds (2,000 x g and 16,500 x g, each for 20 minutes) to progressively remove larger cellular debris. The resulting liquid fraction, enriched in EVs, is then passed through a 0.22 μm filter to eliminate smaller contaminants. The filtrate undergoes ultracentrifugation at 100,000 x g for 70 minutes. This step pellets the EVs based on their density, separating them from the remaining solution. The supernatant is then removed, and the EV pellet is carefully resuspended in a fresh phosphate-buffered saline (PBS) solution for further analysis[260].

Despite various researchers have adopted wide range of methods to isolate placental EVs, it is interesting to note that all of them have utilised differential ultracentrifugation as opposed to other enrichment methods such as density gradient centrifugation, size exclusion chromatography, ultrafiltration, immunoaffinity bead capture, and immunoprecipitation. The unanimous choice for differential ultracentrifugation as the method for EV enrichment could have been possibly influenced by the familiarity of placental EV research fraternity with the method, the popularity of the method, and the use large volume of source materials generated from the two most common placental EV sources; dual lobe placental perfusion (~600 mL of maternal perfusate) and placental explant culture medium (~ 10mL per sample).

Our group has extensive experience in performing dual lobe placental perfusion. The isolated STB-EVs are differentially ultracentrifuged to enrich m/lSTB-EVs and sSTB-EVs. STB-EVs isolated and enriched for the downstream analysis for the purpose of this thesis were obtained from *ex vivo* dual lobe placental perfusions and differential ultracentrifugation.

3.4 Methods

Methods used for isolation, enrichment, and characterisation of STB-EVs have been described in detail in Chapter 2. Briefly, m/lSTB-EVs and sSTB-EVs were isolated by *ex vivo* dual lobe placental perfusion and enriched by differential ultracentrifugation. Enriched STB-EVs were characterized by transmission electron microscopy; flow cytometry; nanoparticle tracking analysis; western blotting; and total protein quantification. Placental cell lysates were used as positive control for placental alkaline phosphatase (PLAP), a specific marker for placental origin of EVs.

3.5 Results

3.5.1 Patient demographics and clinical characteristics

Table 13 presents the demographic details and clinical characteristics of women with placentas that underwent successful *ex vivo* dual lobe placental perfusion (EOPE, n=3 and NP, n=3) after delivery. Due to limitations imposed by the COVID-19 pandemic and the strict criteria for selecting women with EOPE, the number of EOPE placentae obtainable during the study period was restricted.

Women in the EOPE group exhibited significantly higher systolic and diastolic blood pressure readings, as well as a higher sFlt-1:PlGF ratio, compared to the normal pregnancy group ($p < 0.05$). Additionally, they displayed significant proteinuria, delivered at a lower gestational age, and delivered babies with lower birth weights ($p < 0.05$). However, no significant differences were observed in maternal age, weight, height, body mass index, or gravidity between the two groups.

3.5.2 Characterisation of syncytiotrophoblast-derived extracellular vesicles

3.5.2.1 Transmission electron microscopy

Transmission electron microscopy (Figure 8) demonstrated the typical cup-shaped morphology of extracellular vesicles. The 10K STB-EV pellet (Figure 8.A1) showed size heterogeneity characteristic of m/lSTB-EVs (221 – 1000 nm) while the 150K STB-EV pellet (figure 8.A3) showed homogenous EV size profile of that of sSTB-EVs (less than or equal to 220 nm).

3.5.2.2 Nanoparticle tracking analysis

Table 14 summarizes the mean sizes of the 10K STB-EV and 150K STB-EV pellets (EOPE, n=3 and NP, n=3). Figure XX shows a representative NTA graph of a 10K STB-EV (Figure 8.B1) and 150K STB-EV (Figure 8.B2) samples. Based on the physical characteristic (size) of the enriched EVs, the 10K and 150K STB-EV pellets are hereafter renamed as m/lSTB-EVs and sSTB-EVs, respectively.

3.5.2.3 Western blotting

Immunophenotyping (Figure 8.C) detected placental specific marker [PLAP (~66 kDa)]; tetraspanin [CD63 (~30–65 kDa)]; and endosomal trafficking proteins [TSG101 (~46 kDa) and ALIX (~95 kDa)]. The non-EV marker, cytochrome C (~12 kDa) was detected in the placental lysates but not the STB-EVs fractions. The endosomal trafficking proteins were particularly enriched in sSTB-EV fractions than the m/lSTB-EV fractions and the placental lysates.

3.5.2.4 Flow cytometry

Flow cytometry (Figure 9) was only performed on 10K samples due to the sensitivity limit of flow cytometer. 90 ± 3.7 % of qualified events were negative for the following lineage markers [CD41 (platelets); CD235a (RBC); and HLA-I and II (WBC)]. 89.0 ± 1.3 % of the m/lSTB-EVs negative for non-placental markers (listed above) were double positive for BODIPY FL N-(2-aminoethyl)-maleimide (bioM) and PLAP (Figure 9.D). This confirmed that most of the 10K pellets were of placental origin. It was also confirmed that the samples were primarily vesicular as NP-40 treatment only reduced bioM and PLAP double-positive events by 0.7 ± 0.26% (Figure 9.E).

Table 13 - Demographic and clinical characteristics

Characteristic	Normal pregnancy (n = 3)	Early onset preeclampsia (n = 3)	*p* value
Maternal age (*y*)	26.0 ± 1.7	27.7 ± 3.5	> 0.05
Maternal wt. (*kg*)	68.0 ± 12.5	79.4 ± 18.5	> 0.05
Maternal ht. (*cm*)	158.0 ± 7.9	164.3 ± 4.0	> 0.05
Maternal BMI (kgm^{-2})	27.3 ± 5.5	29.2 ± 5.4	> 0.05
Gravidity	3.0 ± 2.7	1.3 ± 0.6	> 0.05
SBP (*mmHg*)	112.3 ± 2.5	159.3 ± 16.2	< 0.01
DBP (*mmHg*)	70.7 ± 9.0	96.3 ± 4.7	< 0.05
Proteinuria (*pluses*)	0.0	2.3 ± 1.2	< 0.05
Gest. age at delivery (*weeks*)	39.7 ± 0.6	30.2 ± 2.3	< 0.05
Birth wt. (*g*)	3492.0 ± 266.3	1770.0 ± 198.4	< 0.001
sFlt-1:PlGF ratio	1.2 ± 0.2	840.0 ± 459.2	< 0.0001

Data are presented as mean ± standard deviation (SD). Two groups were analysed using unpaired student *t-test*. Statistical significance was set at $p < 0.05$ (*$p < 0.05$; **p < 0.01; ***$p < 0.001$).

y – years; wt. – weight; ht. – height; BMI – body mass index; SBP – systolic blood pressure; DBP – diastolic blood pressure; Gest. age – gestational age.

Table 14 - Mean sizes of the 10K and 150K STB-EV pellets

Placental sample	10K STB-EV (nm)	150K STB-EV (nm)
NP – 1	272.8 ± 92.0	189.9 ± 63.5
NP – 2	344.9 ± 112.5	193.5 ± 78.5
NP – 3	355.9 ± 106.3	201.6 ± 83.5
EOPE – 1	269.6 ± 134.6	172.4 ± 88.5
EOPE – 2	322.4 ± 97.8	208.5 ± 97.3
EOPE – 3	311.2 + 99.5	196.4 ± 79.2

Data are presented as mean ± standard deviation

NP – normal pregnancy; EOPE – early-onset preeclampsia

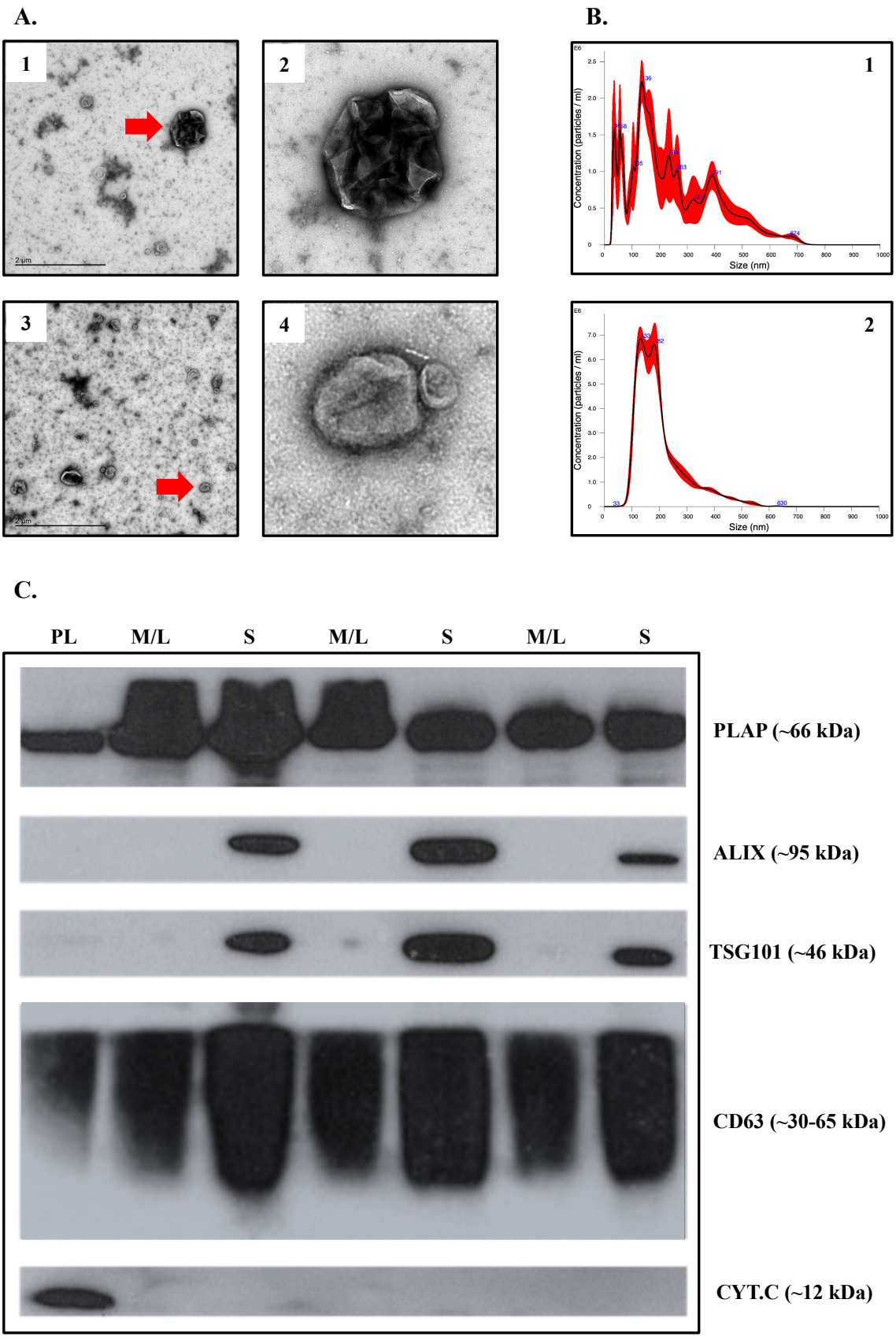


Figure 8 – STB-EV characterisation.
A) Representative TEM images wide with wide view (A1, A3) and cropped view of m/lSTB-EV (A2) and sSTB-EV (A4). **B)** Representative NTA results of (B1) m/lSTB-EVs and (B2) sSTB-EVs. **C)** Representative western blot of placental lysate (PL), m/lSTB-EVs (M/L) and sSTB-EVs (S) showing positivity for CD63, ALIX, TSG101 and PLAP and absence of cytochrome C (CYT.C).

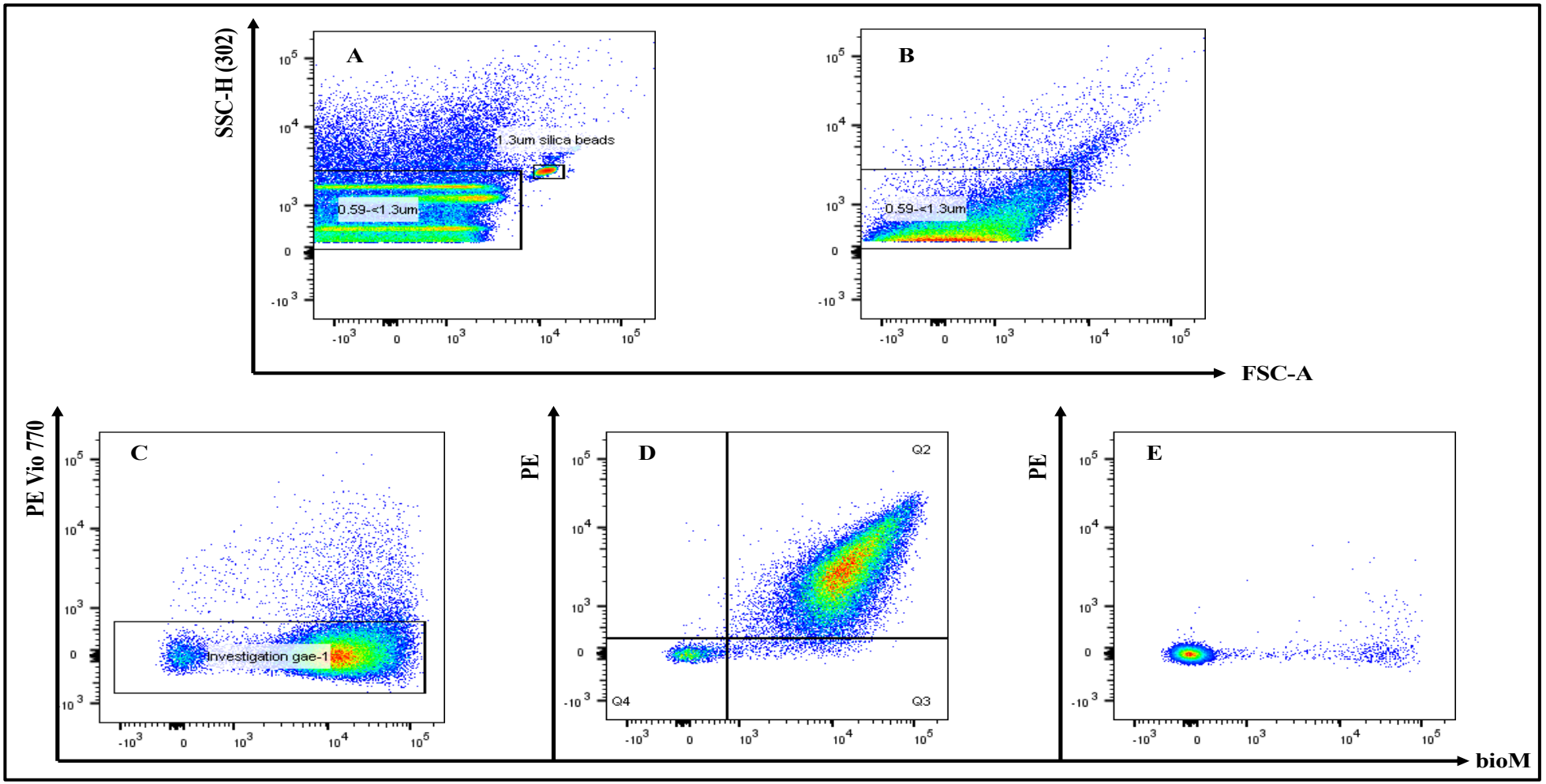


Figure 9 – Representative flow cytometry data of 10K STB-EV pellet.

A) Apogee beads were used to set flow cytometer's light scatter resolution to 0.59-<1.3 µm silica beads; **B)** application of SSC and FSC PMTV determined by apogee beads for analysis of m/lSTB-EVs in the 10K sample; **C)** investigation to exclude particles positive for non-EV markers; **D)** EVs from investigation gate further analysed for expression of PLAP and bioM staining; and **E)** PLAP+ /bioM+ EVs sensitive to NP-40 detergent treatment.

3.6 Discussion

The primary step in isolation and enrichment of EVs is to harvest an EV-containing matrix, such as placental perfusate (perfusion medium obtained after the completion of *ex vivo* dual lobe perfusion). ISEV recommends reporting the source material; the manipulation of the source material to harvest EVs; and experimental conditions[117].

Placenta, the source material, is classified as a solid tissue utilised for EV isolation[117,118,251]. Placenta was transported in warm HBSS solution and processed immediately in the laboratory to maintain the lividity of the tissue. Cannulation of both foetal and maternal facing surfaces of the chosen placental cotyledon with supplemented oxygenated (95% O_2) medium-199 ensured that the perfusate collected EVs produced by the syncytiotrophoblast tissue (STB-EVs) during the perfusion period (3 hours). Perspex water jacket maintained at 37°C; nutritionally supplemented media; dual perfusion; and optimal oxygenation ensured that the placenta was maintained under conditions as close to their in-situ environment as possible. At the end of the three-hour perfusion, the maternal perfusate (~600 mL) containing harvested STB-EVs was immediately processed to enrich m/lSTB-EVs and sSTB-EVs.

Differential ultracentrifugation (dUC), the most commonly used primary EV enrichment technique[261], was the method of choice for STB-EV subtypes' enrichment by our group. The principle of dUC is to apply increasing relative centrifugal forces (RCF = g-force) to the EV-containing fluid[262]. The aim of dUC is to sequentially pellet EVs. The sedimentation velocity of a sphere is determined by Stoke's law equation (Equation 1). The sedimentation velocity, V is proportional to the radii squared (R^2) of the sphere and the density difference between the spherical particle and the fluid[263].

Larger (denser) EVs tend to be pelleted in the initial medium speed + short time centrifugation, while the smallest (least dense) EVs are recovered after higher speed + longer centrifugation[264].

$$V = \frac{2}{9} \frac{(\rho_s - \rho_f)}{\mu} gR^2$$

$V - Sedimentation\ velocity\ of\ the\ sphere\ (m/s)$
$\rho_s - Density\ of\ the\ sphere\ (kg/m^3)$
$\rho_f - Density\ of\ the\ fluid\ (medium)(kg/m^3)$
$\mu - Viscosity\ of\ the\ fluid\ (medium)((kg/m)/s)$
$g - Acceleration\ of\ gravity\ (m/s^2)$
$R - Radius\ of\ the\ sphere\ (m)$

Equation 1 - Stoke's law equation

Sedimentation of sub-types of STB-EVs were performed at three stages. Stage 1 included two low-speed centrifugations at 1,500 x g (2,500 RPM) for 10 minutes at 4°C in Beckman Coulter Avanti J-20XP centrifuge using a Beckman Coulter JS-5.3 swing-out rotor to sediment larger cellular debris. Although there is no unified protocol yet, approximated consensual protocols recommend several centrifugations at speed ranging between ~400 x g to ~2,000 x g to pellet cell debris and apoptotic bodies[265].

Stage 2 involved medium speed centrifugation at 10,000 x g (7,700 RPM) for 35 minutes at 4°C; and stage 3 involved high speed centrifugation at 150,000 x g (29,600 RPM) for 125 minutes at 4°C in a Beckman L8-80M ultracentrifuge and SW 32 Ti swinging-bucket rotor. In steps 2 and 3, the perfusate (~38 mL per tube) was centrifuged in 38.5 mL Ultraclear tubes (Beckman Coulter Life Sciences). The steps 2 and 3 pelleted medium/large EVs and small EVs respectively.

Available literature documents speeds between 10,000 x g to 20,000 x g applied between 10 to 90 minutes to pellet m/lEVs and speeds between 100,000 x g to 200,000 x g applied between 45 to 150 minutes to sediment sEVs[118,262].

As recommended by the ISEV, I have reported centrifugation speed in RPM (and RCF); type of rotors used; duration of centrifugation; temperature during centrifugation; type of tube used for centrifugation; and the sample volume in each tube[118].

While dUC offers a seemingly attractive method for concentrating EVs due to its lack of chemical manipulation, its limitations as a separation technique for EV sub-types cannot be overlooked as it is prone to co-precipitation of contaminants like protein aggregates and other non-EV particles alongside the EVs of interest[266]. To mitigate the co-precipitation of contaminants we have included a washing step at the end of 10,000 x g centrifugation and 150,000 x g centrifugation with fresh fPBS as encouraged[262]. We acknowledge the fact that several researchers' observation on different size distribution in dUC enriched EVs indicative of possible EV aggregation[267–269]. Others have observed higher yield of EVs[270,271] by increasing the number of centrifugations, while some have reported decreased EV recovery[272,273]. Although we acknowledge the limitations of dUC, its suitability for cost effectively processing large volumes (like our ~600 mL starting material) and its widespread use in the context basic research ultimately influenced our choice of technique.

While isolation and enrichment techniques for EVs are constantly evolving, the risk of co-precipitating contaminants remains a significant challenge. This potential for misleading data necessitates a rigorous characterisation process employing a combination of complementary techniques. ISEV outlines a series of recommended practices.

While quantifying the source material is an initial step recommended by ISEV guidelines for EV isolation (number of cells, volume of biofluids, or mass of tissues), this approach offers limited insight into the actual number of EVs isolated. This initial quantification serves primarily as a normalization factor and doesn't account for potential losses during isolation or the presence of co-isolated contaminants.

Therefore, additional characterisation techniques are crucial for establishing the true abundance of EVs within the isolate[117,118]. Particle number quantification offers one approach, with various methods available like light scattering technologies (e.g., NTA) and resistive pulse sensing (RPS) for a wider size range. However, light scattering techniques have limitations in differentiating EVs from other nanoparticles. Flow cytometry is another option for m/lEVs, but this method also relies on specific antibody labelling, which can introduce bias.[274–278]. Total protein quantification provides another data point. Techniques like BCA or Bradford assays (colorimetric methods) and global staining on SDS-PAGE are commonly used. However, these methods assume a proportional relationship between protein content and EV abundance, which may not always hold true. In our study, we quantified STB-EV particle numbers by NTA (presented as concentration ± SEM). m/lSTB-EVs had a particle concentration of $4.88 \times 10^8 \pm 3.32 \times 10^7$ particles/mL and sSTB-EVs: $9.53 \times 10^8 \pm 4.79 \times 10^7$ particles/mL. Additionally, protein concentration of the STB-EV sub-types was measured using a colorimetric method (BCA assay; described in detail in section 2.1.4.5), and all samples had a protein concentration ranging between 2 – 5 μg/μL. However, for a more comprehensive characterisation, other methods like total lipid or RNA quantification could also be considered.

Secondly, the ISEV recommends characterizing EVs by their protein composition. They suggest analysing one protein from each of three categories to demonstrate the presence of EVs (Categories 1 & 2) and assess their purity from common contaminants (Category 3).

- **Category 1 Proteins:** These are transmembrane or GPI-anchored proteins [e.g., Tetraspanins (CD63, CD81, CD82)] localised on the plasma membrane of eukaryotic cells. Their presence confirms the lipid bilayer structure specific to EVs.

- **Category 2 Proteins:** These are cytosolic proteins in a eukaryotic cell [e.g., ESCRT-I/II/III (TSG101) and accessory proteins (ALIX)]. Their presence indicates that the analysed preparation displays the expected structure of lipid bilayers enclosing intracellular material, a hallmark of EVs.

- **Category 3 Proteins:** These are major constituents of non-EV structures often co-precipitated with EVs [e.g., lipoproteins (APOA1/2), albumin, and protein-nucleic acid aggregates (Tamm-Horsfall protein)]. Evaluating their presence helps assess the degree of purity of the EV preparation.

An additional category (Category 4) is recommended if the study focuses on specific EV sub-types. This category includes transmembrane proteins associated with intracellular components other than the plasma or endosomal membrane [e.g., nuclear membrane proteins (histones) or mitochondrial membrane proteins (cytochrome C)].

To characterize the isolated STB-EV preparations, I probed for the following EV marker proteins: **Category 1:** CD63; **Category 2:** TSG101 and ALIX; and **Category 4:** Cytochrome C. As expected, both m/lSTB-EVs and sSTB-EVs were positive for CD63. sSTB-EVs were particularly enriched for TSG101 and ALIX, demonstrating their biogenetic lineage to the intracellular endosomal pathway. All STB-EVs stained negative for cytochrome C, confirming their origin from either the plasma membrane or endosomes. In addition to the ISEV categories, we also probed for placental alkaline phosphatase (PLAP), a specific marker for the syncytiotrophoblast layer, to confirm the tissue of origin of the EVs. As expected, both m/lEVs and sEVs stained positive for PLAP (confirmed by the positive staining in the placental lysate). It's important to note that Category 3 protein selection depends on the source sample.

Lipoproteins and albumin are considered the best negative markers for EVs from plasma or serum samples[279], while Tamm-Horsfall proteins (which form aggregates that co-precipitate with EVs) are most applicable to EVs isolated from urine[280]. Since there are no specific proteins to assess the purity of EVs from placental perfusate, we did not probe for Category 3 proteins in this study.

Building upon the protein characterisation, additional techniques can provide further insights into EV size and morphology. Electron microscopy (EM) offers a high-resolution view of EV morphology, allowing visualization of the characteristic cup-shaped structure delimited by a lipid bilayer membrane. Techniques like transmission electron microscopy (TEM) or scanning electron microscopy (SEM) can be employed, with each offering distinct advantages. TEM provides detailed internal morphology, while SEM excels at revealing the surface features of EVs[281,282]. Furthermore, nanoparticle tracking analysis offers a complementary approach for determining EV size distribution. This non-invasive technique utilizes light scattering to estimate the hydrodynamic diameter of individual EVs in suspension. NTA provides a rapid and high-throughput method for assessing EV size heterogeneity within a population[283]. In our study, we employed both TEM and NTA for further characterisation of the STB-EV isolates. TEM micrographs confirmed the presence of cup shaped EVs with a lipid bilayer membrane and within the expected size ranges for both m/lSTB-EVs and sSTB-EVs. NTA analysis revealed a mean size distributions for m/lSTB-EVs of > 220 nm and for sSTB-EVs < 200 nm. These findings align with the expected size range for these EV sub-types.

By employing a combination of particle quantification, protein characterisation, electron microscopy, and nanoparticle tracking analysis, we were able to comprehensively characterize the isolated STB-EVs, confirming their presence, purity, size distribution, and morphology. This multi-faceted approach strengthens the evidence that the isolated vesicles represent bona fide STB-EVs and paves the way for further investigation of their functional roles.

3.7 Conclusion

This chapter has presented a detailed protocol for the isolation and enrichment of sub-types of STB-EVs from placental perfusate. The method leverages dUC, a widely employed technique, while acknowledging its limitations in potential co-precipitation of contaminants. I have emphasized the importance of rigorous characterisation beyond the initial quantification of source material. My approach incorporated particle number quantification, protein composition analysis, electron microscopy, and nanoparticle tracking analysis. Employing this multi-faceted characterisation strategy, I successfully isolated and enriched m/lSTB-EVs and sSTB-EVs, confirming their presence, purity, size distribution, and characteristic morphology.

3.8 Next steps

Building upon this successful isolation and characterisation protocol, I designed the next steps of my experiment to interrogate the STB-EVs for their protein cargo (Chapter 4) and genetic cargo (miRNAs; Chapter 5). In Chapter 4, I aim to investigate the protein cargo in STB-EVs for the presence of kynurenine metabolising enzymes (kynureninase, kynurenine monooxygenase, and kynurenine aminotransferase); their functionality in kynurenine metabolism; and implications in circulating levels of kynurenine in PE and normal pregnancies. In Chapter 5, I aim to validate the RNA sequencing data obtained from medium/large STB-EVs followed by validation of selected miRNAs in circulating extracellular vesicles isolated from serum samples of PE and normal pregnancies and functional assays to determine their role in regulating processes involved in the pathogenesis of preeclampsia.

CHAPTER 4:

SYNCYTIOTROPHOBLAST-DERIVED EXTRACELLULAR VESICLES CARRY FUNCTIONAL KYNURENINE METABOLIZING ENZYMES

Abstract

Introduction: Preeclampsia (PE) is a complex hypertensive disorder of pregnancy that affects 2-8% of pregnancies. It is characterized by impaired trophoblastic invasion, leading to reduced placental blood flow and oxidative stress. This stress releases anti-angiogenic markers and syncytiotrophoblast-derived extracellular vesicles (STB-EVs), contributing to endothelial dysfunction and vasoconstriction. Kynurenine (Kyn), a tryptophan metabolite, has emerged as a potential therapeutic molecule for maternal features of PE due to its vasodilatory and hypotensive effects.

Methods: This study investigates the presence and functionality of kynurenine metabolising enzymes (KYNME) in STB-EVs and placental tissue. Medium/large and small STB-EVs were isolated from early-onset preeclampsia (EOPE) and normal pregnancy (NP) placentas via *ex vivo* dual lobe placental perfusion and differential ultracentrifugation. Placental tissue underwent immunohistochemical and Western blot analysis for KYNME expression. STB-EVs underwent capillary electrophoresis and Western blot analysis for KYNME expression. Serum kynurenine levels were quantified using gas chromatography-mass spectrometry. Functional assays assessed the ability of STB-EVs to metabolize kynurenine *in vitro*.

Results: Transcriptomic analysis revealed the expression of mRNAs coding for KYNME in placental tissue and STB-EVs from both EOPE and NP pregnancies. Despite similar KYNME content, EOPE women showed significantly reduced serum kynurenine levels compared to NP, indicating higher STB-EV-mediated kynurenine metabolism in EOPE. The study demonstrated that STB-EVs actively metabolize kynurenine, potentially contributing to the pathophysiology of PE by reducing circulating kynurenine levels.

Conclusion: Our findings suggest that STB-EVs play a significant role in regulating kynurenine metabolism in pregnancy, with potential implications for PE management. The elevated release of STB-EVs in EOPE could lead to lower circulating kynurenine levels, exacerbating PE symptoms. These insights raise important questions about the efficacy of kynurenine replacement therapy and suggest exploring specific KYNME inhibitors combined with kynurenine replacement as a therapeutic strategy for PE.

4.1 Introduction

Preeclampsia (PE) is a multifaceted hypertensive disorder of pregnancy that affects 2 – 8% of pregnancies[1,13]. The exact pathophysiological mechanisms underlying placental dysfunction as the direct cause of preeclampsia are still being extensively studied, with the only available definitive treatment being the delivery of placenta[284]. During normal pregnancy, implantation entails trophoblastic invasion of the decidualized endometrium, which facilitates remodelling of spiral arteries and obliteration of the tunica media in myometrial spiral arteries. This process ensures enhanced blood flow to the placenta, independent of maternal vasomotor changes[93]. However in PE, trophoblasts do not adopt an endothelial phenotype, leading to impaired invasion and spiral artery remodelling, which eventually reduces placental blood flow[89]. The resultant placental ischemia leads to oxidative stress of the syncytiotrophoblast layer[94,95], which in turn releases anti-angiogenic markers (sFlt-1, sEng, etc.) and syncytiotrophoblast-derived extracellular vesicles (STB-EVs) which are shown to mediate endothelial dysfunction and vasoconstriction[90,96–98]. The oxidative stress, along with the resultant endothelial dysfunction and vasoconstriction drive the pathophysiology of PE. Therefore, it is imperative to assert that targeting these primary drivers of maternal pathophysiology to attenuate the disease's progression is an attractive therapeutic strategy.

Kynurenine (Kyn), a tryptophan metabolite, came to attention as a potential molecule to treat maternal features of PE[285] during a literature review during my preparation for the DPhil proposal. This led to further exploration of tryptophan metabolism and functional effects of kynurenine in relation to normal and preeclamptic pregnancies.

4.1.1 The kynurenine pathway

The kynurenine (Kyn) pathway (Figure 10) is the primary catabolic route for the essential amino acid tryptophan (Trp) responsible for over 90% of Trp degradation, while the remainder of Trp is either incorporated into proteins, excreted in the urine, or converted into serotonin[286].

The rate-limiting step in the kynurenine (Kyn) pathway involves the conversion of tryptophan (Trp) to N-formylkynurenine by tryptophan 2,3-dioxygenase (TDO), indoleamine 2,3-dioxygenase 1 (IDO1), and indoleamine 2,3-dioxygenase 2 (IDO2)[287]. Subsequently, N-formylkynurenine is converted to Kyn by hydrolase enzymes[288]. The Kyn pathway is not constitutively expressed in many tissues under normal conditions, but key sites of activity include the liver, lungs, small intestine, and, during pregnancy, the placenta. TDO activity is mainly confined to the liver and brain, with hepatic TDO predominantly regulating Trp catabolism under normal conditions.

The placenta has high physiological IDO1 activity during normal pregnancy, making it the most abundant source of IDO1[289,290]. IDO1 expression in vascular endothelium, vascular smooth muscle, and various immune cells is induced by inflammatory markers (IFN-γ and TNF) during tissue stress, hypoxia, and inflammation[289,291,292]. Recently discovered IDO2 (homologous to IDO1) has a much lower affinity for Trp, and its significance in health and disease remains uncertain[293].

Kyn is further metabolised by three different kynurenine metabolising enzymes (KYNME), kynureninase (KYNU), kynurenine monooxygenase (KMO) and kynurenine aminotransferase (KAT-III), to produce several downstream metabolites (Figure 10).

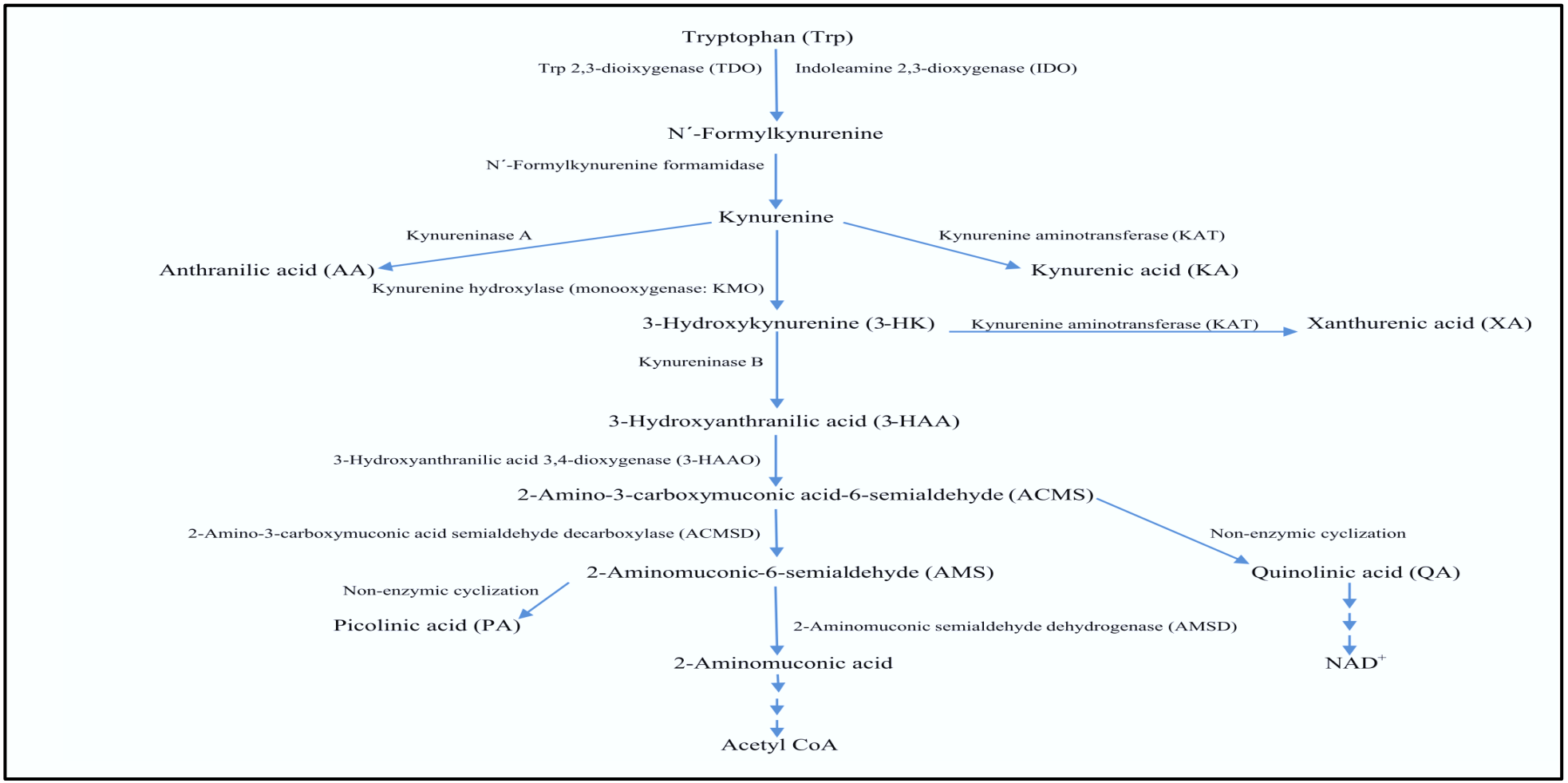


Figure 10 - The kynurenine pathway of tryptophan degradation

Tryptophan (Trp) is broken down to Kyn by TDO (extra-placental) and IDO (placental). Kyn is further broken down to various molecules by three different enzymes: kynureninase A (KYNU); kynurenine aminotransferase (KAT-III) and kynurenine monooxygenase (KMO). Image reproduced from Badawy, (2005)[294].

4.1.2 Kynurenine as an immunoregulator

Kyn is recognized as a physiological ligand of the aryl hydrocarbon receptor (Ahr), a ligand-activated transcription factor[295]. Ahr activation has a wide range of effects depending on the ligand and the context of activation[296]. Prior to the identification of Kyn as a physiological ligand for Ahr, the only known ligands of Ahr were external toxins such as cigarette smoke and dioxins. It was previously hypothesized that Ahr activation in smokers might explain their 33% reduced risk of developing PE[297,298].

4.1.3 Kynurenine as a vasoregulator

In the recent past, a novel role for Kyn as an endothelial-derived regulator of vascular tone has emerged[292,299,300]. In animal models of malaria and endotoxemia, inhibiting IDO activity attenuated the hypotensive response, suggesting that inflammation-induced Kyn production is a key regulator of hypotension in inflammation[292]. This theory is supported by human studies showing an inverse correlation between Kyn pathway activity (measured as the kynurenine:tryptophan ratio) and blood pressure in conditions such as trauma[301], sepsis[302], obesity[303], and preeclampsia[304].

Although Kyn pathway metabolites originate from the vascular endothelium, the vasorelaxant effect of exogenous Kyn was found to be endothelium-independent in animal and non-pregnant human arteries[292,305].

Nitric oxide (NO) is an endothelium-derived vasorelaxant that mediates its effect by binding to guanylate cyclase (GC), a heterodimer with a haem group that exists in redox equilibrium between ferrous (Fe^{2+}) and ferric (Fe^{3+}) forms[306]. NO binding to the ferrous haem group activates GC (ferric form is insensitive to activation by NO), leading to conversion of guanosine

triphosphate (GTP) to the second messenger cyclic guanosine monophosphate (cGMP), which causes vascular smooth muscle relaxation by activating PKG[307]. Kynurenine was shown to activate cGMP-PKG mediated vasorelaxation and its effect was attenuated by PKG inhibitor. Interestingly, the inhibition of guanylate cyclase (an oxidant that oxidises ferrous haem group GC to ferric haem group GC) did not affect Kyn-dependent activation of cGMP-PKG-mediated vasorelaxation, contrary to the attenuated vasorelaxing response to NO. This finding strongly suggests that Kyn operates through a distinct and potentially more robust pathway for inducing vasorelaxation when the effects of NO are attenuated[292]. This is an attractive hypothesis for future application in women with PE, in whom NO pathways are disrupted[308,309].

However, Sakakibara *et al*. found that in rat mesenteric arteries, Kyn-induced relaxation was mediated by voltage-dependent K^+ channel (Kv7 channel) and this hypothesis was further validated by the attenuation of Kyn's hypotensive and vasorelaxant effect by selective inhibition of Kv7 channels using linopirdine[305]. Overall, these findings highlight the complex and context-dependent roles of Kyn in regulating vascular tone and blood pressure.

4.1.4 Kynurenine in pregnancy

In normal pregnancy, IDO expression and kynurenine pathway activity are markedly elevated in the placenta. IDO activity is detectable as early as day six in the trophoblast, increasing significantly by the mid-trimester and plateauing in the third trimester[310,311]. The human placenta contains all three rate-limiting enzymes responsible for converting tryptophan (Trp) to kynurenine, with IDO1 being the most extensively studied[289,312,313]. IDO1 is localised in the syncytiotrophoblast, underlying cytotrophoblast, placental macrophages, and foetal membranes[289]. During pregnancy, the maternal kynurenine:tryptophan (K:T) ratio is significantly elevated in normal pregnancy (0.034 ± 0.004) compared to the non-pregnant state (0.022 ± 0.004)[314], and urinary excretion of kynurenine pathway metabolites increases

accordingly[315]. The placenta likely contributes substantially to these altered maternal levels of Kyn, as suggested by *in vitro* explant models[314,316,317].

In PE, despite an exaggerated inflammatory environment that would typically enhance kynurenine pathway activity, there is a paradoxical reduction in placental IDO1 expression and activity. This reduction results in lower Kyn production compared to normal pregnancies[314,316]. Specifically, placental villous tissue from PE pregnancies produced only 0.63 of the Kyn levels seen in normal pregnancies[316]. Reduction in IDO1 activity in PE was measured objectively in two previous studies by means of K:T ratio with conflicting findings[304,314]. Kudo *et al*. reported an attenuation of the maternal K:T ratio in PE (0.024 ± 0.005) compared to normal pregnancy (0.034 ± 0,004), consistent with decreased placental IDO activity in PE[314]. Conversely, Nishizawa *et al*. found an increased K:T ratio in PE, a discrepancy that remains unexplained[304].

Recent studies have provided further insights into the potential therapeutic implications of Kyn in PE. In experimental models, replacing Kyn in pregnant mice with a PE-like phenotype induced by uni-nephrectomy was sufficient to improve placental blood flow abnormalities and ameliorate the PE-like phenotype[28,318]. These findings support the hypothesis that Kyn replacement therapy may serve as a potential treatment for the clinical syndrome of PE, offering a novel therapeutic approach to managing this condition[318].

While normal pregnancy is characterized by high IDO activity and increased Trp metabolism in the placenta producing enhanced Kyn levels, the attenuation of Kyn level in PE had been attributed exclusively to reduced placental IDO expression and activity. No studies have explored the role of kynurenine metabolising enzymes, kynureninase (KYNU), kynurenine monooxygenase (KMO) and kynurenine aminotransferase (KAT-III) in regulating Kyn levels in pregnancy. Hence, we sought to interrogate the placental tissue and syncytiotrophoblast-derived

extracellular vesicles (STB-EVs) for the presence of KYNME and their functionality in regulating Kyn level in normal and preeclamptic pregnancies.

4.2 Aims

The aims of this chapter are to:

1. investigate the placental tissue and STB-EV cargo for the presence of kynurenine metabolising enzymes (KYNME)
2. assess the functionality of KYNME carried by STB-EVs in an *in vitro* setting
3. compare the serum levels of Kyn in women with EOPE and normal pregnancy

4.3 Methods

The methodologies employed in this chapter are thoroughly detailed in Chapter 2. In summary, medium/large and small STB-EVs were isolated and enriched through *ex vivo* dual lobe placental perfusion followed by dUC (EOPE, n=3; NP, n=3). Biopsies were collected from the corresponding placenta specimens to obtain placental lysates. Placental tissue sections from EOPE (n=3) and NP (n=3) placentae underwent immunohistochemical analysis to detect KYNME expression. Western blot analysis was performed on placental lysates to confirm KYNME expression. Additionally, a Simple Western analysis using the Jess system was conducted on pooled STB-EVs to quantitatively measure KYNME expression. Gas chromatography-mass spectrometry was utilized to (a) quantify Kyn in serum samples from EOPE (n=9) and NP (n=9) mothers and (b) quantify Kyn in *in vitro* experiments designed to assess the functionality of KYNME expressed in STB-EV cargo. Data analysis and representation were carried out using GraphPad Prism (*v10.2.2*, Boston, MA, USA), with statistical significance set at $p < 0.05$.

4.4 Results

4.4.1 Transcriptomic analysis of placental lysate and STB-EVs shows expression of KYNME

Transcriptomic analysis was previously performed[196] on placental tissues, m/lSTB-EVs and sSTB-EVs (n; EOPE=7, NP=6) by Dr Toluwalase Awoyemi (NDWRH, University of Oxford) and the data were re-analysed with the help of Morganne Wilbourne (NDWRH, University of Oxford) to find possible expression of mRNAs coding for KYNME. The analysis revealed that placental tissue, m/lSTB-EVs, and sSTB-EVs obtained from EOPE and NP pregnancies expressed mRNAs coding all three kynurenine metabolising enzymes (KYNU, KMO and KAT-III). Differential Expression Analysis was performed with DESeq2[319] (*v.1.40.2 in* R *v4.3.1*), which showed no significant difference between normal pregnancy and early-onset preeclampsia (False Discovery Rates (FDR) used to correct for multiple testing, adjusted $p > 0.05$ for all 3). Figure 11 shows the normalized counts of the mRNAs coding for KYNME presented as Log_2(Counts).

4.4.2 Demographics and clinical characteristics

Table 15 illustrates the demographic and clinical characteristics of the women from whom the serum samples were obtained for the analysis. As expected, women who were diagnosed with EOPE (n=9) displayed significantly higher systolic and diastolic blood pressure, but lower gestational age at delivery, and had lower birth weight than women with NP (n=9) ($p < 0.0001$). Additionally, the sFlt-1:PlGF ratio was higher in EOPE (599.3) than NP (1.0) women ($p < 0.05$). However, there was no statistically significant differences observed in maternal age, body mass index (BMI), or gestational age at which blood samples were collected.

Table 15 - Demographic and clinical characteristics

Characteristic	NP (n = 9)	EOPE (n = 9)	*p* value
Maternal age (*y*)	28.6 ± 4.2	30.4 ± 4.1	> 0.05
Maternal BMI (kgm^{-2})	24.2 ± 4.0	29.1 ± 7.6	> 0.05
Gest. age at blood collection (*weeks*)	28.3 ± 2.9	28.0 ± 2.7	> 0.05
SBP (*mmHg*)	111.3 ± 7.5	156.3 ± 14.6	< 0.0001
DBP (*mmHg*)	67.3 ± 6.1	100.8 ± 6.6	< 0.0001
Gest. age at delivery (*weeks*)	39.0 ± 1.3	32.3 ± 2.7	< 0.0001
Birth wt. (*g*)	3801 ± 666.3	1815 ± 527.5	< 0.0001
sFlt-1:PlGF	1.0 ± 0.2	599.3 ± 569.5	< 0.05

Data are presented as mean ± standard deviation (SD). Two groups were analysed using unpaired student *t-test*. Statistical significance was set at $p < 0.05$.

NP – normal pregnancy; EOPE – early-onset preeclampsia; *y* – years; BMI – body mass index; SBP – systolic blood pressure; DBP – diastolic blood pressure; Gest. age – gestational age.

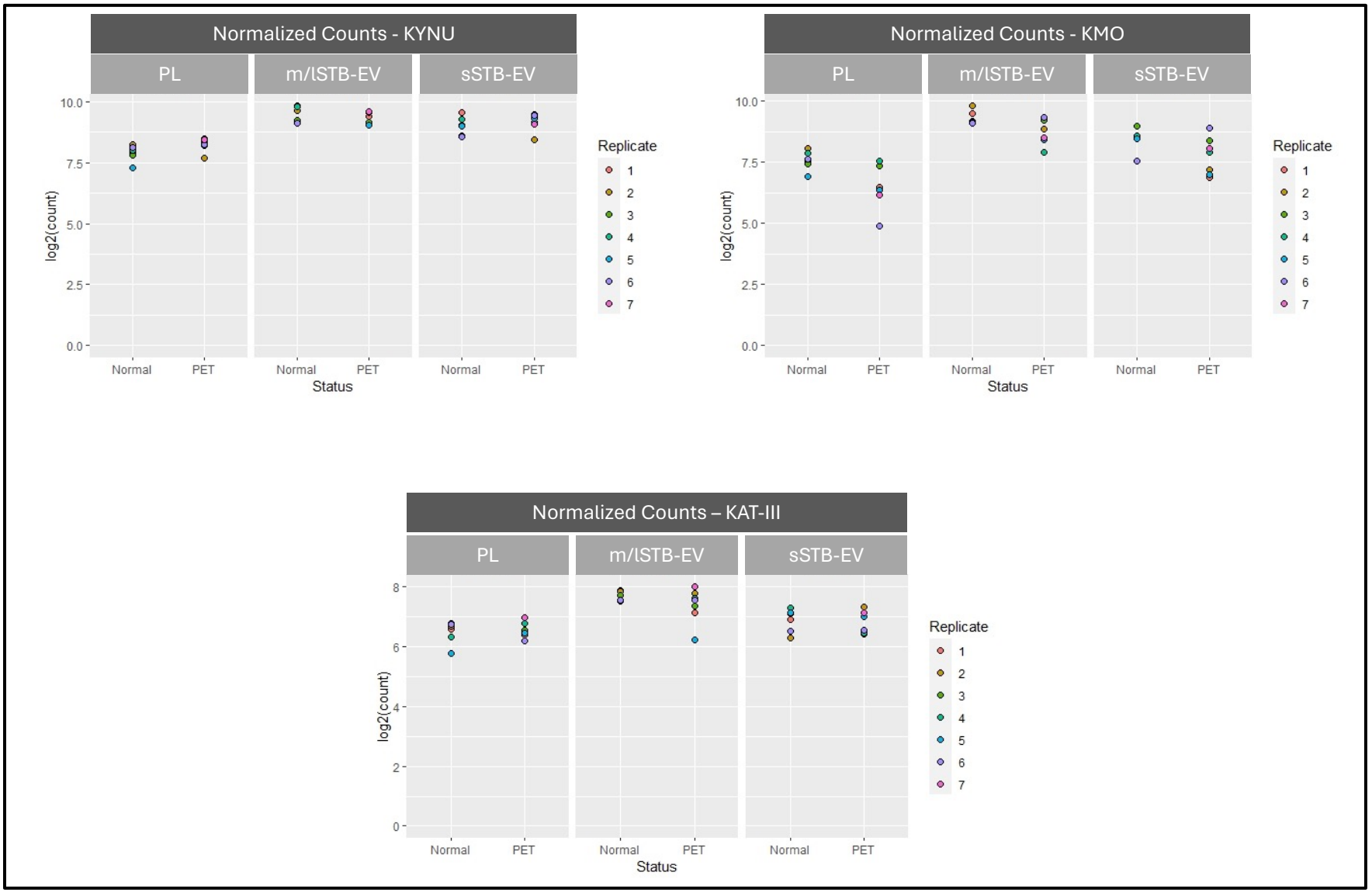


Figure 11 - Normalized counts of mRNAs coding for KYNME expressed in placental tissue and STB-EVs

4.4.3 Syncytiotrophoblast layer is selectively enriched for KYNME

Immunohistochemical staining of placental sections obtained from EOPE and NP pregnancies for KYNME showed selective enrichment of all three enzymes (KYNU, KMO and KAT-III) on syncytiotrophoblast layer (Figure 12.A). Relative qualitative assessment showed no difference in the intensity of staining for KYNME between EOPE and NP placental sections.

4.4.4 Placental lysates express KYNME

Placental lysates and liver cell lysates (positive control for KYNME) were probed for the presence of KYNME by traditional immunoblotting. Placental lysates obtained from EOPE (n=3) and NP (n=3) placentae expressed all three enzymes (Figure 12.B). Qualitative estimation of the intensity of the bands revealed no difference in KYNME expression between EOPE and NP placental lysates.

4.4.5 Identification of KYNME expression in STB-EVs

We aimed to identify KYNME expression in pooled STB-EVs (comprising m/l STB-EVs and sSTB-EVs) obtained from *ex vivo* dual lobe placental perfusion of NP (n=3) and EOPE (n=3) using capillary electrophoresis and western blotting. Liver cell lysate and placental lysate served as positive controls for KYNME and PLAP, respectively. All samples from both NP and EOPE tested positive for the three KYNME markers (KYNU, KMO, and KAT-III) and co-expressed PLAP (Figure 13.A). Total protein analysis was simultaneously conducted to ensure accuracy, and the normalized band densities were analysed using Compass software. There were no statistically significant differences in KYNME expression between NP and EOPE samples (Figure 13.B).

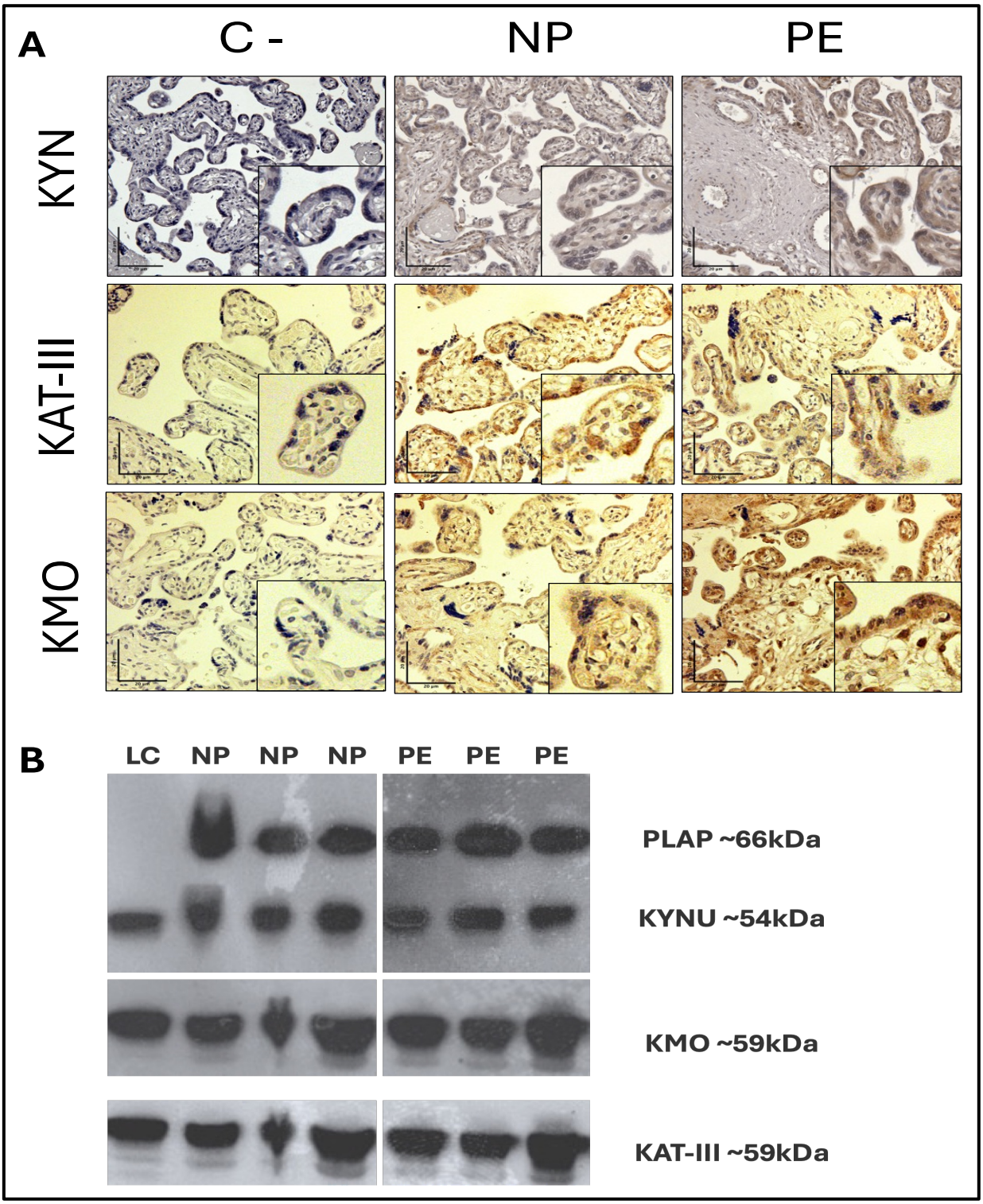


Figure 12 - KYNME expression on placental tissue

A) Immunohistochemistry analysis of placental expression of Anti KYNU; Anti KAT-III; and Anti KMO in NP and EOPE placentae. 'C-' negative control; 'NP' normal pregnancy; 'PE' preeclampsia. **B)** Placental lysates obtained from NP (n=3) and EOPE pregnancies (n=3) probed for KYNME and placental alkaline phosphatase (PLAP). Liver cell lysate used as positive control.

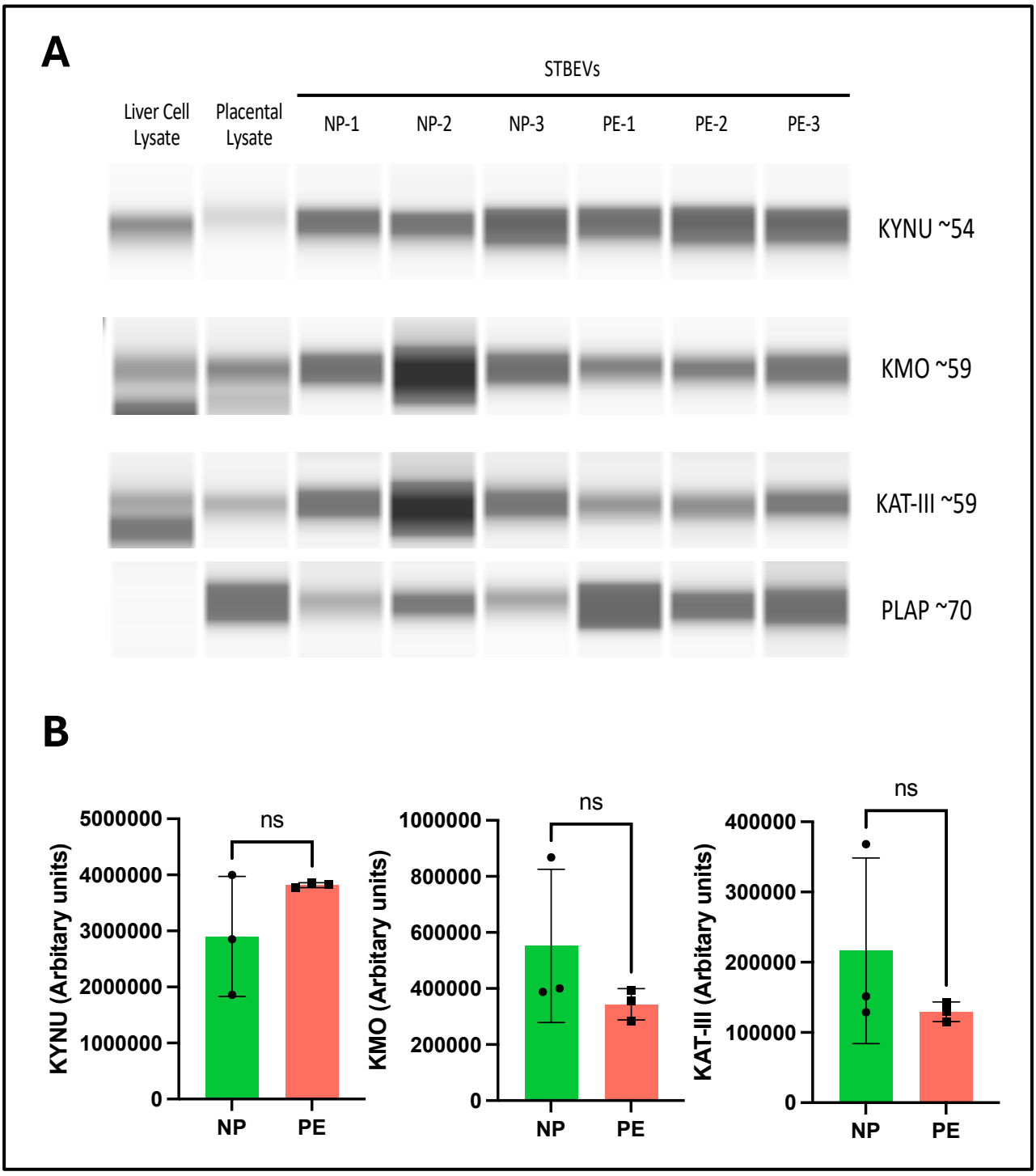


Figure 13 - KYNMEs are expressed by STB-EVs

A) Representative images of capillary electrophoresis of KYNME including KYNU, KMO, and KAT-III in STB-EVs extracted from NP (n=3) and EOPE pregnancies (n=3). PLAP was used as placental marker. Liver cell and placental lysates were used as respective positive and negative controls. **B)** Relative values of KYNMEs after normalizing for total protein. ns, non-statistical significance. Values are presented as mean ± SD.

4.4.6 Functional Assessment of KYNME in STB-EVs

Functional capacity of KYNME expressed in STB-EVs was measured using GCxGC-MS (Figure 14). Kynurenine solution was treated with different amounts of STB-EVs (1 μg and 5 μg of total protein) over two incubation periods (5 min and 60 min). Kynurenine solution incubated with STB-EVs denatured with 100% trifluoroacetic acid was used as control. Both 1 μg and 5 μg of STB-EVs significantly reduced kynurenine levels (~80% and ~90%, respectively), compared to the control condition ($p < 0.05$ for both) (Figures 15.A & 15.B). Furthermore, STB-EVs demonstrated a dose-dependent breakdown of kynurenine, with a significant reduction in kynurenine levels with 5 μg compared to 1 μg of STB-EVs, for both incubation periods ($p < 0.05$ in both cases) (Figures 15.C & 15.D).

4.4.7 Measurement of serum kynurenine

Using GCxGC-MS**,** I measured serum levels of kynurenine in women with EOPE (n=9) and gestationally matched women with NP (n=9) (Figure 16.A). Women with EOPE exhibited significantly lower levels of kynurenine compared with NP women ($p <0.05$) (Figure 16.B).

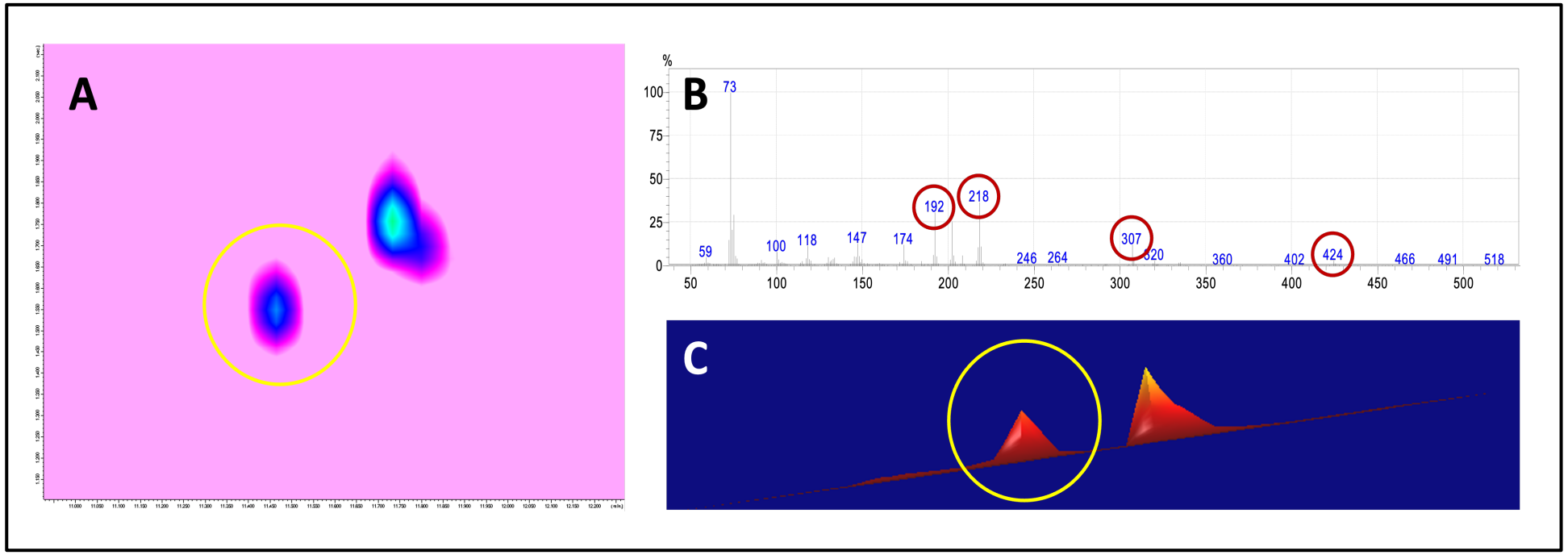


Figure 14 - 2D/3D GC-MS representation of kynurenine

Metabolite Standard Kynurenine (in yellow circle). **A)** 2D Gas chromatograph. **B)** Mass spectrum (fragment ions in red circles used to identify kynurenine in biological samples). **C)** 3D view.

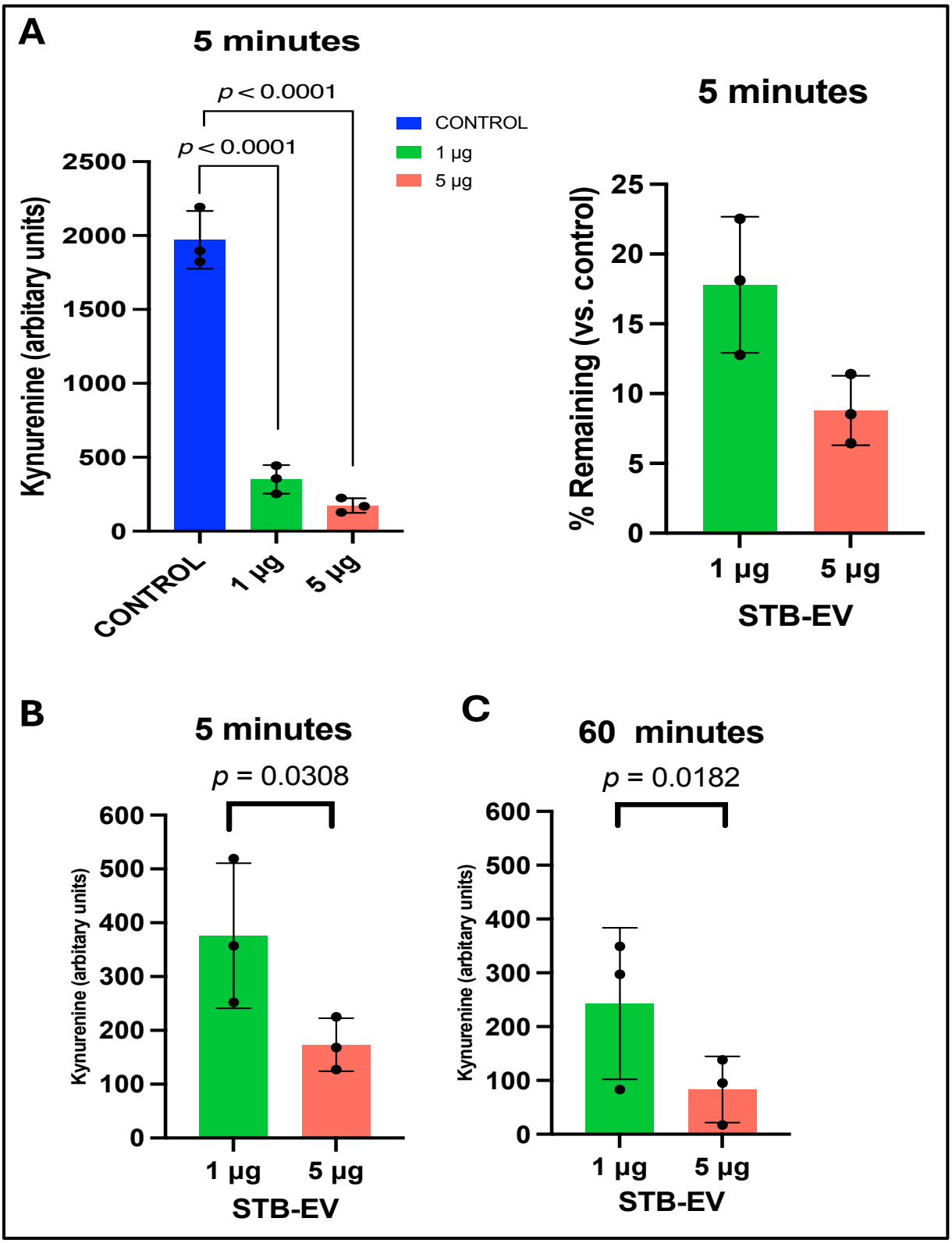


Figure 15 - STB-EVs isolated from normal pregnancy break down kynurenine

A) Kynurenine measured in control (blue bar) and treatment groups (1 µg, green bar; and 5 µg, red bar) and percentage of kynurenine metabolized by 1 µg and 5 µg STB-EVs isolated from NP placentae (n=3). Two different incubation time were tested. **B)** 5 min, and **C)** 60 min of incubation with STB-EVs. Denatured STB-EVs (using 100% trifluoracetic acid) were used as control. Each dot represents an individual STB-EV extraction. Values are presented as mean ± SD. *p* value is indicated in each comparison.

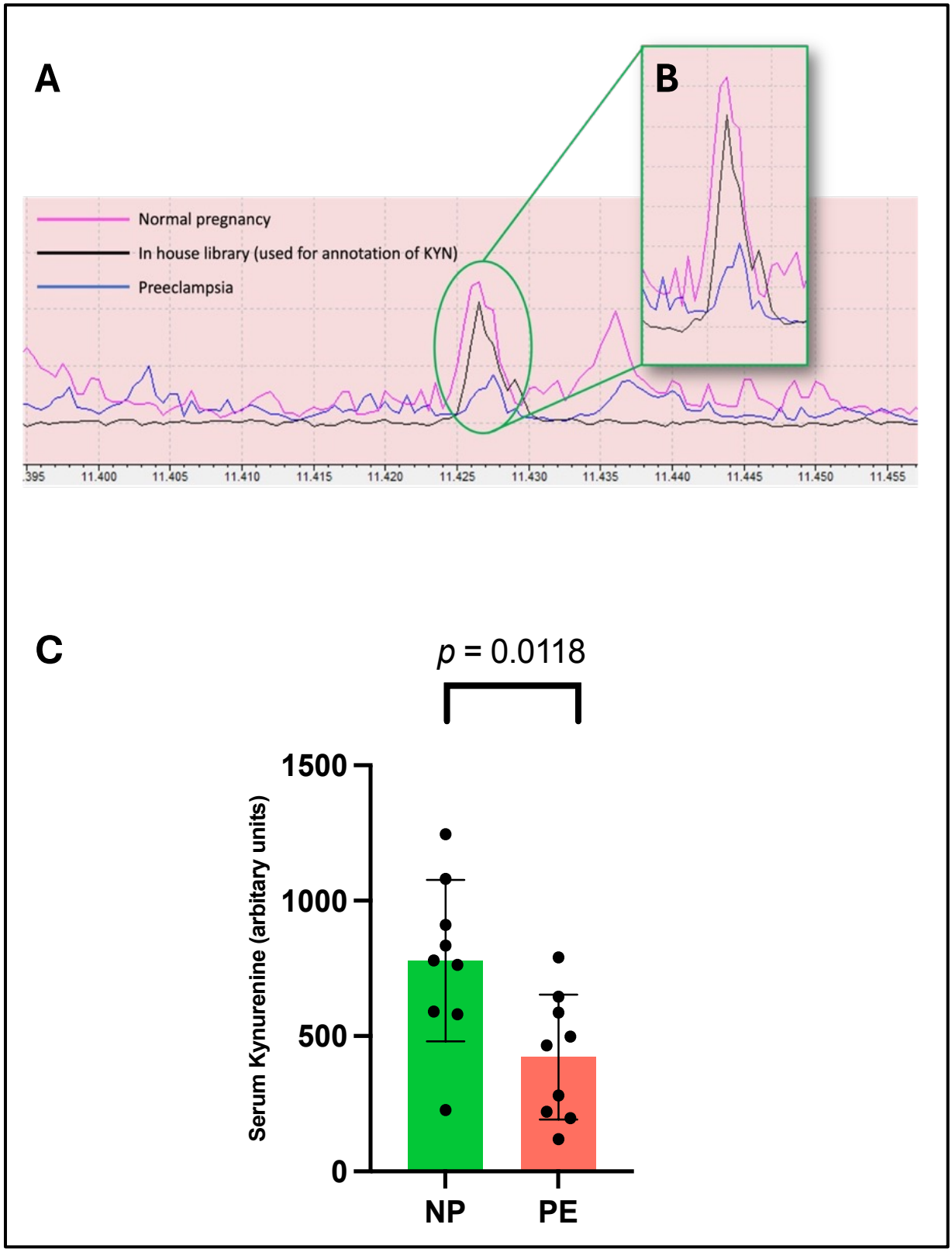


Figure 16 - Serum kynurenine levels in normal and preeclamptic pregnancies

A) Representative chart of gas chromatography mass spectrometry for Kyn detection in serum from NP (n=9, pink) and EOPE pregnancies (n=9, blue). As a control we used an in-house library of Kyn (black). **B)** Amplification of the chromatogram in which KYN is detected. Notice the differences in the peak generated in NP and EOPE samples. **C)** KYN levels presented as mean ± SD. Each dot represents an individual. *p* value is indicated in each comparison.

4.5 Discussion

This study for the first time identified that STB-EVs cargo includes functional kynurenine metabolising enzymes (KYNU, KMO and KAT-III). These enzymes breakdown kynurenine, a biologically active metabolite known for its vasodilatory[292,305] and hypotensive[292] effects. Despite no significant differences in the content of kynurenine metabolising enzymes were found between normal and EOPE STB-EVs, serum levels of kynurenine were significantly reduced in EOPE. These findings suggest that STB-EVs may participate in the regulation of circulating kynurenine levels in NP and EOPE. This is particularly true given that circulating levels of STB-EVs are higher in EOPE compared to NP[108,320]. This dose effect may lead to higher concentrations of kynurenine metabolising enzymes and subsequently to reduced levels of circulating kynurenine. Whether STB-EV-mediated kynurenine metabolism participates in the cascade of placental, angiogenic or vaso-regulatory defects observed in PE requires further investigation.

Single-cell RNA sequencing data obtained from first trimester and term placentae revealed cell-specific (syncytiotrophoblast and cytotrophoblast) expression of mRNA coding for kynurenine metabolising enzymes. Data from the first trimester placenta showed relatively higher expression of mRNAs coding for all three enzymes (KYNU, KMO, and KAT-III) in STB cells[321]. However, studies investigating term placentae presented conflicting evidence: Pique-Regi *et al*. demonstrated varying expressions of mRNAs coding for all three enzymes[322], whereas Tsang *et al*. demonstrated only KMO gene expression in STB cells[323]. My findings from the transcriptomic analysis of placental lysate align with previous studies[321,323], showing the presence of genes coding for all three KYNMEs in placental lysates obtained from both NP and EOPE placentae.

Additionally, my immunohistochemical analysis of NP and EOPE placental sections confirmed the presence of KYNU, KMO, and KAT-III proteins selectively enriched in the STB layer. We further validated the presence of KYNME proteins in placental lysates through traditional western blotting.

To the best of my knowledge, no previous studies have reported the presence of KYNMEs on STB-EVs. For the first time I demonstrated that STB-EVs carry mRNAs coding for KYNMEs and functional KYNME proteins, as shown through transcriptomic analysis, capillary electrophoresis and western blotting, and gas chromatography-mass spectrometry. The expression of KYNME was not significantly different between EOPE and NP groups. But the quantum of KYNME is presumed to be higher in EOPE since EOPE releases more STB-EVs per unit volume of blood compared to NP[108].

Kynurenine was one of the metabolites shown to be released in lower quantities into the culture media by preeclamptic placental villi compared to normal placenta[314,316]. A similar observation was made when the metabolic footprint of culture media obtained from placental villi cultured at hypoxic conditions was compared with placental villi cultured at normoxic conditions[317]. Previous study examining the activity of IDO enzyme (K:T ratio) presented the data on kynurenine and tryptophan measurements made in plasma samples obtained from NP and PE women in third trimester and non-pregnant women by high pressure liquid chromatography. The serum kynurenine level was found to be attenuated in PE samples (1.12 μmol/L) compared to NP (1.02 μmol/L) and non-pregnant samples (1.17 μmol/L), but the observed differences were statistically not significant[314]. We have investigated the serum kynurenine levels in EOPE and NP women (in their late second trimester to early third trimester) using gas chromatography-mass spectrometry and found that women with EOPE had significantly attenuated levels of kynurenine compared to gestationally matched NP women.

Thus, it is established that preeclamptic placentae release low levels of kynurenine and circulating levels of kynurenine is significantly reduced in preeclampsia. Previously, researchers have hypothesized that this reduction in kynurenine in preeclampsia is attributed to the reduced expression of genes coding for IDO enzyme and the IDO protein (responsible for breakdown of Trp to Kyn) in placental tissue[304,314,324,325]. No previous studies have explored the potential of KYNME leading to excess breakdown of Kyn in the context of pregnancy. Thus, we hypothesized that the attenuation of Kyn in preeclampsia is aggravated by the functional KYNME present in circulating STB-EVs. We found that KYNME expressed on STB-EVs demonstrate dose- and time-dependent breakdown of Kyn, proving our hypothesis that attenuation of kynurenine is potentially a combined effect of reduced synthesis (due to reduced levels and activity of IDO) and increased breakdown (due to dose- and time-dependent metabolising effect of KYNME) of Kyn. We acknowledge the fact that the gas chromatography-mass spectrometry experiments were conducted using STB-EVs obtained from *ex vivo* dual lobe placental perfusion of normal pregnancy placentae is a limitation as we have not exclusively investigated the STB-EVs obtained from EOPE placentae. But our group has previously established that EOPE placentae shed higher quantity of STB-EVs per unit volume of blood compared to normal pregnancy[108] and hence, we designed the experiment to assess the dose response of NP STB-EVs on kynurenine metabolism.

With this intriguing finding of the potential functional role of circulating KYNME on STB-EVs, we scrutinized the previously reported findings of Kudo *et al.*[314]. The study quantitatively measured IDO enzyme activity using K:T ratio. The observed ratio in NP, PE and non-pregnant women were 0.034; 0.024; 0.022 respectively. Third trimester of normal pregnancy is characterised by systemic inflammation and increased leukocyte count[326]. Leukocytes and placentae both express IDO and that corresponds well with the observed higher K:T ratio in NP (compared to non-pregnant women). But PE is characterised by even more intense systemic inflammation[327] and it would have been predicted that the K:T ratio to be higher.

Paradoxically, it was observed to be lower than NP and slightly higher than non-pregnant women. Authors attributed the reduced activity and expression of placental IDO in PE for the paradoxical ratio. They also argued that the reduction in placental IDO had significant effect on Trp breakdown compared to the effect of IDO contributed by the leukocytes. Based on this argument, it is prudent to assume that Trp levels to be highest in non-pregnant state, followed by PE and NP; and KYN levels to be highest in NP (higher placental- and leukocyte-derived IDO activity) followed by PE (lower level of placental and higher level of leukocyte-derived IDO activity) and non-pregnant state (no IDO activity). The actual observations from the study showed that Trp levels followed the assumption, but Kyn levels were contradictory. Non-pregnant state had the highest Kyn measurement (1.17 μmol/L), while NP and PE had 1.12 μmol/L and 1.02 μmol/L respectively. This paradox was not further evaluated as the findings were statistically not significant.

Contrary to the findings of Kudo et al., our study and the expectations of the authors, Nishizawa et al. found an elevated plasma Kyn levels in preeclampsia (0.032 and 1.21 μmol/L) compared to normal pregnancy (0.020 and 0.958 μmol/L), despite significant reductions in placental indoleamine 2,3-dioxygenase (IDO) expression and activity[304]. The elevation in Kyn levels despite reduction in IDO enzyme activity remains unexplained.

Our recent findings of the presence of functional KYNME on circulating STB-EVs, which can scavenge Kyn in a dose- and time-dependent manner, potentially elucidate the previously observed paradox. STB-EVs obtained from normal pregnancies have demonstrated the presence of functional KYNME, which could explain the reduction in Kyn levels in NP (1.12 μmol/L) compared to the non-pregnant state (1.17 μmol/L). The dose-dependent effect of STB-EVs' KYNME further explains the reduction in Kyn levels in EOPE (1.02 μmol/L) compared to NP (1.12 μmol/L), as EOPE placenta releases more STB-EVs per unit of blood compared to NP[108]. In EOPE, there is a dual impact on Kyn levels: reduced placental activity of indoleamine 2,3-

dioxygenase (IDO) decreases the synthesis of Kyn, while a higher dose of circulating KYNME on STB-EVs breaks down Kyn. The non-pregnant state had comparatively higher levels of circulating Kyn (1.17 μmol/L) since there are no circulating placental EVs with the potential to break down Kyn.

Recent research has demonstrated that Kyn replacement effectively reversed abnormal placentation and reduced the likelihood of developing preeclampsia in uni-nephrectomized mice[318]. Our study introduces a novel approach to investigate the role of STB-EVs in regulating kynurenine metabolism. Specifically, our findings indicate that exposing Kyn to STB-EVs denatured with 100% trifluoroacetic acid (TFA) results in significantly higher levels of Kyn. This finding suggests that STB-EVs actively metabolize kynurenine and that inhibiting this process could be beneficial. Given these insights, our study raises important questions about the potential effectiveness of kynurenine replacement therapy for managing preeclampsia. Moreover, it suggests that further investigation is warranted to explore the combined use of specific KYNME inhibitors and kynurenine replacement as a more effective strategy for managing the condition. Such an approach could mitigate the breakdown of kynurenine, thereby maintaining its beneficial effects on vascular function and potentially alleviating the clinical symptoms of preeclampsia.

Despite the intriguing findings, my study had several limitations. The stringent criteria to define EOPE to generate a homogeneous disease pathophysiology made recruitment challenging, as EOPE has a distinct phenotype from its late-onset counterpart (LOPE), and its relative rarity at John Radcliffe Hospital, Oxford, similar to other institutions in high-income countries, compounded the difficulty. Additionally, the COVID-19 pandemic significantly disrupted patient recruitment, resulting in a small sample size. Limitation due to the non-availability of adequate EOPE STB-EVs, I could not perform functional assessment of KYNME expressed on EOPE STB-EVs.

4.6 Conclusion

This study unveils the functional expression of KYNME in STB-EVs, offering new insights into the clinical syndrome of preeclampsia. These findings highlight the significant role that STB-EVs may play in regulating kynurenine metabolism, which is known to influence vascular function through its vasodilatory and hypotensive effects. Despite the absence of significant differences in KYNME content between NP and EOPE STB-EVs, we observed significantly reduced serum levels of kynurenine in EOPE. This suggests that STB-EVs might contribute to the regulation of circulating kynurenine levels, particularly since circulating levels of STB-EVs are higher in EOPE compared to NP. This dose-dependent effect could lead to higher concentrations of kynurenine-metabolising enzymes and subsequently reduce circulating kynurenine levels, potentially impacting the pathophysiology of PE.

These findings raise important questions for the potential effectiveness of kynurenine replacement as a strategy for managing preeclampsia and suggest further investigation to explore the role of specific KYNME inhibitors in conjunction with kynurenine replacement as a better alternative for attenuating the maternal syndrome of preeclampsia.

4.7 Future direction

Based on these findings, future research should focus on the following directions:

Therapeutic Potential of Kynurenine Pathway Interventions: Investigate the therapeutic potential of co-administering specific kynurenine metabolising enzyme inhibitors with kynurenine replacement therapy to effectively elevate circulating kynurenine levels in EOPE patients to treat the maternal syndrome of preeclampsia.

Biomarker Development: Examine the feasibility of utilizing downstream metabolites of kynurenine metabolism as biomarkers for early screening and disease monitoring in EOPE patients, which could significantly improve clinical outcomes by enabling earlier and more accurate detection of the condition.

CHAPTER 5

MEDIUM/LARGE SYNCYTIOTROPHOBLAST-DERIVED EXTRACELLULAR VESICLES CARRY ANTI-ANGIOGENIC MICRO RNA IN EARLY-ONSET PREECLAMPSIA

Abstract

Introduction: Preeclampsia (PE), a hypertensive disorder specific to pregnancy, disrupts blood flow regulation and can lead to severe consequences for both mother and foetus. Recent research has unveiled the critical role of microRNAs (miRNAs) in PE, with various miRNAs implicated in processes like trophoblast invasion, angiogenesis, and immune modulation. Among these, *hsa-miR-9-5p* has gained attention due to its overexpression in early-onset PE (EOPE) within medium/large syncytiotrophoblast-derived extracellular vesicles (m/lSTB-EVs) and serum extracellular vesicles (EVs). This study aims to investigate the impact of *hsa-miR-9-5p* on human cerebral microvascular endothelial cells (hCMEC/D3), a validated model for studying the blood-brain barrier, and crucial angiogenic processes.

Methods: Key methodologies include quantitative PCR (qPCR) to validate over-expressed miRNA targets in m/lSTB-EVs and serum EVs from EOPE and normal pregnancy (NP) samples. hCMEC/D3 were transfected with *hsa-miR-9-5p* mimics and controls to measure effects on cell proliferation, viability, and migration using wound healing assays. The expression of angiogenesis-related proteins was assessed using a proteome profiler antibody array, and protein-protein interaction networks were constructed using STRING. Furthermore, the response of *hsa-miR-9-5p* treated cells to TNF-α stimulation was evaluated by measuring VCAM-1 expression.

Results: qPCR validation confirmed the significant overexpression of *hsa-miR-9-5p* within EOPE samples. Functional assays revealed that *hsa-miR-9-5p* significantly suppresses hCMEC/D3 cell proliferation and migration, thereby hindering their angiogenic potential. This finding suggests a novel anti-angiogenic role for *hsa-miR-9-5p* in cerebral microvascular endothelial cells. Additionally, *hsa-miR-9-5p* treated cells maintained their responsiveness to

TNF-α stimulation, suggesting a targeted effect on angiogenesis rather than causing general endothelial dysfunction.

Conclusion: The findings reveal a novel anti-angiogenic role for *hsa-miR-9-5p* in cerebral microvascular endothelial cells, contributing to the pathogenesis of preeclampsia. The study suggests a complex interplay between *hsa-miR-9-5p* and angiogenic factors, necessitating further research to elucidate underlying mechanisms.

5.1 Introduction

Preeclampsia (PE) is a complex multisystemic disorder that arises during pregnancy, primarily characterized by hypertension (systolic blood pressure ≥140 mmHg and/or diastolic pressure ≥90 mmHg) accompanied by either significant proteinuria or indications of maternal acute kidney injury, neurological symptoms, and/or features of utero-placental insufficiency. In severe instances, PE can result in maternal or foetal death[328]. The accurate diagnosis of PE poses significant challenges, and the underlying mechanisms of the disease are not yet fully understood[329,330]. PE is recognized as a disorder driven by syncytiotrophoblast stress[331]. The placenta plays a crucial role in the pathogenesis of PE, primarily through the release of soluble factors and syncytiotrophoblast-derived extracellular vesicles (STB-EVs) into the maternal bloodstream[332]. STB-EVs carry a diverse array of biomolecules, including proteins, messenger RNA (mRNA), micro-RNA (miRNA), and transfer RNA (tRNA)[236,333] (6, 7). STB-EVs are categorized into small STB-EVs (< 220 nm in size) and medium/large STB-EVs (≥ 220 nm in size). The biogenesis and release mechanisms of these EVs are particularly noteworthy; medium/large STB-EVs are typically released in response to cellular stress, whereas small STB-EVs are continuously released under normal physiological conditions[331].

MicroRNAs (miRNAs) are one type of small non-coding RNAs – which can be categorised into miRNA, small nucleolar RNA, piwi-interacting RNA and transfer RNA. MicroRNAs typically consist of 19–24 nucleotides[334,335]. These miRNAs exert their regulatory effects on messenger RNA (mRNA) by either promoting mRNA cleavage or repressing its translation[336,337]. In the bloodstream, miRNAs are transported either by various carriers, including extracellular vesicles, argonaut 2 (AGO2) proteins, high-density lipoprotein, and other ribonucleoprotein complexes, or they circulate freely[338]. In the context of PE, aberrant miRNA expression patterns in both maternal circulation and placenta have been implicated in the disease's pathophysiology. These

alterations in miRNA expression may affect several critical processes, such as angiogenesis, immune functions, and trophoblast proliferation and invasion, all of which are disrupted in PE.

Research into circulating miRNAs in PE has primarily focused on examining cell-free miRNAs in the blood, identifying potential biomarkers, and then inferring their placental origin. Comprehensive reviews published in the recent past have catalogued most of the extracellular miRNAs associated with PE identified to date[339,340]. Additionally, Srinivasan et al. highlighted several novel miRNAs, such as *hsa-miR-941, hsa-miR-516b-5p,* and *hsa-miR-let-7b-5p/hsa-miR-155-5p,* suggesting their placental origin. However, their work did not distinguish which specific subtypes of placental EVs – whether small or medium/large STB-EVs express these miRNAs[340]. In contrast, Sheikh et al. addressed this issue by examining EVs or debris derived from placental explants[339]. In a separate investigation, Wei et al. examined the role of placental EVs in PE and identified a distinct microRNA profile in PE placental EVs generated from placental explants compared to that of normal pregnancies[341]. The small RNA composition of EVs derived from explant cultures differed significantly from that obtained via *ex vivo* dual lobe perfusion. Wei et al. reported that the majority of EVs produced from placental explants primarily contain microRNAs[341]. Conversely, small RNA sequences contained in EVs obtained from *ex vivo* dual lobe perfusion predominantly contained tRNA half fragments[342].

Most researchers have focused on small STB-EVs, or whole serum as biological samples, rather than medium/large STB-EVs. Our group diverged from this trend by concentrating on medium/large STB-EVs (m/lSTB-EVs) in both normal and PE placentae considering that m/lSTB-EVs are released in response to stress, which is a hallmark of PE[331].

Toluwalase Awoyemi (NDWRH, University of Oxford) performed RNA sequencing on m/lSTB-EVs obtained via *ex vivo* dual lobe placental perfusion performed on early-onset PE (EOPE; n = 8) and normal pregnancy (NP, n = 6). Transcriptomic data were subjected to bioinformatic analysis to identify differentially expressed miRNAs (DEMs) in EOPE m/lSTB-EVs.

5.1.1 Differentially expressed miRNAs in preeclamptic m/l STB-EVs

Comparison between DEMs carried in m/lSTB-EVs of EOPE and normal pregnancy showed 47 upregulated miRNAs and 53 down regulated miRNAs that had significant $\log_2$ fold change ($p < 0.05$). Table 16 summarizes the top 20 upregulated DEMs in EOPE. I focussed on upregulated miRNAs since EOPE is characterized by release of increased quantity of STB-EVs per unit volume of blood[108].

Upregulated miRNAs that were not previously described in preeclampsia (*hsa-miR-4488, hsa-miR-3196, hsa-miR-4516,* and *hsa-miR-9-5p*) and those that were not previously described in preeclamptic m/lSTB-EVs (*hsa-miR-193b-5p* and *hsa-miR-210-3p*) were considered for qPCR validation. I primarily focussed on miRNAs that were reported to have a role in regulating angiogenesis.

Table 16 - List of upregulated miRNAs in m/lSTB-EVs

miRNA	Log2 fold change	Adjusted *p* value
hsa-miR-4488*	1.57	< 0.0001
hsa-miR-3196*	1.56	< 0.0001
hsa-miR-4516*	1.54	< 0.0001
hsa-miR-193b-5p^{+}	1.46	< 0.0001
hsa-miR-210-3p^{+}	1.42	< 0.0001
hsa-miR-27a-5p	1.35	< 0.0001
hsa-miR-3656	1.21	< 0.001
p-hsa-miR-113	1.20	< 0.0001
hsa-miR-3960	1.09	< 0.001
hsa-miR-6089	1.05	< 0.001
hsa-miR-127-3p	1.03	< 0.01
p-hsa-miR-317	1.00	< 0.01
p-hsa-miR-338	0.90	< 0.01
hsa-let-7b-5p	0.87	< 0.01
hsa-miR-9-5p*	0.85	< 0.01
hsa-miR-483-3p	0.85	< 0.01
hsa-miR-493-5p	0.83	< 0.01
hsa-miR-455-3p	0.82	< 0.01
hsa-miR-99a-5p	0.81	< 0.01
hsa-miR-370-3p	0.79	< 0.01

* Not previously described in preeclampsia; + Not previously described in preeclamptic m/lSTB-EVs (checked at human microRNA disease database version 3.2)

5.1.2 Angiogenesis

Angiogenesis – the tightly regulated sprouting of new blood vessels from pre-existing vasculature, represents a fundamental process underpinning normal tissue growth and development[343,344]. Tissues with increased demand for more oxygen release vascular endothelial growth factor A (VEGFA) that acts on endothelial cells. VEGFA stimulation leads to a sequential process involving (a) digestion of the basement membrane of the parent vessels; (b) migration of endothelial cells towards the source of the signal and proliferation of cells as they migrate; and (c) formation of a capillary sprout eventually forming a lumen[345–348].

Angiogenesis in normal placental development is a critical physiological process essential for a healthy pregnancy as it creates branched vascular network, crucial for efficient nutrient and oxygen exchange between the mother and the foetus[349]. Proper regulation of angiogenesis is therefore fundamental to placental development and successful pregnancy outcomes. Impaired placental vascular development has been associated with early embryonic mortality[350,351].

Endothelial cells, constituting the endothelium, line the inner surface of the vasculature separating blood products from underlying collagen and smooth muscle[352], and function as a multifaceted endocrine organ, regulating angiogenesis, vascular permeability, inflammation, and a multitude of other physiological processes (Figure 17)[353]. Endothelial cells regulate vascular structure and function through the dynamic release of chemical mediators in response to endothelial stimulation, thereby regulating blood flow[354].

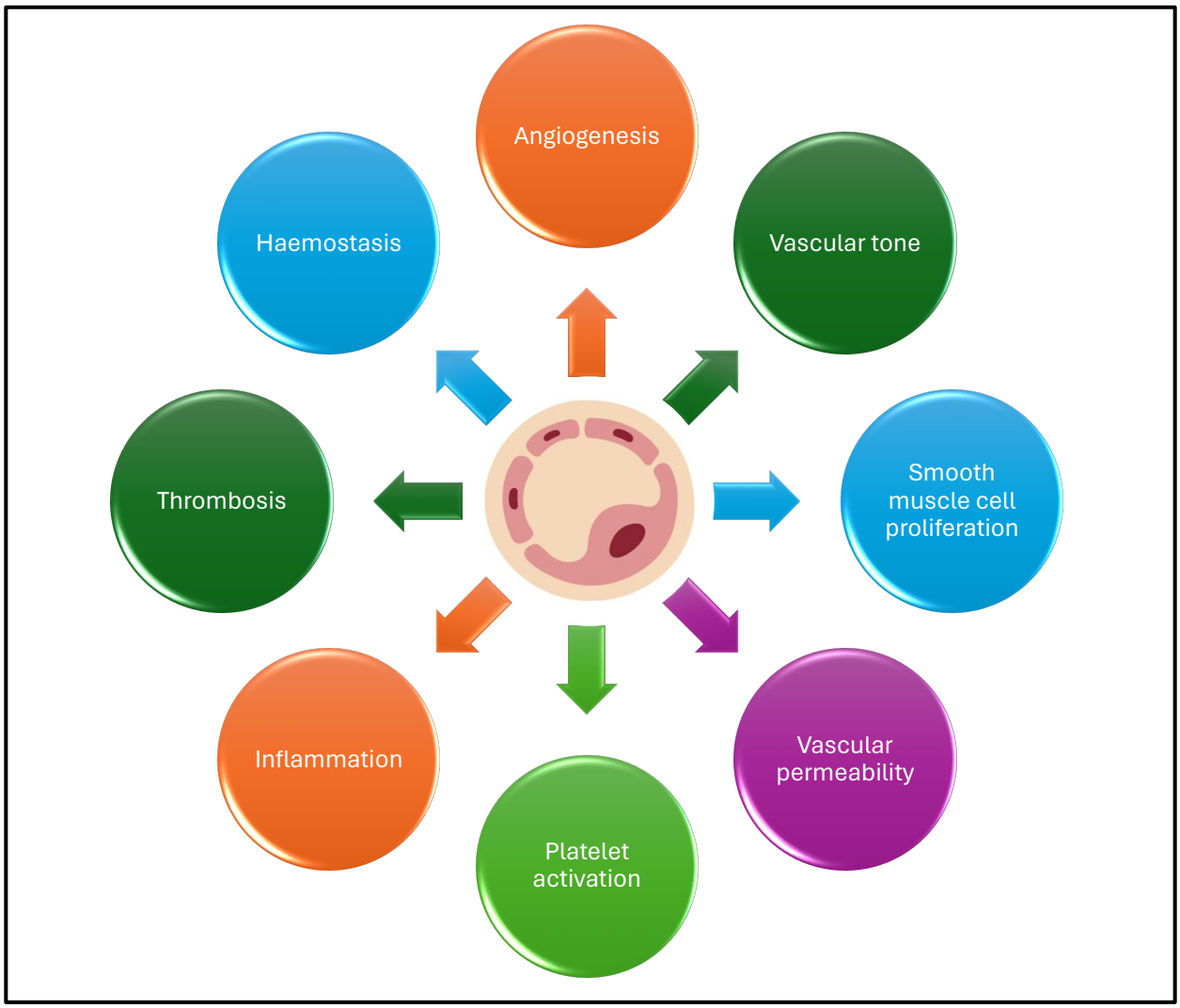


Figure 17 - Multiple functions of endothelial cells

5.1.3 Endothelial dysfunction in preeclampsia

Preeclampsia is characterized by widespread maternal end-organ dysfunction, most notably evident in the brain, kidneys, and liver. A hallmark feature of this condition is the loss of the characteristic flattened morphology and function of endothelial cells within these affected organs[355]. The features of endothelial dysfunction associated with PE is well documented in glomerular endothelium, which show endotheliosis (swelling of endothelial cells) and microvascular obstruction[356]. Similar morphological features were elucidated in endothelial cells of patients who received VEGF blockers (e.g., bevacizumab) as treatment for cancer[357,358], suggesting the potential role of alterations in VEGF signalling in the pathogenesis of preeclampsia.

Soluble fms-like tyrosine kinase-1 (sFlt-1), a factor excessively released by the placenta in preeclampsia[33,109], disrupts vascular function. Elevated circulating sFlt-1 levels correlate with decreased levels of VEGF and PlGF[33]. Animal studies demonstrate that exogenous sFlt-1 administration directly inhibits the pro-angiogenic effects of VEGF and PlGF, leading to microvascular dysfunction[33]. Medical conditions frequently associated with increased incidence of preeclampsia, including diabetes mellitus, autoimmune vascular diseases, and hypertension, all share a component of microvascular dysfunction in their pathogenesis[355]. These compelling facts suggest that preeclampsia is characterized by microvascular disease.

5.1.4 Cerebral circulation in preeclampsia

In normal pregnancy, maternal organs such as the uterus, kidneys, and heart undergo adaptations to accommodate the increased perfusion resulting from hormonal and cardiovascular changes. The brain, however, adapts its circulation to maintain stability and safeguard its intricate milieu.

The adaptations in cerebral circulation include structural remodelling of the brain parenchymal micro-circulation involving arteriogenesis and angiogenesis [359].

Preeclampsia is associated with notable structural and functional alterations in the brain[360–362], potentially increasing the risk of both immediate[363,364] and long-term adverse outcomes, including three-fold increase in risk of vascular dementia[365] and two-fold increase in risk of stroke[366]. Preclinical studies investigating the effect of plasma of preeclamptic women on animal blood vessels demonstrated signs of blood-brain barrier (BBB) disruption[367,368]. Similar findings were demonstrated *in vitro* on human cerebral microvascular endothelial cells (hCMEC/D3)[369,370].

I hypothesized that impairment of new blood vessel formation in the brain parenchyma during preeclampsia may underlie the potential immediate and long-term cerebrovascular alterations. Studying angiogenic capacity of cerebral blood vessels in pregnancy is ethically questionable and technically difficult. To overcome this issue, we used cell-based model as an alternative, as it allows to explore events at cellular level. Investigators have used human cerebral microvascular endothelial cells (hCMEC/D3) as a reliable cell-based model to investigate cerebral vascular functions[369]. Previously it has been shown the STB-EVs enter target cells and deliver their cargo, including miRNA, and alter intracellular signalling pathways[168,371]. Thus, I decided to use hCMEC/D3 as primary cell model to investigate the effects of differentially expressed miRNAs in m/lSTB-EVs on angiogenesis.

5.2 Aims

The aims of this chapter are to:

1. validate selected over-expressed miRNAs from the RNA sequencing data of m/lSTB-EVs
2. validate selected miRNA from m/lSTB-EVs in serum samples obtained from EOPE and NP women
3. investigate the effect of *hsa-miR-9-5p* on cell proliferation, viability and migration of hCMEC/D3
4. investigate the effect of *hsa-miR-9-5p* on angiogenesis related protein expression of hCMEC/D3

5.3 Methods

The methodologies employed in this chapter are detailed in Chapter 2. In summary, qPCR was performed to validate over-expressed miRNA targets in m/lSTB-EVs obtained from *ex vivo* dual lobe placental perfusion of EOPE (n=4) and NP (n=4) women and validate *hsa-miR-9-5p* on EVs isolated from serum of women with EOPE (n=8) and NP (n=8). hCMEC/D3 transfected with *hsa-miR-9-5p* mimic (treatment group) and negative scramble (control group) were assessed for cell proliferation, cell viability, and cell migration. The impact of *hsa-miR-9-5p* treatment on the expression of angiogenesis-related proteins in hCMEC/D3 was assessed using the Proteome Profiler™ Human Angiogenesis Antibody Array Kit. Protein-protein interaction (PPI) networks of differentially expressed proteins were constructed using STRING online tool and relevant gene ontology terms and KEGG pathways were delineated. VCAM-1 expression in TNF-α stimulated hCMEC/D3 (treatment and control groups) was assessed using ELISA. Data analysis and representation were carried out using R (*v4.3.1*) and GraphPad Prism (*v10.2.2*, Boston, MA, USA), with statistical significance set at $p < 0.05$.

5.4 Results

5.4.1 Patient characteristics of the m/lSTB-EV samples used for validation

Table 17 summarizes comparative analysis between women with EOPE and NP, examining various parameters, including maternal age, body mass index (BMI), systolic and diastolic blood pressure measurements, proteinuria manifestation, gestational age at delivery, birth weight and incidence of intrauterine growth restriction (IUGR).

Notably, the two cohorts demonstrated statistically significant differences across several metrics. Women with EOPE exhibited elevated systolic and diastolic blood pressure readings, proteinuria, and increased incidence of IUGR, compared to their normal counterparts ($p < 0.001$).

Furthermore, the gestational age at delivery and birth weight of the newborn were significantly reduced in EOPE cases ($p < 0.001$). However, parameters such as maternal age, and BMI did not demonstrate statistically significant discrepancies between the two groups.

5.4.2 qPCR validation of selected miRNA targets on m/lSTB-EVs

I performed validation of selected upregulated miRNAs (*hsa-miR-4488, hsa-miR-3196, hsa-miR-4516, hsa-miR-9-5p, hsa-miR-193b-5p* and *hsa-miR-210-3p*) jointly with Toluwalase Awoyemi (NDWRH, Oxford) on m/lSTB-EVs obtained from *ex vivo* dual lobe placental perfusions performed on placentae of women with EOPE (n = 6) and normal pregnancy (n = 6). Figure 18 and Table 18 compares the RNA sequencing data and qPCR results of the selected miRNA targets.

qPCR validation identified four significantly over-expressed miRNA targets (*hsa-miR-3196, hsa-miR-9-5p, hsa-miR-193b-5p* and *hsa-miR-210-3p*) in EOPE compared to NP ($p < 0.05$) and were further considered for validation in serum samples and downstream analysis.

Literature review and review of the miRNA disease database (version 3.2) search revealed that *hsa-miR-9-5p* and *hsa-miR-3196* had not previously been reported in preeclampsia. *hsa-miR-3196* was primarily reported to play a role in tumourigenesis while several studies reported the role of *hsa-miR-9-5p* on tumour angiogenesis.

The potential effect of *hsa-miR-9-5p* on angiogenesis and the role of impaired angiogenesis in the pathogenesis of preeclampsia provoked interest to study *hsa-miR-9-5p* in depth in relation to the pathophysiology of preeclampsia.

Table 17 - Patient characteristics of m/lSTB-EV samples

Characteristic	NP (n = 6)	EOPE (n = 6)	*p* value
Maternal age (*y*)	33.8 ± 5.6	34.1 ± 4.4	> 0.05
Maternal BMI (kgm^{-2})	27.8 ± 7.4	28.7 ± 8.4	> 0.05
SBP (*mmHg*)	122.3 ± 8.5	162.1 ± 13.7	< 0.001
DBP (*mmHg*)	74.2 ± 4.6	102.6 ± 8.4	< 0.001
Proteinuria (*pluses*)	0	2.2 ± 1.2	< 0.001
Gest. age at delivery (*weeks*)	39.3 ± 0.7	31.9 ± 3.5	< 0.001
Birth wt. (*g*)	3641.3 ± 578.7	1532.3 ± 686.6	< 0.001
IUGR (*%*)	0	83.3	< 0.05

Data are presented as mean ± standard deviation (SD). Two groups were analysed using unpaired student *t-test*. Statistical significance was set at $p < 0.05$.

NP – normal pregnancy; EOPE – early-onset preeclampsia; *y* – years; BMI – body mass index; SBP – systolic blood pressure; DBP – diastolic blood pressure; Gest. age – gestational age; IUGR – intrauterine growth restriction.

Table 18 - Log fold change and log fold standard error of selected miRNAs

miRNA	RNA Seq			qPCR		
	LFC	**LSE**	***p* value**	**LFC**	**LSE**	***p* value**
hsa-miR-4488	1.57	0.32	< 0.0001	1.22	-1.23	0.08
hsa-miR-3196	**1.56**	**0.25**	**< 0.0001**	**0.89**	**-2.60**	**< 0.05**
hsa-miR-4516	1.54	0.30	< 0.0001	0.53	-1.32	0.20
hsa-miR-193b-5p	**1.46**	**0.25**	**< 0.0001**	**2.02**	**-0.02**	**< 0.05**
hsa-miR-210-3p	**1.42**	**0.27**	**< 0.0001**	**4.58**	**2.87**	**< 0.01**
hsa-miR-9-5p	**0.85**	**0.31**	**< 0.01**	**4.73**	**3.30**	**< 0.001**

RNA Seq – RNA sequencing; qPCR – quantitative polymerase chain reaction; LFC – $\log_2$ fold change; LSE – log standard error

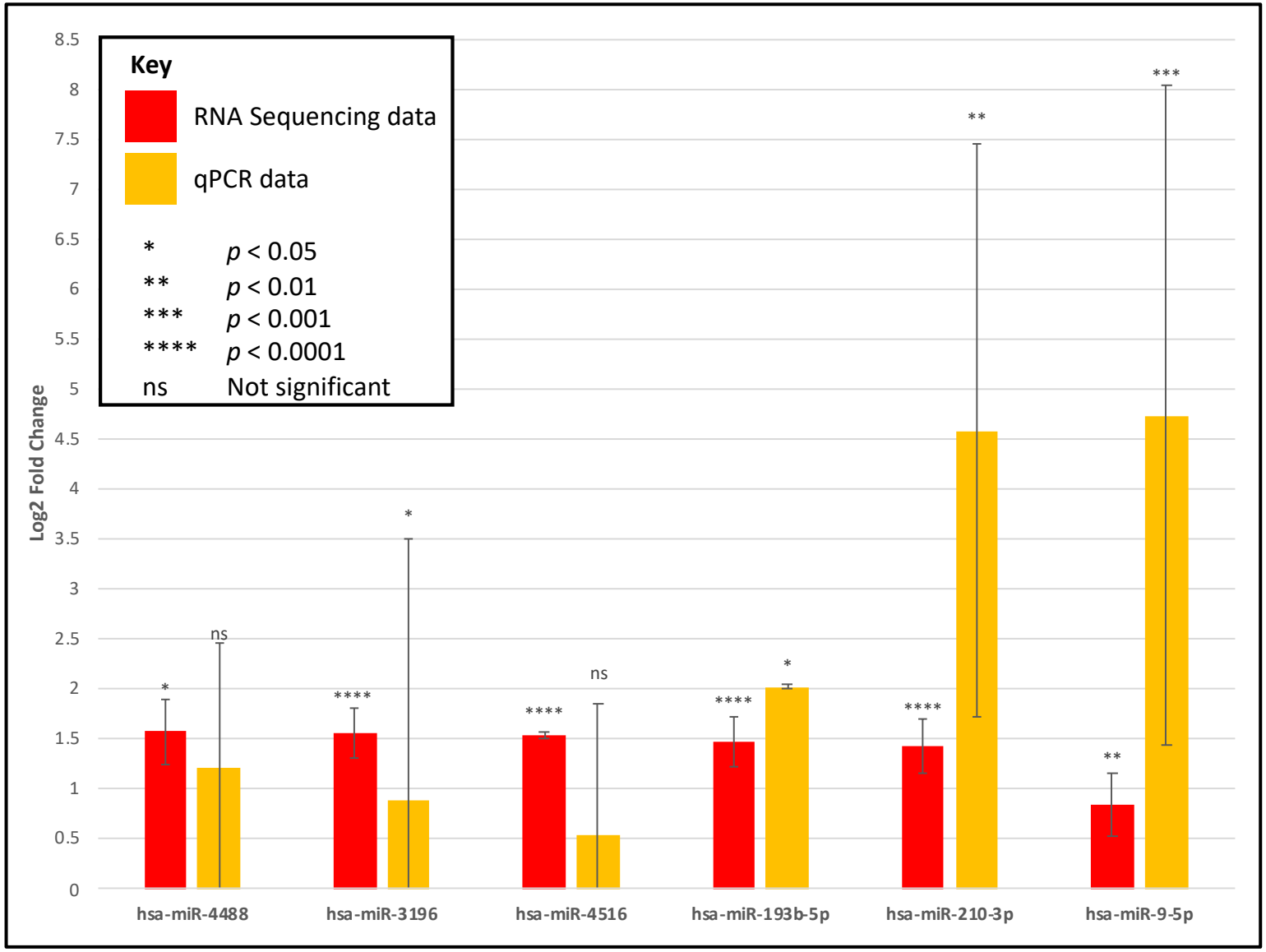


Figure 18 - RNA Sequencing and qPCR data of selected miRNA targets

5.4.3 Patient characteristics of the serum extracellular vesicles used for validation

Table 19 presents a comprehensive comparative analysis between normal pregnancies and those affected by EOPE. The two cohorts demonstrated statistically significant disparities across several metrics. EOPE pregnancies exhibited markedly elevated systolic and diastolic blood pressure readings, a notable prevalence of proteinuria, higher incidence of IUGR, and elevated sFlt-1:PlGF ratio relative to their normal counterparts ($p < 0.05$). The gestational age at delivery and the birth weight of the newborn were significantly reduced in EOPE cases ($p < 0.05$). Parameters such as maternal age, BMI and gestational age at sample collection were not significantly different between the groups.

5.4.4 qPCR validation of *hsa-miR-9-5p* on serum EV samples

qPCR validation on serum EVs revealed that EOPE women over-expressed *hsa-miR-9-5p* compared to women with NP (LFC = 1.03; $p < 0.05$). Figure 19 compares the $\log_2$ fold changes of *hsa-miR-9-5p* in RNA sequencing and qPCR data obtained from m/lSTB-EVs and qPCR data obtained from serum EVs.

After establishing and validating the over expression of *hsa-miR-9-5p* in m/lSTB-EVs and serum EVs obtained from women with EOPE, I sought to investigate the effect of synthetic *hsa-miR-9-5p* on human cerebral microvascular endothelial cells (hCMEC/D3).

Table 19 - Patient characteristics of serum samples

Characteristic	NP (n = 8)	EOPE (n = 8)	*p* value
Maternal age (*y*)	30.0 ± 5.7	35.6 ± 6.4	> 0.05
Maternal BMI (kgm^{-2})	33.7 ± 13.8	28.1 ± 12.3	> 0.05
Gest. age at blood collection (*weeks*)	30.3 ± 2.6	30.1 ± 2.2	> 0.05
SBP (*mmHg*)	127.8 ± 8.3	170.0 ± 32.4	< 0.05
DBP (*mmHg*)	77.6 ± 4.5	111.3 ± 24.3	< 0.05
Proteinuria (*pluses*)	0	2.8 ± 1.5	< 0.001
Gest. age at delivery (*weeks*)	38.3 ± 1.3	33.1 ± 3.7	< 0.001
Birth wt. (*g*)	3083.1 ± 604.4	1770.3 ± 962.8	< 0.05
IUGR (*%*)	0	87.5	< 0.001
sFlt-1:PlGF	5.4 ± 3.9	461.1 ± 166.5	< 0.001

Data are presented as mean ± standard deviation (SD). Two groups were analysed using unpaired student *t-test*. Statistical significance was set at $p < 0.05$.

NP – normal pregnancy; EOPE – early-onset preeclampsia; *y* – years; BMI – body mass index; SBP – systolic blood pressure; DBP – diastolic blood pressure; Gest. age – gestational age; IUGR – intrauterine growth restriction.

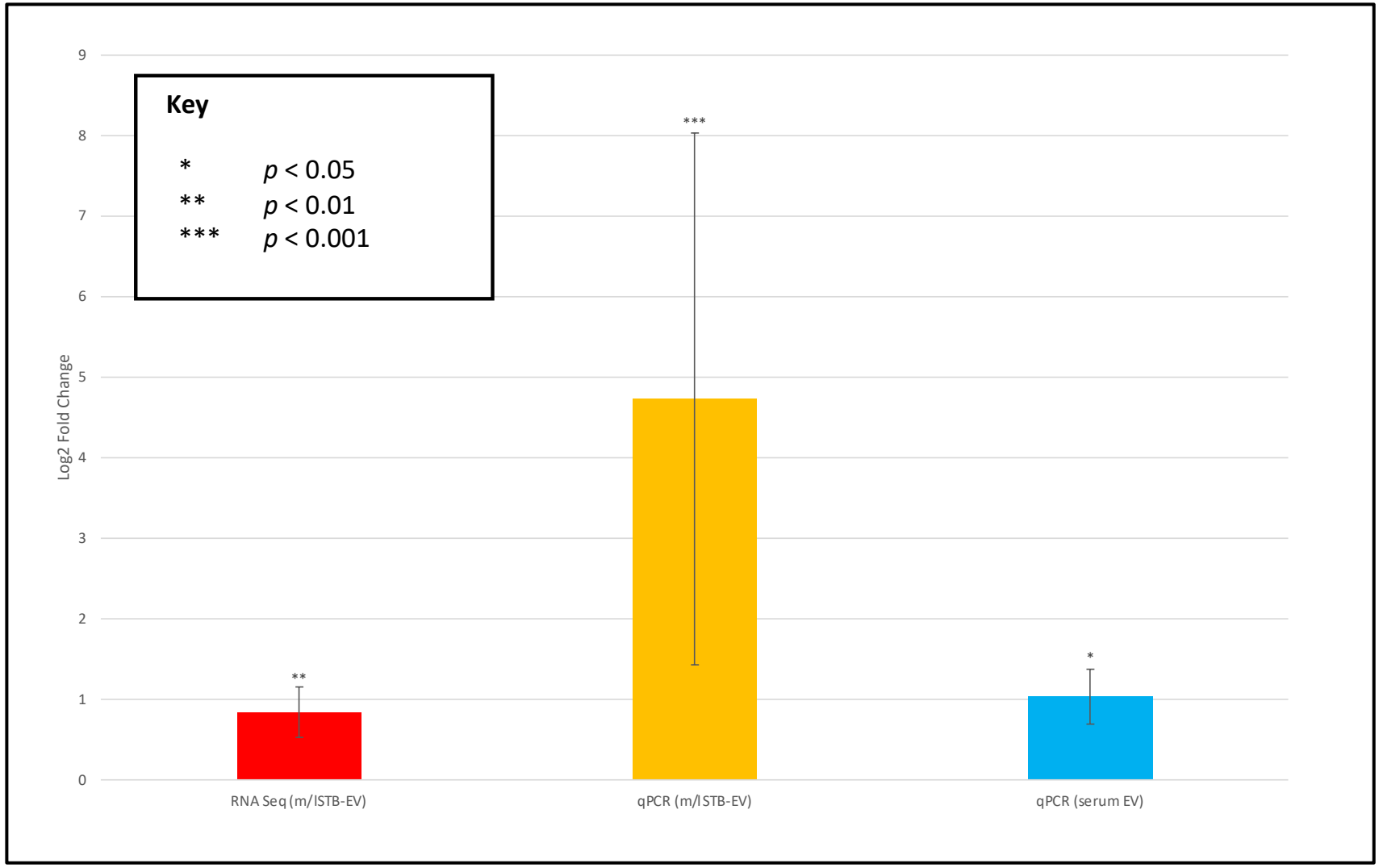


Figure 19 - Log fold changes for *hsa-miR-9-5p* in m/lSTB-EVs and serum EVs

5.4.5 *hsa-miR-9-5p* attenuates hCMEC/D3 proliferation

The effect of *hsa-miR-9-5p* on hCMEC/D3 cell proliferation was assessed by comparing the absolute live cell counts after co-culturing hCMEC/D3 with negative scramble, *hsa-miR-9-5p* [5 nM], and *hsa-miR-9-5p* [10 nM] after 2, 24 and 48 hours of treatment. Compared to the control group transfected with scramble miRNA, the cell viability of hCMEC/D3 remained unaffected after exposure to *hsa-miR-9-5p* at concentrations of 5 nM and 10 nM, as illustrated in Figure 20.A. This indicated that *hsa-miR-9-5p* did not exert any immediate cytotoxic effects at these concentrations.

Nevertheless, a different trend was observed when examining cell proliferation over time. At both 24- and 48-hours post-treatment, hCMEC/D3 treated with *hsa-miR-9-5p* displayed a pronounced and statistically significant reduction in cell proliferation in a dose-dependent manner, in comparison to the control group, as shown in Figure 20.B ($p < 0.05$).

This suggests that *hsa-miR-9-5p* significantly inhibits the proliferative capacity of hCMEC/D3 over time in a dose dependent manner, while having no impact on cell viability, highlighting its potential role in regulating endothelial cell proliferation.

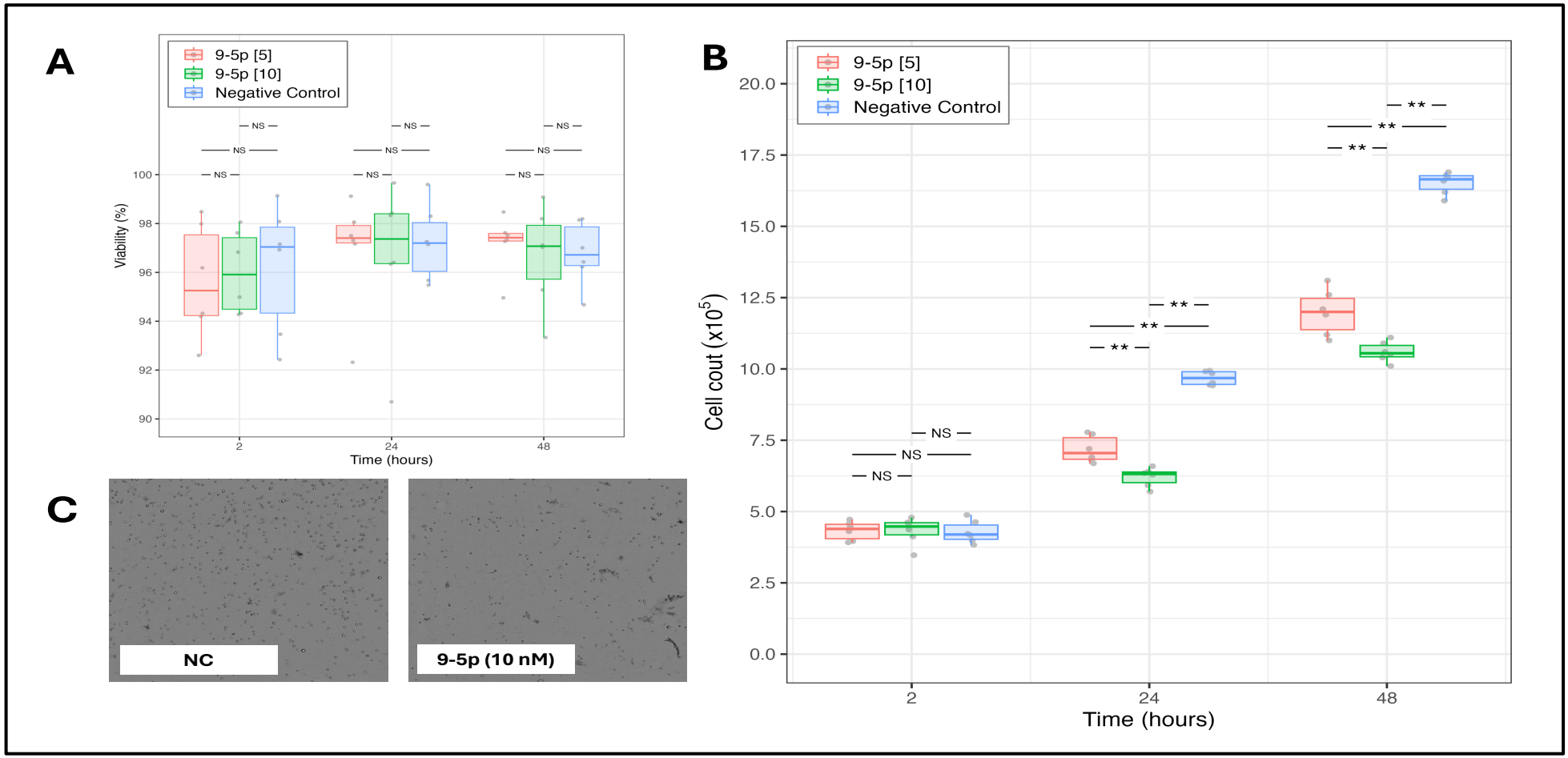


Figure 20 - miR-9-5p attenuates microvascular endothelial cell proliferation

A) Control and treatment groups (*hsa-miR-9-5p* 5 nM and 10 nM) showed no difference in cell viability. **B)** Treatment groups showed significant dose-dependent attenuation in hCMEC/D3 cell proliferation at 24- and 48-hours post-treatment. **C)** Representative images of live cells captured by the automated cell counter show significant reduction in cell number in treatment group compared (9-5p) to control group (NC). The groups were compared using two-way ANOVA followed by Turkey's post hoc test and statistical significance was set at $p < 0.05$ (NS – Not significant; $^{**}p < 0.01$).

5.4.6 *hsa-miR-9-5p* attenuates hCMEC/D3 migration

To further investigate the impact of *hsa-miR-9-5p* on angiogenic capacity of endothelial cells, I performed wound healing assay on hCMEC/D3 treated with *hsa-miR-9-5p* and negative scramble.

Initial optimization experiment was performed to determine the time taken for gap-closure by the hCMEC/D3 when treated with growth medium (Figure 21.A). Based on the findings, it was determined that hCMEC/D3 achieved significant wound gap-closure by 16 hours. Subsequently, I optimized the dose of *hsa-miR-9-5p* by comparing the wound gap-closure achieved with negative scramble and *hsa-miR-9-5p* at 5 nM and 10 nM concentrations (Figure 21.B). Based on the results, I selected 10 nM concentration of *hsa-miR-9-5p* for the wound healing assay. The findings revealed that treatment with *hsa-miR-9-5p* significantly impaired hCMEC/D3 cell migration compared to the control group, as depicted in Figure 22.A ($p < 0.05$).

Specifically, at 16 hours post-treatment, cells treated with *hsa-miR-9-5p* achieved approximately 50% gap closure, while the control group achieved 90% closure. By 24 hours, the gap closure in the *hsa-miR-9-5p* treated group reached about 70%, in stark contrast to the 95% closure observed in the control group (Figure 22.B). These substantial reductions in gap closure indicate that *hsa-miR-9-5p* markedly attenuated the ability of hCMEC/D3 to migrate.

The results from both proliferation and wound healing assays suggested that *hsa-miR-9-5p* significantly diminished the pro-angiogenic potential of hCMEC/D3.

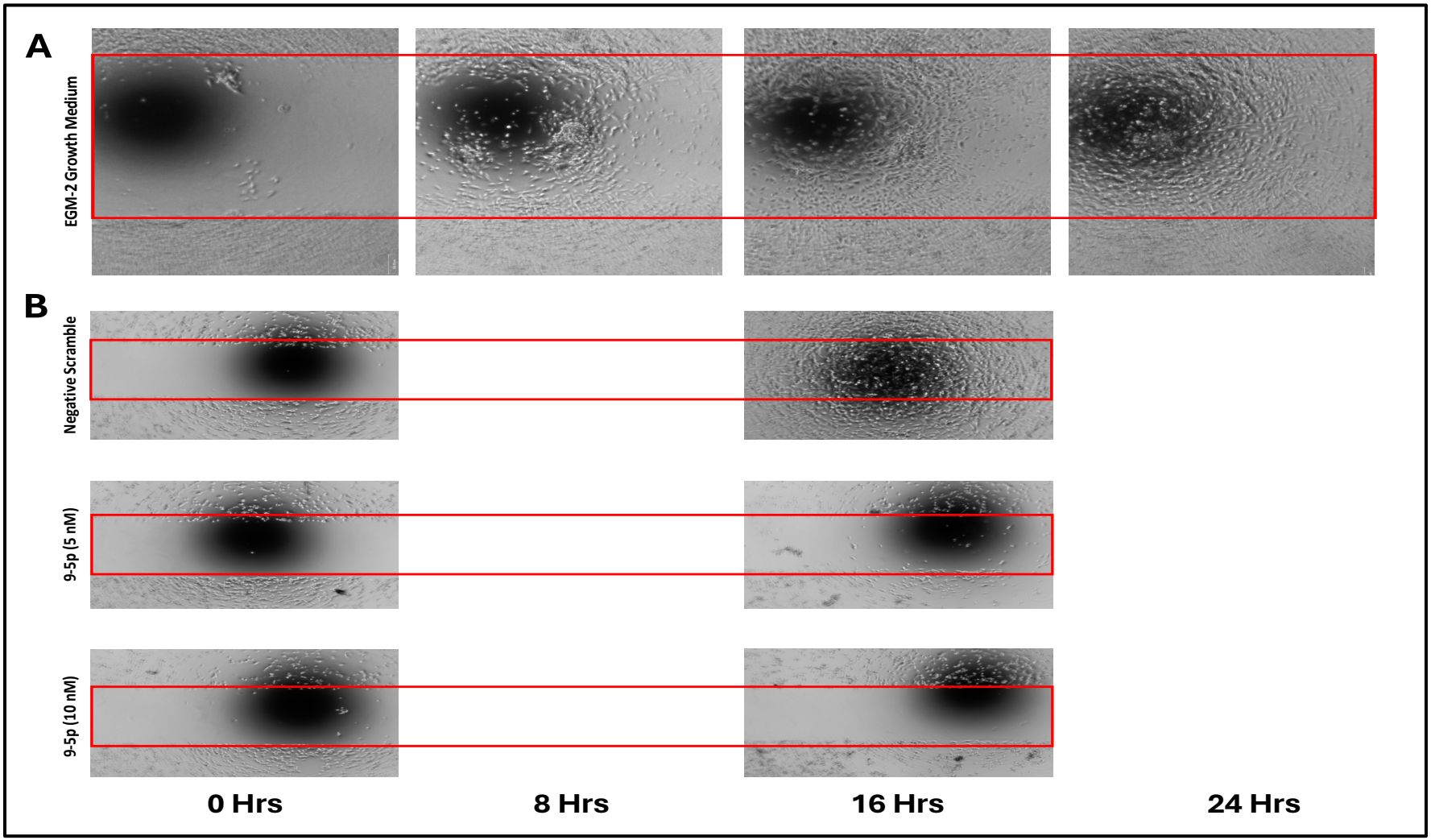


Figure 21 - Optimization experiments for wound healing assay

A) hCMEC/D3 treated with EGM-2 growth medium achieved wound closure in 16 hours. **B)** hCMEC/D3 treated with negative scramble achieved wound closure in 16 hours while cells treated with *hsa-miR-9-5p* (5 nM and 10 nM) showed attenuated cell migration.

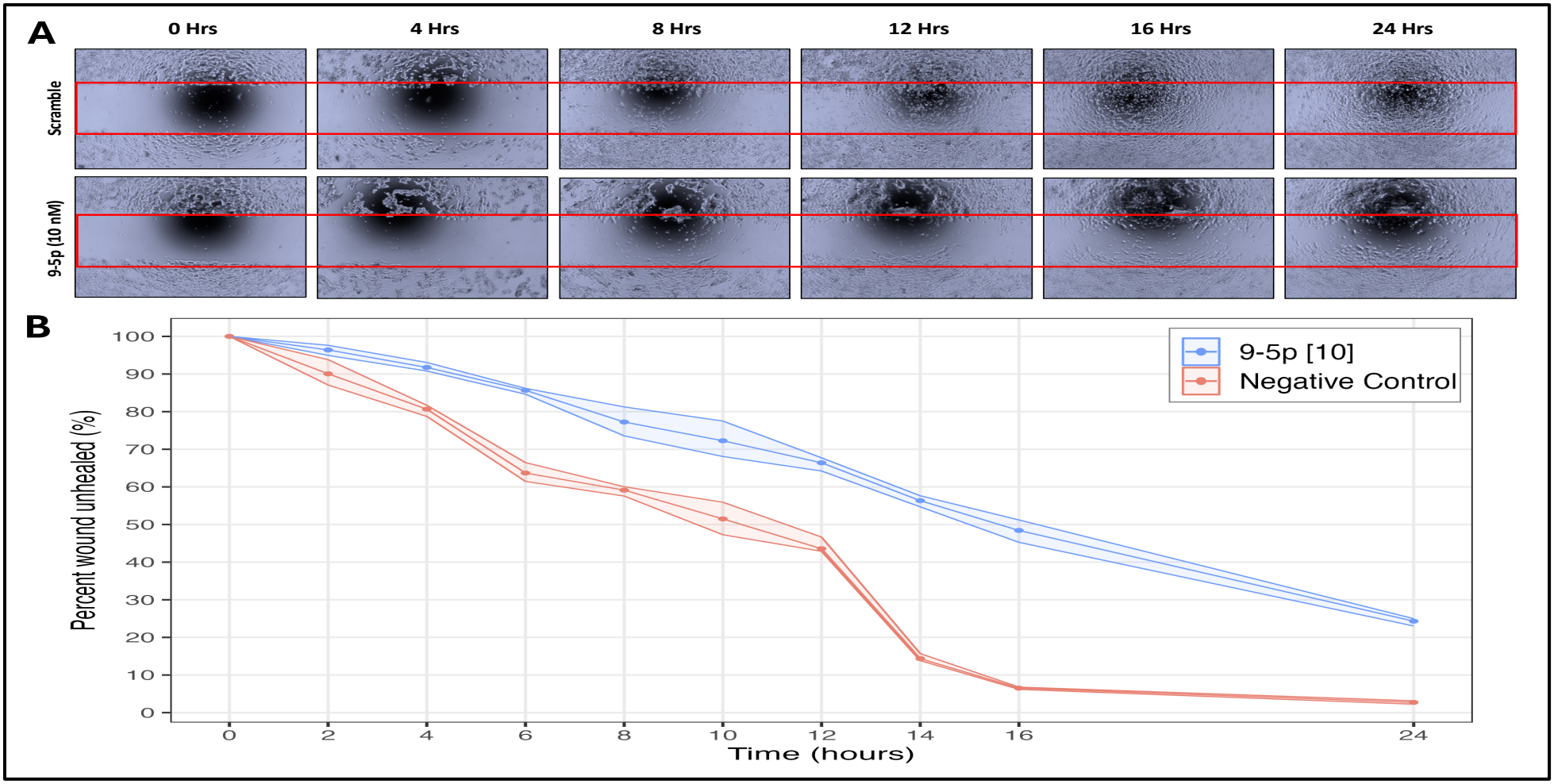


Figure 22 - miR-9-5p attenuates hCMEC/D3 cell migration

A) Representative images of wound healing assay performed on hCMEC/D3 treated with negative scramble and *hsa-miR-9-5p* (10 nM) captured at 0-, 4-, 8-, 12-, 16-, and 24-hours. **B)** Graph demonstrating the wound gap over the time course. The treatment and control groups were compared using student's T-test with Bonferroni correction at each time point. The differences were significant for all time points > 0 hours ($p < 0.001$).

5.4.7 *hsa-miR-9-5p* alters the angiogenic-protein profile of hCMEC/D3

To substantiate the observed attenuation of pro-angiogenic processes, I conducted an angiogenesis proteomic array analysis. The array investigated the expression of 55 angiogenesis-related proteins and measurement of mean pixel density obtained from the experiment revealed hCMEC/D3 treated with *hsa-miR-9-5p* (10 nM) differentially expressed 47 angiogenesis-related proteins (11 over-expressed and 36 under-expressed) compared to control group (Figure 23). From these differentially expressed proteins, I selected 19 proteins that exhibited a $\log_2$ fold change > 0.5 for further analysis (Table 20).

5.4.8 Protein-protein interaction network and functional enrichment of differentially expressed angiogenesis-related proteins

I generated and visualized protein-protein interaction (PPI) networks for the differentially expressed proteins (DEPs) using the STRING tool with a high confidence threshold of 0.70 and including a maximum of 10 interacting proteins in the second shell (Figure 24). The observed changes in endothelial cell proliferation and migration were found to be associated with alterations in the expression of these specific proteins in hCMEC/D3.

Furthermore, I identified and annotated the interactions between proteins that regulate vascular endothelial cell proliferation and migration with a false discovery rate (FDR) of less than 0.001.

Among the positive regulators of endothelial cell proliferation, PDGFB, VEGFC and PGF (PlGF) were prominent, while THBS1, PRL and VASH1 were identified as negative regulators (Figure 25.A). FGF2, KDR, FLT4, TEK and FLT1 identified as regulators of proliferation are interacting proteins in the 2nd shelf. Figure 25.B depicts the $\log_2$ fold changes of identified

positive and negative regulators of endothelial cell proliferation, suggesting an overall attenuation of hCMEC/D3 proliferation. This claim needs to be validated with further investigations.

Among the regulators of vascular endothelial cell migration, PDGFB, VEGFC, and PLG were found to be prominent positive regulators, while ANGPT2 and VASH1 were identified as negative regulators. THBS1 and TGFB1 were identified as regulators of endothelial migration with the ability of positive and negative regulation depending on the target receptors (Figure 26.A). KDR and FGF2 identified as regulators of migration are interacting proteins in the 2nd shelf. Figure 26.B depicts the $\log_2$ fold changes of identified positive and negative regulators of endothelial cell migration, suggesting an overall attenuation of hCMEC/D3 migration. This claim also needs to be validated with further investigations.

Additionally, the protein-protein interaction (PPI) network and KEGG pathways associated with preeclampsia were also identified. Focal adhesions, ECM receptor interactions, PI3k/Akt signalling pathway and HIF-1 signalling pathway were identified to be associated with the interrogated PPI network that were previously reported to be associated with preeclampsia. Table 21 summarizes the top 30 gene ontology (GO) terms (biological processes), and table 22 summarizes top 30 KEGG pathways associated with the established PPI network according to their strength of evidence (FDR < 0.05).

This comprehensive analysis underscores the complex regulatory network influenced by *hsa-miR-9-5p*, providing deeper insights into its role in modulating angiogenesis in cerebral microvascular endothelial cells and its potential implications in preeclampsia.

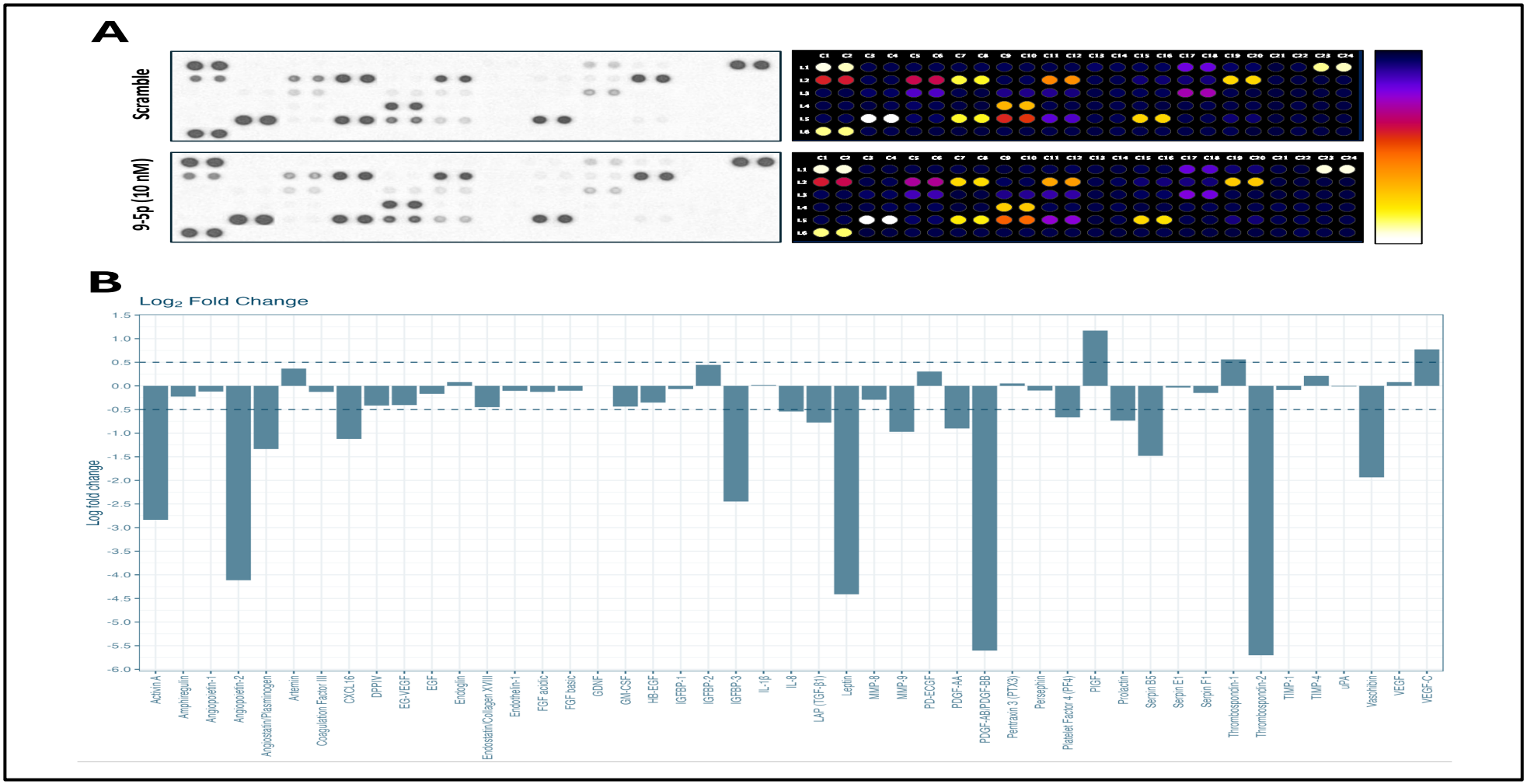


Figure 23 - Altered angiogenesis-related protein profile of hCMEC/D3

A) X-ray images and colour-coded band density images obtained Protein Array Analyzer plugin from angiogenesis-related proteome profiler array of hCMEC/D3 treated with negative scramble (top panel) and *hsa-miR-9-5p* (10 nM) bottom panel. **B)** Graphical representation of log-transformed normalized data of differentially expressed angiogenesis-related proteins in the treatment group.

Table 20 - Log fold changes of differentially expressed angiogenesis-related proteins in hCMEC/D3 treated with miR-9-5p (10 nM)

Under-expressed proteins	LFC	Over-expressed proteins	LFC
Thrombospondin-2 (THBS2)	-5.70	Placental growth factor (PlGF/PGF)	1.17
Platelet-derived growth factor-BB (PDGFB)	-5.60	Vascular endothelial growth factor-C (VEGFC)	0.77
Leptin (LEP)	-4.41	Thrombospondin-1 (THBS1)	0.56
Angiopoeitin-2 (ANGPT2)	-4.11		
Activin-A (INHBA)	-2.84		
Insulin-like growth factor binding protein-3 (IGFBP3)	-2.45		
Vasohibin (VASH1)	-1.94		
Serpin B5 (SERPINB5)	-1.48		
Plasminogen (PLG)	-1.34		
Chemokine (C-X-C motif) ligand 16 (CXCL16)	-1.12		
Matrix metalloproteinase-9 (MMP9)	-0.97		
Platelet-derived growth factor-AA (PDGFA)	-0.90		
Transforming growth factor beta-1 (TGFB1)	-0.78		
Prolactin (PRL)	-0.74		
Platelet factor 4 (PF4)	-0.67		
Interleukin 8 (CXCL8)	-0.54		

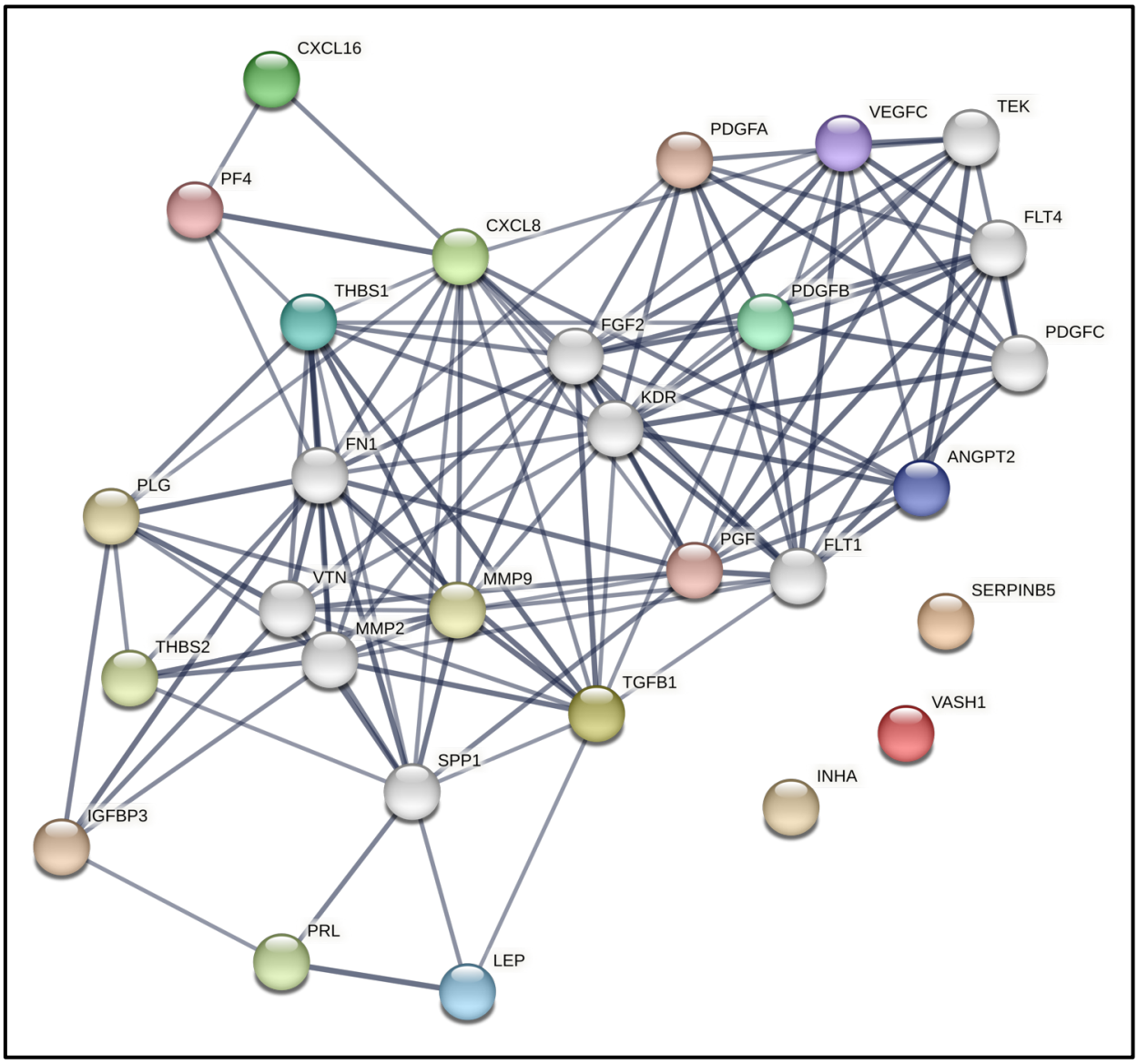


Figure 24 – PPI network of differentially expressed angiogenesis-related proteins

The proteins differentially expressed by the hCMEC/D3 are denoted by the coloured shells and interactors are denoted by grey shells.

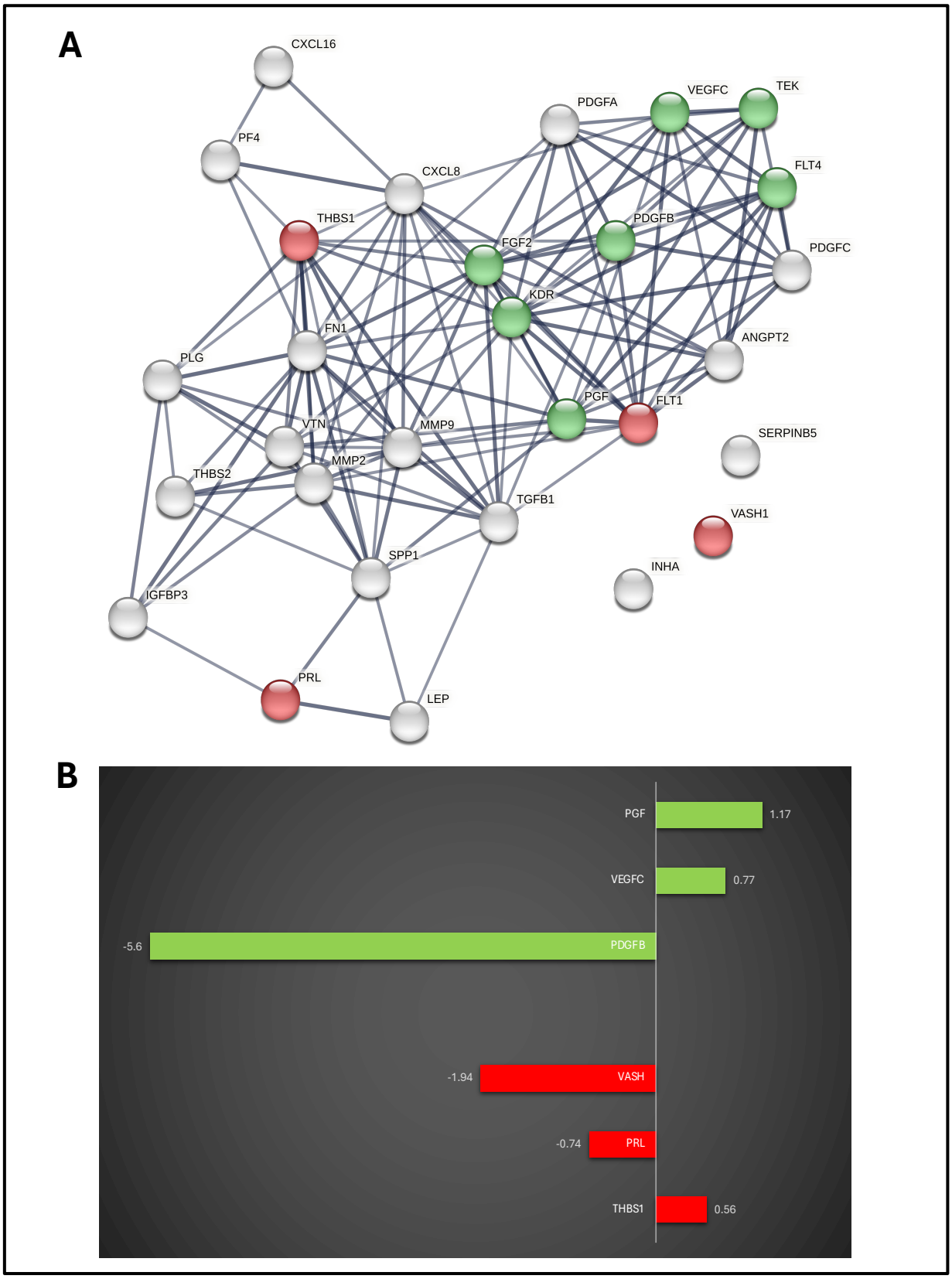


Figure 25 - Regulators of endothelial cell proliferation

A) The protein-protein interaction network highlighting the proteins involved in regulating endothelial cell proliferation. Green shells demonstrate positive regulators and red shells demonstrate negative regulators of endothelial cell proliferation. **B)** Graphical representation of $\log_2$ fold changes of the differentially expressed proteins by hCMEC/D3 treated with *hsa-miR-9-5p* (10 nM).

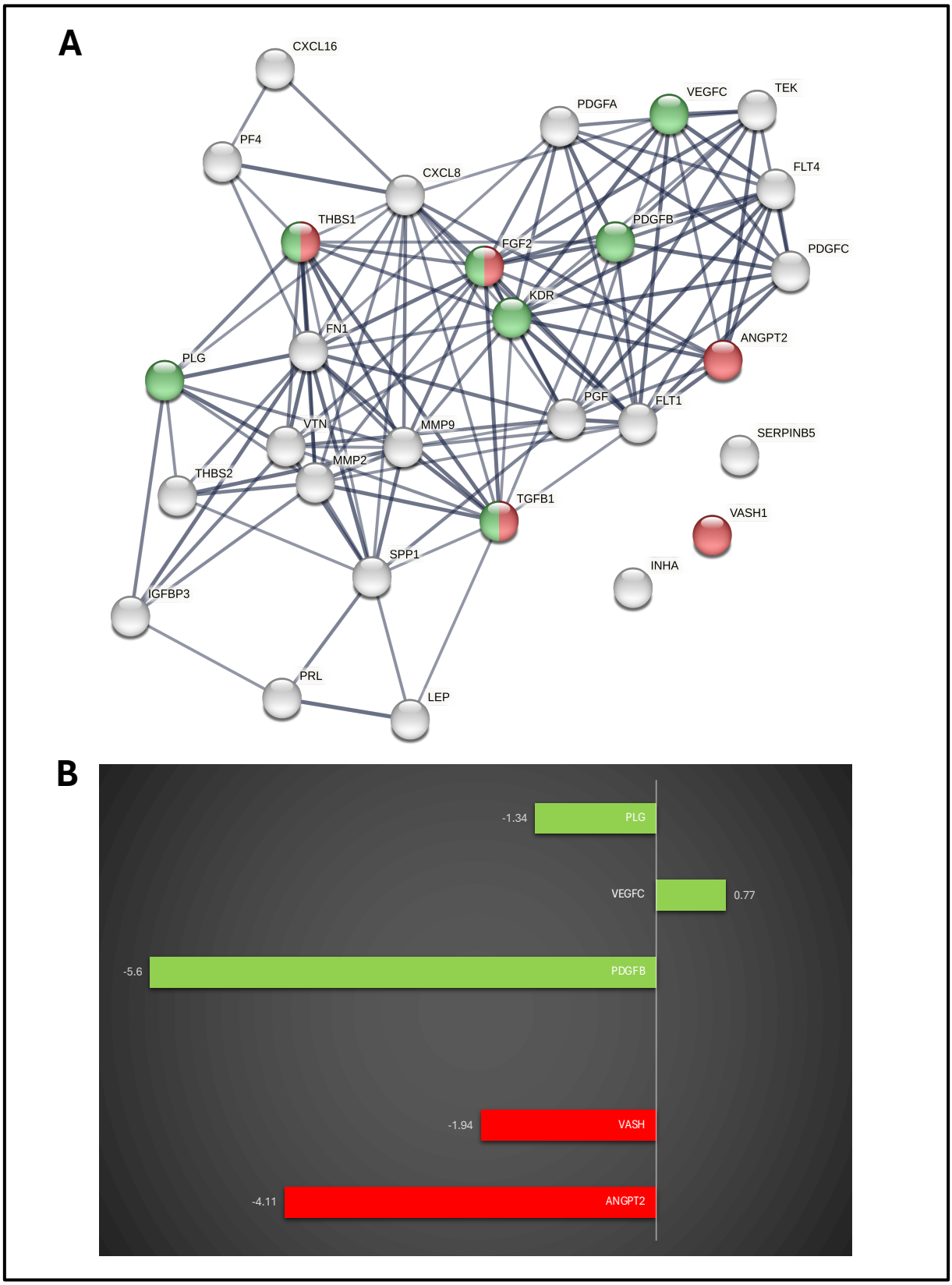


Figure 26 - Regulators of endothelial cell migration

A) The protein-protein interaction network highlighting the proteins involved in regulating endothelial cell migration. Green shells demonstrate positive regulators and red shells demonstrate negative regulators of endothelial cell migration. **B)** Graphical representation of $\log_2$ fold changes of the differentially expressed proteins by hCMEC/D3 treated with *hsa-miR-9-5p* (10 nM).

Table 21 - Gene ontology terms (biological processes) associated with established PPI network

Biological processes	Strength
Negative regulation of phosphatidylinositol biosynthetic process	2.83
Positive regulation of metanephric mesenchymal cell migration by PDGF-receptor-beta signalling pathway	2.66
Tie signalling pathway	2.53
Positive regulation of mast cell chemotaxis	2.43
Regulation of lymphangiogenesis	2.43
Positive regulation of follicle-stimulating hormone secretion	2.35
Paracrine signalling	2.29
Regulation of blood vessel remodelling	2.29
Negative regulation of vasoconstriction	2.23
Regulation of hyaluronan biosynthetic process	2.23
VEGF signalling pathway	2.21
Negative regulation of fibrinolysis	2.20
Induction of positive chemotaxis	2.16
Ovulation from ovarian follicle	2.13
Hyaluronan catabolic process	2.13
Regulation of positive chemotaxis	2.12
Cellular response to UV-A	2.09
Positive regulation of positive chemotaxis	2.04
Positive regulation of protein autophosphorylation	2.02
VEGF-receptor signalling pathway	2.01
Regulation of endothelial cell chemotaxis	2.01
Negative regulation of blood vessel endothelial cell migration	1.99
Positive regulation of phosphatidylinositol 3-kinase activity	1.99
Glomerulus vasculature development	1.99
Positive regulation of endothelial cell chemotaxis	1.99
Surfactant homeostasis	1.96
Positive regulation of blood vessel endothelial cell migration	1.95
Regulation of macrophage differentiation	1.95
Positive regulation of fibroblast migration	1.93
Regulation of blood vessel endothelial cell migration	1.93

Table 22 - KEGG pathways associated with established PPI network

KEGG pathways	Strength
Bladder cancer	1.83
Malaria	1.77
Focal adhesion	1.66
EGFR tyrosine kinase inhibitor resistance	1.64
Rap1 signalling pathway	1.61
ECM-receptor interaction	1.59
Melanoma	1.58
AGE-RAGE signalling pathway in diabetic complications	1.55
PI3K-Akt signalling pathway	1.52
Ras signalling pathway	1.52
Rheumatoid arthritis	1.52
MAPK signalling pathway	1.45
Proteoglycans in cancer	1.45
Prostate cancer	1.45
p53 signalling pathway	1.45
Fluid sheer stress and atherosclerosis	1.42
Gap junction	1.37
MicroRNAs in cancer	1.33
Relaxin signalling pathway	1.33
Choline metabolism in cancer	1.33
Renal cell carcinoma	1.32
Transcriptional misregulation in cancer	1.30
HIF-1 signalling pathway	1.30
Amoebiasis	1.30
Glioma	1.28
Phospholipase D signalling pathway	1.27
JAK-STAT signalling pathway	1.24
Cytokine-cytokine receptor interaction	1.23
Regulation of actin cytoskeleton	1.21
Pathways in cancer	1.16

5.4.9 miR-9-5p does not affect the ability of hCMEC/D3's response to TNF-α stimuli

I sought to determine whether the changes seen with cell proliferation, migration and angiogenesis-related proteome profiler array represent endothelial dysfunction in general or isolated effect of *hsa-miR-9-5p* on angiogenesis processes. To determine this, I investigated the response of hCMEC/D3 treated with negative scramble and *hsa-miR-9-5p* (10nM) to TNF-α stimulation. Cells treated with scramble and *hsa-miR-9-5p* (10nM) without TNF-α stimulation were used as controls. The expression of VCAM-1, a marker of endothelial cell activation, was analysed in the culture supernatants. Results indicated that hCMEC/D3 treated with *hsa-miR-9-5p* (10nM) showed enhanced response to TNF- α stimulation suggesting that treatment with *hsa-miR-9-5p* did not impair the capacity of hCMEC/D3 to respond to TNF-α (Figure 27). Microvascular endothelial cells treated with *hsa-miR-9-5p* (10nM) without TNF-α stimulation also showed enhanced expression of VCAM-1 compared to cells treated with scramble, but the difference was not statistically significant.

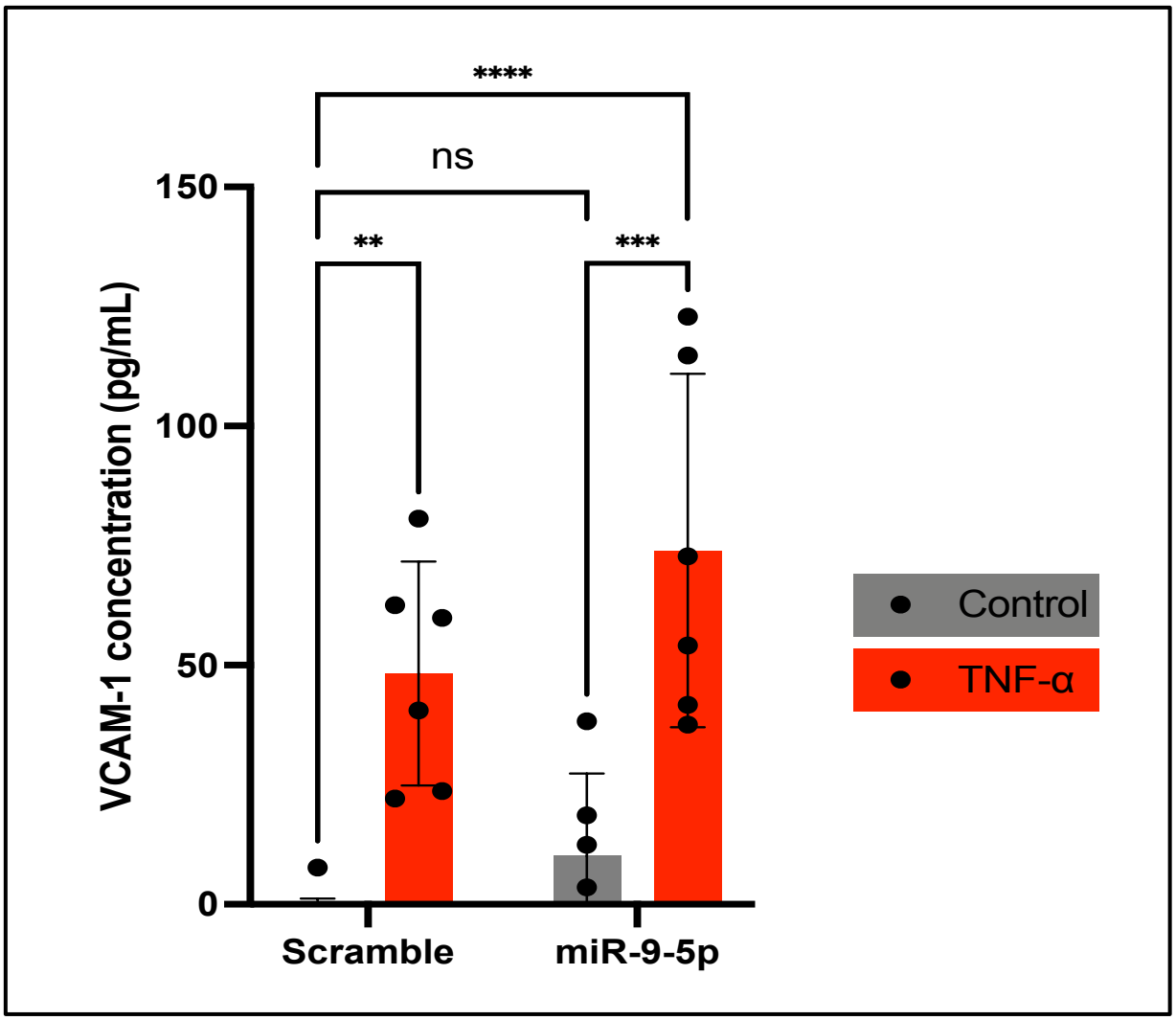


Figure 27 - VCAM-1 expression in cell culture supernatants

The groups were compared using two-way ANOVA followed by Turkey's post hoc test and statistical significance was set at $p < 0.05$ (ns – not significant; **$p < 0.01$; ***$p < 0.001$; ****$p < 0.0001$).

5.5 Discussion

This study presents the first evidence of *hsa-miR-9-5p* overexpression in m/lSTB-EVs (isolated from dual lobe placental perfusion) and serum EVs from women with EOPE. This finding is coupled with the observed attenuation of pro-angiogenic parameters like endothelial cell proliferation and migration in hCMEC/D3 treated with *hsa-miR-9-5p*. The altered expression profile of angiogenesis-related proteins in these cells further strengthens this association. Notably, despite the anti-angiogenic effect, *hsa-miR-9-5p*-treated hCMEC/D3 retained their responsiveness to TNF-α stimulation, as evidenced by VCAM-1 expression. These observations collectively support our hypothesis that impaired angiogenesis within the brain parenchyma contributes to the cerebrovascular alterations observed in preeclampsia.

Furthermore, this study proposes a potential mechanism linking the high circulating levels of m/lSTB-EVs in EOPE to cerebral microvascular endothelial dysfunction. The unpublished RNA sequencing data from our group demonstrates that *hsa-miR-9-5p* expression in small STB-EVs is not significantly different between EOPE and normal pregnancy (L2FC 0.33, $p > 0.05$). This finding suggests a critical distinction in cargo sorting into EVs under cellular stress conditions (as seen in the excessive release of m/lSTB-EVs during EOPE) compared to the physiological release of sSTB-EVs. This differential sorting could be a key factor in the pathogenesis of preeclampsia-related cerebrovascular complications.

Severe preeclampsia represents a significant risk factor for a spectrum of maternal neurological complications including posterior reversible encephalopathy syndrome (PRES)[372], cerebral white matter abnormalities[373], cognitive changes[374], and stroke[375]. These complications are a leading cause of maternal mortality associated with preeclampsia, contributing to 40-70% of

deaths[376,377]. The underlying mechanisms responsible for preeclampsia-induced cerebrovascular complications remain under active investigation. However, growing evidence suggests the involvement of circulating factors originating from the placenta and present in the maternal circulation could potentially mediate the cerebrovascular alterations[378]. These circulating factors are thought to disrupt the blood-brain barrier (BBB), induce cerebral vasoconstriction, and promote vasogenic oedema, potentially leading to cerebrovascular complications and eclampsia[379,380]. Preeclamptic placentas are known to release a variety of factors and molecules, including STB-EVs, which may contribute to the observed cerebrovascular manifestations[231,381]. Elucidating the specific roles of these placental factors in disrupting cerebrovascular function holds immense potential for improving our understanding of the pathophysiology of preeclampsia-associated neurological complications.

The human brain is distinguished by a unique confluence of characteristics: (a) high metabolic demands, consuming approximately 20% of the body's oxygen at rest, (b) a limited tolerance for fluctuations in blood flow, ion concentrations, and water balance, and (c) a rigid cranial enclosure provided by the skull[382]. This unique confluence of characteristics renders the cerebral system highly vulnerable to detrimental increases in intracranial pressure as a result of elevated vascular permeability or circulatory volume. These disruptions can culminate in serious neurological complications, including brain herniation and even death.

Paradoxically, normal pregnancy is characterized by significant haemodynamic adaptations that could theoretically threaten the cerebral internal milieu. These adaptations include a decrease in vascular resistance and an increase in vascular permeability and cardiac output[383–385]. While these physiological changes are essential to compensate for the expanding plasma volume and ensure adequate perfusion of vital organs, particularly the uterus and placenta, they come with a potential risk to the cerebral system. To mitigate this risk, the cerebral vasculature undergoes crucial changes during pregnancy to compensate for the global haemodynamic shifts.

Cerebral vasculature, similar to vasculature of many other organ systems, undergoes selective structural remodeling during pregnancy. Selective arteriogenesis (development of new arteries from existing arterioles) of parenchymal arterioles (as opposed to large intracranial arteries)[386] and increased angiogenesis (formation of new capillary sprouts from existing blood vessels) in the posterior cerebral cortex (as opposed to anterior cerebral cortex)[379] are driven by peroxisome proliferator-activated receptor-gamma (PPARγ) activation by circulating relaxin[379,386]. Increase in capillary density in the posterior cerebral cortex may be attributed to the increased demand of blood supply to neuro-endocrine glands that enlarge during pregnancy[387].

On the other hand, cerebral vasculature maintains the integrity of BBB despite a substantial rise in circulating factors like vascular endothelial growth factor (VEGF)[368] and placental growth factor (PlGF)[388] during normal pregnancy, which are known to enhance blood-brain barrier (BBB) permeability[368,389]. Cerebral endothelial cells forming the BBB remarkably maintain their tight junction proteins (claudin-1, claudin-5, occludin, and zona occludens-1)[379], maintain normal hydraulic conductivity[390], and preserve normal paracellular and transcellular transport processes across the BBB during normal pregnancy[379]. The selective binding of VEGF and PlGF to soluble fms-like tyrosine kinase-1 (sFlt-1) is believed to reduce bioavailability of VEGF and PlGF and is regarded as an important mechanism limiting the permeability enhancing effect at the BBB[389].

My investigation identified a novel microRNA, *hsa-miR-9-5p*, abundantly carried by m/lSTB-EVs isolated from EOPE patients. This miRNA significantly attenuated the proliferation and migration of hCMEC/D3, processes considered hallmarks of the initial stages of angiogenesis. However, the precise mechanisms underlying *hsa-miR-9-5p's* anti-angiogenic effect remain to be elucidated.

Indirect evidence from studies on choroidal melanoma suggests a potential role for *hsa-miR-9-5p* in inhibiting the proliferation and migration of choroidal melanoma eye cells (MUM-2B and MUM-2C) by targeting the V-raf murine sarcoma viral homolog B1 (BRAF) gene[391]. However, these findings were observed in a distinct cell type and may not directly translate to the context of cerebral angiogenesis.

Furthermore, some prior studies suggest a pro-angiogenic role for *hsa-miR-9-5p* in human umbilical vein endothelial cells (HUVECs)[392,393]. These studies suggest *hsa-miR-9-5p* may promote angiogenesis by positively regulating the expression of vascular endothelial growth factor (VEGF) and its receptor, VEGFR2[392], or by targeting CXC chemokine receptor-4 (CXCR4)[393]. These seemingly contradictory findings highlight the importance of considering cell type specificity when investigating microRNA function. Our investigation employed hCMEC/D3, a microvascular endothelial cell type and a well-established model for studying the blood-brain barrier (BBB) with a maternal origin[369]. In contrast, the aforementioned studies utilized HUVECs, which are of foetal origin and represent a macrovascular endothelial cell phenotype. Additionally, our study focused on cell proliferation and migration as indicators of angiogenic potential, whereas the previous studies relied solely on the tube formation assay.

Proteome Profiler™ Human Angiogenesis Antibody Array Kit analysis yielded interesting results. In contrast to our expectations, hCMEC/D3 treated with *hsa-miR-9-5p* over-expressed PlGF and VEGFC, two pro-angiogenic proteins which have been shown to disrupt BBB in animal models in previous studies[389,394,395]. Investigators have shown similar disruption in BBB in rats when their cerebral veins were treated with plasma obtained from women with early-onset preclampsia[367]. Another study found that addition of plasma of women with preeclampsia to rodent brain blood vessels *ex vivo* activated VEGFR2 receptor[368]. VEGFR2 is predominantly expressed in vascular endothelial cells and its activation is linked to increased BBB permeability[396]. Out of the 11 major autophosphorylation sites on VEGFR2, each responsible

for activating distinct intracellular signalling pathways, the phosphorylation of tyrosine residue 951 (pY951-VEGFR2) has been linked to regulation of endothelial cell permeability[397], while phosphorylation of tyrosine residue 1175 (pY1175-VEGFR2) is associated with regulation of endothelial cell proliferation[398]. Investigators have found that hCMEC/D3 treated with plasma from women with PE showed signs of BBB disruption and simultaneous increase in selective phosphorylation of pY951-VEGFR2 and decrease in phosphorylation of pY1175-VEGFR2, responsible for cell proliferation[369]. In the light of our findings of over-expression of *hsa-miR-9-5p* in m/lSTB-EVs and serum EVs in preeclampsia, its attenuating effect on microvascular endothelial cell proliferation and migration despite over-expression of pro-angiogenic VEGFC and PlGF by hCMEC/D3 treated with *hsa-miR-9-5p,* it would be interesting to study the effect of *hsa-miR-9-5p* on selective phosphorylation of VEGFR2 tyrosine kinase residues. It is worth noting that several studies investigating the allelic variation of VEGFC identified single nucleotide polymorphisms in VEGFC gene were associated with increased risk of preeclampsia[399,400]. These findings suggest a complex interplay between VEGFC and its receptors in regulating angiogenesis in various physiological and pathological contexts.

Functional enrichment analysis of the PPI network established using STRING tool identified various biological processes that were potentially regulated by the interacting proteins' network. Positive and negative regulators of endothelial cell proliferation and migration were of special interest. PDGFB, identified as a positive regulator of endothelial cell proliferation and migration, was also found to be under-expressed in hCMEC/D3 treated with *hsa-miR-9-5p* (log_2 fold change -5.60). The PPI network also identified KDR (also known as VEGFR2) as an interacting protein in the 2nd shelf as a positive regulator of endothelial cell proliferation and migration. Owing to the complexity of downstream effects due to selective phosphorylation of different tyrosine kinase residues in VEGFR2 (KDR), it would be interesting to evaluate the effects of PDGFB via VEGFR2 on hCMEC/D3 to further elucidate their role in regulating cerebral angiogenesis.

Another key biological process identified with the PPI network was the regulation of glomerular vasculature. Glomerular endothelial dysfunction is a well-known pathological feature in preeclampsia. Previously, investigators have shown glomerular endothelial cell swelling (glomerular endotheliosis) as a feature in preeclampsia[401–403]. The potential contribution of *hsa-miR-9-5p* carried within m/lSTB-EVs to endothelial dysfunction in renal glomeruli warrants further investigation.

Delineated KEGG pathways have identified several pathways that have been previously attributed to preeclampsia: *focal adhesions*[404], *ECM receptor interaction*[404], *PI3K/Akt signalling pathway*[405] and *HIF-1 signalling*[406].

Focal adhesion pathway is activated by extracellular matrix (ECM)-receptor interaction[407] and it mediates interaction between cells and their environment during early human development[408,409] and stimulates trophoblast differentiation, migration and invasion at the foeto-maternal interface[410,411]. Phosphoinositide 3-kinase (PI3K)/ Akt signalling pathway is also known to regulate cell proliferation, migration, and invasion[412,413], including trophoblast migration and invasion[414,415]. Investigators have shown that selective inhibition of PI3K/Akt signalling pathway significantly attenuated trophoblast cell proliferation and invasion, and enhanced cell apoptosis[416]. Preeclampsia is characterized by poor differentiation and shallow invasion of trophoblasts[417] that impede uterine spiral arterial remodelling resulting in placental hypoxia[418,419]. Hypoxia inducible factor 1 alpha (HIF-1α), a key biomarker of placental function and vascular adaptation in pregnancy[420], is secreted in response to hypoxic states[421]. HIF-1α induces expression of anti-angiogenic factors and suppress expression of proangiogenic factors; and enhances renin-angiotensin system activity by increasing circulating angiotensin II causing peripheral vasoconstriction and endothelial dysfunction[422]. This intricate interplay between cell-matrix interactions and cell signalling pathways, underscores the need for further investigation into the precise role of *hsa-miR-9-5p* in the pathogenesis of preeclampsia.

My findings also confirmed that the observed anti-angiogenic effects of *hsa-miR-9-5p* on hCMEC/D3 may be specific as confirmed by VCAM-1 expression analysis. The treated cells and control cells retained the ability to respond to stimulus (TNF-α) ascertaining that the miRNA did not induce global dysfunction in hCMEC/D3.

I acknowledge that following limitations should be considered while interpreting the presented results. First, the *in vitro* cell culture model using hCMEC/D3 (well-established BBB model), cannot fully recapitulate the complex *in vivo* environment within human brain during pregnancy. Second, our study focused on the effects of *hsa-miR-9-5p* in isolation, while the cargo of m/lSTB-EVs likely contain a multitude of biomolecules that could interact with *hsa-miR-9-5p* and influence its overall effect. Third, the sample size in this study was relatively small (n = 3 for cell proliferation and cell migration assay and n = 1 for angiogenesis proteome profiler array kit analysis), and further investigation with larger cohorts is needed to confirm our findings. Finally, we only investigated the impact of *hsa-miR-9-5p* on endothelial cell proliferation and migration. Future studies should explore the broader effects of *hsa-miR-9-5p* on other cellular processes relevant to angiogenesis and preeclampsia.

Despite these limitations, our findings provide a valuable starting point for further research into the role of *hsa-miR-9-5p* in the pathogenesis of preeclampsia and its cerebrovascular complications.

5.6 Conclusion

In conclusion, this study identified a novel role for *hsa-miR-9-5p*, a microRNA abundantly carried by m/lSTB-EVs and serum EVs isolated from EOPE patients. We demonstrated that *hsa-miR-9-5p* attenuates the proliferation and migration of human cerebral microvascular endothelial cells (hCMEC/D3), processes crucial for initial stages of angiogenesis. However, the precise mechanisms underlying this anti-angiogenic effect remain unclear. Our findings suggest a complex interplay between *hsa-miR-9-5p* and the delicate balance of pro- and anti-angiogenic factors released by the cerebral microvascular endothelial cells.

5.7 Future direction

Several key areas warrant further investigation to elucidate the role of *hsa-miR-9-5p* in preeclampsia:

VEGFR2 signalling: We observed paradoxical over-expression of pro-angiogenic factors (PlGF and VEGFC) in hCMEC/D3 treated with *hsa-miR-9-5p* despite its anti-angiogenic effect. Investigating the effect of *hsa-miR-9-5p* on the selective phosphorylation of VEGFR2 tyrosine kinase residues could shed light on this discrepancy and improve our understanding of VEGF signalling pathways in the context of preeclampsia.

The PPI network analysis identified PDGFB, a positive regulator of endothelial cell proliferation and migration, as downregulated in hCMEC/D3 treated with *hsa-miR-9-5p*. Evaluating the effects of PDGFB via VEGFR2 on hCMEC/D3 could further elucidate their role in regulating cerebral angiogenesis during preeclampsia.

Renal glomerular endothelial dysfunction: My findings suggest a theoretical relationship between *hsa-miR-9-5p* carried by m/lSTB-EVs and endothelial dysfunction in the renal glomeruli (as identified by functional enrichment analysis). Future studies should investigate this potential link in greater detail.

Biomarker development: I identified elevated levels of *hsa-miR-9-5p* in serum EVs isolated from EOPE women (< 34 weeks). However, the precise timeframe during pregnancy when miR-9-5p expression changes remains unclear. To address this knowledge gap, I propose evaluating serum EV expression of miR-9-5p in blood samples collected during early pregnancy. This approach has the potential to establish miR-9-5p as a biomarker or predictor of cerebrovascular complications associated with preeclampsia.

CHAPTER 6:

PREDICTIVE VALUE OF sFlt-1:PlGF RATIO IN WOMEN WITH SUSPECTED PREECLAMPSIA IN SRI LANKA – CLINICAL TRIAL

6.1 Introduction

Preeclampsia, a pregnancy-specific hypertensive disorder, remains a significant global health concern[423,424]. Early and accurate identification of women at risk is crucial for timely intervention and improved maternal and foetal outcomes. While the soluble fms-like tyrosine kinase-1 (sFlt-1): placental growth factor (PlGF) ratio has emerged as a promising non-invasive screening tool for preeclampsia[425–428]. However, existing validation data primarily originates from Western and Asian populations.

This knowledge gap regarding the generalizability of the sFlt1:PlGF ratio across diverse ethnicities warranted further investigation. South Asian populations, in particular, may exhibit distinct preeclampsia risk factors and clinical presentations. To address this gap and ensure the effectiveness of screening strategies for all women, I decided to establish a clinical trial to assess the predictive value of sFlt-1:PlGF ratio in women suspected with preeclampsia in Sri Lanka.

This clinical trial served another key objective within the context of my broader research paradigm. My research in University of Oxford focused on syncytiotrophoblast-derived extracellular vesicles (STB-EVs) and their potential role in preeclampsia. STB-EVs are membrane-bound particles released by placental cells and contain valuable information regarding placental health. Through STB-EV research, potential preeclampsia biomarkers were identified in a smaller study population. However, robust validation of these markers necessitated a larger study population with confirmed preeclampsia cases.

Therefore, the Sri Lankan clinical trial aimed to achieve a two-fold purpose: firstly, to assess the predictive value of the sFlt1:PlGF ratio in a South Asian population, and secondly, to establish a stratified biobank. This biobank would categorize serum and plasma samples based on the sFlt1:PlGF ratio and confirmed clinical diagnosis of preeclampsia. This resource would then

serve as a valuable tool for validating the potential preeclampsia biomarkers identified through my STB-EV research at University of Oxford. By analysing samples from a larger South Asian cohort with confirmed preeclampsia status, the biobank would enable the validation and refinement of these markers, potentially leading to the development of novel preeclampsia diagnostic tools.

In the subsequent sections I have detailed the trial protocol that was developed, annexed the confirmation of the ethical approval from the Ethics Review Committee, Faculty of Medicine, University of Colombo, Sri Lanka, and discussed the current progress of the trial despite the challenges due to COVID-19 lockdown followed by the economic crisis in Sri Lanka.

6.2 Study protocol

The study protocol submitted to the Ethics Review Committee, Faculty of Medicine, University of Colombo on 10th March 2020 is attached herewith:

PREDICTIVE VALUE OF THE

sFlt-1:PlGF RATIO

IN WOMEN WITH

SUSPECTED PREECLAMPSIA

IN SRI LANKA

STUDY PROTOCOL

Collaborative Study between
Department of Obstetrics & Gynaecology and Department of Biochemistry, Faculty of Medicine, University of Colombo, Sri Lanka
And
Nuffield Department of Women's & Reproductive Health, Medical Sciences Division, University of Oxford, United Kingdom

Investigators
Dr Asanka Jayawardane, University of Colombo
Professor Chandrika Wijeyaratne, University of Colombo
Dr Dilanthi Warawita, University of Colombo
Dr Manu Vatish, University of Oxford
Dr Sofia Cerdeira, University of Oxford
Dr Prassana Logenthiran, University of Oxford*
**Lead investigator*

Abbreviations

AC	-	abdominal circumference
AE	-	adverse event
AST	-	aspartate transaminase
EFW	-	estimated foetal weight
IUGR	-	intrauterine growth restriction
L	-	litre
LDH	-	lactate dehydrogenase
LMP	-	last menstrual period
mg	-	milligram
mL	-	millilitre
mmHg	-	millimetre mercury
NICU	-	neonatal intensive care unit
PE	-	preeclampsia
PI	-	pulsatility index
PlGF	-	placental growth factor
SAE	-	serious adverse event
sFlt-1	-	soluble fms-like tyrosine kinase 1
SGA	-	small for gestational age
µL	-	microlitre
VEGF	-	vascular endothelial growth factor
VEGFR-1	-	vascular endothelial growth factor receptor 1

1. Introduction

1.1 Background

Hypertensive disorders are one of the common medical problems encountered in pregnancy, affecting up to 15% of pregnancies and accounting for approximately 25% of antenatal admissions[429]. Notably preeclampsia (PE) is a major cause of maternal and foetal or neonatal morbidity and mortality[430]. Preeclampsia complicates 5% to 7% of all pregnancies worldwide[431]. Each year, it is estimated that 50,000 women die from PE globally[429,432].

Preeclampsia is currently diagnosed based on the following criteria: new onset of hypertension (systolic blood pressure ≥ 140mmHg, or diastolic blood pressure ≥ 90mmHg at least on 2 determinations) and proteinuria (≥ 300mg/day) after 20 weeks of gestation. Women with moderate disease generally have no symptoms. Women with severe disease may feel unwell and report symptoms such as headache, upper abdominal pain, or visual disturbances. Preeclampsia presents with systemic vasospasm causing decreased perfusion of virtually all organ systems. Rare but serious complications are eclampsia (generalized seizures superimposed on PE), HELLP syndrome, and disseminated intravascular coagulation (DIC). Severe morbidity associated with eclampsia and PE includes renal failure, stroke, cardiac arrest, adult respiratory distress syndrome, and liver failure. As the placenta is involved and placental hypoperfusion is present, there are increased risks for the foetus. The most common abnormalities are intrauterine growth restriction due to placental insufficiency, preterm birth, hypoxic neurological injury, perinatal death, and long-term risks associated with low birth weight and prematurity[429,431–433].

Maternal and perinatal morbidity and mortality are increased in developing countries, especially in women who develop the complication before 34 weeks of gestation (early-onset PE, EOPE), and in those with pre-existing medical disorders such as hypertension and diabetes mellitus[429]. To date no treatment is available to prevent PE or halt the progression of the disease. Delivery

of the placenta (regardless of the gestational age) is currently the only cure for the condition[434,435]. Current antenatal management is focused on close monitoring of PE-complicated pregnancies in combination with treatment of hypertension and (early) delivery when indicated[429,434,436,437].

Early-onset preeclampsia appears to progress in two stages. The first, preclinical stage, is characterized by poor placentation, resulting from insufficient endovascular invasion of foetal extra-villous trophoblasts into the maternal spiral arterioles. The second stage is characterized by clinical manifestation, reflecting generalized endothelial dysfunction, leading to generalized vasoconstriction and end organ damage[438,439]. Conversely, late-onset preeclampsia (LOPE) may arise from a mismatch between normal maternal perfusion and increased metabolic demands of the placenta and foetus, exacerbated by maternal factors such as obesity, pre-existing hypertension, or increased susceptibility to inflammation[99].

The exact aetiology of the disease has not yet been completely understood. Nevertheless, changes in circulating placental angiogenic factors appear to play a key role in the pathogenesis of PE. Soluble fms-like tyrosine kinase-1 (sFlt-1) is an alternatively spliced and truncated version of vascular endothelial growth factor receptor-1 (VEGFR1). sFlt-1 contains the extracellular ligand binding domain but lacks the transmembrane and cytoplasmic portions of VEGFR1. Therefore, circulating free sFlt-1 is able to bind with both vascular endothelial growth factor (VEGF) and placental growth factor (PlGF) and diminish binding of these pro-angiogenic factors (PlGF and VEGF) to their respective receptors[440,441]. In patients with PE, increased levels of sFlt-1 is associated with decreased levels of free VEGF an PlGF resulting in a net anti-angiogenic state causing endothelial dysfunction[442–444].

Investigators have found the sFlt-1 concentration to be high and concentrations of free VEGF and PlGF to be low several weeks prior to the clinical manifestations of PE[438]. Although sFlt-1

may be a key player of the mechanism linking the irregular placentation with maternal endothelial dysfunction, derangements in other angiogenic molecules have also been observed. Maternal serum levels of endostatin and soluble endoglin (inhibitors of angiogenesis) were also found to be elevated in PE. Soluble endoglin antagonizes the pro-angiogenic effects of transforming growth factor-β (TGF-β) and thereby amplifies the sFlt-1 mediated vascular damage[438,440].

Although no definitive therapeutic or preventive strategy is available yet, clinical experience suggests that early detection, monitoring, and supportive care are beneficial to the mother and the foetus. To optimize the expectant management, reliable prediction of PE would be helpful allowing closer prenatal monitoring, timely diagnosis, and timely intervention with antihypertensive treatment, bed rest, corticosteroids to promote foetal lung maturity, magnesium as seizure prophylaxis, and – if needed – expeditious delivery.

Increased levels of sFlt-1 and reduced levels of PlGF herald the onset of PE, whereas the ratio of sFlt-1/PlGF, an index reflecting changes in both bio markers, is a better predictor of PE than either measure alone[445–448]. The intra-individual rate of change of the sFlt-1/PlGF ratio is highly predictive of overall PE risk[449]. Severity of disease and time of onset (early onset vs. late onset PE) seem to correlate with the dimension of change in serum levels of either sFlt-1 or PlGF[445,450].

The Roche immunoassays for sFlt-1 and PlGF have recently been investigated in clinical trials conducted in Europe[442,448] and Japan[444]. Verlohren et al. (2010), conducted a multicentre case control study enrolling 71 patients with PE and 280 gestational age matched controls[442]. They established gestational age dependent reference ranges for sFlt-1, PlGF and sFlt-1:PlGF ratio. Maternal serum concentrations of sFlt-1 and PlGF significantly differed in women with PE compared to controls. The sFlt-1/PlGF ratio performed best (AUC 0.95) in the diagnosis of all

PE compared to the sole measurement of sFlt-1 (AUC 0.91) or PlGF (AUC 0.92) ($p < 0.05$). The best sensitivity and specificity were observed in the subgroup of early onset PE (AUC 0.97 for sFlt-1:PlGF ratio). A cut off value of 85 for sFlt-1:PlGF ratio resulted in the best sensitivity and specificity for the diagnosis of all PE (82% and 95%, respectively) and for the diagnosis of early-onset PE (89% and 97%, respectively).

Zeisler et al. (2016), in a larger multicentre trial reported sFlt-1:PlGF ratio ≤ 38 had a negative predictive value (NPV, no preeclampsia in the subsequent week) of 99.3% (95% CI, 97.9 – 99.9), with a sensitivity and specificity of 80.0% and 78.3% respectively. The positive predictive value (PPV) of an sFlt-1:PlGF ratio > 38 for a diagnosis of PE within 4 weeks was 36.7% (95% CI, 28.4 – 45.7), with 66.2% sensitivity and 83.1% specificity[448].

The Japanese trial collected plasma samples from women diagnosed with PE and women who had normal pregnancy. Reference ranges for sFlt-1, PlGF, and sFlt-1:PlGF ratio were determined during the second half of pregnancy. The sFlt-1:PlGF ratio showed the best diagnostic power for both early-onset and late-onset PE (AUC 0.975)[444].

1.2 Study Rationale & Justification

The traditional definition of PE hinges on the *de novo* development of hypertension and proteinuria after 20 weeks' gestation. While this definition serves well in routine clinical practice, recent evidences highlight its limitations. Namely, some pregnancies can progress to severe PE, eclampsia, or HELLP syndrome without meeting either proteinuria or hypertension criteria. Therefore, the conventional definition proves inadequate for diagnosing these complications in such cases. Furthermore, the temporal disparity observed in clinical practice between the onset of hypertension and proteinuria in women meeting traditional PE criteria presents an additional challenge. This variability can significantly hinder timely management

decisions for pregnant women exhibiting signs or symptoms suggestive of PE, yet falling outside the current diagnostic parameters for PE, eclampsia, or HELLP syndrome[451].

Hypertension and/or proteinuria can arise from various aetiologies unrelated to preeclampsia. Women may even remain asymptomatic despite harbouring severe preeclampsia, leading to unnecessary admissions, interventions (e.g., labour induction), or conversely, missed diagnoses. Building on the data presented regarding the performance of Roche Elecsys® assays for sFlt-1 and PlGF, routine clinical implementation of these markers, particularly the sFlt-1:PlGF ratio, holds significant potential. This approach aligns with findings from other clinical studies suggesting the ability of sFlt-1 and PlGF to predict the onset of PE, eclampsia, or HELLP syndrome weeks before the full clinical syndrome manifests. The incorporation of these angiogenic factors could facilitate earlier diagnoses compared to the traditional criteria, potentially improving patient management strategies[445,452].

Assays for the sFlt-1:PlGF ratio and PlGF (measured alone) are readily available for clinical use[442,448,453]. These assays have been endorsed by the National Institute for Clinical Excellence (NICE) for ruling out preeclampsia in patients presenting with suspected disease[454]. However, it is crucial to acknowledge that the NICE recommendation primarily stemmed from clinical evidence associated with the Roche Elecsys® assays for sFlt-1:PlGF ratio and the Quidel® PlGF assay. Notably, these two assays boast the most extensive body of clinical research supporting their efficacy.

The research group at the University of Oxford possesses extensive experience in the clinical application of the sFlt-1:PlGF ratio for preeclampsia diagnosis. Leveraging this expertise, we propose to investigate the utility of this biomarker in the Sri Lankan context.

Zeisler et al. demonstrated that a sFlt-1:PlGF ratio ≤ 38 effectively excluded PE within the following week, boasting a high negative predictive value (NPV) of 99.3%, alongside a sensitivity of 80% and specificity of 78.3%. This high NPV signifies a low likelihood of PE development in near future, empowering treating obstetricians to prioritize and optimize treatment strategies while offering reassurance to patients.

The recent PROGNOSIS-Asia study, encompassing 25 centres across Asia, further corroborated the exceptional NPV of the 38 cutoff in populations from China, Korea, Thailand, Singapore, and Japan[455]. However, the performance of this biomarker in Sri Lankan patients remains unexplored. This proposed study presents a unique opportunity to evaluate the sFlt-1:PlGF ratio for predicting adverse outcomes in pregnant women suspected of preeclampsia within Sri Lanka. By implementing expertise from the University of Oxford and addressing a critical knowledge gap, this research has the potential to significantly improve diagnostic accuracy and patient management in Sri Lanka.

Benefit of the Test in Clinical Practice

The incorporation of sFlt-1 and PlGF measurements into clinical practice holds promise for improved risk stratification, leading to more optimized patient admissions and reduced maternal-foetal complications[456,457]. The landmark INSPIRE trial[456] served as the first real-world assessment of the sFlt-1:PlGF ratio in suspected preeclampsia. The INSPIRE trial successfully validated the previously reported NPV (99.3%) for sFlt-1:PlGF ≤ 38 and further demonstrated that integrating the sFlt-1:PlGF ratio into clinical management significantly improved the profile of patient admissions, without altering the overall admission rate. Notably, the study found that 100% of patients who developed PE within a week were admitted when using the test, compared to 83% with standard clinical practice alone ($p < 0.05$). Additionally, the INSPIRE trial identified a reduction in adverse maternal and foetal outcomes, highlighting the test's ability to optimize current practice by effectively stratifying

patients into high-risk and low-risk groups, thereby enabling more targeted admission decisions[456].

1.3 Objectives of the Study

The main objective of the present study is to assess the short-term prediction potential of the sFlt-1:PlGF ratio for development of PE / eclampsia / HELLP in Sri Lankan pregnant women with clinical suspicion of PE.

1.3.1 Primary Objectives

1. To demonstrate that low ratios of sFlt-1:PlGF in Sri Lankan pregnant women predict absence of PE / eclampsia / HELLP syndrome (according to diagnostic criteria) within one week after the start visit (= visit 1).
2. To demonstrate that high ratios of sFlt-1:PlGF in Sri Lankan pregnant women predict PE / eclampsia / HELLP syndrome (according to diagnostic criteria) within four weeks after the start visit (= visit 1).

1.3.2 Secondary Objectives

1. To collect evidence that low ratios of sFlt-1:PlGF correlate with absence of PE-related adverse outcomes (other than PE / eclampsia / HELLP being part of the primary objective) of the mother within one week after start visit (= Visit 1) as follows: maternal death, pulmonary oedema, acute renal failure.
2. To collect evidence that low ratios of sFlt-1:PlGF correlate with absence of PE-related adverse outcomes of the foetus within one week after start visit (= Visit 1) as follows: perinatal/foetal death, IUGR, placental abruption, respiratory distress.
3. To collect evidence that high ratios of sFlt-1:PlGF correlate with the mother's adverse PE-related outcomes (other than PE / eclampsia / HELLP being part of the primary objective) within four weeks after start visit (= Visit 1) as follows: maternal death, pulmonary oedema, acute renal failure.

4. To collect evidence that high ratios of sFlt-1:PlGF correlate with the foetus' adverse PE related outcomes within four weeks after start visit (= Visit 1) as follows: perinatal/foetal death, IUGR, placental abruption, respiratory distress.
5. To evaluate sFlt-1 and PlGF values and the sFlt-1:PlGF ratio in diagnosed cases of PE / eclampsia / HELLP in comparison to corresponding parameters in controls.
6. To collect evidence that ratios of sFlt-1:PlGF correlate with time of delivery.
7. To investigate the economic benefit of considering the sFlt-1:PlGF ratio for decision on the length of hospitalization of women with clinical suspicion of PE and of the new-born.

2. Study design and assessments

2.1 Overview of study design

The study is planned in accordance with the principles of evidence-based medicine using the PICO criteria[458]. The present study is an observational single centre, prospective, double-blinded, non-interventional study in patients with suspected preeclampsia (as defined below). In this trial only patients with clinical suspicion of PE will be enrolled. Patients included who will develop PE, eclampsia or HELLP will be compared to gestational age-matched controls. The recruitment of the patients will occur at the antenatal clinic and outpatient department of the De Soysa Hospital for Women, Colombo. Subsequent data collection will occur at intervals and the site of data collection could be either the ward or the antenatal clinic.

It is planned to enrol 250 eligible pregnant women with suspected preeclampsia. Apart from sampling material (planned 2mL of serum corresponding to 4mL full blood and 2mL plasma corresponding to 4mL of full blood) and the stipulation that routine safety laboratory variables should be assessed at all visits during pregnancy and the visit at the delivery, the study is non-interventional in the sense that it does not have any further impact on the patient's health and does not interfere with therapeutic decisions of the treating obstetrician.

2.1.1 Blinding of the study

The study will be conducted at De Soysa Hospital for Women in a double-blind fashion. At the clinical site neither the treating obstetrician nor the patient will know the results of the sFlt-1 and PlGF assessments. The results of the sFlt-1:PlGF assay will be conducted at intervals at the Department of Biochemistry, Faculty of Medicine, University of Colombo and the results not be divulged to the treating obstetrician. This will not affect the standard antenatal care currently provided to the pregnant mothers with suspected preeclampsia. Thus, standard of care will be maintained.

2.1.2 Study population: classification of cases and controls

Standard diagnostic criteria will be used throughout the study period to ensure consistent classification of disorders (see section 2.5).

For the primary study objective, cases will be divided into three categories:

- Patients who develop PE/eclampsia/HELLP within one week after start visit (=Visit 1)
- Patients who develop PE / eclampsia / HELLP between one and four weeks after start visit (=Visit 1)
- Patients who develop PE / eclampsia / HELLP between four weeks after start visit (=Visit 1) and four to six weeks postpartum

Controls:

- Controls are patients who do not develop PE / eclampsia / HELLP / IUGR throughout the entire pregnancy up to 4 to 6 weeks (28 days to 42 days) postpartum.

2.2 Acceptance criteria

All patients must meet all inclusion criteria without violating any of the exclusion criteria listed below.

2.2.1 Inclusion criteria

- Pregnant women aged ≥18 years
- Gestational week > 20+0 days
- Signed written informed consent
- Suspicion of clinical diagnosis of PE based on one or more of the following criteria:
- New onset elevated BP
- Aggravation of preexisting hypertension

- New onset proteinuria
- Aggravation of preexisting proteinuria
- One or more other reason(s) for clinical suspicion of PE:(to be determined by the attending clinician as this reflects the practical clinical situation studied)
- PE-related symptoms: epigastric pain, excessive oedema, severe swelling (face, hands, feet), headache, visual disturbances, sudden weight gain (>1kg/week)
- PE-related findings: low platelets, elevated liver transaminases, IUGR, abnormal uterine perfusion detected by Doppler sonography with mean PI > 95th percentile in second trimester and/or bilateral notch.

2.2.2 Exclusion Criteria

- Preeclampsia: Proteinuria ≥2 (dipstick) (or in case available ≥0.3 g protein/24 hours or ≥30 mg/dL protein in spot urine or spot urine protein/creatinine ratio ≥30 mg protein/mmol creatinine) AND elevated BP (≥ 140 mmHg systolic and/or ≥90 mmHg diastolic, reproducible on two occasions)
- Proteinuria ≥2+ (dipstick) (or in case available ≥0.3 g protein/24 hours or ≥30 mg/dL protein in spot urine or spot urine protein/creatinine ratio ≥30 mg protein/mmol creatinine) AND current anti-hypertensive treatment
- Confirmed diagnosis of HELLP syndrome
- Employee at the investigational site, or relative or spouse of the investigators/treating obstetricians

2.3 Assessments for documentation

2.3.1 Data collection overview

	Visit 1	Visit 2	Visit 3	Delivery	Postpartum	Unscheduled Visit
Informed consent	X					
Inclusion/Exclusion criteria	X					
Demographic data	X					
Medical history						
Specific pre-pregnancy diseases	X					
Concomitant medication	X	X	X	X	X	X
Pregnancy assessment	X					
Body weight	X	X	X			X
Blood pressure	X	X	X	X	X	X
Assessment of proteinuria	X	X	X		X	X
PE status, symptoms		X	X	X	X	X
Maternal status		X	X	X	X	X
IUGR and SGA	X	X	X	X		X
Fetal/neonatal status				X		
Laboratory parameters	X	X	X			X
Sonographic data	X	X	X			X
Sample material (sFlt-1/PlGF)	X	X	X	X	X	X
Neonatal disorders				X	X	
Delivery outcome				X		
AEs/SAEs	X	X	X	X	X	X

Recruitment Process:

- Patient meets the acceptance criteria as described above (Section 2.2)
- Informed written consent is obtained for participating in the study
- Data collection at visit 1 and other subsequent visits
- Blood collection as described above (Sample collection)

2.3.2 Data collected during assessment period

The study will include enrolment visit (= visit 1), assessment at the time of delivery and a postpartum documentation. Patients will be included into the study after they have given their informed consent in writing. On occurrence of pregnancy complications further visits during pregnancy are possible and data will be collected during these unscheduled visits. In order to obtain consistent data across study sites the diagnostic criteria described in section 2.5 will have to be adhered to by the investigators and treating obstetricians.

Schedule of visits:

- Start visit (= Visit 1 = Day of enrolment; 0 weeks)
- Visit 2 (exactly in 1 week from the day enrolment
- Visit 3 (exactly in 4 weeks from the day of enrolment)
- Delivery
- Unscheduled visits due to onset of pregnancy related complications
- Postpartum documentation

Start visit / visit 1

At visit 1 the following will be performed, assessed and documented:

- Informed consent
- Inclusion/Exclusion criteria
- Demographic data (age, ethnicity, smoker, height, weight)
- Medical history including history of PE / eclampsia / HELLP / IUGR in previous pregnancies as well as family history of PE, other chronic diseases
- Specific pre-pregnancy diseases. Classification according to ICD 10: pre-existing hypertension, pre-existing diabetes, pre-existing renal disease, pre-existing proteinuria, autoimmune diseases, thrombophilia
- Concomitant medication
- Pregnancy assessment (gravidity, parity, first USS date, LMP, age of gestation, multiple pregnancy, number of foetuses)
- Body weight
- Systolic, diastolic BP according to ISSHP guidelines[459]
- Assessment of proteinuria (protein dip stick, spot urine protein, spot urine protein/creatinine ratio)
- IUGR/SGA
- Laboratory parameters: ALT, AST, Thrombocytes, Serum creatinine
- Doppler USS of uterine arteries at current visit in second trimester
- Collection of blood sample: 4mL of blood for serum and 4mL of blood for plasma
- AEs/SAEs

Visit 2 and visit 3

At visits 2 and 3 the following will be performed, assessed and documented:

- Concomitant medication
- Body weight
- Systolic, diastolic BP according to ISSHP guidelines[459]
- Assessment of proteinuria (protein dip stick, spot urine protein, spot urine protein/creatinine ratio)
- IUGR/SGA
- Laboratory parameters: ALT, AST, Thrombocytes, Serum creatinine (if clinically indicated)
- Doppler USS of uterine arteries at current visit in second trimester
- Collection of blood sample: 4mL of blood for serum and 4mL of blood for plasma (if blood is collected for any clinical indications, additional blood will be collected for sFlt-1 and PlGF assays)
- AEs/SAEs

Visit at delivery

By the time of delivery, the following will be assessed and documented:

- Concomitant medication
- Systolic, diastolic BP according to ISSHP guidelines[459]
- PE status, symptoms: no PE, suspected PE, PE, severe PE, superimposed PE, eclampsia, HELLP, date of diagnosis of PE, neurological symptoms (headache, visual disturbances), epigastric pain, severe oedema, oliguria
- Maternal status: maternal death, pulmonary oedema, acute renal failure, cerebral haemorrhage, cerebral thrombosis, DIC, hospitalization: admission day, days in hospital, days in ICU
- IUGR, SGA

- Fetal/neonatal status: perinatal/foetal death, placental abruption, gender, weight, height, Apgar score
- Laboratory parameters: ALT, AST, thrombocytes, serum creatinine (if clinically indicated)
- Collection of blood sample: 4mL of blood for serum and 4mL of blood for plasma (if blood is collected for any clinical indications, additional blood will be collected for sFlt-1 and PlGF assays)
- Neonatal disorders: respiratory distress syndrome, necrotizing enterocolitis, intraventricular haemorrhage, hospitalization: admission day, days in hospital, days in NICU
- Delivery outcome: date of delivery, mode of delivery, pre-term delivery, delivery < 34 weeks (iatrogenic).
- AEs/SAEs

Postpartum documentation

Postpartum within 48 hours from the delivery, the following will be assessed and documented:

- Concomitant medication
- Systolic, diastolic BP according to ISSHP guidelines[459]
- PE status, symptoms: no PE, suspected PE, PE, severe PE, superimposed PE, eclampsia, HELLP, date of diagnosis of PE, neurological symptoms (headache, visual disturbances), epigastric pain, severe oedema, oliguria
- Maternal status: maternal death, pulmonary oedema, acute renal failure, cerebral haemorrhage, cerebral thrombosis, DIC, hospitalization: admission day, days in hospital, days in ICU
- Collection of blood sample: 4mL of blood for serum and 4mL of blood for plasma (will be used to assess the sFlt-1 and PlGF assays in PE related adverse outcomes reported during postpartum period)

- Neonatal disorders: respiratory distress syndrome, necrotizing enterocolitis, intraventricular haemorrhage, hospitalization: admission day, days in hospital, days in NICU
- AEs/SAEs

Unscheduled visits during pregnancy

In case of pregnancy complications unscheduled visits may take place during pregnancy where the following will be assessed and documented:

- Concomitant medication
- Body weight (optional)
- Systolic and diastolic BP according to ISSHP guidelines[459]
- Assessment of proteinuria (protein dip stick, spot urine protein, spot urine protein/creatinine ratio, 24-h urine for confirmation of diagnosis of PE: determined not more than 5 days before actual visit)
- PE status, symptoms: no PE, suspected PE, PE, severe PE, superimposed PE, eclampsia, HELLP, date of diagnosis of PE, neurological symptoms (headache, visual disturbances), epigastric pain, severe oedema, oliguria
- Maternal status: maternal death, pulmonary oedema, acute renal failure, cerebral haemorrhage, cerebral thrombosis, DIC, hospitalization: admission day, days in hospital, days in ICU
- IUGR, SGA
- Laboratory parameters: AST, thrombocytes, LDH, serum creatinine
- Optional: Doppler sonography of uterine arteries at current visit in second trimester (notching, PI)
- AEs/SAEs

2.4 Endpoints of the study

2.4.1 Primary endpoints

Value of the sFlt-1:PlGF ratio at Visit 1 to predict preeclampsia / eclampsia / HELLP syndrome (according to diagnostic criteria) within one and four weeks from Visit 1

2.4.2 Secondary endpoints

- Value of the sFlt-1:PlGF ratio at Visit 1 to evaluate PE-related adverse outcomes other than PE / eclampsia / HELLP of mother and foetus within one and four weeks from Visit 1
- Systolic, diastolic BP
- Proteinuria (protein dipstick, spot urine protein, spot urine protein/creatinine ratio)
- PE status Maternal death, pulmonary oedema, acute renal failure
- Neurological symptoms (headache, visual disturbances), epigastric pain, severe oedema, oliguria
- Perinatal/foetal death, IUGR, SGA, placental abruption
- Laboratory parameters: AST, thrombocytes, LDH, serum creatinine
- Date and mode of delivery
- Data of the newborn: weight, height, Apgar score, NICU admission

2.4.3 Safety variables

Adverse effects (AEs) and Serious Adverse Effects (SAEs) will be classified into Anticipated and Unanticipated AEs/SAEs in the study population. Anticipated AEs/SAEs will be captured in the data collection sheet as part of the documentation at scheduled visits. Unanticipated AEs/SAEs will be recorded separately and will be reported immediately to the treating obstetrician.

2.4.4 Health-economic variables

Costs of hospitalization of the mother (admission to hospital, days in hospital, days in ICU)

Costs for hospitalization of the newborn (admission to hospital, days in hospital, days in NICU)

2.5 Diagnostic criteria for classification of disorders in this study

As there is still a lack of consensus on classification and diagnosis of hypertensive disorders in pregnancy which could lead to controversial documentation of outcomes, the diagnostic criteria mentioned below will be used by the investigators.

Hypertension[433,459]

- Systolic BP ≥140 mmHg and/or diastolic BP ≥90 mmHg (on two occasions ≥6 hour apart, but within 1 week)
- Hypertension according to diagnostic criteria above (documented in medical history) controlled by antihypertensive drug use irrespective of current systolic and diastolic BP values

Chronic Hypertension[459]

- Hypertension (systolic BP ≥140 mmHg and/or diastolic BP ≥90 mmHg) diagnosed preconceptionally or in the first half of pregnancy (<20 weeks of gestation) persisting >12 weeks postpartum

Proteinuria[459]

- ≥0.3 g protein/24 hours (or in emergency cases only if a 24-h urine protein collection cannot be obtained dipstick ≥2+ or ≥30 mg/dL protein in spot urine or spot urine protein/creatinine ratio ≥30 mg protein/mmol creatinine)

Gestational hypertension[459]

- New onset of hypertension (systolic BP ≥140 mmHg and/or diastolic BP ≥90 mmHg) alone without proteinuria after gestational week 20

Preeclampsia[459]

- New onset of both hypertension (systolic BP ≥140 mmHg and/or diastolic BP ≥90 mmHg) and proteinuria after 20 weeks' gestation

Suspected Preeclampsia

- Suspicion of clinical diagnosis of PE according to inclusion criteria (see section 2.2)

Severe Preeclampsia[433]

Preeclampsia *plus* one or more of the following criteria:

- Systolic BP ≥160 mmHg and/or diastolic BP ≥110 mmHg (on two occasions ≥6 hours apart, but within 1 week)
- Proteinuria (>5 g protein/24 hours or dipstick ≥3+ on two random urine samples collected at least 4 hours apart)
- Impaired renal function (serum creatinine ≥0.9 mg/dL or oliguria <500 mL/24 hours)
- Pulmonary oedema
- Impaired liver function (elevated liver enzymes, epigastric or right upper-quadrant pain)
- Neurological symptoms (cerebral or visual disturbances, severe headache)
- Haematological disorders (thrombocytopenia, haemolysis)
- IUGR

Eclampsia[433]

- New onset of tonic-clonic seizures in a woman with PE which cannot be assigned to any other cause

Superimposed preeclampsia

- Chronic hypertension plus new onset of proteinuria after gestational week 20 or
- Chronic hypertension and proteinuria before gestational week 20

AND

  - Sudden increase of proteinuria or
  - Sudden increase of BP or
  - Clinical or laboratory signs/symptoms of severe PE

Early-onset / Late-onset Preeclampsia[460]

- Early-onset PE: onset of the disease < 34+0 weeks of gestation
- Late-onset PE: onset of the disease ≥ 34+0 weeks of gestation

HELLP Syndrome[461]

- Increased AST (>70 IU/L)
- Reduced thrombocytes count (<100,000/µL)
- Increased LDH level (>600IU/L)

IUGR[456]

- EFW <10 percentile (adjusted for gender and ethnicity according to the charts routinely used at the study site)
- Presence of pathologic process that inhibits expression of normal intrinsic growth potential. Pathologic process to be demonstrated on at least one occasion after gestational week 22 by one of the below criteria:
  - Oligohydramnios (Amniotic Fluid Index <10th percentile)
  - Pathologic flow in umbilical artery (PI >95th percentile)
- Serial ultrasonography growth curve anomalies

SGA[456]

- EFW or AC <5th percentile (adjusted for gender and ethnicity according to the charts routinely used at the study site)
- Absence of pathologic process

Preterm Delivery[462]

- Birth before the completion of 37 weeks of gestation (< 37+0 weeks of gestation)

3. Statistical plan

Descriptive statistics will be employed to compare clinical subgroups. Boxplots, for instance, will be generated to visualize the distribution of sFlt-1:PlGF ratio results across different groups. Correlation analyses will be performed if deemed appropriate, examining the relationships between laboratory parameters and clinical characteristics such as age, body mass index (BMI), and gestational age.

For continuous variables within distinct clinical groups, parametric tests (ANOVA, t-tests) will be applied if the data meet the necessary assumptions. Non-parametric tests (Wilcoxon signed-rank test, Kruskal-Wallis test) will be employed as alternatives when data normality assumptions are violated. Categorical variables will be compared using chi-square tests. All *p*-values will be two-tailed.

ROC analysis will be performed if appropriate to assess the area under the curve (AUC) and evaluate the sensitivity and specificity of the diagnostic algorithm as a function of gestational week at the time of calculation. Logistic regression will be used within the ROC analysis to investigate the influence of covariates such as gestational week, maternal age, and BMI. For any covariates identified as statistically significant, additional descriptive analyses (e.g., boxplots of marker results) will be presented.

4. Sample collection

4.1 Patient recruitment

The recruitment will be done in compliance with all applicable ethical and legal principles and under consideration of patient's rights and patient's safety.

4.2 Blood sampling

The patients should have rested for at least 10 minutes in a sitting or supine position before blood withdrawal. A ligature should be applied for no longer than 2 minutes and should be open before aspiration of blood. Aseptic technique will be used to perform the venepuncture.

4.3 Patient ID

On enrolment, each patient will be assigned a study specific number to protect their anonymity during the study. All collected samples will be labelled with this study specific number to allow tracking and identification of the sample while maintaining subject anonymity. The patient numbers will be used in tracking any aliquots prepared from the original blood and in the sample programming on the laboratory analysers.

4.4 Types of sample material

Minimum of 2mL of serum (corresponding to 4 mL of whole blood)

Minimum of 2mL of plasma (corresponding to 4 mL of whole blood)

4.5 Sample processing

The samples will be processed according to the protocol issued by the Roche Elecsys® sFlt-1 and PlGF immunoassay kits.

4.6 Sample storage

The collected serum and plasma samples will be stored in a -80°C freezer for a maximum period of 10 years from the date of collection. The samples will be stored for assessing biomarkers that are being currently investigated in relation to preeclampsia. The biobank will serve as a rich source of material for future research. Biomarkers could be studied in serum and plasma samples only up to 10 years from the date of collection and hence the samples are stored for a maximum of 10 years.

5. Ethical considerations

5.1 Confidentiality

All personal data will be entered onto a Microsoft Access database which will be password protected and maintained on a secure server. Clinical data will be stored on a secure server with access restricted to appropriate personnel. Storage is on a restricted area of a file server. Authorisation to access the restricted area of the file server is strictly limited. Data will be processed on a workstation by authorised staff only. The workstations access the network via a log in name and password (changed regularly). No data are stored on individual workstations.

Personal data and information required for the study will be collected directly from trial participants and extracted manually from the woman's hospital notes. All staff involved in the study share the same duty of care to prevent unauthorized disclosure of personal information. The principal investigator and the study trial team members will ensure that the patients' anonymity is maintained. Personal data will be anonymized. Access to the anonymized data will be granted to the Principal Investigator at the host institution (Faculty of Medicine, University of Colombo) and the regulatory authorities to permit trial related monitoring, audits and inspections. Consent will be gained for this.

All personal information received in paper format for the trial will be held securely within the Department of Obstetrics & Gynaecology, Faculty of Medicine, University of Colombo and treated as strictly confidential. All the participants will be identified only by a unique study ID number on manual data collection sheet and on any electronic database.

5.2 Rights of the study participants

The participants will be recruited to the study only after obtaining written informed consent. The consenting will be done by a member of the study team or a trained research assistant under supervision of the research team. Prior to obtaining consent, patients will be briefed about the study and the its objectives; the samples to be collected; risks associated with sample collection; measures to minimize the risks during sample collection and the benefit of the study to the future generation of pregnant women in Sri Lanka. The patients will be offered a chance to discuss their concerns or questions with a member of the study team. The patients will also be provided with written material explaining the study in simple language translated into Sinhala and Tamil. Contact details of the principal investigator will be shared to the participants in the Information Sheet.

The participant any time can raise concerns or lodge complaint to the principal investigator during the study period via the contact information shared on the Information Sheet.

The study participant can withdraw from the study at any point after recruitment by informing any one of the team members of the study. Withdrawing from the study will not have any impact on the routine antenatal, obstetric and postnatal care that the patient would receive from De Soysa Hospital for Women.

The patient will be briefed about the necessity to visit the hospital for one to two additional visits in order to collect data and blood samples. Written informed consent will be obtained for these additional visits.

5.3 Publication and dissemination

The results of the study will be disseminated via conference presentations, publication in peer reviewed journals and publication on website and other media channels like newspaper. No personal identifiable data will be used in any form of publication.

5.4 Ethics approval

Ethical approval will be obtained from the Ethics Review Committee, Faculty of Medicine, University of Colombo and Ethics Committee of the De Soysa Hospital for Women, Colombo prior to the onset of the study.

6. References

1. Huda SS, Freeman DJ, Nelson SM. Short- and long-term strategies for the management of hypertensive disorders of pregnancy. *Expert Rev Cardiovasc Ther*. 2009;7(12):1581-1594. doi:10.1586/ERC.09.147

2. Sibai B, Dekker G, Kupferminc M. Pre-eclampsia. *Lancet*. 2005;365(9461):785-799. doi:10.1016/S0140-6736(05)17987-2

3. Wagner LK. Diagnosis and management of preeclampsia. *Am Fam Physician*. 2004;70(12):2317-2324.

4. Duley L. The global impact of pre-eclampsia and eclampsia. *Semin Perinatol*. 2009;33(3):130-137. doi:10.1053/J.SEMPERI.2009.02.010

5. ACOG Committee on Obstetric Practice. ACOG practice bulletin. Diagnosis and management of preeclampsia and eclampsia. Number 33, January 2002. *Obstetrics and gynecology*. 2002;99(1):159-167. doi:10.1016/S0029-7844(01)01747-1

6. Chappell LC, Brocklehurst P, Green ME, et al. Planned early delivery or expectant management for late preterm pre-eclampsia (PHOENIX): a randomised controlled trial. *The Lancet*. 2019;394(10204):1181-1190. doi:10.1016/S0140-6736(19)31963-4

7. Roberts JM, Escudero C. The placenta in preeclampsia. *Pregnancy Hypertension: An International Journal of Women's Cardiovascular Health*. 2012;2(2):72-83. doi:10.1016/j.preghy.2012.01.001

8. Haddad B, Sibai BM. Expectant management in pregnancies with severe pre-eclampsia. *Semin Perinatol*. 2009;33(3):143-151. doi:10.1053/J.SEMPERI.2009.02.002

9. Koopmans CM, Bijlenga D, Groen H, et al. Induction of labour versus expectant monitoring for gestational hypertension or mild pre-eclampsia after 36 weeks' gestation (HYPITAT): a multicentre, open-label randomised controlled trial. *Lancet*. 2009;374(9694):979-988. doi:10.1016/S0140-6736(09)60736-4

10. Foidart JM, Schaaps JP, Chantraine F, Munaut C, Lorquet S. Dysregulation of anti-angiogenic agents (sFlt-1, PLGF, and sEndoglin) in preeclampsia--a step forward but not the definitive answer. *J Reprod Immunol*. 2009;82(2):106-111. doi:10.1016/J.JRI.2009.09.001

11. Cudihy D, Lee R V. The pathophysiology of pre-eclampsia: current clinical concepts. *J Obstet Gynaecol*. 2009;29(7):576-582. doi:10.1080/01443610903061751

12. McLaughlin K, Zhang J, Lye SJ, Parker JD, Kingdom JC. Phenotypes of Pregnant Women Who Subsequently Develop Hypertension in Pregnancy. *J Am Heart Assoc*. 2018;7(14). doi:10.1161/JAHA.118.009595

13. Maynard S, Epstein FH, Karumanchi SA. Preeclampsia and angiogenic imbalance. *Annu Rev Med*. 2008;59:61-78. doi:10.1146/ANNUREV.MED.59.110106.214058

14. Levine RJ, Karumanchi SA. Circulating Angiogenic Factors in Preeclampsia. *Clin Obstet Gynecol*. 2005;48(2):372-386. doi:10.1097/01.grf.0000160313.82606.d7

15. Verlohren S, Galindo A, Schlembach D, et al. An automated method for the determination of the sFlt-1/PIGF ratio in the assessment of preeclampsia. *Am J Obstet Gynecol*. 2010;202(2):161.e1-161.e11. doi:10.1016/J.AJOG.2009.09.016

16. Sunderji S, Gaziano E, Wothe D, et al. Automated assays for sVEGF R1 and PlGF as an aid in the diagnosis of preterm preeclampsia: a prospective clinical study. *Am J Obstet Gynecol*. 2010;202(1):40.e1-40.e7. doi:10.1016/J.AJOG.2009.07.025

17. Ohkuchi A, Hirashima C, Suzuki H, et al. Evaluation of a new and automated electrochemiluminescence immunoassay for plasma sFlt-1 and PlGF levels in women with preeclampsia. *Hypertens Res*. 2010;33(5):422-427. doi:10.1038/HR.2010.15

18. Levine RJ, Maynard SE, Qian C, et al. Circulating angiogenic factors and the risk of preeclampsia. *N Engl J Med*. 2004;350(7):672-683. doi:10.1056/NEJMOA031884

19. Levine RJ, Lam C, Qian C, et al. Soluble endoglin and other circulating antiangiogenic factors in preeclampsia. *N Engl J Med*. 2006;355(10):992-1005. doi:10.1056/NEJMOA055352

20. Vatten LJ, Eskild A, Nilsen TIL, Jeansson S, Jenum PA, Staff AC. Changes in circulating level of angiogenic factors from the first to second trimester as predictors of preeclampsia. *Am J Obstet Gynecol*. 2007;196(3):239.e1-239.e6. doi:10.1016/J.AJOG.2006.10.909

21. Zeisler H, Llurba E, Chantraine F, et al. Predictive Value of the sFlt-1:PlGF Ratio in Women with Suspected Preeclampsia. *New England Journal of Medicine*. 2016;374(1):13-22. doi:10.1056/NEJMoa1414838

22. Moore Simas TA, Crawford SL, Solitro MJ, Frost SC, Meyer BA, Maynard SE. Angiogenic factors for the prediction of preeclampsia in high-risk women. *Am J Obstet Gynecol*. 2007;197(3):244.e1-244.e8. doi:10.1016/J.AJOG.2007.06.030

23. Rana S, Karumanchi SA, Levine RJ, et al. Sequential changes in antiangiogenic factors in early pregnancy and risk of developing preeclampsia. *Hypertension*. 2007;50(1):137-142. doi:10.1161/HYPERTENSIONAHA.107.087700

24. Sibai BM, Stella CL. Diagnosis and management of atypical preeclampsia-eclampsia. *Am J Obstet Gynecol*. 2009;200(5):481.e1-481.e7. doi:10.1016/J.AJOG.2008.07.048

25. Romero R, Nien JK, Espinoza J, et al. A longitudinal study of angiogenic (placental growth factor) and anti-angiogenic (soluble endoglin and soluble vascular endothelial growth factor receptor-1) factors in normal pregnancy and patients destined to develop preeclampsia and deliver a small for gestational age neonate. *J Matern Fetal Neonatal Med*. 2008;21(1):9-23. doi:10.1080/14767050701830480

26. Chappell LC, Duckworth S, Seed PT, et al. Diagnostic accuracy of placental growth factor in women with suspected preeclampsia: a prospective multicenter study. *Circulation*. 2013;128(19):2121-2131. doi:10.1161/CIRCULATIONAHA.113.003215

27. NICE. *"PlGF-Based Testing to Help Diagnose Suspected Pre-Eclampsia (Triage PlGF Test, Elecsys Immunoassay SFlt-1/PlGF Ratio, DELFIA Xpress PlGF 1-2-3 Test, and BRAHMS SFlt-1 Kryptor/BRAHMS PlGF plus Kryptor PE Ratio),."*; 2016.

28. Bian X, Biswas A, Huang X, et al. Short-Term Prediction of Adverse Outcomes Using the sFlt-1 (Soluble fms-Like Tyrosine Kinase 1)/PlGF (Placental Growth Factor) Ratio in Asian

Women With Suspected Preeclampsia. *Hypertension*. 2019;74(1):164-172. doi:10.1161/HYPERTENSIONAHA.119.12760

29. Cerdeira AS, O'Sullivan J, Ohuma EO, et al. Randomized Interventional Study on Prediction of Preeclampsia/Eclampsia in Women With Suspected Preeclampsia: INSPIRE. *Hypertension*. 2019;74(4):983-990. doi:10.1161/HYPERTENSIONAHA.119.12739

30. Duhig KE, Myers J, Seed PT, et al. Placental growth factor testing to assess women with suspected pre-eclampsia: a multicentre, pragmatic, stepped-wedge cluster-randomised controlled trial. *Lancet*. 2019;393(10183):1807-1818. doi:10.1016/S0140-6736(18)33212-4

31. Sackett DL, Straus SE, Richardson WS, Rosenberg W, Haynes RB. *Evidence-Based Medicine: How to Practice and Teach EBM.* 2nd ed. Churchill Livingstone; 2000.

32. Brown MA, Magee LA, Kenny LC, et al. The hypertensive disorders of pregnancy: ISSHP classification, diagnosis & management recommendations for international practice. *Pregnancy Hypertens*. 2018;13:291-310. doi:10.1016/J.PREGHY.2018.05.004

33. Von Dadelszen P, Magee LA, Roberts JM. Subclassification of preeclampsia. *Hypertens Pregnancy*. 2003;22(2):143-148. doi:10.1081/PRG-120021060

34. Magann EF, Martin JN. Twelve steps to optimal management of HELLP syndrome. *Clin Obstet Gynecol*. 1999;42(3):532-550. doi:10.1097/00003081-199909000-00009

35. Simhan HN, Cartis SN. Prevention of preterm delivery. *N Engl J Med*. 2007;357(5):477-487. doi: 10.1056/NEJMra050435

6.3 Trial progress

The initiation of our preeclampsia clinical trial in Sri Lanka, despite establishing strong collaborations with the University of Colombo and the University of Oxford, encountered a series of unforeseen obstacles. Following the meticulous development of the trial protocol, it was submitted to the Ethics Review Committee at the Faculty of Medicine, University of Colombo, Sri Lanka, for ethical approval. The committee's rigorous review process culminated in ethical approval being granted on 20th August 2020 (EC-20-037; Figure 28). However, this initial success coincided with a significant national lockdown in Sri Lanka, creating difficulties into our patient recruitment efforts.

The impact of the COVID-19 pandemic lockdown on patient recruitment was multifaceted. Firstly, it resulted in a dramatic decrease in overall patient turnover at hospitals. Pregnant women, unless experiencing emergencies or complications, often delayed seeking prenatal care during this period due to fear of exposure or following lockdown restrictions. This limited pool of potential participants significantly hampered our ability to identify and enroll women who met the study criteria.

Secondly, even after the lockdown lifted, patient flow within hospitals remained limited. Healthcare facilities prioritized high-risk pregnancies and those with established diagnoses. Women with potentially relevant symptoms, such as those suspected of developing preeclampsia but not yet presenting with full-blown signs, may have been less likely to seek care at major hospitals during this recovery period. Additionally, resource constraints within the healthcare system may have led to a shift in care delivery, with some women with less severe symptoms being managed at peripheral hospitals or clinics outside our designated recruitment

site. This limited access to the target population significantly impeded our progress in enrolling participants.

Further roadblocks emerged in 2022 as Sri Lanka faced a crippling economic crisis and political turmoil. These events had a cascading effect, hindering the trial's advancement in several ways. The economic crisis placed a significant strain on the healthcare system, leading to shortages in essential medical supplies and equipment. This, coupled with rising costs of transportation and potential disruptions in daily routines, may have further discouraged some women from seeking prenatal care at hospitals, further impacting our recruitment pool.

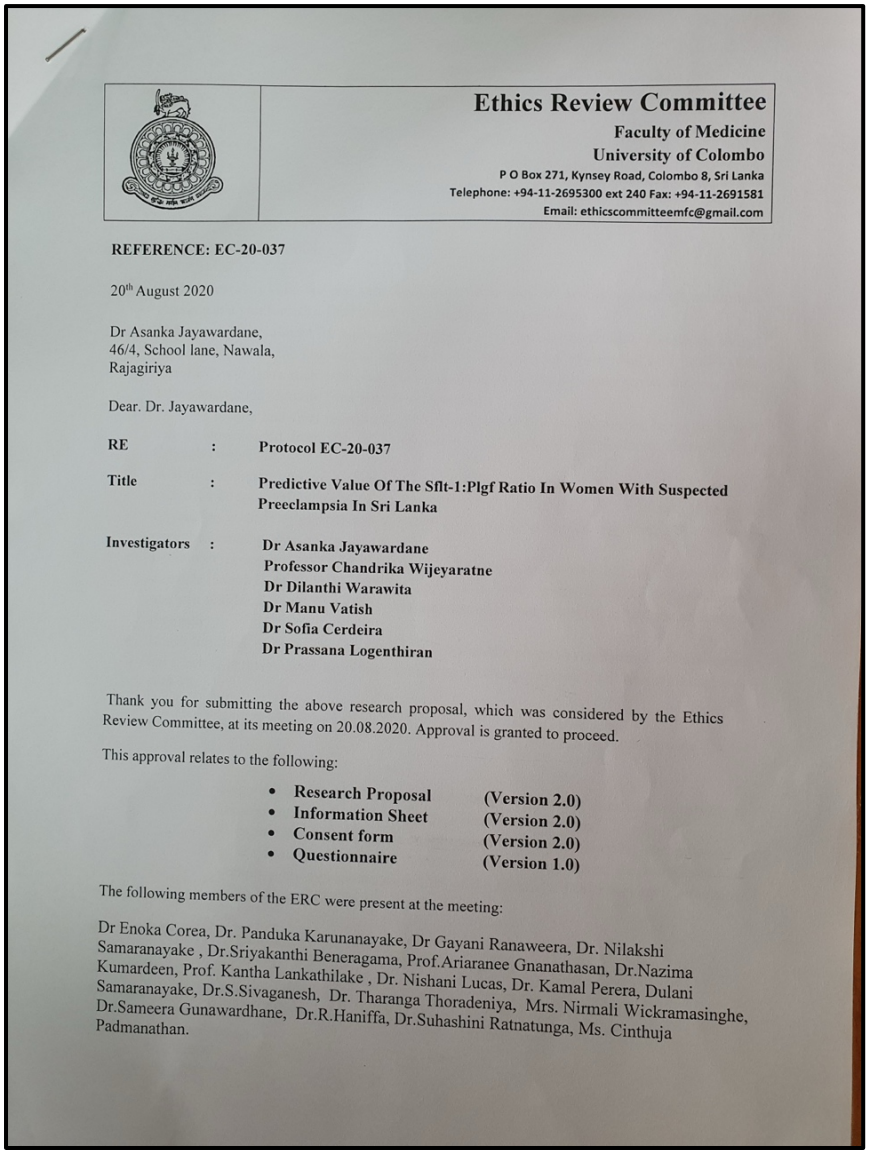
The political turmoil also presented unforeseen challenges. A temporary freeze on all recruitment within state institutions by the Sri Lankan government made it impossible to hire research assistants and data collectors. This unexpected bureaucratic hurdle significantly delayed the trial's launch.

Despite these initial setbacks, the unwavering commitment of the research team and the importance of the study's objectives ultimately paved the way for a successful launch. In March 2023, when the temporary freeze for recruitments was lifted, we were able to recruit a committed research assistant who began recruiting patients for the trial in May 2023. Through their dedicated efforts, we were able to enroll 30 patients who met the study criteria and consented to participate. While this represents approximately 15% of our target sample size, it signifies a crucial first step towards achieving our recruitment goals.

We are determined to continue recruiting patients for the study and are confident of reaching the final numbers within the next 2-3 years. Several strategies are being implemented to expedite this process. Firstly, we are expanding our recruitment efforts to include collaborating with peripheral hospitals and clinics that may manage a higher proportion of women with early

signs or suspicions of preeclampsia. Secondly, we are exploring the possibility of implementing alternative methods for patient outreach and education, such as utilizing community health workers to reach a wider geographical area. Finally, we are actively seeking additional research assistants to bolster our recruitment capacity.

The findings from this study have the potential to significantly improve preeclampsia screening strategies in South Asian populations, ultimately leading to better maternal and foetal outcomes. Beyond patient enrolment, a critical aspect of this study is the establishment of a comprehensive biobank. This biobank will store serum and plasma samples collected from participants, categorized based on the sFlt1:PlGF ratio and confirmed clinical diagnosis of preeclampsia. This valuable resource will serve as a foundation for future research endeavors. The biobank will enable the validation and refinement of potential preeclampsia biomarkers identified through my STB-EV research at University of Oxford.



Ethics Review Committee
Faculty of Medicine
University of Colombo
P O Box 271, Kynsey Road, Colombo 8, Sri Lanka
Telephone: +94-11-2695300 ext 240 Fax: +94-11-2691581
Email: ethicscommitteemfc@gmail.com

REFERENCE: EC-20-037

20th August 2020

Dr Asanka Jayawardane,
46/4, School lane, Nawala,
Rajagiriya

Dear. Dr. Jayawardane,

RE : Protocol EC-20-037

Title : Predictive Value Of The Sflt-1:Plgf Ratio In Women With Suspected Preeclampsia In Sri Lanka

Investigators :
Dr Asanka Jayawardane
Professor Chandrika Wijeyaratne
Dr Dilanthi Warawita
Dr Manu Vatish
Dr Sofia Cerdeira
Dr Prassana Logenthiran

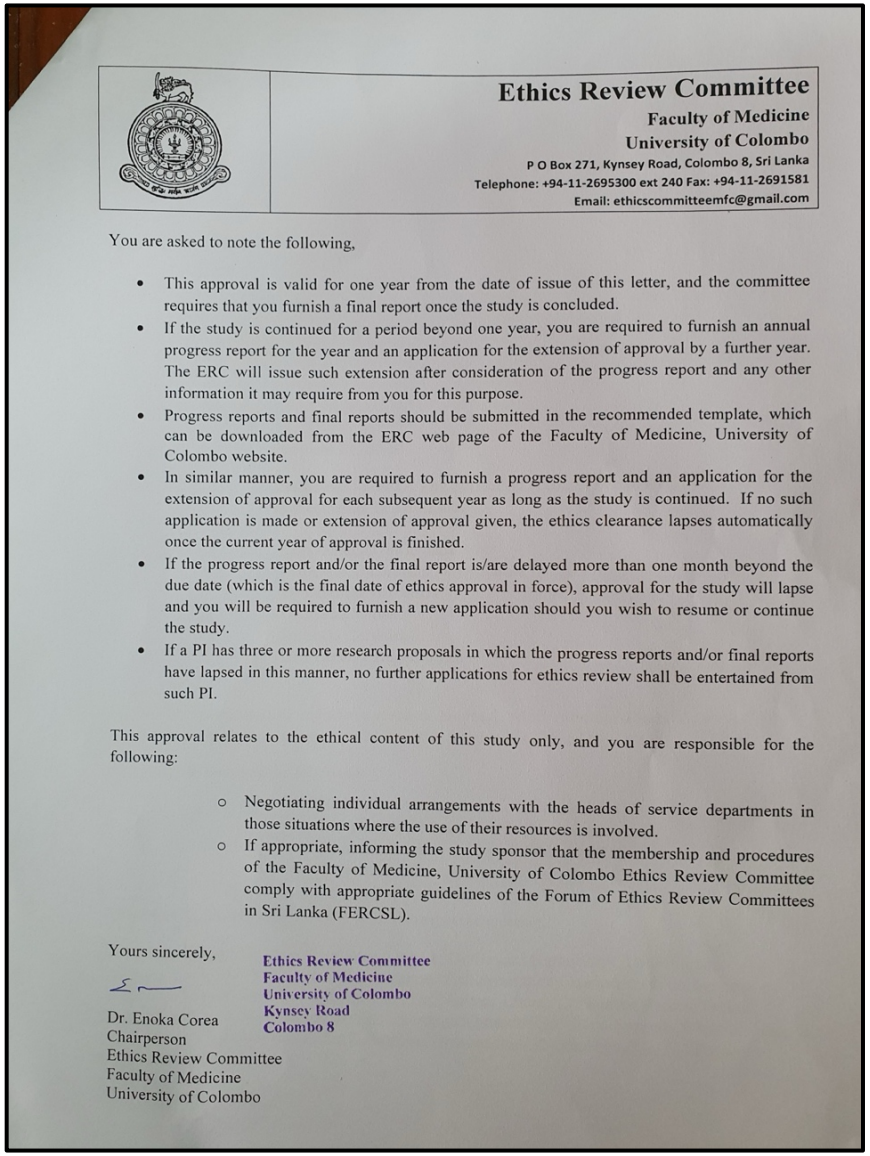
Thank you for submitting the above research proposal, which was considered by the Ethics Review Committee, at its meeting on 20.08.2020. Approval is granted to proceed.

This approval relates to the following:

- **Research Proposal (Version 2.0)**
- **Information Sheet (Version 2.0)**
- **Consent form (Version 2.0)**
- **Questionnaire (Version 1.0)**

The following members of the ERC were present at the meeting:

Dr Enoka Corea, Dr. Panduka Karunanayake, Dr Gayani Ranaweera, Dr. Nilakshi Samaranayake , Dr.Sriyakanthi Beneragama, Prof.Ariaranee Gnanathasan, Dr.Nazima Kumardeen, Prof. Kantha Lankathilake , Dr. Nishani Lucas, Dr. Kamal Perera, Dulani Samaranayake, Dr.S.Sivaganesh, Dr. Tharanga Thoradeniya, Mrs. Nirmali Wickramasinghe, Dr.Sameera Gunawardhane, Dr.R.Haniffa, Dr.Suhashini Ratnatunga, Ms. Cinthuja Padmanathan.



Ethics Review Committee
Faculty of Medicine
University of Colombo
P O Box 271, Kynsey Road, Colombo 8, Sri Lanka
Telephone: +94-11-2695300 ext 240 Fax: +94-11-2691581
Email: ethicscommitteemfc@gmail.com

You are asked to note the following,

- This approval is valid for one year from the date of issue of this letter, and the committee requires that you furnish a final report once the study is concluded.
- If the study is continued for a period beyond one year, you are required to furnish an annual progress report for the year and an application for the extension of approval by a further year. The ERC will issue such extension after consideration of the progress report and any other information it may require from you for this purpose.
- Progress reports and final reports should be submitted in the recommended template, which can be downloaded from the ERC web page of the Faculty of Medicine, University of Colombo website.
- In similar manner, you are required to furnish a progress report and an application for the extension of approval for each subsequent year as long as the study is continued. If no such application is made or extension of approval given, the ethics clearance lapses automatically once the current year of approval is finished.
- If the progress report and/or the final report is/are delayed more than one month beyond the due date (which is the final date of ethics approval in force), approval for the study will lapse and you will be required to furnish a new application should you wish to resume or continue the study.
- If a PI has three or more research proposals in which the progress reports and/or final reports have lapsed in this manner, no further applications for ethics review shall be entertained from such PI.

This approval relates to the ethical content of this study only, and you are responsible for the following:

- Negotiating individual arrangements with the heads of service departments in those situations where the use of their resources is involved.
- If appropriate, informing the study sponsor that the membership and procedures of the Faculty of Medicine, University of Colombo Ethics Review Committee comply with appropriate guidelines of the Forum of Ethics Review Committees in Sri Lanka (FERCSL).

Yours sincerely,

Ethics Review Committee
Faculty of Medicine
University of Colombo
Kynsey Road
Colombo 8

Dr. Enoka Corea
Chairperson
Ethics Review Committee
Faculty of Medicine
University of Colombo

Figure 28 - Ethics approval for the clinical trial in Sri Lanka

CHAPTER 7:

SUMMARY AND FUTURE DIRECTION

7.1 Summary

This thesis investigates the role of syncytiotrophoblast-derived extracellular vesicles (STB-EVs) in the pathophysiology of preeclampsia (PE). It addresses four key aims:

1. **STB-EV isolation, enrichment, and characterisation:** This established a foundation for subsequent analyses by isolating and enriching STB-EVs, while simultaneously confirming their origin through size, morphology, and immunophenotypic characterisation.

2. **STB-EVs and kynurenine metabolism:** I investigated the role of isolated STB-EVs in kynurenine metabolism during pregnancy, aiming to elucidate a potential mechanism by which STB-EVs contribute to preeclampsia pathophysiology.

3. **miRNA-mediated angiogenesis in PE:** Building on the identification of differentially expressed miRNAs in STB-EVs, I explored the functional impact of a specific miRNA (*hsa-miR-9-5p*) on the process of angiogenesis in the context of preeclampsia.

4. **Clinical trial of angiogenic biomarkers:** I established a clinical trial in Sri Lanka to evaluate the predictive value of angiogenic biomarkers for preeclampsia in women with suspected symptoms. Additionally, a biobank of stratified serum and plasma samples is being created to support future research endeavors.

Key Findings:

- STB-EVs were successfully isolated from *ex vivo* dual lobe placental perfusion. These isolated vesicles were then characterized based on their physical properties, categorized as m/lSTB-EVs and sSTB-EVs, and employed for subsequent experiments.

- Analysis revealed that STB-EVs obtained from early-onset PE (EOPE) and normal pregnancy express kynurenine metabolising enzymes (kynureninase, KYNU; kynurenine aminotransferase, KAT-III; and kynurenine monooxygenase, KMO). These enzymes demonstrated the potential to attenuate kynurenine levels in a dose-dependent manner.

- The study identified *hsa-miR-9-5p* (over-expressed miRNA in EOPE) as a miRNA that attenuated endothelial cell proliferation and cell migration in human cerebral microvascular endothelial cells (hCMEC/D3). This suggests a potential anti-angiogenic role of *hsa-miR-9-5p* in cerebral microvascular endothelial cells in EOPE.

- Following ethical approval from the Ethics Review Committee, Faculty of Medicine, University of Colombo (EC-20-037), the clinical trial was successfully established in Sri Lanka. Despite unforeseen challenges presented by the COVID-19 pandemic and local political and economic circumstances, the trial is currently ongoing with 30 patients successfully recruited.

Chapter summaries:

- **Chapter 1:** Introduction to PE and STB-EVs, encompassing clinical definitions, current knowledge on PE pathophysiology, prevention strategies, therapeutic options, and potential complications. This chapter also details the biogenesis of extracellular vesicles, their uptake by target cells, and their ability to modulate downstream pathways. Additionally, it explores the mechanisms of STB-EVs in PE, their potential as biomarkers, and their biodistribution.

- **Chapter 2:** Methodology, detailing STB-EV isolation procedures using *ex vivo* dual lobe placental perfusion and differential ultracentrifugation. Characterisation methods employed to confirm STB-EV identity include transmission electron microscopy (TEM), nanoparticle tracking analysis (NTA), Western blot, flow cytometry, and protein quantification, all adhering to the guidelines set by the International Society of Extracellular Vesicles (ISEV).

  This chapter also details the specific methodologies used in the thesis: immunohistochemistry, capillary electrophoresis and western blot, gas chromatography mass spectrometry, quantitative polymerase chain reaction, hCMEC/D3 culture, cell proliferation and viability assay, cell migration assay, Proteome profiler angiogenesis array analysis, protein-protein interaction network construction and cluster analysis and VCAM-1 expression analysis following TNF-α stimulation.

- **Chapter 3:** Results of STB-EV isolation, enrichment, and characterisation obtained via *ex vivo* dual lobe placental perfusion. This chapter further compares available STB-EV isolation methods, highlighting their advantages and limitations.

- **Chapter 4:** Investigation of kynurenine metabolising enzymes within STB-EV cargo, their functionality, and a comparison of *in vivo* kynurenine levels between PE and normal pregnancy.

- **Chapter 5:** Validation of selected miRNA targets within medium/large STB-EVs and serum extracellular vesicles obtained from PE and normal pregnancies. This chapter also explores the effect of the selected miRNA target (*hsa-miR-9-5p*) on the angiogenic processes of hCMEC/D3.

- **Chapter 6:** Summarizes the establishment of a clinical trial in Sri Lanka to evaluate the predictive value of the angiogenic biomarkers in identifying women at risk of PE. Additionally, it details the creation of a sample biobank to validate the findings of Chapters 4 and 5 on a larger sample size.

Overall, this thesis contributes valuable insights into the role of different cargo carried in STB-EVs: kynurenine metabolising enzymes (protein cargo) regulating kynurenine metabolism and the potential involvement of *hsa-miR-9-5p* (genetic cargo) in PE-related angiogenesis in cerebral microvascular endothelium.

7.2 Future work

Based on the findings of this thesis, future research efforts could explore several promising avenues:

1. **Investigate the therapeutic potential of specific kynurenine metabolising enzyme inhibitors:**

   Future studies should investigate whether specific inhibitors of kynurenine metabolising enzymes could salvage kynurenine levels when exposed to higher doses of STB-EVs. The findings of such *in vitro* studies will guide shed more light on the therapeutic efficacy of kynurenine replacement in preeclampsia.

2. **Investigate the feasibility of utilizing downstream metabolites of kynurenine metabolism and *hsa-miR-9-5p* as biomarkers for early screening and disease monitoring in EOPE patients:**

   Identifying and validating specific downstream metabolites of kynurenine metabolism and validating *hsa-miR-9-5p* levels in early pregnancy blood samples could lead to the development of easily detectable biomarkers. These biomarkers could facilitate early screening and disease monitoring for EOPE, particularly for cerebrovascular complications associated with preeclampsia (*hsa-miR-9-5p)*. Early and accurate detection has the potential to significantly improve clinical outcomes by enabling timely intervention and improved patient management strategies.

3. **Identify downstream targets of *hsa-miR-9-5p*:**

This research could involve employing RNA sequencing identify the specific genes and pathways regulated by *hsa-miR-9-5p* in endothelial cells. Understanding these downstream targets is crucial for deciphering the precise molecular mechanisms by which *hsa-miR-9-5p* exerts its anti-angiogenic effects in PE.

4. **Investigate the molecular mechanisms of *hsa-miR-9-5p* mediated anti-angiogenic effects in hCMEC/D3:**

The complex relationships between VEGFC, PlGF, PDGFB (proangiogenic proteins) and VEGFR2 warrants further investigation. The effect of hsa-miR-9-5p or PDGFB, VEGFC and PlGF on differential phosphorylation of tyrosine residues in VEGFR2 causing different downstream effects on hCMEC/D3 could be studied further to explore potential regulatory networks or compensatory mechanisms that might explain the anti-angiogenic phenomenon.

5. **Investigate the effect of *hsa-miR-9-5p* on other microvascular endothelial cells:**

This study revealed that *hsa-miR-9-5p* exerts anti-angiogenic effects on hCMEC/D3, a cell model replicating the blood-brain barrier. Since the blood-brain barrier is compromised in preeclampsia, these findings suggest a potential role for *hsa-miR-9-5p* in the disease. Future research should investigate the impact of *hsa-miR-9-5p* on endothelial cells from other organs significantly affected in preeclampsia, such as the kidneys, liver, and heart. Understanding how *hsa-miR-9-5p* influences endothelial function across these organs could provide a more comprehensive picture of its contribution to preeclampsia pathophysiology.

6. *In vivo* models:

While this study utilized an *in vitro* model of hCMEC/D3, future research could incorporate *in vivo* animal models to assess the effects of *hsa-miR-9-5p* manipulation on PE development and progression. This would provide valuable insights into the functional significance of *hsa-miR-9-5p* in a more complex physiological setting.

In conclusion, I believe this thesis will contribute valuable insights into the role of different cargo carried by STB-EVs (kynurenine metabolising enzymes and *hsa-miR-9-5p*) in preeclampsia. This newfound knowledge can potentially serve as a springboard for further investigation, ultimately leading to improved clinical practices and better health outcomes for women experiencing preeclampsia.

LIST OF PUBLICATIONS

8.1 Published papers

Syncytiotrophoblast extracellular vesicles contain functional kynurenine metabolising enzymes: potential implications for preeclampsia (Preprint)

Prassana Varun Logenthiran, Toluwalase A Awoyemi, Morganne Wilbourne, Zhanru Yu, Benedikt Kessler, Carlos Escudero, Wei Zhang, Ana Sofia Cerdeira & Manu Vatish (2024)

MedRxiv

https://doi.org/10.1101/2024.05.25.24307626

MicroRNA analysis of medium/large placenta extracellular vesicles in normal and preeclampsia pregnancies.

Toluwalase Awoyemi, Shuhan Jiang, Maryam Rahbar, **Prasanna Logenthiran**, Gavin Collett, Wei Zhang, Adam Cribbs, Sofia Cerdeira & Manu Vatish (2024)

Frontiers in Cardiovascular Medicine. 11:1371168

http://dx.doi.org/10.3389/fcvm.2024.1371168

Identification of Novel Syncytiotrophoblast Membrane Extracellular Vesicles Derived Protein Biomarkers in Early-onset Preeclampsia: A Cross-Sectional Study.

Awoyemi, T., Jiang, S., Bjarkadóttir, B., Rahbar, M., **Logenthiran, P.**, Collett, G., Zhang, W., Cribbs, A., Cerdeira, A. S., & Vatish, M. (2024)

eLife. 12: RP88841

https://doi.org/10.7554/eLife.88841.2

Early screening for preeclampsia: A myth or a reality?

Sailakshmi Logeeswaran, Indu Asanka Jaywardane & **Prassana Logenthiran** (2023)

Sri Lanka Journal of Obstetrics and Gynaecology. 45(4): 170-178

http://dx.doi.org/10.4038/sljog.v45i4.8094

A cross-sectional analysis of syncytiotrophoblast membrane extracellular vesicles–derived transcriptomic biomarkers in early-onset preeclampsia.

Toluwalase Awoyemi, Wei Zhang, Maryam Rahbar, Adam Cribbs, **Prasanna Logenthiran**, Shuhan Jiang, Gavin Collett, Ana Sofia Cerdeira & Manu Vatish (2023)

Frontiers in Cardiovascular Medicine. 10:1291642

http://dx.doi.org/10.3389/fcvm.2023.1291642

Preeclampsia and syncytiotrophoblast membrane extracellular vesicles (STB-EVs).

Awoyemi, T., Cerdeira, A., Zhang, W., Jiang, S., Rahbar, M., **Logenthiran, P.**, Redman, C., & Vatish, M. (2022)

Clinical Science. 136(24): 1793-1807

https://doi.org/10.1042/cs20220149

8.2 Submitted manuscripts (under review)

Syncytiotrophoblast extracellular vesicles contain functional kynurenine metabolising enzymes: potential implications for preeclampsia (under review)

Prassana Varun Logenthiran, Toluwalase A Awoyemi, Morganne Wilbourne, Zhanru Yu, Benedikt Kessler, Carlos Escudero, Wei Zhang, Ana Sofia Cerdeira & Manu Vatish

Effect of seminal fluid extracellular vesicles on fertility in men with normal and abnormal sperm parameters: protocol for systematic literature review (under review)

Nishadi Rodrigo, **Prassana Logenthiran** & Sharaine Fernando

8.3 Abstracts

Systematic characterisation of urine small extracellular vesicles from normal pregnancy and early-onset preeclampsia.

Qian Chen, Shuhan Jiang, Maryam Rahbar, **Prassana Logenthiran**, Wei Zhang & Manu Vatish (2023)

Plaventa. 140: e13-e14

http://dx.doi.org/10.1016/j.placenta.2023.07.058

The Influence of Normal and Preeclamptic Syncytiotrophoblast Extracellular Vesicles on Human Podocytes.

Jiang, Shuhan; Awoyemi, Toluwalase; Rahbar, Maryam; **Logenthiran, Prassana V.**; Zhang, Wei; Tuffin, Jack P.; Saleem, Moin; & Vatish, Manu (2022)

Journal of the American Society of Nephrology. 33(11S):p 262

http://dx.doi.org/10.1681/ASN.20223311S1262a

Syncytiotrophoblast and syncytiotrophoblast derived extracellular vesicles express kynurenine metabolising enzymes.

Logenthiran, P., Awoyemi, T., Jiang, S., Rahbar, M., Kandzija, N., Zhang, W., Cerdeira, S., & Vatish, M. (2021)

Placenta. 112: e83

https://doi.org/10.1016/j.placenta.2021.07.266

Investigating the roles of small STBEV's microRNAs in the pathogenesis of early-onset preeclampsia through bioinformatics.

Awoyemi, T., Zhang, W., Tanetta, D., Collett, G., **Logenthiran, P.**, Kandzija, N., Rahbar, M., Jiang, S., Redman, C., & Vatish, M. (2021)

Placenta, 112: e24

https://doi.org/10.1016/j.placenta.2021.07.080

REFERENCES

1. Brown MA, Magee LA, Kenny LC, et al. The hypertensive disorders of pregnancy: ISSHP classification, diagnosis & management recommendations for international practice. *Pregnancy Hypertens*. 2018;13. doi:10.1016/j.preghy.2018.05.004
2. Magee LA, Brown MA, Hall DR, et al. The 2021 International Society for the Study of Hypertension in Pregnancy classification, diagnosis & management recommendations for international practice. *Pregnancy Hypertens*. 2022;27:148-169. doi:10.1016/j.preghy.2021.09.008
3. Saudan PJ, Brown MA, Farrell T, Shaw L. Improved methods of assessing proteinuria in hypertensive pregnancy. *BJOG*. 1997;104(10):1159-1164. doi:10.1111/J.1471-0528.1997.TB10940.X
4. Côté AM, Brown MA, Lam E, et al. Diagnostic accuracy of urinary spot protein:creatinine ratio for proteinuria in hypertensive pregnant women: systematic review. *BMJ*. 2008;336(7651):1003-1006. doi:10.1136/BMJ.39532.543947.BE
5. Waugh J, Hooper R, Lamb E, et al. Spot protein-creatinine ratio and spot albumin-creatinine ratio in the assessment of pre-eclampsia: a diagnostic accuracy study with decision-analytic model-based economic evaluation and acceptability analysis. *Health Technol Assess (Rockv)*. 2017;21(61):1-90. doi:10.3310/HTA21610
6. Phelan LK, Brown MA, Davis GK, Mangos G. A prospective study of the impact of automated dipstick urinalysis on the diagnosis of preeclampsia. *Hypertens Pregnancy*. 2004;23(2):135-142. doi:10.1081/PRG-120028289
7. Cade TJ, Gilbert SA, Polyakov A, Hotchin A. The accuracy of spot urinary protein-to-creatinine ratio in confirming proteinuria in pre-eclampsia. *Aust N Z J Obstet Gynaecol*. 2012;52(2):179-182. doi:10.1111/J.1479-828X.2011.01409.X

8. Ness RB, Roberts JM. Heterogeneous causes constituting the single syndrome of preeclampsia: A hypothesis and its implications. *Am J Obstet Gynecol*. 1996;175(5):1365-1370. doi:10.1016/S0002-9378(96)70056-X

9. von Dadelszen P, Magee LA, Roberts JM. Subclassification of Preeclampsia. *Hypertens Pregnancy*. 2003;22(2):143-148. doi:10.1081/PRG-120021060

10. Boyd HA, Tahir H, Wohlfahrt J, Melbye M. Associations of Personal and Family Preeclampsia History With the Risk of Early-, Intermediate- and Late-Onset Preeclampsia. *Am J Epidemiol*. 2013;178(11):1611-1619. doi:10.1093/aje/kwt189

11. Phillips JK, Janowiak M, Badger GJ, Bernstein IM. Evidence for distinct preterm and term phenotypes of preeclampsia. *The Journal of Maternal-Fetal & Neonatal Medicine*. 2010;23(7):622-626. doi:10.3109/14767050903258746

12. NICE. *Hypertension in Adults: Diagnosis and Management*.; 2019.

13. Lisonkova S, Joseph KS. Incidence of preeclampsia: risk factors and outcomes associated with early- versus late-onset disease. *Am J Obstet Gynecol*. 2013;209(6):544.e1-544.e12. doi:10.1016/j.ajog.2013.08.019

14. Jeyabalan A. Epidemiology of preeclampsia: impact of obesity. *Nutr Rev*. 2013;71:S18-S25. doi:10.1111/nure.12055

15. Lisonkova S, Joseph KS. Incidence of preeclampsia: risk factors and outcomes associated with early- versus late-onset disease. *Am J Obstet Gynecol*. 2013;209(6):544.e1-544.e12. doi:10.1016/j.ajog.2013.08.019

16. Duley L. The Global Impact of Pre-eclampsia and Eclampsia. *Semin Perinatol*. 2009;33(3):130-137. doi:10.1053/j.semperi.2009.02.010

17. von Dadelszen P, Magee LA. Preventing deaths due to the hypertensive disorders of pregnancy. *Best Pract Res Clin Obstet Gynaecol*. 2016;36:83-102. doi:10.1016/j.bpobgyn.2016.05.005

18. Kenny LC, Black MA, Poston L, et al. Early Pregnancy Prediction of Preeclampsia in Nulliparous Women, Combining Clinical Risk and Biomarkers. *Hypertension*. 2014;64(3):644-652. doi:10.1161/HYPERTENSIONAHA.114.03578

19. Scholten RR, Thijssen DJH, Lotgering FK, Hopman MTE, Spaanderman MEA. Cardiovascular effects of aerobic exercise training in formerly preeclamptic women and healthy parous control subjects. *Am J Obstet Gynecol*. 2014;211(5):516.e1-516.e11. doi:10.1016/j.ajog.2014.04.025

20. Barry DR, Utzschneider KM, Tong J, et al. Intraabdominal fat, insulin sensitivity, and cardiovascular risk factors in postpartum women with a history of preeclampsia. *Am J Obstet Gynecol*. 2015;213(1):104.e1-104.e11. doi:10.1016/j.ajog.2015.05.040

21. Akhter T, Larsson M, Wikström AK, Naessen T. Thicknesses of individual layers of artery wall indicate increased cardiovascular risk in severe pre-eclampsia. *Ultrasound in Obstetrics & Gynecology*. 2014;43(6):675-680. doi:10.1002/uog.13289

22. Sibai BM. Preeclampsia As a Cause of Preterm and Late Preterm (Near-Term) Births. *Semin Perinatol*. 2006;30(1):16-19. doi:10.1053/j.semperi.2006.01.008

23. Herrera-Garcia G, Contag S. Maternal Preeclampsia and Risk for Cardiovascular Disease in Offspring. *Curr Hypertens Rep*. 2014;16(9):475. doi:10.1007/s11906-014-0475-3

24. Scott G, Gillon TE, Pels A, von Dadelszen P, Magee LA. Guidelines—similarities and dissimilarities: a systematic review of international clinical practice guidelines for pregnancy hypertension. *Am J Obstet Gynecol*. 2022;226(2):S1222-S1236. doi:10.1016/j.ajog.2020.08.018

25. Davidson KW, Barry MJ, Mangione CM, et al. Aspirin Use to Prevent Preeclampsia and Related Morbidity and Mortality. *JAMA*. 2021;326(12):1186. doi:10.1001/jama.2021.14781

26. Wright D, Wright A, Nicolaides KH. The competing risk approach for prediction of preeclampsia. *Am J Obstet Gynecol*. 2020;223(1):12-23.e7. doi:10.1016/j.ajog.2019.11.1247

27. Al-Rubaie Z, Askie L, Ray J, Hudson H, Lord S. The performance of risk prediction models for pre-eclampsia using routinely collected maternal characteristics and comparison with models that include specialised tests and with clinical guideline decision rules: a systematic review. *BJOG*. 2016;123(9):1441-1452. doi:10.1111/1471-0528.14029

28. Levine RJ, Maynard SE, Qian C, et al. Circulating Angiogenic Factors and the Risk of Preeclampsia. *New England Journal of Medicine*. 2004;350(7). doi:10.1056/NEJMoa031884

29. Poon LC, Nicolaides KH. First-trimester maternal factors and biomarker screening for preeclampsia. *Prenat Diagn*. 2014;34(7):618-627. doi:10.1002/pd.4397

30. Kane SC, Da Silva Costa F, Brennecke SP. New directions in the prediction of pre-eclampsia. *Australian and New Zealand Journal of Obstetrics and Gynaecology*. 2014;54(2):101-107. doi:10.1111/ajo.12151

31. Brunelli V, Prefumo F. Quality of first trimester risk prediction models for pre-eclampsia: a systematic review. *BJOG*. 2015;122(7):904-914. doi:10.1111/1471-0528.13334

32. Anderson UD, Gram M, Åkerström B, Hansson SR. First Trimester Prediction of Preeclampsia. *Curr Hypertens Rep*. 2015;17(9):74. doi:10.1007/s11906-015-0584-7

33. Maynard SE, Min JY, Merchan J, et al. Excess placental soluble fms-like tyrosine kinase 1 (sFlt1) may contribute to endothelial dysfunction, hypertension, and proteinuria in preeclampsia. *Journal of Clinical Investigation*. 2003;111(5). doi:10.1172/JCI17189

34. Levine RJ, Lam C, Qian C, et al. Soluble Endoglin and Other Circulating Antiangiogenic Factors in Preeclampsia. *New England Journal of Medicine*. 2006;355(10):992-1005. doi:10.1056/NEJMoa055352

35. Verlohren S, Galindo A, Schlembach D, et al. An automated method for the determination of the sFlt-1/PIGF ratio in the assessment of preeclampsia. *Am J Obstet Gynecol*. 2010;202(2):161.e1-161.e11. doi:10.1016/j.ajog.2009.09.016

36. Verlohren S, Herraiz I, Lapaire O, et al. The sFlt-1/PlGF ratio in different types of hypertensive pregnancy disorders and its prognostic potential in preeclamptic patients. *Am J Obstet Gynecol*. 2012;206(1):58.e1-58.e8. doi:10.1016/j.ajog.2011.07.037

37. Villa PM, Hämäläinen E, Mäki A, et al. Vasoactive agents for the prediction of early- and late-onset preeclampsia in a high-risk cohort. *BMC Pregnancy Childbirth*. 2013;13(1):110. doi:10.1186/1471-2393-13-110

38. Rana S, Powe CE, Salahuddin S, et al. Angiogenic Factors and the Risk of Adverse Outcomes in Women With Suspected Preeclampsia. *Circulation*. 2012;125(7):911-919. doi:10.1161/CIRCULATIONAHA.111.054361

39. Vatten LJ, Eskild A, Nilsen TIL, Jeansson S, Jenum PA, Staff AC. Changes in circulating level of angiogenic factors from the first to second trimester as predictors of preeclampsia. *Am J Obstet Gynecol*. 2007;196(3):239.e1-239.e6. doi:10.1016/j.ajog.2006.10.909

40. Zeisler H, Llurba E, Chantraine F, et al. Predictive Value of the sFlt-1:PlGF Ratio in Women with Suspected Preeclampsia. *New England Journal of Medicine*. 2016;374(1). doi:10.1056/NEJMoa1414838

41. Verlohren S, Herraiz I, Lapaire O, et al. New Gestational Phase–Specific Cutoff Values for the Use of the Soluble fms-Like Tyrosine Kinase-1/Placental Growth Factor Ratio as a Diagnostic Test for Preeclampsia. *Hypertension*. 2014;63(2):346-352. doi:10.1161/HYPERTENSIONAHA.113.01787

42. Kenny L, English F, McCarthy F. Risk factors and effective management of preeclampsia. *Integr Blood Press Control*. Published online March 2015:7. doi:10.2147/IBPC.S50641

43. Surapaneni T, Bada VP, Nirmalan CPK. Risk for Recurrence of Pre-eclampsia in the Subsequent Pregnancy. *J Clin Diagn Res*. 2013;7(12):2889-2891. doi:10.7860/JCDR/2013/7681.3785

44. Esplin MS, Fausett MB, Fraser A, et al. Paternal and Maternal Components of the Predisposition to Preeclampsia. *New England Journal of Medicine*. 2001;344(12):867-872. doi:10.1056/NEJM200103223441201

45. Lie RT, Rasmussen S, Brunborg H, Gjessing HK, Lie-Nielsen E, Irgens LM. Fetal and maternal contributions to risk of pre-eclampsia: population based study. *BMJ*. 1998;316(7141):1343-1347. doi:10.1136/bmj.316.7141.1343

46. Hoy J, Venn A, Halliday J, Kovacs G, Waalwyk K. Perinatal and obstetric outcomes of donor insemination using cryopreserved semen in Victoria, Australia. *Human Reproduction*. 1999;14(7):1760-1764. doi:10.1093/humrep/14.7.1760

47. Duley L, Meher S, Hunter KE, Seidler AL, Askie LM. Antiplatelet agents for preventing pre-eclampsia and its complications. *Cochrane Database of Systematic Reviews*. 2019;2019(10). doi:10.1002/14651858.CD004659.pub3

48. Rolnik DL, Wright D, Poon LC, et al. Aspirin versus Placebo in Pregnancies at High Risk for Preterm Preeclampsia. *New England Journal of Medicine*. 2017;377(7):613-622. doi:10.1056/NEJMoa1704559

49. Davenport MH, Ruchat SM, Poitras VJ, et al. Prenatal exercise for the prevention of gestational diabetes mellitus and hypertensive disorders of pregnancy: a systematic review and meta-analysis. *Br J Sports Med*. 2018;52(21):1367-1375. doi:10.1136/bjsports-2018-099355

50. Woo Kinshella M, Sarr C, Sandhu A, et al. Calcium for pre-eclampsia prevention: A systematic review and network meta-analysis to guide personalised antenatal care. *BJOG*. 2022;129(11):1833-1843. doi:10.1111/1471-0528.17222

51. Mottola MF, Davenport MH, Ruchat SM, et al. No. 367-2019 Canadian Guideline for Physical Activity throughout Pregnancy. *Journal of Obstetrics and Gynaecology Canada*. 2018;40(11):1528-1537. doi:10.1016/j.jogc.2018.07.001

52. Hofmeyr GJ, Lawrie TA, Atallah ÁN, Duley L, Torloni MR. Calcium supplementation during pregnancy for preventing hypertensive disorders and related problems. *Cochrane Database of Systematic Reviews*. Published online June 24, 2014. doi:10.1002/14651858.CD001059.pub4

53. Döbert M, Varouxaki AN, Mu AC, et al. Pravastatin Versus Placebo in Pregnancies at High Risk of Term Preeclampsia. *Circulation*. 2021;144(9):670-679. doi:10.1161/CIRCULATIONAHA.121.053963

54. Wen SW, White RR, Rybak N, et al. Effect of high dose folic acid supplementation in pregnancy on pre-eclampsia (FACT): double blind, phase III, randomised controlled, international, multicentre trial. *BMJ*. Published online September 12, 2018:k3478. doi:10.1136/bmj.k3478

55. Cruz-Lemini M, Vázquez JC, Ullmo J, Llurba E. Low-molecular-weight heparin for prevention of preeclampsia and other placenta-mediated complications: a systematic review and meta-analysis. *Am J Obstet Gynecol*. 2022;226(2):S1126-S1144.e17. doi:10.1016/j.ajog.2020.11.006

56. Syngelaki A, Nicolaides KH, Balani J, et al. Metformin versus Placebo in Obese Pregnant Women without Diabetes Mellitus. *New England Journal of Medicine*. 2016;374(5):434-443. doi:10.1056/NEJMoa1509819

57. Tong S, Kaitu'u-Lino TJ, Hastie R, Brownfoot F, Cluver C, Hannan N. Pravastatin, proton-pump inhibitors, metformin, micronutrients, and biologics: new horizons for the

prevention or treatment of preeclampsia. *Am J Obstet Gynecol*. 2022;226(2):S1157-S1170. doi:10.1016/j.ajog.2020.09.014

58. Masini G, Foo LF, Tay J, et al. Preeclampsia has two phenotypes which require different treatment strategies. *Am J Obstet Gynecol*. 2022;226(2S):S1006-S1018. doi:10.1016/J.AJOG.2020.10.052

59. Improving Health Care Response to Hypertensive Disorders of Pregnancy | California Maternal Quality Care Collaborative. Accessed May 2, 2024. https://www.cmqcc.org/resource/improving-health-care-response-hypertensive-disorders-pregnancy

60. Chappell LC, Duckworth S, Seed PT, et al. Diagnostic Accuracy of Placental Growth Factor in Women With Suspected Preeclampsia. *Circulation*. 2013;128(19):2121-2131. doi:10.1161/CIRCULATIONAHA.113.003215

61. Von Dadelszen P, Payne B, Li J, et al. Prediction of adverse maternal outcomes in pre-eclampsia: development and validation of the fullPIERS model. *Lancet*. 2011;377(9761):219-227. doi:10.1016/S0140-6736(10)61351-7

62. Ukah UV, Payne B, Karjalainen H, et al. Temporal and external validation of the fullPIERS model for the prediction of adverse maternal outcomes in women with pre-eclampsia. *Pregnancy Hypertens*. 2019;15:42-50. doi:10.1016/J.PREGHY.2018.01.004

63. Duhig KE, Seed PT, Placzek A, et al. Prognostic indicators of severe disease in late preterm pre-eclampsia to guide decision making on timing of delivery: The PEACOCK study. *Pregnancy Hypertens*. 2021;24:90-95. doi:10.1016/J.PREGHY.2021.02.012

64. Ukah UV, Payne BA, Hutcheon JA, et al. Placental growth factor for the prognosis of women with preeclampsia (fullPIERS model extension): context matters. *BMC Pregnancy Childbirth*. 2020;20(1). doi:10.1186/S12884-020-03332-W

65. Magee LA, von Dadelszen P, Rey E, et al. Less-Tight versus Tight Control of Hypertension in Pregnancy. *New England Journal of Medicine*. 2015;372(5):407-417.

doi:10.1056/NEJMOA1404595/SUPPL_FILE/NEJMOA1404595_DISCLOSURES.PDF

66. Cleary KL, Siddiq Z, Ananth C V., et al. Use of Antihypertensive Medications During Delivery Hospitalizations Complicated by Preeclampsia. *Obstetrics and gynecology*. 2018;131(3):441. doi:10.1097/AOG.0000000000002479

67. Abalos E, Duley L, Steyn DW, Gialdini C. Antihypertensive drug therapy for mild to moderate hypertension during pregnancy. *Cochrane Database Syst Rev*. 2018;10(10). doi:10.1002/14651858.CD002252.PUB4

68. Weber-Schoendorfer C, Kayser A, Tissen-Diabaté T, et al. Fetotoxic risk of AT1 blockers exceeds that of angiotensin-converting enzyme inhibitors. *J Hypertens*. 2020;38(1):133-141. doi:10.1097/HJH.0000000000002233

69. Booker WA, Gyamfi-Bannerman C, Sheen JJ, et al. Maternal Outcomes by Race for Women Aged 40 Years or Older. *Obstetrics and gynecology*. 2018;132(2):404-413. doi:10.1097/AOG.0000000000002751

70. Identification and Management of Neonatal Hypoglycaemia in the Full Term Infant (2017) | British Association of Perinatal Medicine. Accessed May 3, 2024. https://www.bapm.org/resources/40-identification-and-management-of-neonatal-hypoglycaemia-in-the-full-term-infant-2017

71. Butalia S, Audibert F, Côté AM, et al. Hypertension Canada's 2018 Guidelines for the Management of Hypertension in Pregnancy. *Canadian Journal of Cardiology*. 2018;34(5):526-531. doi:10.1016/j.cjca.2018.02.021

72. Magee LA, von Dadelszen P, Singer J, et al. The CHIPS Randomized Controlled Trial (Control of Hypertension in Pregnancy Study). *Hypertension*. 2016;68(5):1153-1159. doi:10.1161/HYPERTENSIONAHA.116.07862

73. Gupta M, Greene N, Kilpatrick SJ. Timely treatment of severe maternal hypertension and reduction in severe maternal morbidity. *Pregnancy Hypertens*. 2018;14:55-58. doi:10.1016/j.preghy.2018.07.010

74. Scott G, Gillon TE, Pels A, von Dadelszen P, Magee LA. Guidelines—similarities and dissimilarities: a systematic review of international clinical practice guidelines for pregnancy hypertension. *Am J Obstet Gynecol*. 2022;226(2):S1222-S1236. doi:10.1016/j.ajog.2020.08.018

75. Sridharan K, Sequeira RP. Drugs for treating severe hypertension in pregnancy: a network meta-analysis and trial sequential analysis of randomized clinical trials. *Br J Clin Pharmacol*. 2018;84(9):1906-1916. doi:10.1111/bcp.13649

76. Alavifard S, Chase R, Janoudi G, et al. First-line antihypertensive treatment for severe hypertension in pregnancy: A systematic review and network meta-analysis. *Pregnancy Hypertens*. 2019;18:179-187. doi:10.1016/j.preghy.2019.09.019

77. Magpie Trial Follow-Up Study Collaborative Group. The Magpie Trial: a randomised trial comparing magnesium sulphate with placebo for pre-eclampsia. Outcome for women at 2 years. *BJOG*. 2007;114(3):300-309. doi:10.1111/j.1471-0528.2006.01166.x

78. Duley L. Do women with pre-eclampsia, and their babies, benefit from magnesium sulphate? The Magpie Trial: A randomised placebo-controlled trial. *Lancet*. 2002;359(9321):1877-1890. doi:10.1016/S0140-6736(02)08778-0

79. Duley L, Graham KM. Magnesium sulphate in eclampsia. Eclampsia Trial Collaborative Group. *Lancet*. 1998;352(9121):67-68. doi:10.1016/S0140-6736(05)79550-7

80. McGoldrick E, Stewart F, Parker R, Dalziel SR. Antenatal corticosteroids for accelerating foetal lung maturation for women at risk of preterm birth. *Cochrane Database Syst Rev*. 2020;12(12). doi:10.1002/14651858.CD004454.PUB4

81. Gyamfi-Bannerman C, Thom EA, Blackwell SC, et al. Antenatal Betamethasone for Women at Risk for Late Preterm Delivery. *New England Journal of Medicine*. 2016;374(14):1311-1320. doi:10.1056/NEJMOA1516783/SUPPL_FILE/NEJMOA1516783_DISCLOSURES.PDF

82. Ganzevoort W, Sibai BM. Temporising versus interventionist management (preterm and at term). *Best Pract Res Clin Obstet Gynaecol*. 2011;25(4):463-476. doi:10.1016/J.BPOBGYN.2011.01.004

83. Sibai BM, Barton JR. Expectant management of severe preeclampsia remote from term: patient selection, treatment, and delivery indications. *Am J Obstet Gynecol*. 2007;196(6):514.e1-514.e9. doi:10.1016/J.AJOG.2007.02.021

84. Knight M, Bunch K, Tuffnell D, et al. *Saving Lives, Improving Mothers' Care: Lessons Learned to Inform Maternity Care from the UK and Ireland Confidential Enquiries into Maternal Deaths and Morbidity 2015-17*.; 2019.

85. Koopmans CM, Bijlenga D, Groen H, et al. Induction of labour versus expectant monitoring for gestational hypertension or mild pre-eclampsia after 36 weeks' gestation (HYPITAT): a multicentre, open-label randomised controlled trial. *Lancet*. 2009;374(9694):979-988. doi:10.1016/S0140-6736(09)60736-4

86. Khosla K, Heimberger S, Nieman KM, et al. Long-Term Cardiovascular Disease Risk in Women After Hypertensive Disorders of Pregnancy: Recent Advances in Hypertension. *Hypertension*. 2021;78(4):927-935. doi:10.1161/HYPERTENSIONAHA.121.16506

87. Theilen LH, Fraser A, Hollingshaus MS, et al. All-Cause and Cause-Specific Mortality After Hypertensive Disease of Pregnancy. *Obstetrics & Gynecology*. 2016;128(2):238-244. doi:10.1097/AOG.0000000000001534

88. Tooher J, Thornton C, Makris A, Ogle R, Korda A, Hennessy A. All Hypertensive Disorders of Pregnancy Increase the Risk of Future Cardiovascular Disease. *Hypertension*. 2017;70(4):798-803. doi:10.1161/HYPERTENSIONAHA.117.09246

89. Sircar M, Thadhani R, Karumanchi SA. Pathogenesis of preeclampsia. *Curr Opin Nephrol Hypertens*. 2015;24(2):131-138. doi:10.1097/MNH.0000000000000105

90. Jim B, Karumanchi SA. Preeclampsia: Pathogenesis, Prevention, and Long-Term Complications. *Semin Nephrol*. 2017;37(4):386-397. doi:10.1016/J.SEMNEPHROL.2017.05.011

91. Brosens I, Pijnenborg R, Vercruysse L, Romero R. The "Great Obstetrical Syndromes" are associated with disorders of deep placentation. *Am J Obstet Gynecol*. 2011;204(3). doi:10.1016/j.ajog.2010.08.009

92. Pankiewicz K, Szczerba E, Maciejewski T, Fijałkowska A. Non-obstetric complications in preeclampsia. *Menopause Review/Przegląd Menopauzalny*. 2019;18(2):99-109. doi:10.5114/PM.2019.85785

93. Phipps E, Prasanna D, Brima W, Jim B. Preeclampsia: Updates in pathogenesis, definitions, and guidelines. *Clinical Journal of the American Society of Nephrology*. 2016;11(6):1102-1113. doi:10.2215/CJN.12081115

94. Hubel CA. Oxidative Stress in the Pathogenesis of Preeclampsia. *Proceedings of the Society for Experimental Biology and Medicine*. 1999;222(3):222-235. doi:10.1046/j.1525-1373.1999.d01-139.x

95. Myatt L, Cui X. Oxidative stress in the placenta. *Histochem Cell Biol*. 2004;122(4):369-382. doi:10.1007/s00418-004-0677-x

96. El-Sayed AAF. Preeclampsia: A review of the pathogenesis and possible management strategies based on its pathophysiological derangements. *Taiwan J Obstet Gynecol*. 2017;56(5):593-598. doi:10.1016/J.TJOG.2017.08.004

97. Tannetta D, Masliukaite I, Vatish M, Redman C, Sargent I. Update of syncytiotrophoblast derived extracellular vesicles in normal pregnancy and preeclampsia. *J Reprod Immunol*. 2017;119:98-106. doi:10.1016/j.jri.2016.08.008

98. Redman CW, Sargent IL, Staff AC. IFPA Senior Award Lecture: Making sense of pre-eclampsia – Two placental causes of preeclampsia? *Placenta*. 2014;35:S20-S25. doi:10.1016/j.placenta.2013.12.008

99. McLaughlin K, Zhang J, Lye SJ, Parker JD, Kingdom JC. Phenotypes of Pregnant Women Who Subsequently Develop Hypertension in Pregnancy. *J Am Heart Assoc*. 2018;7(14). doi:10.1161/JAHA.118.009595

100. Redman CW, Sargent IL. Latest Advances in Understanding Preeclampsia. *Science (1979)*. 2005;308(5728):1592-1594. doi:10.1126/science.1111726

101. Roberts J. Endothelial Dysfunction in Preeclampsia. *Semin Reprod Med*. 1998;16(01):5-15. doi:10.1055/s-2007-1016248

102. Porto LB, Brandão AHF, Leite HV, Cabral ACV. Longitudinal evaluation of uterine perfusion, endothelial function and central blood flow in early onset pre-eclampsia. *Pregnancy Hypertens*. 2017;10:161-164. doi:10.1016/j.preghy.2017.08.005

103. Roberts JM, Lain KY. Recent Insights into the Pathogenesis of Pre-eclampsia. *Placenta*. 2002;23(5):359-372. doi:10.1053/plac.2002.0819

104. Cindrova-Davies T, Fogarty NME, Jones CJP, Kingdom J, Burton GJ. Evidence of oxidative stress-induced senescence in mature, post-mature and pathological human placentas. *Placenta*. 2018;68:15-22. doi:10.1016/j.placenta.2018.06.307

105. Johnson MR, Anim-Nyame N, Johnson P, Sooranna SR, Steer PJ. Does endothelial cell activation occur with intrauterine growth restriction? *BJOG*. 2002;109(7):836-839. doi:10.1111/j.1471-0528.2002.01045.x

106. Sekizawa A, Jimbo M, Saito H, et al. Cell-free foetal DNA in the plasma of pregnant women with severe foetal growth restriction. *Am J Obstet Gynecol*. 2003;188(2):480-484. doi:10.1067/mob.2003.27

107. Laivuori H, Gallaher MJ, Collura L, et al. Relationships between maternal plasma leptin, placental leptin mRNA and protein in normal pregnancy, pre-eclampsia and intrauterine growth restriction without pre-eclampsia. *MHR: Basic science of reproductive medicine*. 2006;12(9):551-556. doi:10.1093/molehr/gal064

108. Goswami D, Tannetta DS, Magee LA, et al. Excess syncytiotrophoblast microparticle shedding is a feature of early-onset pre-eclampsia, but not normotensive intrauterine growth restriction. *Placenta*. 2006;27(1). doi:10.1016/j.placenta.2004.11.007

109. Shibata E, Rajakumar A, Powers RW, et al. Soluble fms-Like Tyrosine Kinase 1 Is Increased in Preeclampsia But Not in Normotensive Pregnancies with Small-for-Gestational-Age Neonates: Relationship to Circulating Placental Growth Factor. *J Clin Endocrinol Metab*. 2005;90(8):4895-4903. doi:10.1210/jc.2004-1955

110. Mizuuchi M, Cindrova-Davies T, Olovsson M, Charnock-Jones DS, Burton GJ, Yung HW. Placental endoplasmic reticulum stress negatively regulates transcription of placental growth factor via ATF4 and ATF6β: implications for the pathophysiology of human pregnancy complications. *J Pathol*. 2016;238(4):550-561. doi:10.1002/path.4678

111. Redman CWG, Tannetta DS, Dragovic RA, et al. Review: Does size matter? Placental debris and the pathophysiology of pre-eclampsia. *Placenta*. 2012;33:S48-S54. doi:10.1016/j.placenta.2011.12.006

112. Rusterholz C, Messerli M, Hoesli I, Hahn S. Placental Microparticles, DNA, and RNA in Preeclampsia. *Hypertens Pregnancy*. 2011;30(3):364-375. doi:10.3109/10641951003599571

113. Nakahara A, Nair S, Ormazabal V, et al. Circulating Placental Extracellular Vesicles and Their Potential Roles During Pregnancy. *Ochsner Journal*. 2020;20(4):439-445. doi:10.31486/toj.20.0049

114. Gupta AK, Rusterholz C, Huppertz B, et al. A comparative study of the effect of three different syncytiotrophoblast micro-particles preparations on endothelial cells. *Placenta*. 2005;26(1):59-66. doi:10.1016/j.placenta.2004.04.004

115. Cronqvist T, Saljé K, Familari M, et al. Syncytiotrophoblast Vesicles Show Altered micro-RNA and Haemoglobin Content after Ex-vivo Perfusion of Placentas with

Haemoglobin to Mimic Preeclampsia. *PLoS One*. 2014;9(2):e90020. doi:10.1371/journal.pone.0090020

116. Dragovic RA, Southcombe JH, Tannetta DS, Redman CWG, Sargent IL. Multicolor Flow Cytometry and Nanoparticle Tracking Analysis of Extracellular Vesicles in the Plasma of Normal Pregnant and Pre-eclamptic Women1. *Biol Reprod*. 2013;89(6). doi:10.1095/biolreprod.113.113266

117. Théry C, Witwer KW, Aikawa E, et al. Minimal information for studies of extracellular vesicles 2018 (MISEV2018): a position statement of the International Society for Extracellular Vesicles and update of the MISEV2014 guidelines. *J Extracell Vesicles*. 2018;7(1). doi:10.1080/20013078.2018.1535750

118. Welsh JA, Goberdhan DCI, O'Driscoll L, et al. Minimal information for studies of extracellular vesicles (MISEV2023): From basic to advanced approaches. *J Extracell Vesicles*. 2024;13(2). doi:10.1002/jev2.12404

119. Santavanond JP, Rutter SF, Atkin-Smith GK, Poon IKH. Apoptotic Bodies: Mechanism of Formation, Isolation and Functional Relevance. In: ; 2021:61-88. doi:10.1007/978-3-030-67171-6_4

120. Kerr JFR, Wyllie AH, Currie AR. Apoptosis: A Basic Biological Phenomenon with Wideranging Implications in Tissue Kinetics. *Br J Cancer*. 1972;26(4):239-257. doi:10.1038/bjc.1972.33

121. Reddy A, Zhong XY, Rusterholz C, et al. The Effect of Labour and Placental Separation on the Shedding of Syncytiotrophoblast Microparticles, Cell-free DNA and mRNA in Normal Pregnancy and Pre-eclampsia. *Placenta*. 2008;29(11):942-949. doi:10.1016/j.placenta.2008.08.018

122. Rajakumar A, Cerdeira AS, Rana S, et al. Transcriptionally Active Syncytial Aggregates in the Maternal Circulation May Contribute to Circulating Soluble Fms-Like Tyrosine Kinase 1 in Preeclampsia. *Hypertension*. 2012;59(2):256-264. doi:10.1161/HYPERTENSIONAHA.111.182170

123. Scott CC, Vacca F, Gruenberg J. Endosome maturation, transport and functions. *Semin Cell Dev Biol*. 2014;31:2-10. doi:10.1016/j.semcdb.2014.03.034

124. Doyle LM, Wang MZ. Overview of Extracellular Vesicles, Their Origin, Composition, Purpose, and Methods for Exosome Isolation and Analysis. *Cells*. 2019;8(7). doi:10.3390/CELLS8070727

125. Raposo G, Stoorvogel W. Extracellular vesicles: Exosomes, microvesicles, and friends. *Journal of Cell Biology*. 2013;200(4):373-383. doi:10.1083/jcb.201211138

126. Janas AM, Sapoń K, Janas T, Stowell MHB, Janas T. Exosomes and other extracellular vesicles in neural cells and neurodegenerative diseases. *Biochimica et Biophysica Acta (BBA) - Biomembranes*. 2016;1858(6):1139-1151. doi:10.1016/j.bbamem.2016.02.011

127. Janas T, Janas MM, Sapoń K, Janas T. Mechanisms of RNA loading into exosomes. *FEBS Lett*. 2015;589(13):1391-1398. doi:10.1016/J.FEBSLET.2015.04.036

128. Zhang Y, Liu Y, Liu H, Tang WH. Exosomes: biogenesis, biologic function and clinical potential. *Cell Biosci*. 2019;9(1). doi:10.1186/S13578-019-0282-2

129. Van Niel G, D'Angelo G, Raposo G. Shedding light on the cell biology of extracellular vesicles. *Nat Rev Mol Cell Biol*. 2018;19(4):213-228. doi:10.1038/NRM.2017.125

130. Regina Todeschini A, Hakomori S itiroh. Functional role of glycosphingolipids and gangliosides in control of cell adhesion, motility, and growth, through glycosynaptic microdomains. *Biochimica et Biophysica Acta (BBA) - General Subjects*. 2008;1780(3):421-433. doi:10.1016/j.bbagen.2007.10.008

131. Charrin S, Manié S, Thiele C, et al. A physical and functional link between cholesterol and tetraspanins. *Eur J Immunol*. 2003;33(9):2479-2489. doi:10.1002/eji.200323884

132. Essandoh K, Fan GC. Insights into the Mechanism of Exosome Formation and Secretion. In: *Mesenchymal Stem Cell Derived Exosomes*. Elsevier; 2015:1-19. doi:10.1016/B978-0-12-800164-6.00001-0

133. Hessvik NP, Llorente A. Current knowledge on exosome biogenesis and release. *Cellular and Molecular Life Sciences*. 2018;75(2):193-208. doi:10.1007/s00018-017-2595-9

134. McCullough J, Fisher RD, Whitby FG, Sundquist WI, Hill CP. ALIX-CHMP4 interactions in the human ESCRT pathway. *Proceedings of the National Academy of Sciences*. 2008;105(22):7687-7691. doi:10.1073/pnas.0801567105

135. Baietti MF, Zhang Z, Mortier E, et al. Syndecan–syntenin–ALIX regulates the biogenesis of exosomes. *Nat Cell Biol*. 2012;14(7):677-685. doi:10.1038/ncb2502

136. Goñi FM, Alonso A. Effects of ceramide and other simple sphingolipids on membrane lateral structure. *Biochimica et Biophysica Acta (BBA) - Biomembranes*. 2009;1788(1):169-177. doi:10.1016/j.bbamem.2008.09.002

137. Chairoungdua A, Smith DL, Pochard P, Hull M, Caplan MJ. Exosome release of β-catenin: a novel mechanism that antagonizes Wnt signaling. *Journal of Cell Biology*. 2010;190(6):1079-1091. doi:10.1083/jcb.201002049

138. van Niel G, Charrin S, Simoes S, et al. The Tetraspanin CD63 Regulates ESCRT-Independent and -Dependent Endosomal Sorting during Melanogenesis. *Dev Cell*. 2011;21(4):708-721. doi:10.1016/j.devcel.2011.08.019

139. Doyle LM, Wang MZ. Overview of Extracellular Vesicles, Their Origin, Composition, Purpose, and Methods for Exosome Isolation and Analysis. *Cells*. 2019;8(7). doi:10.3390/CELLS8070727

140. Makrygianni EA, Chrousos GP. Extracellular Vesicles and the Stress System. *Neuroendocrinology*. 2023;113(2):120-167. doi:10.1159/000527182

141. Tricarico C, Clancy J, D'Souza-Schorey C. Biology and biogenesis of shed microvesicles. *Small GTPases*. 2017;8(4):220-232. doi:10.1080/21541248.2016.1215283

142. Villarroya-Beltri C, Baixauli F, Gutiérrez-Vázquez C, Sánchez-Madrid F, Mittelbrunn M. Sorting it out: Regulation of exosome loading. *Semin Cancer Biol*. 2014;28:3-13. doi:10.1016/j.semcancer.2014.04.009

143. Moreno-Gonzalo O, Villarroya-Beltri C, SÃ¡nchez-Madrid F. Post-Translational Modifications of Exosomal Proteins. *Front Immunol*. 2014;5. doi:10.3389/fimmu.2014.00383

144. Mittelbrunn M, Gutiérrez-Vázquez C, Villarroya-Beltri C, et al. Unidirectional transfer of microRNA-loaded exosomes from T cells to antigen-presenting cells. *Nat Commun*. 2011;2(1):282. doi:10.1038/ncomms1285

145. Yuyama K, Sun H, Mitsutake S, Igarashi Y. Sphingolipid-modulated Exosome Secretion Promotes Clearance of Amyloid-β by Microglia. *Journal of Biological Chemistry*. 2012;287(14):10977-10989. doi:10.1074/jbc.M111.324616

146. Garcia-Martin R, Wang G, Brandão BB, et al. MicroRNA sequence codes for small extracellular vesicle release and cellular retention. *Nature*. 2022;601(7893):446-451. doi:10.1038/s41586-021-04234-3

147. Groot M, Lee H. Sorting Mechanisms for MicroRNAs into Extracellular Vesicles and Their Associated Diseases. *Cells*. 2020;9(4):1044. doi:10.3390/cells9041044

148. McKenzie AJ, Hoshino D, Hong NH, et al. KRAS-MEK Signaling Controls Ago2 Sorting into Exosomes. *Cell Rep*. 2016;15(5):978-987. doi:10.1016/j.celrep.2016.03.085

149. Shurtleff MJ, Temoche-Diaz MM, Karfilis K V, Ri S, Schekman R. Y-box protein 1 is required to sort microRNAs into exosomes in cells and in a cell-free reaction. *Elife*. 2016;5. doi:10.7554/eLife.19276

150. Guduric-Fuchs J, O'Connor A, Camp B, O'Neill CL, Medina RJ, Simpson DA. Selective extracellular vesicle-mediated export of an overlapping set of microRNAs from multiple cell types. *BMC Genomics*. 2012;13(1):357. doi:10.1186/1471-2164-13-357

151. Villarroya-Beltri C, Gutiérrez-Vázquez C, Sánchez-Cabo F, et al. Sumoylated hnRNPA2B1 controls the sorting of miRNAs into exosomes through binding to specific motifs. *Nat Commun*. 2013;4(1):2980. doi:10.1038/ncomms3980

152. Anand S, Samuel M, Kumar S, Mathivanan S. Ticket to a bubble ride: Cargo sorting into exosomes and extracellular vesicles. *Biochimica et Biophysica Acta (BBA) - Proteins and Proteomics*. 2019;1867(12):140203. doi:10.1016/j.bbapap.2019.02.005

153. Christianson HC, Svensson KJ, Van Kuppevelt TH, Li JP, Belting M. Cancer cell exosomes depend on cell-surface heparan sulfate proteoglycans for their internalization and functional activity. *Proc Natl Acad Sci U S A*. 2013;110(43):17380-17385. doi:10.1073/PNAS.1304266110/-/DCSUPPLEMENTAL/PNAS.201304266SI.PDF

154. Escrevente C, Keller S, Altevogt P, Costa J. Interaction and uptake of exosomes by ovarian cancer cells. *BMC Cancer*. 2011;11(1):108. doi:10.1186/1471-2407-11-108

155. Valapala M, Vishwanatha JK. Lipid raft endocytosis and exosomal transport facilitate extracellular trafficking of annexin A2. *J Biol Chem*. 2011;286(35):30911-30925. doi:10.1074/JBC.M111.271155

156. Costa Verdera H, Gitz-Francois JJ, Schiffelers RM, Vader P. Cellular uptake of extracellular vesicles is mediated by clathrin-independent endocytosis and macropinocytosis. *Journal of Controlled Release*. 2017;266:100-108. doi:10.1016/j.jconrel.2017.09.019

157. Fitzner D, Schnaars M, van Rossum D, et al. Selective transfer of exosomes from oligodendrocytes to microglia by macropinocytosis. *J Cell Sci*. 2011;124(3):447-458. doi:10.1242/jcs.074088

158. Parolini I, Federici C, Raggi C, et al. Microenvironmental pH Is a Key Factor for Exosome Traffic in Tumor Cells. *Journal of Biological Chemistry*. 2009;284(49):34211-34222. doi:10.1074/jbc.M109.041152

159. Franzen CA, Simms PE, Van Huis AF, Foreman KE, Kuo PC, Gupta GN. Characterization of Uptake and Internalization of Exosomes by Bladder Cancer Cells. *Biomed Res Int*. 2014;2014:1-11. doi:10.1155/2014/619829

160. Barrès C, Blanc L, Bette-Bobillo P, et al. Galectin-5 is bound onto the surface of rat reticulocyte exosomes and modulates vesicle uptake by macrophages. *Blood*. 2010;115(3):696-705. doi:10.1182/blood-2009-07-231449

161. Skokos D, Botros HG, Demeure C, et al. Mast Cell-Derived Exosomes Induce Phenotypic and Functional Maturation of Dendritic Cells and Elicit Specific Immune Responses In Vivo. *The Journal of Immunology*. 2003;170(6):3037-3045. doi:10.4049/jimmunol.170.6.3037

162. Hao S, Bai O, Li F, Yuan J, Laferte S, Xiang J. Mature dendritic cells pulsed with exosomes stimulate efficient cytotoxic T-lymphocyte responses and antitumour immunity. *Immunology*. 2007;120(1):90-102. doi:10.1111/j.1365-2567.2006.02483.x

163. Atay S, Gercel-Taylor C, Taylor DD. Human Trophoblast-Derived Exosomal Fibronectin Induces Pro-Inflammatory Il-1β Production by Macrophages. *American Journal of Reproductive Immunology*. 2011;66(4):259-269. doi:10.1111/j.1600-0897.2011.00995.x

164. Izquierdo-Useros N, Naranjo-Gómez M, Archer J, et al. Capture and transfer of HIV-1 particles by mature dendritic cells converges with the exosome-dissemination pathway. *Blood*. 2009;113(12):2732-2741. doi:10.1182/blood-2008-05-158642

165. Montecalvo A, Larregina AT, Shufesky WJ, et al. Mechanism of transfer of functional microRNAs between mouse dendritic cells via exosomes. *Blood*. 2012;119(3):756-766. doi:10.1182/blood-2011-02-338004

166. Svensson KJ, Christianson HC, Wittrup A, et al. Exosome Uptake Depends on ERK1/2-Heat Shock Protein 27 Signaling and Lipid Raft-mediated Endocytosis Negatively Regulated by Caveolin-1. *Journal of Biological Chemistry*. 2013;288(24):17713-17724. doi:10.1074/jbc.M112.445403

167. Feng D, Zhao WL, Ye YY, et al. Cellular Internalization of Exosomes Occurs Through Phagocytosis. *Traffic*. 2010;11(5):675-687. doi:10.1111/j.1600-0854.2010.01041.x

168. Cronqvist T, Tannetta D, Mörgelin M, et al. Syncytiotrophoblast derived extracellular vesicles transfer functional placental miRNAs to primary human endothelial cells. *Sci Rep*. 2017;7(1):4558. doi:10.1038/s41598-017-04468-0

169. Vargas A, Zhou S, Éthier-Chiasson M, et al. Syncytin proteins incorporated in placenta exosomes are important for cell uptake and show variation in abundance in serum exosomes from patients with preeclampsia. *The FASEB Journal*. 2014;28(8):3703-3719. doi:10.1096/fj.13-239053

170. Bobek G, Surmon L, Mirabito KM, Makris A, Hennessy A. Placental Regulation of Inflammation and Hypoxia after TNF-α Infusion in Mice. *American Journal of Reproductive Immunology*. 2015;74(5):407-418. doi:10.1111/aji.12417

171. Al-Ofi E, Anumba DOC, Coffelt S. OS006. Functional expression of endogenous ligands of Toll like receptor4 on monocytes and placentae from women during normal pregnancy andpre-eclampsia. *Pregnancy Hypertension: An International Journal of Women's Cardiovascular Health*. 2012;2(3):178. doi:10.1016/j.preghy.2012.04.008

172. Awoyemi T, Motta-Mejia C, Zhang W, et al. Syncytiotrophoblast Extracellular Vesicles From Late-Onset Preeclampsia Placentae Suppress Pro-Inflammatory Immune Response in THP-1 Macrophages. *Front Immunol*. 2021;12. doi:10.3389/fimmu.2021.676056

173. Messerli M, May K, Hansson SR, et al. Feto-maternal interactions in pregnancies: Placental microparticles activate peripheral blood monocytes. *Placenta*. 2010;31(2):106-112. doi:10.1016/j.placenta.2009.11.011

174. Gupta AK, Rusterholz C, Holzgreve W, Hahn S. Syncytiotrophoblast micro-particles do not induce apoptosis in peripheral T lymphocytes, but differ in their activity depending on the mode of preparation. *J Reprod Immunol*. 2005;68(1-2):15-26. doi:10.1016/j.jri.2005.05.003

175. Joerger-Messerli MS, Hoesli IM, Rusterholz C, Lapaire O. Stimulation of Monocytes by Placental Microparticles Involves Toll-Like Receptors and Nuclear Factor Kappa-Light-Chain-Enhancer of Activated B Cells. *Front Immunol*. 2014;5. doi:10.3389/fimmu.2014.00173

176. Motta-Mejia C, Kandzija N, Zhang W, et al. Placental Vesicles Carry Active Endothelial Nitric Oxide Synthase and Their Activity is Reduced in Preeclampsia. *Hypertension*. 2017;70(2):372-381. doi:10.1161/HYPERTENSIONAHA.117.09321

177. Chang X, Yao J, He Q, Liu M, Duan T, Wang K. Exosomes From Women With Preeclampsia Induced Vascular Dysfunction by Delivering sFlt (Soluble Fms-Like Tyrosine Kinase)-1 and sEng (Soluble Endoglin) to Endothelial Cells. *Hypertension*. 2018;72(6):1381-1390. doi:10.1161/HYPERTENSIONAHA.118.11706

178. Tannetta DS, Dragovic RA, Gardiner C, Redman CW, Sargent IL. Characterisation of syncytiotrophoblast vesicles in normal pregnancy and pre-eclampsia: expression of Flt-1 and endoglin. *PLoS One*. 2013;8(2). doi:10.1371/JOURNAL.PONE.0056754

179. Tannetta DS, Hunt K, Jones CI, et al. Syncytiotrophoblast Extracellular Vesicles from Pre-Eclampsia Placentas Differentially Affect Platelet Function. *PLoS One*. 2015;10(11):e0142538. doi:10.1371/journal.pone.0142538

180. Gardiner C, Tannetta DS, Simms CA, Harrison P, Redman CWG, Sargent IL. Syncytiotrophoblast Microvesicles Released from Pre-Eclampsia Placentae Exhibit Increased Tissue Factor Activity. *PLoS One*. 2011;6(10):e26313. doi:10.1371/journal.pone.0026313

181. Owens AP, Mackman N. Microparticles in Hemostasis and Thrombosis. *Circ Res*. 2011;108(10):1284-1297. doi:10.1161/CIRCRESAHA.110.233056

182. Guller S, Tang Z, Ma YY, Di Santo S, Sager R, Schneider H. Protein composition of microparticles shed from human placenta during placental perfusion: Potential role in angiogenesis and fibrinolysis in preeclampsia. *Placenta*. 2011;32(1):63-69. doi:10.1016/j.placenta.2010.10.011

183. Gunel T, Hosseini MK, Gumusoglu E, Kisakesen HI, Benian A, Aydinli K. Expression profiling of maternal plasma and placenta microRNAs in preeclamptic pregnancies by microarray technology. *Placenta*. 2017;52:77-85. doi:10.1016/j.placenta.2017.02.019

184. Ura B, Feriotto G, Monasta L, Bilel S, Zweyer M, Celeghini C. Potential role of circulating microRNAs as early markers of preeclampsia. *Taiwan J Obstet Gynecol*. 2014;53(2):232-234. doi:10.1016/j.tjog.2014.03.001

185. Stubert J, Koczan D, Richter DU, et al. miRNA expression profiles determined in maternal sera of patients with HELLP syndrome. *Hypertens Pregnancy*. 2014;33(2):215-235. doi:10.3109/10641955.2013.858743

186. Wu L, Zhou H, Lin H, et al. Circulating microRNAs are elevated in plasma from severe preeclamptic pregnancies. *REPRODUCTION*. 2012;143(3):389-397. doi:10.1530/REP-11-0304

187. Yang Q, Lu J, Wang S, Li H, Ge Q, Lu Z. Application of next-generation sequencing technology to profile the circulating microRNAs in the serum of preeclampsia versus normal pregnant women. *Clinica Chimica Acta*. 2011;412(23-24):2167-2173. doi:10.1016/j.cca.2011.07.029

188. Gill M, Motta-Mejia C, Kandzija N, et al. Placental Syncytiotrophoblast-Derived Extracellular Vesicles Carry Active NEP (Neprilysin) and Are Increased in Preeclampsia. *Hypertension*. 2019;73(5):1112-1119. doi:10.1161/HYPERTENSIONAHA.119.12707

189. Landers KA, Mortimer RH, Richard K. Transthyretin and the human placenta. *Placenta*. 2013;34(7):513-517. doi:10.1016/j.placenta.2013.04.013

190. Tong M, Cheng S bin, Chen Q, et al. Aggregated transthyretin is specifically packaged into placental nano-vesicles in preeclampsia. *Sci Rep*. 2017;7(1):6694. doi:10.1038/s41598-017-07017-x

191. Awoyemi T, Tannetta D, Zhang W, et al. Glycosylated Siglec-6 expression in syncytiotrophoblast-derived extracellular vesicles from preeclampsia placentas. *Biochem Biophys Res Commun*. 2020;533(4):838-844. doi:10.1016/j.bbrc.2020.09.081

192. Cerdeira AS, O'Sullivan J, Ohuma EO, et al. Randomized Interventional Study on Prediction of Preeclampsia/Eclampsia in Women With Suspected Preeclampsia. *Hypertension*. 2019;74(4). doi:10.1161/HYPERTENSIONAHA.119.12739

193. Dragovic RA, Collett GP, Hole P, et al. Isolation of syncytiotrophoblast microvesicles and exosomes and their characterisation by multicolour flow cytometry and fluorescence Nanoparticle Tracking Analysis. *Methods*. 2015;87:64-74. doi:10.1016/j.ymeth.2015.03.028

194. Jiang S, Zhang W, Cao Q, et al. ExoCounter Assays Identify Women Who May Develop Early-Onset Preeclampsia From 12.5 μL First-Trimester Serum by Characterizing Placental Small Extracellular Vesicles. *Hypertension*. 2023;80(7):1439-1451. doi:10.1161/HYPERTENSIONAHA.123.20907

195. Awoyemi T, Jiang S, Rahbar M, et al. MicroRNA analysis of medium/large placenta extracellular vesicles in normal and preeclampsia pregnancies. *Front Cardiovasc Med*. 2024;11. doi:10.3389/fcvm.2024.1371168

196. Awoyemi T, Zhang W, Rahbar M, et al. A cross-sectional analysis of syncytiotrophoblast membrane extracellular vesicles–derived transcriptomic biomarkers in early-onset preeclampsia. *Front Cardiovasc Med*. 2023;10. doi:10.3389/fcvm.2023.1291642

197. Thomas T, Gopikrishna V, Kandaswamy D. Comparative evaluation of maintenance of cell viability of an experimental transport media "coconut water" with Hank′s balanced salt solution and milk, for transportation of an avulsed tooth: An *in vitro* cell culture study. *Journal of Conservative Dentistry*. 2008;11(1):22. doi:10.4103/0972-0707.43414

198. Yu Z, Huang H, Zhang H, Kessler BM. Improved profiling of polyamines using two-dimensional gas chromatography mass spectrometry. *Talanta*. 2019;199:184-188. doi:10.1016/j.talanta.2019.02.062

199. Hill AF, Pegtel DM, Lambertz U, et al. ISEV position paper: extracellular vesicle RNA analysis and bioinformatics. *J Extracell Vesicles*. 2013;2(1). doi:10.3402/jev.v2i0.22859

200. Livak KJ, Schmittgen TD. Analysis of Relative Gene Expression Data Using Real-Time Quantitative PCR and the 2−ΔΔCT Method. *Methods*. 2001;25(4):402-408. doi:10.1006/meth.2001.1262

201. Szklarczyk D, Gable AL, Lyon D, et al. STRING v11: protein–protein association networks with increased coverage, supporting functional discovery in genome-wide experimental datasets. *Nucleic Acids Res*. 2019;47(D1):D607-D613. doi:10.1093/nar/gky1131

202. Akbar N, Braithwaite AT, Corr EM, et al. Rapid neutrophil mobilization by VCAM-1+ endothelial cell-derived extracellular vesicles. *Cardiovasc Res*. 2023;119(1):236-251. doi:10.1093/cvr/cvac012

203. Stein JM, Luzio JP. Ectocytosis caused by sublytic autologous complement attack on human neutrophils. The sorting of endogenous plasma-membrane proteins and lipids into shed vesicles. *Biochemical Journal*. 1991;274(2):381-386. doi:10.1042/bj2740381

204. Cocucci E, Meldolesi J. Ectosomes and exosomes: shedding the confusion between extracellular vesicles. *Trends Cell Biol*. 2015;25(6):364-372. doi:10.1016/j.tcb.2015.01.004

205. Mir B, Goettsch C. Extracellular Vesicles as Delivery Vehicles of Specific Cellular Cargo. *Cells*. 2020;9(7):1601. doi:10.3390/cells9071601

206. Yates AG, Pink RC, Erdbrügger U, et al. In sickness and in health: The functional role of extracellular vesicles in physiology and pathology in vivo. *J Extracell Vesicles*. 2022;11(1). doi:10.1002/jev2.12151

207. Nair S, Razo-Azamar M, Jayabalan N, et al. Advances in extracellular vesicles as mediators of cell-to-cell communication in pregnancy. *Cytokine Growth Factor Rev*. 2024;76:86-98. doi:10.1016/j.cytogfr.2023.12.004

208. Caruso Bavisotto C, Scalia F, Marino Gammazza A, et al. Extracellular Vesicle-Mediated Cell–Cell Communication in the Nervous System: Focus on Neurological Diseases. *Int J Mol Sci*. 2019;20(2):434. doi:10.3390/ijms20020434

209. Vader P, Breakefield XO, Wood MJA. Extracellular vesicles: emerging targets for cancer therapy. *Trends Mol Med*. 2014;20(7):385-393. doi:10.1016/j.molmed.2014.03.002

210. Mulcahy LA, Pink RC, Carter DRF. Routes and mechanisms of extracellular vesicle uptake. *J Extracell Vesicles*. 2014;3(1). doi:10.3402/jev.v3.24641

211. Kanada M, Bachmann MH, Hardy JW, et al. Differential fates of biomolecules delivered to target cells via extracellular vesicles. *Proceedings of the National Academy of Sciences*. 2015;112(12). doi:10.1073/pnas.1418401112

212. Schulz-Siegmund M, Aigner A. Nucleic acid delivery with extracellular vesicles. *Adv Drug Deliv Rev*. 2021;173:89-111. doi:10.1016/j.addr.2021.03.005

213. Capra E, Lange-Consiglio A. The Biological Function of Extracellular Vesicles during Fertilization, Early Embryo—Maternal Crosstalk and Their Involvement in Reproduction: Review and Overview. *Biomolecules*. 2020;10(11):1510. doi:10.3390/biom10111510

214. Adam S, Elfeky O, Kinhal V, et al. Review: Fetal-maternal communication via extracellular vesicles – Implications for complications of pregnancies. *Placenta*. 2017;54:83-88. doi:10.1016/j.placenta.2016.12.001

215. Nair S, Salomon C. Extracellular vesicles as critical mediators of maternal-foetal communication during pregnancy and their potential role in maternal metabolism. *Placenta*. 2020;98:60-68. doi:10.1016/j.placenta.2020.06.011

216. Szuszkiewicz J, Myszczynski K, Reliszko ZP, Heifez Y, Kaczmarek MM. Early steps of embryo implantation are regulated by exchange of extracellular vesicles between the embryo and the endometrium. *The FASEB Journal*. 2022;36(8). doi:10.1096/fj.202200677R

217. Godakumara K, Ord J, Lättekivi F, et al. Trophoblast derived extracellular vesicles specifically alter the transcriptome of endometrial cells and may constitute a critical component of embryo-maternal communication. *Reproductive Biology and Endocrinology*. 2021;19(1):115. doi:10.1186/s12958-021-00801-5

218. Salomon C, Rice GE. Role of Exosomes in Placental Homeostasis and Pregnancy Disorders. In: ; 2017:163-179. doi:10.1016/bs.pmbts.2016.12.006

219. Escudero CA, Herlitz K, Troncoso F, et al. Role of Extracellular Vesicles and microRNAs on Dysfunctional Angiogenesis during Preeclamptic Pregnancies. *Front Physiol*. 2016;7. doi:10.3389/fphys.2016.00098

220. Zhang Y, Fei M, Xue G, et al. Elevated levels of hypoxia-inducible microRNA-210 in pre-eclampsia: new insights into molecular mechanisms for the disease. *J Cell Mol Med*. 2012;16(2):249-259. doi:10.1111/j.1582-4934.2011.01291.x

221. Hedlund M, Stenqvist AC, Nagaeva O, et al. Human Placenta Expresses and Secretes NKG2D Ligands via Exosomes that Down-Modulate the Cognate Receptor Expression: Evidence for Immunosuppressive Function. *The Journal of Immunology*. 2009;183(1):340-351. doi:10.4049/jimmunol.0803477

222. Gutierrez-Franco J, Hernandez-Gutierrez R, Bueno-Topete MR, et al. Characterization of B7H6, an endogenous ligand for the NK cell activating receptor NKp30, reveals the identity of two different soluble isoforms during normal human pregnancy. *Immunobiology*. 2018;223(1):57-63. doi:10.1016/j.imbio.2017.10.012

223. ISHIDA Y, ZHAO D, OHKUCHI A, et al. Maternal peripheral blood natural killer cells incorporate placenta-associated microRNAs during pregnancy. *Int J Mol Med*. 2015;35(6):1511-1524. doi:10.3892/ijmm.2015.2157

224. Bai K, Lee CL, Liu X, et al. Human placental exosomes induce maternal systemic immune tolerance by reprogramming circulating monocytes. *J Nanobiotechnology*. 2022;20(1):86. doi:10.1186/s12951-022-01283-2

225. Atay S, Gercel-Taylor C, Suttles J, Mor G, Taylor DD. Trophoblast-Derived Exosomes Mediate Monocyte Recruitment and Differentiation. *American Journal of Reproductive Immunology*. 2011;65(1):65-77. doi:10.1111/j.1600-0897.2010.00880.x

226. Atay S, Gercel-Taylor C, Taylor DD. Human Trophoblast-Derived Exosomal Fibronectin Induces Pro-Inflammatory Il-1β Production by Macrophages. *American Journal of Reproductive Immunology*. 2011;66(4):259-269. doi:10.1111/j.1600-0897.2011.00995.x

227. Lokossou AG, Toudic C, Nguyen PT, et al. Endogenous retrovirus-encoded Syncytin-2 contributes to exosome-mediated immunosuppression of T cells†. *Biol Reprod*. Published online July 18, 2019. doi:10.1093/biolre/ioz124

228. Kovács ÁF, Fekete N, Turiák L, et al. Unravelling the Role of Trophoblastic-Derived Extracellular Vesicles in Regulatory T Cell Differentiation. *Int J Mol Sci*. 2019;20(14):3457. doi:10.3390/ijms20143457

229. Salomon C, Torres MJ, Kobayashi M, et al. A Gestational Profile of Placental Exosomes in Maternal Plasma and Their Effects on Endothelial Cell Migration. *PLoS One*. 2014;9(6):e98667. doi:10.1371/journal.pone.0098667

230. Gebara N, Correia Y, Wang K, Bussolati B. Angiogenic Properties of Placenta-Derived Extracellular Vesicles in Normal Pregnancy and in Preeclampsia. *Int J Mol Sci*. 2021;22(10):5402. doi:10.3390/ijms22105402

231. Awoyemi T, Cerdeira AS, Zhang W, et al. Preeclampsia and syncytiotrophoblast membrane extracellular vesicles (STB-EVs). *Clin Sci*. 2022;136(24):1793-1807. doi:10.1042/CS20220149

232. Kandzija N, Zhang W, Motta-Mejia C, et al. Placental extracellular vesicles express active dipeptidyl peptidase IV; levels are increased in gestational diabetes mellitus. *J Extracell Vesicles*. 2019;8(1). doi:10.1080/20013078.2019.1617000

233. Bobek G, Surmon L, Mirabito KM, Makris A, Hennessy A. Placental Regulation of Inflammation and Hypoxia after TNF-α Infusion in Mice. *American Journal of Reproductive Immunology*. 2015;74(5):407-418. doi:10.1111/aji.12417

234. Al-Ofi E, Anumba DOC, Coffelt S. Functional expression of endogenous ligands of Toll like receptor4 on monocytes and placentae from women during normal pregnancy andpre-eclampsia. *Pregnancy Hypertension: An International Journal of Women's Cardiovascular Health*. 2012;2(3):178. doi:10.1016/j.preghy.2012.04.008

235. Sammar M, Dragovic R, Meiri H, et al. Reduced placental protein 13 (PP13) in placental derived syncytiotrophoblast extracellular vesicles in preeclampsia – A novel tool to study the impaired cargo transmission of the placenta to the maternal organs. *Placenta*. 2018;66:17-25. doi:10.1016/j.placenta.2018.04.013

236. Cronqvist T, Tannetta D, Mörgelin M, et al. Syncytiotrophoblast derived extracellular vesicles transfer functional placental miRNAs to primary human endothelial cells. *Sci Rep*. 2017;7(1):4558. doi:10.1038/s41598-017-04468-0

237. Tannetta DS, Dragovic RA, Gardiner C, Redman CW, Sargent IL. Characterisation of Syncytiotrophoblast Vesicles in Normal Pregnancy and Pre-Eclampsia: Expression of Flt-1 and Endoglin. *PLoS One*. 2013;8(2):e56754. doi:10.1371/journal.pone.0056754

238. Gardiner C, Tannetta DS, Simms CA, Harrison P, Redman CWG, Sargent IL. Syncytiotrophoblast Microvesicles Released from Pre-Eclampsia Placentae Exhibit Increased Tissue Factor Activity. *PLoS One*. 2011;6(10):e26313. doi:10.1371/journal.pone.0026313

239. Thamotharan S, Ghosh S, James-Allan L, Lei MYY, Janzen C, Devaskar SU. Circulating extracellular vesicles exhibit a differential miRNA profile in gestational

diabetes mellitus pregnancies. *PLoS One*. 2022;17(5):e0267564. doi:10.1371/journal.pone.0267564

240. Gillet V, Ouellet A, Stepanov Y, et al. miRNA Profiles in Extracellular Vesicles From Serum Early in Pregnancies Complicated by Gestational Diabetes Mellitus. *J Clin Endocrinol Metab*. 2019;104(11):5157-5169. doi:10.1210/jc.2018-02693

241. Konoshenko MYu, Lekchnov EA, Vlassov A V., Laktionov PP. Isolation of Extracellular Vesicles: General Methodologies and Latest Trends. *Biomed Res Int*. 2018;2018:1-27. doi:10.1155/2018/8545347

242. Kenigsberg S, Wyse BA, Librach CL, da Silveira JC. Protocol for Exosome Isolation from Small Volume of Ovarian Follicular Fluid: Evaluation of Ultracentrifugation and Commercial Kits. In: ; 2017:321-341. doi:10.1007/978-1-4939-7253-1_26

243. Brennan K, Martin K, FitzGerald SP, et al. A comparison of methods for the isolation and separation of extracellular vesicles from protein and lipid particles in human serum. *Sci Rep*. 2020;10(1):1039. doi:10.1038/s41598-020-57497-7

244. Sidhom K, Obi PO, Saleem A. A Review of Exosomal Isolation Methods: Is Size Exclusion Chromatography the Best Option? *Int J Mol Sci*. 2020;21(18):6466. doi:10.3390/ijms21186466

245. Deregibus MC, Figliolini F, D'antico S, et al. Charge-based precipitation of extracellular vesicles. *Int J Mol Med*. 2016;38(5):1359-1366. doi:10.3892/ijmm.2016.2759

246. Böing AN, van der Pol E, Grootemaat AE, Coumans FAW, Sturk A, Nieuwland R. Single-step isolation of extracellular vesicles by size-exclusion chromatography. *J Extracell Vesicles*. 2014;3(1). doi:10.3402/jev.v3.23430

247. Witwer KW, Buzás EI, Bemis LT, et al. Standardization of sample collection, isolation and analysis methods in extracellular vesicle research. *J Extracell Vesicles*. 2013;2(1). doi:10.3402/jev.v2i0.20360

248. Gupta AK, Holzgreve W, Huppertz B, Malek A, Schneider H, Hahn S. Detection of Fetal DNA and RNA in Placenta-Derived Syncytiotrophoblast Microparticles Generated in Vitro. *Clin Chem*. 2004;50(11):2187-2190. doi:10.1373/clinchem.2004.040196

249. Gupta AK, Holzgreve W, Hahn S. Decrease in lipid levels of syncytiotrophoblast micro-particles reduced their potential to inhibit endothelial cell proliferation. *Arch Gynecol Obstet*. 2008;277(2):115-119. doi:10.1007/s00404-007-0425-2

250. SMITH NC, BRUSH MG, LUCKETT S. Preparation of human placental villous surface membrane. *Nature*. 1974;252(5481):302-303. doi:10.1038/252302b0

251. Gupta AK, Rusterholz C, Huppertz B, et al. A comparative study of the effect of three different syncytiotrophoblast micro-particles preparations on endothelial cells. *Placenta*. 2005;26(1):59-66. doi:10.1016/j.placenta.2004.04.004

252. Tong M, Chamley LW. Placental Extracellular Vesicles and Feto-Maternal Communication. *Cold Spring Harb Perspect Med*. 2015;5(3):a023028-a023028. doi:10.1101/cshperspect.a023028

253. Tong M, Chamley LW. Isolation and Characterization of Extracellular Vesicles from Ex Vivo Cultured Human Placental Explants. In: ; 2018:117-129. doi:10.1007/978-1-4939-7498-6_9

254. Levine L, Habertheuer A, Ram C, et al. Syncytiotrophoblast extracellular microvesicle profiles in maternal circulation for noninvasive diagnosis of preeclampsia. *Sci Rep*. 2020;10(1):6398. doi:10.1038/s41598-020-62193-7

255. Cross CE, Tolba MF, Rondelli CM, Xu M, Abdel-Rahman SZ. Oxidative Stress Alters miRNA and Gene Expression Profiles in Villous First Trimester Trophoblasts. *Biomed Res Int*. 2015;2015:1-11. doi:10.1155/2015/257090

256. Chern SR, Li SH, Chiu CL, Chang HH, Chen CP, Tsuen Chen EI. Spatiotemporal expression of SERPINE2 in the human placenta and its role in extravillous trophoblast migration and invasion. *Reprod Biol Endocrinol*. 2011;9:106. doi:10.1186/1477-7827-9-106

257. Chen CP, Chang SC, Vivian Yang WC. High glucose alters proteoglycan expression and the glycosaminoglycan composition in placentas of women with gestational diabetes mellitus and in cultured trophoblasts. *Placenta*. 2007;28(2-3):97-106. doi:10.1016/j.placenta.2006.02.009

258. Lee SM, Romero R, Lee YJ, Park IS, Park CW, Yoon BH. Systemic inflammatory stimulation by microparticles derived from hypoxic trophoblast as a model for inflammatory response in preeclampsia. *Am J Obstet Gynecol*. 2012;207(4):337.e1-337.e8. doi:10.1016/j.ajog.2012.06.047

259. Hunkapiller NM, Fisher SJ. Chapter 12 Placental Remodeling of the Uterine Vasculature. In: ; 2008:281-302. doi:10.1016/S0076-6879(08)03012-7

260. Taylor SK, Houshdaran S, Robinson JF, et al. Cytotrophoblast extracellular vesicles enhance decidual cell secretion of immune modulators via TNF-alpha. *Development*. Published online January 1, 2020. doi:10.1242/dev.187013

261. Gardiner C, Di Vizio D, Sahoo S, et al. Techniques used for the isolation and characterization of extracellular vesicles: results of a worldwide survey. *J Extracell Vesicles*. 2016;5(1). doi:10.3402/jev.v5.32945

262. Théry C, Amigorena S, Raposo G, Clayton A. Isolation and Characterization of Exosomes from Cell Culture Supernatants and Biological Fluids. *Curr Protoc Cell Biol*. 2006;30(1). doi:10.1002/0471143030.cb0322s30

263. Wang S, Fu J, Zhang C, Yang J. Slurry treatment for shield tunnelling and waste slurry recycling. In: *Shield Tunnel Engineering*. Elsevier; 2021:491-521. doi:10.1016/B978-0-12-823992-6.00010-2

264. Kowal J, Arras G, Colombo M, et al. Proteomic comparison defines novel markers to characterize heterogeneous populations of extracellular vesicle subtypes. *Proceedings of the National Academy of Sciences*. 2016;113(8). doi:10.1073/pnas.1521230113

265. Clos-Sansalvador M, Monguió-Tortajada M, Roura S, Franquesa M, Borràs FE. Commonly used methods for extracellular vesicles' enrichment: Implications in

downstream analyses and use. *Eur J Cell Biol*. 2022;101(3):151227. doi:10.1016/j.ejcb.2022.151227

266. Cvjetkovic A, Lötvall J, Lässer C. The influence of rotor type and centrifugation time on the yield and purity of extracellular vesicles. *J Extracell Vesicles*. 2014;3(1). doi:10.3402/jev.v3.23111

267. Ramirez MI, Amorim MG, Gadelha C, et al. Technical challenges of working with extracellular vesicles. *Nanoscale*. 2018;10(3):881-906. doi:10.1039/C7NR08360B

268. Linares R, Tan S, Gounou C, Arraud N, Brisson AR. High-speed centrifugation induces aggregation of extracellular vesicles. *J Extracell Vesicles*. 2015;4(1). doi:10.3402/jev.v4.29509

269. McNamara RP, Caro-Vegas CP, Costantini LM, et al. Large-scale, cross-flow based isolation of highly pure and endocytosis-competent extracellular vesicles. *J Extracell Vesicles*. 2018;7(1). doi:10.1080/20013078.2018.1541396

270. Welton JL, Webber JP, Botos L, Jones M, Clayton A. Ready-made chromatography columns for extracellular vesicle isolation from plasma. *J Extracell Vesicles*. 2015;4(1). doi:10.3402/jev.v4.27269

271. Baranyai T, Herczeg K, Onódi Z, et al. Isolation of Exosomes from Blood Plasma: Qualitative and Quantitative Comparison of Ultracentrifugation and Size Exclusion Chromatography Methods. *PLoS One*. 2015;10(12):e0145686. doi:10.1371/journal.pone.0145686

272. Livshits MA, Khomyakova E, Evtushenko EG, et al. Isolation of exosomes by differential centrifugation: Theoretical analysis of a commonly used protocol. *Sci Rep*. 2015;5(1):17319. doi:10.1038/srep17319

273. Webber J, Clayton A. How pure are your vesicles? *J Extracell Vesicles*. 2013;2(1). doi:10.3402/jev.v2i0.19861

274. de Vrij J, Maas SL, van Nispen M, et al. Quantification of nanosized extracellular membrane vesicles with scanning ion occlusion sensing. *Nanomedicine*. 2013;8(9):1443-1458. doi:10.2217/nnm.12.173

275. Arraud N, Linares R, Tan S, et al. Extracellular vesicles from blood plasma: determination of their morphology, size, phenotype and concentration. *Journal of Thrombosis and Haemostasis*. 2014;12(5):614-627. doi:10.1111/jth.12554

276. van der Vlist EJ, Nolte-'t Hoen ENM, Stoorvogel W, Arkesteijn GJA, Wauben MHM. Fluorescent labeling of nano-sized vesicles released by cells and subsequent quantitative and qualitative analysis by high-resolution flow cytometry. *Nat Protoc*. 2012;7(7):1311-1326. doi:10.1038/nprot.2012.065

277. Cointe S, Judicone C, Robert S, et al. Standardization of microparticle enumeration across different flow cytometry platforms: results of a multicenter collaborative workshop. *Journal of Thrombosis and Haemostasis*. 2017;15(1):187-193. doi:10.1111/jth.13514

278. Kormelink TG, Arkesteijn GJA, Nauwelaers FA, van den Engh G, Nolte-'t Hoen ENM, Wauben MHM. Prerequisites for the analysis and sorting of extracellular vesicle subpopulations by high-resolution flow cytometry. *Cytometry Part A*. 2016;89(2):135-147. doi:10.1002/cyto.a.22644

279. Karimi N, Cvjetkovic A, Jang SC, et al. Detailed analysis of the plasma extracellular vesicle proteome after separation from lipoproteins. *Cellular and Molecular Life Sciences*. 2018;75(15):2873-2886. doi:10.1007/s00018-018-2773-4

280. Musante L, Saraswat M, Duriez E, et al. Biochemical and Physical Characterisation of Urinary Nanovesicles following CHAPS Treatment. *PLoS One*. 2012;7(7):e37279. doi:10.1371/journal.pone.0037279

281. Wu Y, Deng W, Klinke II DJ. Exosomes: improved methods to characterize their morphology, RNA content, and surface protein biomarkers. *Analyst*. 2015;140(19):6631-6642. doi:10.1039/C5AN00688K

282. Noble JM, Roberts LM, Vidavsky N, et al. Direct comparison of optical and electron microscopy methods for structural characterization of extracellular vesicles. *J Struct Biol*. 2020;210(1):107474. doi:10.1016/j.jsb.2020.107474

283. Bordanaba-Florit G, Royo F, Kruglik SG, Falcón-Pérez JM. Using single-vesicle technologies to unravel the heterogeneity of extracellular vesicles. *Nat Protoc*. 2021;16(7):3163-3185. doi:10.1038/s41596-021-00551-z

284. Redman C. Pre-eclampsia: A complex and variable disease. *Pregnancy Hypertension: An International Journal of Women's Cardiovascular Health*. 2014;4(3):241-242. doi:10.1016/j.preghy.2014.04.009

285. Worton SA, Greenwood SL, Wareing M, Heazell AEP, Myers J. The kynurenine pathway; A new target for treating maternal features of preeclampsia? *Placenta*. 2019;84:44-49. doi:10.1016/j.placenta.2019.04.007

286. Massudi H, Grant R, Guillemin GJ, Braidy N. NAD+ metabolism and oxidative stress: the golden nucleotide on a crown of thorns. *Redox Report*. 2012;17(1):28-46. doi:10.1179/1351000212Y.0000000001

287. Ball HJ, Sanchez-Perez A, Weiser S, et al. Characterization of an indoleamine 2,3-dioxygenase-like protein found in humans and mice. *Gene*. 2007;396(1):203-213. doi:10.1016/j.gene.2007.04.010

288. Seifert J, Casida JE. Multiple forms of chicken kynurenine formamidase. *Comparative Biochemistry and Physiology Part C: Comparative Pharmacology*. 1979;63(1):123-127. doi:10.1016/0306-4492(79)90140-0

289. Sedlmayr P, Blaschitz A, Stocker R. The Role of Placental Tryptophan Catabolism. *Front Immunol*. 2014;5. doi:10.3389/fimmu.2014.00230

290. Kamimura S, Eguchi K, Yonezawa M, Sekiba K. Localization and developmental change of indoleamine 2,3-dioxygenase activity in the human placenta. *Acta Med Okayama*. 1991;45(3):135-139. doi:10.18926/AMO/32206

291. McGaha TL, Huang L, Lemos H, et al. Amino acid catabolism: a pivotal regulator of innate and adaptive immunity. *Immunol Rev*. 2012;249(1):135-157. doi:10.1111/j.1600-065X.2012.01149.x

292. Wang Y, Liu H, McKenzie G, et al. Kynurenine is an endothelium-derived relaxing factor produced during inflammation. *Nature Medicine 2010 16:3*. 2010;16(3):279-285. doi:10.1038/nm.2092

293. Yuasa HJ, Ball HJ, Ho YF, et al. Characterization and evolution of vertebrate indoleamine 2, 3-dioxygenases. *Comp Biochem Physiol B Biochem Mol Biol*. 2009;153(2):137-144. doi:10.1016/j.cbpb.2009.02.002

294. Badawy AAB. Kynurenine pathway of tryptophan metabolism: Regulatory and functional aspects. *International Journal of Tryptophan Research*. 2017;10(1). doi:10.1177/1178646917691938

295. Mezrich JD, Fechner JH, Zhang X, Johnson BP, Burlingham WJ, Bradfield CA. An Interaction between Kynurenine and the Aryl Hydrocarbon Receptor Can Generate Regulatory T Cells. *The Journal of Immunology*. 2010;185(6):3190-3198. doi:10.4049/jimmunol.0903670

296. Noakes R. The Aryl Hydrocarbon Receptor: A Review of Its Role in the Physiology and Pathology of the Integument and Its Relationship to the Tryptophan Metabolism. *International Journal of Tryptophan Research*. 2015;8:IJTR.S19985. doi:10.4137/IJTR.S19985

297. Conde-Agudelo A, Althabe F, Belizán JM, Kafury-Goeta AC. Cigarette smoking during pregnancy and risk of preeclampsia: A systematic review. *Am J Obstet Gynecol*. 1999;181(4):1026-1035. doi:10.1016/S0002-9378(99)70341-8

298. Wang K, Zhou Q, He Q, Tong G, Zhao Z, Duan T. The possible role of AhR in the protective effects of cigarette smoke on preeclampsia. *Med Hypotheses*. 2011;77(5):872-874. doi:10.1016/j.mehy.2011.07.061

299. Stanley JL, Sulek K, Andersson IJ, et al. Sildenafil Therapy Normalizes the Aberrant Metabolomic Profile in the Comt−/− Mouse Model of Preeclampsia/Fetal Growth Restriction. *Sci Rep*. 2015;5(1):18241. doi:10.1038/srep18241

300. Watts SW, Shaw S, Burnett R, Dorrance AM. Indoleamine 2,3-diooxygenase in periaortic fat: mechanisms of inhibition of contraction. *American Journal of Physiology-Heart and Circulatory Physiology*. 2011;301(4):H1236-H1247. doi:10.1152/ajpheart.00384.2011

301. Pellegrin K, Neurauter G, Wirleitner B, Fleming AW, Peterson VM, Fuchs D. Enhanced enzymatic degradation of tryptophan by indoleamine 2,3-dioxygenase contributes to the tryptophan-deficient state seen after major trauma. *Shock*. 2005;23(3):209-215.

302. Changsirivathanathamrong D, Wang Y, Rajbhandari D, et al. Tryptophan metabolism to kynurenine is a potential novel contributor to hypotension in human sepsis*. *Crit Care Med*. 2011;39(12):2678-2683. doi:10.1097/CCM.0b013e31822827f2

303. Wolowczuk I, Hennart B, Leloire A, et al. Tryptophan metabolism activation by indoleamine 2,3-dioxygenase in adipose tissue of obese women: an attempt to maintain immune homeostasis and vascular tone. *American Journal of Physiology-Regulatory, Integrative and Comparative Physiology*. 2012;303(2):R135-R143. doi:10.1152/ajpregu.00373.2011

304. Nishizawa H, Hasegawa K, Suzuki M, et al. The Etiological Role of Allogeneic Fetal Rejection in Pre-Eclampsia. *American Journal of Reproductive Immunology*. 2007;58(1):11-20. doi:10.1111/j.1600-0897.2007.00484.x

305. Sakakibara K, Feng GG, Li J, et al. Kynurenine causes vasodilation and hypotension induced by activation of KCNQ-encoded voltage-dependent K+ channels. *J Pharmacol Sci*. 2015;129(1). doi:10.1016/j.jphs.2015.07.042

306. Stasch JP, Schmidt PM, Nedvetsky PI, et al. Targeting the heme-oxidized nitric oxide receptor for selective vasodilatation of diseased blood vessels. *Journal of Clinical Investigation*. 2006;116(9):2552-2561. doi:10.1172/JCI28371

307. Denninger JW, Marletta MA. Guanylate cyclase and the ·NO/cGMP signaling pathway. *Biochimica et Biophysica Acta (BBA) - Bioenergetics*. 1999;1411(2-3):334-350. doi:10.1016/S0005-2728(99)00024-9

308. Norris L. Nitric oxide in the uteroplacental, foetoplacental, and peripheral circulations in preeclampsia. *Obstetrics & Gynecology*. 1999;93(6):958-963. doi:10.1016/S0029-7844(99)00007-1

309. Suzuki Y, Yamamoto T. PP041. The underlying mechanisms in reduced action of endothelial nitric oxide in resistance artery in preeclampsia. *Pregnancy Hypertension: An International Journal of Women's Cardiovascular Health*. 2013;3(2):81. doi:10.1016/j.preghy.2013.04.068

310. Kamimura S, Eguchi K, Sekiba K. Tryptophan and its metabolite concentrations in human plasma and breast milk during the perinatal period. *Acta Med Okayama*. 1991;45(2):101-106. doi:10.18926/AMO/32183

311. Kamimura S, Eguchi K, Yonezawa M, Sekiba K. Localization and developmental change of indoleamine 2,3-dioxygenase activity in the human placenta. *Acta Med Okayama*. 1991;45(3):135-139. doi:10.18926/AMO/32206

312. Minatogawa Y, Suzuki S, Ando Y, Tone S, Takikawa O. Tryptophan pyrrole ring cleavage enzymes in placenta. *Adv Exp Med Biol*. 2003;527:425-434. doi:10.1007/978-1-4615-0135-0_50

313. Blaschitz A, Gauster M, Fuchs D, et al. Vascular Endothelial Expression of Indoleamine 2,3-Dioxygenase 1 Forms a Positive Gradient towards the Feto-Maternal Interface. *PLoS One*. 2011;6(7):e21774. doi:10.1371/journal.pone.0021774

314. Kudo Y, Boyd CAR, Sargent IL, Redman CWG. Decreased tryptophan catabolism by placental indoleamine 2,3-dioxygenase in preeclampsia. *Am J Obstet Gynecol*. 2003;188(3):719-726. doi:10.1067/mob.2003.156

315. Rose DP, Braidman IP. Excretion of tryptophan metabolites as affected by pregnancy, contraceptive steroids, and steroid hormones. *Am J Clin Nutr*. 1971;24(6):673-683. doi:10.1093/ajcn/24.6.673

316. Dunn WB, Brown M, Worton SA, et al. Changes in the Metabolic Footprint of Placental Explant-Conditioned Culture Medium Identifies Metabolic Disturbances Related to Hypoxia and Pre-Eclampsia. *Placenta*. 2009;30(11). doi:10.1016/j.placenta.2009.08.008

317. Heazell AEP, Brown M, Dunn WB, et al. Analysis of the Metabolic Footprint and Tissue Metabolome of Placental Villous Explants Cultured at Different Oxygen Tensions Reveals Novel Redox Biomarkers. *Placenta*. 2008;29(8):691-698. doi:10.1016/j.placenta.2008.05.002

318. Dupont V, Berg AH, Yamashita M, et al. Impaired renal reserve contributes to preeclampsia via the kynurenine and soluble fms-like tyrosine kinase 1 pathway. *Journal of Clinical Investigation*. Published online August 9, 2022. doi:10.1172/JCI158346

319. Love MI, Huber W, Anders S. Moderated estimation of fold change and dispersion for RNA-seq data with DESeq2. *Genome Biol*. 2014;15(12):550. doi:10.1186/s13059-014-0550-8

320. Knight M, Redman CWG, Linton EA, Sargent IL. Shedding of syncytiotrophoblast microvilli into the maternal circulation in pre-eclamptic pregnancies. *BJOG*. 1998;105(6):632-640. doi:10.1111/j.1471-0528.1998.tb10178.x

321. Vento-Tormo R, Efremova M, Botting RA, et al. Single-cell reconstruction of the early maternal-fetal interface in humans. *Nature*. 2018;563(7731):347-353. doi:10.1038/S41586-018-0698-6

322. Pique-Regi R, Romero R, Tarca AL, et al. Single cell transcriptional signatures of the human placenta in term and preterm parturition. *Elife*. 2019;8. doi:10.7554/ELIFE.52004

323. Tsang JCH, Vong JSL, Ji L, et al. Integrative single-cell and cell-free plasma RNA transcriptomics elucidates placental cellular dynamics. *Proc Natl Acad Sci U S A*. 2017;114(37):E7786-E7795. doi:10.1073/PNAS.1710470114

324. Chang RQ, Li DJ, Li MQ. The role of indoleamine-2,3-dioxygenase in normal and pathological pregnancies. *American Journal of Reproductive Immunology*. 2018;79(4):e12786. doi:10.1111/AJI.12786

325. Kudo Y, Sugimoto J. The Role of the Placental Enzyme Indoleamine 2,3-Dioxygenase in Normal and Abnormal Human Pregnancy. *International Journal of Molecular Sciences 2024, Vol 25, Page 4577*. 2024;25(8):4577. doi:10.3390/IJMS25084577

326. Redman CWG, Sacks GP, Sargent IL. Preeclampsia: An excessive maternal inflammatory response to pregnancy. *Am J Obstet Gynecol*. 1999;180(2):499-506. doi:10.1016/S0002-9378(99)70239-5

327. Sacks GP, Studena K, Sargent IL, Redman CWG. Normal pregnancy and preeclampsia both produce inflammatory changes in peripheral blood leukocytes akin to those of sepsis. *Am J Obstet Gynecol*. 1998;179(1):80-86. doi:10.1016/S0002-9378(98)70254-6

328. Gestational Hypertension and Preeclampsia. *Obstetrics & Gynecology*. 2020;135(6):e237-e260. doi:10.1097/AOG.0000000000003891

329. Hurrell A, Beardmore-Gray A, Duhig K, Webster L, Chappell L, Shennan A. Placental growth factor in suspected preterm pre-eclampsia: a review of the evidence and practicalities of implementation. *BJOG*. 2020;127(13):1590-1597. doi:10.1111/1471-0528.16425

330. Fox R, Kitt J, Leeson P, Aye CYL, Lewandowski AJ. Preeclampsia: Risk Factors, Diagnosis, Management, and the Cardiovascular Impact on the Offspring. *J Clin Med*. 2019;8(10):1625. doi:10.3390/jcm8101625

331. Redman CWG, Staff AC, Roberts JM. Syncytiotrophoblast stress in preeclampsia: the convergence point for multiple pathways. *Am J Obstet Gynecol*. 2022;226(2):S907-S927. doi:10.1016/j.ajog.2020.09.047

332. Redman CWG, Staff AC. Preeclampsia, biomarkers, syncytiotrophoblast stress, and placental capacity. *Am J Obstet Gynecol*. 2015;213(4). doi:10.1016/j.ajog.2015.08.003

333. Teng F, Fussenegger M. Shedding Light on Extracellular Vesicle Biogenesis and Bioengineering. *Advanced Science*. 2021;8(1). doi:10.1002/advs.202003505

334. Massoud SMA, Agwa SHA, Gomaa AA, Sayed ARM, Hamdy SM. Novel Micro Non-coding RNAs (miRNA-221 and miRNA-197) As Biomarkers for Acute Myocardial Infarction Diagnosis. *Biochemistry Letters*. 2022;18(1):103-118. doi:10.21608/BLJ.2022.277168

335. Norouzi-Barough L, Sarookhani MR, Sharifi M, Moghbelinejad S, Jangjoo S, Salehi R. Molecular mechanisms of drug resistance in ovarian cancer. *J Cell Physiol*. 2018;233(6):4546-4562. doi:10.1002/jcp.26289

336. Raisch J. Role of microRNAs in the immune system, inflammation and cancer. *World J Gastroenterol*. 2013;19(20):2985. doi:10.3748/wjg.v19.i20.2985

337. Acunzo M, Romano G, Wernicke D, Croce CM. MicroRNA and cancer – A brief overview. *Adv Biol Regul*. 2015;57:1-9. doi:10.1016/j.jbior.2014.09.013

338. Pös O, Biró O, Szemes T, Nagy B. Circulating cell-free nucleic acids: characteristics and applications. *European Journal of Human Genetics*. 2018;26(7):937-945. doi:10.1038/s41431-018-0132-4

339. Sheikh AM, Small HY, Currie G, Delles C. Systematic Review of Micro-RNA Expression in Pre-Eclampsia Identifies a Number of Common Pathways Associated with the Disease. *PLoS One*. 2016;11(8):e0160808. doi:10.1371/journal.pone.0160808

340. Srinivasan S, Treacy R, Herrero T, et al. Discovery and Verification of Extracellular miRNA Biomarkers for Non-invasive Prediction of Pre-eclampsia in Asymptomatic Women. *Cell Rep Med*. 2020;1(2):100013. doi:10.1016/j.xcrm.2020.100013

341. Wei J, Blenkiron C, Tsai P, et al. Placental trophoblast debris mediated feto-maternal signalling via small RNA delivery: implications for preeclampsia. *Sci Rep*. 2017;7(1):14681. doi:10.1038/s41598-017-14180-8

342. Cooke WR, Cribbs A, Zhang W, et al. Maternal circulating syncytiotrophoblast-derived extracellular vesicles contain biologically active 5'-tRNA halves. *Biochem Biophys Res Commun*. 2019;518(1):107-113. doi:10.1016/j.bbrc.2019.08.015

343. Klagsbrun M, D'Amore PA. Regulators of Angiogenesis. *Annu Rev Physiol*. 1991;53(1):217-239. doi:10.1146/annurev.ph.53.030191.001245

344. Reynolds LP, Killilea SD, Redmer DA. Angiogenesis in the female reproductive system. *FASEB J*. 1992;6(3):886-892.

345. Gupta MK. Mechanism and its regulation of tumour-induced angiogenesis. *World J Gastroenterol*. 2003;9(6):1144. doi:10.3748/wjg.v9.i6.1144

346. Bellon G, Martiny L, Robinet A. Matrix metalloproteinases and matrikines in angiogenesis. *Crit Rev Oncol Hematol*. 2004;49(3):203-220. doi:10.1016/j.critrevonc.2003.10.004

347. Bussolino F, Mantovani A, Persico G. Molecular mechanisms of blood vessel formation. *Trends Biochem Sci*. 1997;22(7):251-256. doi:10.1016/S0968-0004(97)01074-8

348. Kalebic T, Garbisa S, Glaser B, Liotta LA. Basement Membrane Collagen: Degradation by Migrating Endothelial Cells. *Science (1979)*. 1983;221(4607):281-283. doi:10.1126/science.6190230

349. Reynolds LP, Redmer DA. Angiogenesis in the Placenta. *Biol Reprod*. 2001;64(4):1033-1040. doi:10.1095/biolreprod64.4.1033

350. Bassil S, Magritte JP, Roth J, Nisolle M, Donnez J, Gordts S. Uterine vascularity during stimulation and its correlation with implantation in in-vitro fertilization. *Human Reproduction*. 1995;10(6):1497-1501. doi:10.1093/HUMREP/10.6.1497

351. Meegdes BHLM, Ingenhoes R, Peeters LLH, Exalto N. Early pregnancy wastage: relationship between chorionic vascularization and embryonic development. *Fertil Steril*. 1988;49(2):216-220. doi:10.1016/S0015-0282(16)59704-0

352. Jaffe EA. Cell biology of endothelial cells. *Hum Pathol*. 1987;18(3):234-239. doi:10.1016/S0046-8177(87)80005-9

353. Félétou M. The Endothelium, Part I: Multiple Functions of the Endothelial Cells -- Focus on Endothelium-Derived Vasoactive Mediators. *Colloquium Series on Integrated Systems Physiology: From Molecule to Function*. 2011;3(4):1-306. doi:10.4199/C00031ED1V01Y201105ISP019

354. Alberts B, Johnson A, Lewis J, Raff M, Roberts K, Walter P. Blood Vessels and Endothelial Cells. In: *Molecular Biology of the Cell*. 4th ed. Garland Science; 2002.

355. Roberts JM, Taylor RN, Musci TJ, Rodgers GM, Hubel CA, McLaughlin MK. Preeclampsia: An endothelial cell disorder. *Am J Obstet Gynecol*. 1989;161(5):1200-1204. doi:10.1016/0002-9378(89)90665-0

356. Stillman IE, Karumanchi SA. The Glomerular Injury of Preeclampsia. *Journal of the American Society of Nephrology*. 2007;18(8):2281-2284. doi:10.1681/ASN.2007020255

357. Eremina V, Jefferson JA, Kowalewska J, et al. VEGF Inhibition and Renal Thrombotic Microangiopathy. *New England Journal of Medicine*. 2008;358(11):1129-1136. doi:10.1056/nejmoa0707330

358. Eremina V, Sood M, Haigh J, et al. Glomerular-specific alterations of VEGF-A expression lead to distinct congenital and acquired renal diseases. *J Clin Invest*. 2003;111(5):707-716. doi:10.1172/JCI17423

359. Johnson AC, Cipolla MJ. The Cerebral Circulation During Pregnancy: Adapting to Preserve Normalcy. *Physiology*. 2015;30(2):139-147. doi:10.1152/physiol.00048.2014

360. Siepmann T, Boardman H, Bilderbeck A, et al. Long-term cerebral white and gray matter changes after preeclampsia. *Neurology*. 2017;88(13):1256-1264. doi:10.1212/WNL.0000000000003765

361. Wiegman MJ, Zeeman GG, Aukes AM, et al. Regional distribution of cerebral white matter lesions years after preeclampsia and eclampsia. *Obstetrics and gynecology*. 2014;123(4):790-795. doi:10.1097/AOG.0000000000000162

362. Mielke MM, Milic NM, Weissgerber TL, et al. Impaired Cognition and Brain Atrophy Decades After Hypertensive Pregnancy Disorders. *Circ Cardiovasc Qual Outcomes*. 2016;9(2 Suppl 1):S70-S76. doi:10.1161/CIRCOUTCOMES.115.002461

363. Ibarra AJ, Butters MA, Lim G, et al. Longitudinal cognitive evaluation before and after delivery among people with preeclampsia. *Am J Obstet Gynecol MFM*. 2023;5(7):100966. doi:10.1016/j.ajogmf.2023.100966

364. Bergman L, Thorgeirsdottir L, Elden H, et al. Cognitive impairment in preeclampsia complicated by eclampsia and pulmonary edema after delivery. *Acta Obstet Gynecol Scand*. 2021;100(7):1280-1287. doi:10.1111/aogs.14100

365. Samara AA, Liampas I, Dadouli K, et al. Preeclampsia, gestational hypertension and incident dementia: A systematic review and meta-analysis of published evidence. *Pregnancy Hypertens*. 2022;30:192-197. doi:10.1016/j.preghy.2022.10.008

366. Brohan MP, Daly FP, Kelly L, et al. Hypertensive disorders of pregnancy and long-term risk of maternal stroke—a systematic review and meta-analysis. *Am J Obstet Gynecol*. 2023;229(3):248-268. doi:10.1016/j.ajog.2023.03.034

367. Schreurs MPH, Hubel CA, Bernstein IM, Jeyabalan A, Cipolla MJ. Increased oxidized low-density lipoprotein causes blood-brain barrier disruption in early-onset preeclampsia through LOX-1. *FASEB J*. 2013;27(3):1254-1263. doi:10.1096/FJ.12-222216

368. Amburgey ÖA, Chapman AC, May V, Bernstein IM, Cipolla MJ. Plasma from preeclamptic women increases blood-brain barrier permeability: role of vascular endothelial growth factor signaling. *Hypertension*. 2010;56(5):1003-1008. doi:10.1161/HYPERTENSIONAHA.110.158931

369. Bergman L, Acurio J, Leon J, et al. Preeclampsia and Increased Permeability Over the Blood-Brain Barrier: A Role of Vascular Endothelial Growth Receptor 2. *Am J Hypertens*. 2021;34(1):73-81. doi:10.1093/AJH/HPAA142

370. Friis T, Wikström AK, Acurio J, et al. Cerebral Biomarkers and Blood-Brain Barrier Integrity in Preeclampsia. *Cells*. 2022;11(5):789. doi:10.3390/CELLS11050789/S1

371. Ouyang Y, Mouillet JF, Coyne CB, Sadovsky Y. Review: placenta-specific microRNAs in exosomes - good things come in nano-packages. *Placenta*. 2014;35 Suppl(SUPPL). doi:10.1016/J.PLACENTA.2013.11.002

372. Manfredi M, Beltramello A, Bongiovanni LG, Polo A, Pistoia L, Rizzuto N. Eclamptic encephalopathy: imaging and pathogenetic considerations. *Acta Neurol Scand*. 1997;96(5):277-282. doi:10.1111/J.1600-0404.1997.TB00284.X

373. Wiegman MJ, Zeeman GG, Aukes AM, et al. Regional distribution of cerebral white matter lesions years after preeclampsia and eclampsia. *Obstetrics and gynecology*. 2014;123(4):790-795. doi:10.1097/AOG.0000000000000162

374. Aukes AM, Wessel I, Dubois AM, Aarnoudse JG, Zeeman GG. Self-reported cognitive functioning in formerly eclamptic women. *Am J Obstet Gynecol*. 2007;197(4):365.e1-365.e6. doi:10.1016/J.AJOG.2007.06.044

375. Leffert LR, Clancy CR, Bateman BT, Bryant AS, Kuklina E V. Hypertensive disorders and pregnancy-related stroke: frequency, trends, risk factors, and outcomes. *Obstetrics and gynecology*. 2015;125(1):124-131. doi:10.1097/AOG.0000000000000590

376. Ghulmiyyah L, Sibai B. Maternal mortality from preeclampsia/eclampsia. *Semin Perinatol*. 2012;36(1):56-59. doi:10.1053/J.SEMPERI.2011.09.011

377. Fishel Bartal M, Sibai BM. Eclampsia in the 21st century. *Am J Obstet Gynecol*. 2022;226(2S):S1237-S1253. doi:10.1016/J.AJOG.2020.09.037

378. Escudero C, Kupka E, Ibañez B, et al. Brain Vascular Dysfunction in Mothers and Their Children Exposed to Preeclampsia. *Hypertension*. 2023;80(2):242-256. doi:10.1161/HYPERTENSIONAHA.122.19408

379. Cipolla MJ, Sweet JG, Chan SL. Cerebral vascular adaptation to pregnancy and its role in the neurological complications of eclampsia. *J Appl Physiol (1985)*. 2011;110(2):329-339. doi:10.1152/JAPPLPHYSIOL.01159.2010

380. Johnson AC, Hammer ES, Sakkaki S, Tremble SM, Holmes GL, Cipolla MJ. Inhibition of blood-brain barrier efflux transporters promotes seizure in pregnant rats: Role of circulating factors. *Brain Behav Immun*. 2018;67:13-23. doi:10.1016/J.BBI.2017.07.017

381. León J, Acurio J, Bergman L, et al. Disruption of the Blood-Brain Barrier by Extracellular Vesicles From Preeclampsia Plasma and Hypoxic Placentae: Attenuation by Magnesium Sulfate. *Hypertension*. 2021;78(5):1423-1433. doi:10.1161/HYPERTENSIONAHA.121.17744

382. Siegel GJ, Agranoff BW, Albers RW, Fisher SK, Uhler MD. *Basic Neurochemistry*. Lippincott-Raven; 1999. Accessed June 19, 2024. https://www.ncbi.nlm.nih.gov/books/NBK20385/

383. Palmer SK, Zamudio S, Coffin C, Parker S, Stamm E, Moore LG. Quantitative estimation of human uterine artery blood flow and pelvic blood flow redistribution in pregnancy. *Obstetrics and gynecology*. 1992;80(6):1000-1006.

384. Duvekot JJ, Peeters LLH. Maternal cardiovascular hemodynamic adaptation to pregnancy. *Obstet Gynecol Surv*. 1994;49(12 Suppl):S1-S14. doi:10.1097/00006254-199412011-00001

385. Clapp JF, Capeless E. Cardiovascular function before, during, and after the first and subsequent pregnancies. *Am J Cardiol*. 1997;80(11):1469-1473. doi:10.1016/S0002-9149(97)00738-8

386. Chan S, Cipolla MJ. Relaxin causes selective outward remodeling of brain parenchymal arterioles via activation of peroxisome proliferator-activated receptor-γ. *FASEB J*. 2011;25(9):3229-3239. doi:10.1096/FJ.10-175471

387. Gonzalez J g., Elizondo G, Saldivar D, Nanez H, Todd LE, Villarreal JZ. Pituitary gland growth during normal pregnancy: an in vivo study using magnetic resonance imaging. *Am J Med*. 1988;85(2):217-220. doi:10.1016/S0002-9343(88)80346-2

388. Krauss T, Pauer HU, Augustin HG. Prospective analysis of placenta growth factor (PlGF) concentrations in the plasma of women with normal pregnancy and pregnancies complicated by preeclampsia. *Hypertens Pregnancy*. 2004;23(1):101-111. doi:10.1081/PRG-120028286

389. Schreurs MPH, Houston EM, May V, Cipolla MJ. The adaptation of the blood-brain barrier to vascular endothelial growth factor and placental growth factor during pregnancy. *FASEB J*. 2012;26(1):355-362. doi:10.1096/FJ.11-191916

390. Cipolla MJ, Pusic AD, Grinberg YY, Chapman AC, Poynter ME, Kraig RP. Pregnant serum induces neuroinflammation and seizure activity via TNFα. *Exp Neurol*. 2012;234(2):398-404. doi:10.1016/J.EXPNEUROL.2012.01.005

391. Ying M, Feng H, Zhang X, Liu R, Ning H. MiR-9-5p Inhibits the Proliferation, Migration and Invasion of Choroidal Melanoma by Targeting BRAF. *Technol Cancer Res Treat*. 2020;19. doi:10.1177/1533033820956987

392. Wei YZ, Jiao XL, Zhang SY, Xu Y, Li S, Kong B. MiR-9-5p could promote angiogenesis and radiosensitivity in cervical cancer by targeting SOCS5. *Eur Rev Med Pharmacol Sci*. 2019;23(17):7314-7326. doi:10.26355/EURREV_201909_18837

393. Yi J, Gao ZF. MicroRNA-9-5p promotes angiogenesis but inhibits apoptosis and inflammation of high glucose-induced injury in human umbilical vascular endothelial cells by targeting CXCR4. *Int J Biol Macromol*. 2019;130:1-9. doi:10.1016/J.IJBIOMAC.2019.02.003

394. Mayhan WG. VEGF increases permeability of the blood-brain barrier via a nitric oxide synthase/cGMP-dependent pathway. *Am J Physiol*. 1999;276(5). doi:10.1152/AJPCELL.1999.276.5.C1148

395. Olsson AK, Dimberg A, Kreuger J, Claesson-Welsh L. VEGF receptor signalling - in control of vascular function. *Nat Rev Mol Cell Biol*. 2006;7(5):359-371. doi:10.1038/NRM1911

396. Hudson N, Powner MB, Sarker MH, et al. Differential apicobasal VEGF signaling at vascular blood-neural barriers. *Dev Cell*. 2014;30(5):541-552. doi:10.1016/J.DEVCEL.2014.06.027

397. Sun Z, Li X, Massena S, et al. VEGFR2 induces c-Src signaling and vascular permeability in vivo via the adaptor protein TSAd. *Journal of Experimental Medicine*. 2012;209(7):1363-1377. doi:10.1084/jem.20111343

398. Koch S, Claesson-Welsh L. Signal Transduction by Vascular Endothelial Growth Factor Receptors. *Cold Spring Harb Perspect Med*. 2012;2(7). doi:10.1101/CSHPERSPECT.A006502

399. Srinivas SK, Morrison AC, Andrela CM, Elovitz MA. Allelic variations in angiogenic pathway genes are associated with preeclampsia. *Am J Obstet Gynecol*. 2010;202(5):445.e1-445.e11. doi:10.1016/j.ajog.2010.01.040

400. Agarwal I, Karumanchi SA. Preeclampsia and the Anti-Angiogenic State. *Pregnancy Hypertens*. 2011;1(1):17. doi:10.1016/J.PREGHY.2010.10.007

401. Gaber LW, Spargo BH, Lindheimer MD. 12 Renal pathology in pre-eclampsia. *Baillieres Clin Obstet Gynaecol*. 1987;1(4):971-995. doi:10.1016/S0950-3552(87)80045-7

402. Spargo BH, Lichtig C, Luger AM, Katz AI, Lindheimer MD. The renal lesion in preeclampsia. *Perspect Nephrol Hypertens*. 1976;5:129-137.

403. Lafayette RA, Druzin M, Sibley R, et al. Nature of glomerular dysfunction in pre-eclampsia. *Kidney Int*. 1998;54(4):1240-1249. doi:10.1046/j.1523-1755.1998.00097.x

404. He P, Shao D, Ye M, Zhang G. Analysis of gene expression identifies candidate markers and pathways in pre-eclampsia. *J Obstet Gynaecol (Lahore)*. 2015;35(6):578-584. doi:10.3109/01443615.2014.990430

405. Li X, Fang Y. Bioinformatics identification of potential genes and pathways in preeclampsia based on functional gene set enrichment analyses. *Exp Ther Med*. 2019;18(3). doi:10.3892/ETM.2019.7749

406. Guo F, Zhang B, Yang H, et al. Systemic transcriptome comparison between early- And late-onset pre-eclampsia shows distinct pathology and novel biomarkers. *Cell Prolif*. 2021;54(2). doi:10.1111/CPR.12968

407. Birnie R, Bryce SD, Roome C, et al. Gene expression profiling of human prostate cancer stem cells reveals a pro-inflammatory phenotype and the importance of extracellular matrix interactions. *Genome Biol*. 2008;9(5). doi:10.1186/GB-2008-9-5-R83

408. Kim J, Zhao K, Jiang P, et al. Transcriptome landscape of the human placenta. *BMC Genomics*. 2012;13(1):1-21. doi:10.1186/1471-2164-13-115/COMMENTS

409. Rozario T, DeSimone DW. The extracellular matrix in development and morphogenesis: a dynamic view. *Dev Biol*. 2010;341(1):126-140. doi:10.1016/J.YDBIO.2009.10.026

410. Damsky C, Sutherland A, Fisher S. Extracellular matrix 5: adhesive interactions in early mammalian embryogenesis, implantation, and placentation. *FASEB J*. 1993;7(14):1320-1329. doi:10.1096/FASEBJ.7.14.8224605

411. Bruchova H, Vasikova A, Merkerova M, et al. Effect of maternal tobacco smoke exposure on the placental transcriptome. *Placenta*. 2010;31(3):186-191. doi:10.1016/J.PLACENTA.2009.12.016

412. Lu Q, Liu Z, Li Z, et al. TIPE2 Overexpression Suppresses the Proliferation, Migration, and Invasion in Prostate Cancer Cells by Inhibiting PI3K/Akt Signaling Pathway. *Oncology Research Featuring Preclinical and Clinical Cancer Therapeutics*. 2016;24(5):305-313. doi:10.3727/096504016X14666990347437

413. Peng X, Wang Z, Liu Y, et al. Oxyfadichalcone C inhibits melanoma A375 cell proliferation and metastasis via suppressing PI3K/Akt and MAPK/ERK pathways. *Life Sci*. 2018;206:35-44. doi:10.1016/j.lfs.2018.05.032

414. Prast J, Saleh L, Husslein H, Sonderegger S, Helmer H, Knöfler M. Human Chorionic Gonadotropin Stimulates Trophoblast Invasion through Extracellularly Regulated Kinase and AKT Signaling. *Endocrinology*. 2008;149(3):979-987. doi:10.1210/en.2007-1282

415. Qiu Q, Yang M, Tsang BK, Gruslin A. EGF-induced trophoblast secretion of MMP-9 and TIMP-1 involves activation of both PI3K and MAPK signalling pathways. *Reproduction*. 2004;128(3):355-363. doi:10.1530/rep.1.00234

416. Xu Y, Sui L, Qiu B, Yin X, Liu J, Zhang X. ANXA4 promotes trophoblast invasion via the PI3K/akt/eNOS pathway in preeclampsia. *Am J Physiol Cell Physiol*. 2019;316(4):C481-C491. doi:10.1152/AJPCELL.00404.2018/ASSET/IMAGES/LARGE/ZH00031984010006.JPEG

417. Kaufmann P, Black S, Huppertz B. Endovascular trophoblast invasion: implications for the pathogenesis of intrauterine growth retardation and preeclampsia. *Biol Reprod*. 2003;69(1):1-7. doi:10.1095/BIOLREPROD.102.014977

418. Ji L, Brkić J, Liu M, Fu G, Peng C, Wang YL. Placental trophoblast cell differentiation: physiological regulation and pathological relevance to preeclampsia. *Mol Aspects Med*. 2013;34(5):981-1023. doi:10.1016/J.MAM.2012.12.008

419. Wang S, He G, Yang Y, et al. Reduced expression of Enac in Placenta tissues of patients with severe preeclampsia is related to compromised trophoblastic cell migration and invasion during pregnancy. *PLoS One*. 2013;8(8). doi:10.1371/JOURNAL.PONE.0072153

420. Pringle KG, Kind KL, Sferruzzi-Perri AN, Thompson JG, Roberts CT. Beyond oxygen: complex regulation and activity of hypoxia inducible factors in pregnancy. *Hum Reprod Update*. 2010;16(4):415-431. doi:10.1093/HUMUPD/DMP046

421. Berra E, Benizri E, Ginouvès A, Volmat V, Roux D, Pouysségur J. HIF prolyl-hydroxylase 2 is the key oxygen sensor setting low steady-state levels of HIF-1alpha in normoxia. *EMBO J*. 2003;22(16):4082-4090. doi:10.1093/EMBOJ/CDG392

422. Tal R. The role of hypoxia and hypoxia-inducible factor-1alpha in preeclampsia pathogenesis. *Biol Reprod*. 2012;87(6). doi:10.1095/BIOLREPROD.112.102723

423. Erez O, Romero R, Jung E, et al. Preeclampsia and eclampsia: the conceptual evolution of a syndrome. *Am J Obstet Gynecol*. 2022;226(2):S786-S803. doi:10.1016/j.ajog.2021.12.001

424. Martin JN, Morris RF. Preeclampsia-Spectrum Hypertensive Disorders of Pregnancy: Gestational Hypertension, Preeclampsia, Eclampsia, Chronic Hypertension, and HELLP Syndrome. In: *Sex Differences in Cardiovascular Physiology and Pathophysiology*. Elsevier; 2019:121-136. doi:10.1016/B978-0-12-813197-8.00008-7

425. Agrawal S, Cerdeira AS, Redman C, Vatish M. Meta-Analysis and Systematic Review to Assess the Role of Soluble FMS-Like Tyrosine Kinase-1 and Placenta Growth Factor Ratio in Prediction of Preeclampsia. *Hypertension*. 2018;71(2):306-316. doi:10.1161/HYPERTENSIONAHA.117.10182

426. Cerdeira AS, Karumanchi SA. Biomarkers in Preeclampsia. In: *Biomarkers of Kidney Disease*. Elsevier; 2011:385-426. doi:10.1016/B978-0-12-375672-5.10011-8

427. Yamazaki T, Cerdeira AS, Agrawal S, et al. Predictive Accuracy of Soluble FMS-Like Tyrosine Kinase-1/Placental Growth Factor Ratio for Preeclampsia in Japan: A Systematic Review. *Hypertension Research in Pregnancy*. 2021;9(1):1-7. doi:10.14390/jsshp.HRP2020-012

428. Verlohren S, Brennecke SP, Galindo A, et al. Clinical interpretation and implementation of the sFlt-1/PlGF ratio in the prediction, diagnosis and management of preeclampsia. *Pregnancy Hypertens*. 2022;27:42-50. doi:10.1016/j.preghy.2021.12.003

429. Huda SS, Freeman DJ, Nelson SM. Short- and long-term strategies for the management of hypertensive disorders of pregnancy. *Expert Rev Cardiovasc Ther*. 2009;7(12):1581-1594. doi:10.1586/ERC.09.147

430. Sibai B, Dekker G, Kupferminc M. Pre-eclampsia. *Lancet*. 2005;365(9461):785-799. doi:10.1016/S0140-6736(05)17987-2

431. Wagner LK. Diagnosis and management of preeclampsia. *Am Fam Physician*. 2004;70(12):2317-2324.

432. Duley L. The global impact of pre-eclampsia and eclampsia. *Semin Perinatol*. 2009;33(3):130-137. doi:10.1053/J.SEMPERI.2009.02.010

433. ACOG Committee on Obstetric Practice. ACOG practice bulletin. Diagnosis and management of preeclampsia and eclampsia. Number 33, January 2002. *Obstetrics and gynecology*. 2002;99(1):159-167. doi:10.1016/S0029-7844(01)01747-1

434. Chappell LC, Brocklehurst P, Green ME, et al. Planned early delivery or expectant management for late preterm pre-eclampsia (PHOENIX): a randomised controlled trial. *The Lancet*. 2019;394(10204):1181-1190. doi:10.1016/S0140-6736(19)31963-4

435. Roberts JM, Escudero C. The placenta in preeclampsia. *Pregnancy Hypertension: An International Journal of Women's Cardiovascular Health*. 2012;2(2):72-83. doi:10.1016/j.preghy.2012.01.001

436. Haddad B, Sibai BM. Expectant management in pregnancies with severe pre-eclampsia. *Semin Perinatol*. 2009;33(3):143-151. doi:10.1053/J.SEMPERI.2009.02.002

437. Koopmans CM, Bijlenga D, Groen H, et al. Induction of labour versus expectant monitoring for gestational hypertension or mild pre-eclampsia after 36 weeks' gestation (HYPITAT): a multicentre, open-label randomised controlled trial. *Lancet*. 2009;374(9694):979-988. doi:10.1016/S0140-6736(09)60736-4

438. Foidart JM, Schaaps JP, Chantraine F, Munaut C, Lorquet S. Dysregulation of anti-angiogenic agents (sFlt-1, PLGF, and sEndoglin) in preeclampsia--a step forward but not the definitive answer. *J Reprod Immunol*. 2009;82(2):106-111. doi:10.1016/J.JRI.2009.09.001

439. Cudihy D, Lee R V. The pathophysiology of pre-eclampsia: current clinical concepts. *J Obstet Gynaecol*. 2009;29(7):576-582. doi:10.1080/01443610903061751

440. Maynard S, Epstein FH, Karumanchi SA. Preeclampsia and angiogenic imbalance. *Annu Rev Med*. 2008;59:61-78. doi:10.1146/ANNUREV.MED.59.110106.214058

441. Levine RJ, Karumanchi SA. Circulating Angiogenic Factors in Preeclampsia. *Clin Obstet Gynecol*. 2005;48(2):372-386. doi:10.1097/01.grf.0000160313.82606.d7

442. Verlohren S, Galindo A, Schlembach D, et al. An automated method for the determination of the sFlt-1/PIGF ratio in the assessment of preeclampsia. *Am J Obstet Gynecol*. 2010;202(2):161.e1-161.e11. doi:10.1016/J.AJOG.2009.09.016

443. Sunderji S, Gaziano E, Wothe D, et al. Automated assays for sVEGF R1 and PlGF as an aid in the diagnosis of preterm preeclampsia: a prospective clinical study. *Am J Obstet Gynecol*. 2010;202(1):40.e1-40.e7. doi:10.1016/J.AJOG.2009.07.025

444. Ohkuchi A, Hirashima C, Suzuki H, et al. Evaluation of a new and automated electrochemiluminescence immunoassay for plasma sFlt-1 and PlGF levels in women with preeclampsia. *Hypertens Res*. 2010;33(5):422-427. doi:10.1038/HR.2010.15

445. Levine RJ, Maynard SE, Qian C, et al. Circulating angiogenic factors and the risk of preeclampsia. *N Engl J Med*. 2004;350(7):672-683. doi:10.1056/NEJMOA031884

446. Levine RJ, Lam C, Qian C, et al. Soluble endoglin and other circulating antiangiogenic factors in preeclampsia. *N Engl J Med*. 2006;355(10):992-1005. doi:10.1056/NEJMOA055352

447. Vatten LJ, Eskild A, Nilsen TIL, Jeansson S, Jenum PA, Staff AC. Changes in circulating level of angiogenic factors from the first to second trimester as predictors of

preeclampsia. *Am J Obstet Gynecol*. 2007;196(3):239.e1-239.e6. doi:10.1016/J.AJOG.2006.10.909

448. Zeisler H, Llurba E, Chantraine F, et al. Predictive Value of the sFlt-1:PlGF Ratio in Women with Suspected Preeclampsia. *New England Journal of Medicine*. 2016;374(1):13-22. doi:10.1056/NEJMoa1414838

449. Moore Simas TA, Crawford SL, Solitro MJ, Frost SC, Meyer BA, Maynard SE. Angiogenic factors for the prediction of preeclampsia in high-risk women. *Am J Obstet Gynecol*. 2007;197(3):244.e1-244.e8. doi:10.1016/J.AJOG.2007.06.030

450. Rana S, Karumanchi SA, Levine RJ, et al. Sequential changes in antiangiogenic factors in early pregnancy and risk of developing preeclampsia. *Hypertension*. 2007;50(1):137-142. doi:10.1161/HYPERTENSIONAHA.107.087700

451. Sibai BM, Stella CL. Diagnosis and management of atypical preeclampsia-eclampsia. *Am J Obstet Gynecol*. 2009;200(5):481.e1-481.e7. doi:10.1016/J.AJOG.2008.07.048

452. Romero R, Nien JK, Espinoza J, et al. A longitudinal study of angiogenic (placental growth factor) and anti-angiogenic (soluble endoglin and soluble vascular endothelial growth factor receptor-1) factors in normal pregnancy and patients destined to develop preeclampsia and deliver a small for gestational age neonate. *J Matern Fetal Neonatal Med*. 2008;21(1):9-23. doi:10.1080/14767050701830480

453. Chappell LC, Duckworth S, Seed PT, et al. Diagnostic accuracy of placental growth factor in women with suspected preeclampsia: a prospective multicenter study. *Circulation*. 2013;128(19):2121-2131. doi:10.1161/CIRCULATIONAHA.113.003215

454. NICE. *"PlGF-Based Testing to Help Diagnose Suspected Pre-Eclampsia (Triage PlGF Test, Elecsys Immunoassay SFlt-1/PlGF Ratio, DELFIA Xpress PlGF 1-2-3 Test, and BRAHMS SFlt-1 Kryptor/BRAHMS PlGF plus Kryptor PE Ratio),."*; 2016.

455. Bian X, Biswas A, Huang X, et al. Short-Term Prediction of Adverse Outcomes Using the sFlt-1 (Soluble fms-Like Tyrosine Kinase 1)/PlGF (Placental Growth Factor) Ratio

in Asian Women With Suspected Preeclampsia. *Hypertension*. 2019;74(1):164-172. doi:10.1161/HYPERTENSIONAHA.119.12760

456. Cerdeira AS, O'Sullivan J, Ohuma EO, et al. Randomized Interventional Study on Prediction of Preeclampsia/Eclampsia in Women With Suspected Preeclampsia: INSPIRE. *Hypertension*. 2019;74(4):983-990. doi:10.1161/HYPERTENSIONAHA.119.12739

457. Duhig KE, Myers J, Seed PT, et al. Placental growth factor testing to assess women with suspected pre-eclampsia: a multicentre, pragmatic, stepped-wedge cluster-randomised controlled trial. *Lancet*. 2019;393(10183):1807-1818. doi:10.1016/S0140-6736(18)33212-4

458. Sackett DL, Straus SE, Richardson WS, Rosenberg W, Haynes RB. *Evidence-Based Medicine: How to Practice and Teach EBM.* 2nd ed. Churchill Livingstone; 2000.

459. Brown MA, Magee LA, Kenny LC, et al. The hypertensive disorders of pregnancy: ISSHP classification, diagnosis & management recommendations for international practice. *Pregnancy Hypertens*. 2018;13:291-310. doi:10.1016/J.PREGHY.2018.05.004

460. Von Dadelszen P, Magee LA, Roberts JM. Subclassification of preeclampsia. *Hypertens Pregnancy*. 2003;22(2):143-148. doi:10.1081/PRG-120021060

461. Magann EF, Martin JN. Twelve steps to optimal management of HELLP syndrome. *Clin Obstet Gynecol*. 1999;42(3):532-550. doi:10.1097/00003081-199909000-00009

462. Tsatsaris V, Azria E, Goffinet F. Prevention of preterm delivery. *N Engl J Med*. 2007;357(19):1979; author reply 1979-80. doi:10.1056/NEJMc072557